

PyCAMA report generated by trop12-proc

trop12-proc

2023-09-27 (05:15)

1 Short Introduction

1.1 The list of parameters

You may want to keep the list given in table 1 at hand when viewing the results.

2 Definitions

The averages shown here are *unweighted* averages:

$$\bar{x} = \frac{1}{N} \sum_{i=1}^N x_i \quad (1)$$

with N the number of observations in the dataset.

The spread of the measurements is indicated with the variance $V(x)$, or rather the standard deviation $\sigma(x) = \sqrt{V(x)}$.

$$V(x) = \frac{1}{N-1} \sum_{i=1}^N (x_i - \bar{x})^2 \quad (2)$$

We also report the more robust statistics median, minimum, maximum, various percentiles and inter quartile range.

The median m is the value of parameter x for which half of the observations of x is smaller than m :

$$P(x \leq m) = P(x \geq m) = \int_{-\infty}^m f(x) dx = \frac{1}{2} \quad (3)$$

with $f(x)$ the probability density function.

The median is a special case of a percentile. Instead of $1/2$ in equation 3, other threshold values can be used. We report results for 1 %, 5 %, 10 %, 15.9 %, 25 %, 75 %, 84.1 %, 90 %, 95 % and 99 %. The inter quartile range is the difference between the 75 % and 25 % percentiles. Similarly the minimum and maximum values correspond to the 0 % and 100 % percentiles respectively.

For normally distributed parameters the mean and median are the same, while the $\mu \pm \sigma$ values and the 15.9 % and 84.1 % percentiles coincide.

To get a measure for the relation of one variable $x_{(k)}$ with another $x_{(l)}$, we calculate the covariance matrix C_{kl} .

$$C_{kl} = C(x_{(k)}, x_{(l)}) = \frac{1}{N-1} \sum_{i=1}^N (x_{(k),i} - \bar{x}_{(k)})(x_{(l),i} - \bar{x}_{(l)}) \quad (4)$$

Rather than a dimensionally dependent covariance, it is often easier to interpret a correlation matrix R_{kl} , a matrix of Pearson's r coefficients:

$$R_{kl} = R(x_{(k)}, x_{(l)}) = \frac{C_{kl}}{\sqrt{C_{kk}C_{ll}}} = \frac{C_{kl}}{\sqrt{V(x_k)V(x_l)}} \quad (5)$$

The diagonal elements of the covariance matrix are the variances of the elements, $V(x_{(k)}) = C_{kk}$ and obviously $R_{kk} = 1$.

| Variable |
|---|
| qa value [1] |
| formaldehyde tropospheric vertical column [mol m ⁻²] |
| formaldehyde tropospheric vertical column precision [mol m ⁻²] |
| formaldehyde tropospheric vertical column correction [mol m ⁻²] |
| formaldehyde slant column density window1 [mol m ⁻²] |
| formaldehyde slant column density window1 precision [mol m ⁻²] |
| formaldehyde tropospheric air mass factor [1] |
| formaldehyde tropospheric air mass factor precision [1] |
| formaldehyde clear air mass factor [1] |
| integrated formaldehyde profile apriori [mol m ⁻²] |
| fitted wavelength radiance shift [nm] |
| fitted wavelength radiance squeeze [1] |
| fitted root mean square win1 [1] |
| formaldehyde slant column delta [mol m ⁻²] |

Table 1: Parameterlist and basic statistics for the analysis

| mean $\pm \sigma$ | Count | Mode | IQR | Median | Minimum | Maximum |
|---------------------------------------|----------|-------------------------|------------------------|-------------------------|-------------------------|------------------------|
| 0.682 ± 0.346 | 20362022 | 0.995 | 0.690 | 0.900 | 1.000×10^{-2} | 1.000 |
| $(6.658 \pm 14.875) \times 10^{-5}$ | 20362022 | 3.250×10^{-5} | 1.384×10^{-4} | 4.933×10^{-5} | -2.374×10^{-3} | 5.924×10^{-3} |
| $(9.043 \pm 10.018) \times 10^{-5}$ | 20362022 | 2.500×10^{-6} | 9.049×10^{-5} | 6.406×10^{-5} | 7.176×10^{-13} | 5.428×10^{-3} |
| $(4.103 \pm 4.127) \times 10^{-5}$ | 20362022 | 5.025×10^{-5} | 3.394×10^{-5} | 3.481×10^{-5} | -5.446×10^{-6} | 7.796×10^{-4} |
| $(1.684 \pm 13.601) \times 10^{-5}$ | 20362022 | 1.500×10^{-5} | 1.714×10^{-4} | 1.471×10^{-5} | -3.206×10^{-3} | 1.937×10^{-3} |
| $(1.331 \pm 0.450) \times 10^{-4}$ | 20362022 | 1.125×10^{-4} | 4.484×10^{-5} | 1.224×10^{-4} | 4.625×10^{-5} | 1.525×10^{-3} |
| 1.43 ± 0.62 | 20362022 | 1.23 | 0.635 | 1.28 | 0.100 | 4.12 |
| 0.172 ± 0.127 | 20362022 | 7.500×10^{-2} | 0.188 | 0.131 | 9.181×10^{-3} | 1.60 |
| 1.35 ± 0.52 | 20362022 | 1.23 | 0.268 | 1.24 | 0.541 | 4.08 |
| $(5.862 \pm 7.842) \times 10^{-5}$ | 20362022 | 4.750×10^{-5} | 4.963×10^{-5} | 4.686×10^{-5} | 6.460×10^{-7} | 1.988×10^{-3} |
| $(-8.309 \pm 340.324) \times 10^{-5}$ | 20362022 | -2.000×10^{-4} | 2.114×10^{-3} | -1.407×10^{-4} | -5.782×10^{-2} | 4.486×10^{-2} |
| $(1.561 \pm 6.767) \times 10^{-5}$ | 20362022 | 1.500×10^{-5} | 8.470×10^{-5} | 1.377×10^{-5} | -1.141×10^{-2} | 7.614×10^{-3} |
| $(7.929 \pm 2.687) \times 10^{-4}$ | 20362022 | 6.500×10^{-4} | 2.673×10^{-4} | 7.294×10^{-4} | 2.749×10^{-4} | 9.055×10^{-3} |
| $(8.402 \pm 18.654) \times 10^{-6}$ | 20362022 | 2.500×10^{-6} | 2.370×10^{-5} | 7.440×10^{-6} | -9.959×10^{-5} | 1.293×10^{-4} |

| Variable | 1 % | 5 % | 10 % | 15.9 % | 25 % | 75 % | 84.1 % | 90 % | 95 % | 99 % |
|---|-------------------------|-------------------------|-------------------------|-------------------------|-------------------------|------------------------|------------------------|------------------------|------------------------|------------------------|
| qa value [1] | 9.000×10^{-2} | 0.200 | 0.200 | 0.210 | 0.310 | 1.000 | 1.000 | 1.000 | 1.000 | 1.000 |
| formaldehyde tropospheric vertical column [mol m ⁻²] | -2.246×10^{-4} | -1.161×10^{-4} | -7.287×10^{-5} | -4.385×10^{-5} | -1.325×10^{-5} | 1.252×10^{-4} | 1.706×10^{-4} | 2.168×10^{-4} | 2.923×10^{-4} | 5.491×10^{-4} |
| formaldehyde tropospheric vertical column precision [mol m ⁻²] | 1.126×10^{-6} | 5.639×10^{-6} | 1.132×10^{-5} | 1.808×10^{-5} | 2.900×10^{-5} | 1.195×10^{-4} | 1.557×10^{-4} | 1.938×10^{-4} | 2.562×10^{-4} | 4.510×10^{-4} |
| formaldehyde tropospheric vertical column correction [mol m ⁻²] | 3.353×10^{-7} | 3.365×10^{-6} | 7.782×10^{-6} | 1.253×10^{-5} | 1.856×10^{-5} | 5.251×10^{-5} | 5.806×10^{-5} | 6.582×10^{-5} | 9.072×10^{-5} | 2.191×10^{-4} |
| formaldehyde slant column density window1 [mol m ⁻²] | -3.036×10^{-4} | -2.003×10^{-4} | -1.500×10^{-4} | -1.125×10^{-4} | -7.036×10^{-5} | 1.010×10^{-4} | 1.450×10^{-4} | 1.850×10^{-4} | 2.405×10^{-4} | 3.630×10^{-4} |
| formaldehyde slant column density window1 precision [mol m ⁻²] | 6.823×10^{-5} | 8.354×10^{-5} | 9.191×10^{-5} | 9.798×10^{-5} | 1.050×10^{-4} | 1.498×10^{-4} | 1.671×10^{-4} | 1.848×10^{-4} | 2.146×10^{-4} | 3.072×10^{-4} |
| formaldehyde tropospheric air mass factor [1] | 0.283 | 0.587 | 0.803 | 0.922 | 1.06 | 1.70 | 2.02 | 2.30 | 2.69 | 3.44 |
| formaldehyde tropospheric air mass factor precision [1] | 3.813×10^{-2} | 4.833×10^{-2} | 5.540×10^{-2} | 5.994×10^{-2} | 6.581×10^{-2} | 0.254 | 0.310 | 0.354 | 0.410 | 0.560 |
| formaldehyde clear air mass factor [1] | 0.780 | 0.880 | 0.953 | 1.02 | 1.11 | 1.37 | 1.47 | 1.61 | 2.72 | 3.60 |
| integrated formaldehyde profile a priori [mol m ⁻²] | 1.741×10^{-6} | 3.872×10^{-6} | 6.633×10^{-6} | 1.105×10^{-5} | 1.720×10^{-5} | 6.682×10^{-5} | 8.453×10^{-5} | 1.100×10^{-4} | 1.591×10^{-4} | 3.966×10^{-4} |
| fitted wavelength radiance shift [nm] | -1.061×10^{-2} | -5.309×10^{-3} | -3.316×10^{-3} | -2.144×10^{-3} | -1.157×10^{-3} | 9.575×10^{-4} | 2.011×10^{-3} | 3.237×10^{-3} | 5.295×10^{-3} | 1.075×10^{-2} |
| fitted wavelength radiance squeeze [1] | -1.425×10^{-4} | -9.073×10^{-5} | -6.613×10^{-5} | -4.800×10^{-5} | -2.771×10^{-5} | 5.699×10^{-5} | 7.921×10^{-5} | 9.953×10^{-5} | 1.277×10^{-4} | 1.896×10^{-4} |
| fitted root mean square win1 [1] | 4.066×10^{-4} | 4.973×10^{-4} | 5.471×10^{-4} | 5.834×10^{-4} | 6.254×10^{-4} | 8.927×10^{-4} | 9.961×10^{-4} | 1.102×10^{-3} | 1.280×10^{-3} | 1.832×10^{-3} |
| formaldehyde slant column delta [mol m ⁻²] | -4.002×10^{-5} | -1.868×10^{-5} | -1.212×10^{-5} | -8.059×10^{-6} | -3.392×10^{-6} | 2.031×10^{-5} | 2.656×10^{-5} | 3.160×10^{-5} | 3.776×10^{-5} | 5.227×10^{-5} |

Table 3: Parameterlist and basic statistics for the analysis for observations in the northern hemisphere

| Variable | mean $\pm \sigma$ | Count | IQR | Median | Minimum | Maximum | 25 % percentile | 75 % percentile |
|---|-------------------------------------|----------|------------------------|------------------------|-------------------------|------------------------|-------------------------|------------------------|
| qa value [1] | 0.676 ± 0.348 | 11463426 | 0.700 | 0.900 | 1.000×10^{-2} | 1.000 | 0.300 | 1.000 |
| formaldehyde tropospheric vertical column [mol m ⁻²] | $(8.085 \pm 15.874) \times 10^{-5}$ | 11463426 | 1.442×10^{-4} | 6.010×10^{-5} | -1.193×10^{-3} | 5.384×10^{-3} | -4.267×10^{-6} | 1.400×10^{-4} |
| formaldehyde tropospheric vertical column precision [mol m ⁻²] | $(9.434 \pm 10.686) \times 10^{-5}$ | 11463426 | 9.411×10^{-5} | 6.629×10^{-5} | 7.176×10^{-13} | 4.984×10^{-3} | 2.990×10^{-5} | 1.240×10^{-4} |
| formaldehyde tropospheric vertical column correction [mol m ⁻²] | $(5.133 \pm 4.717) \times 10^{-5}$ | 11463426 | 3.118×10^{-5} | 4.665×10^{-5} | 6.078×10^{-6} | 7.796×10^{-4} | 2.622×10^{-5} | 5.740×10^{-5} |
| formaldehyde slant column density window1 [mol m ⁻²] | $(2.428 \pm 13.584) \times 10^{-5}$ | 11463426 | 1.689×10^{-4} | 2.274×10^{-5} | -1.448×10^{-3} | 1.741×10^{-3} | -6.139×10^{-5} | 1.075×10^{-4} |
| formaldehyde slant column density window1 precision [mol m ⁻²] | $(1.329 \pm 0.474) \times 10^{-4}$ | 11463426 | 4.732×10^{-5} | 1.211×10^{-4} | 4.625×10^{-5} | 1.127×10^{-3} | 1.032×10^{-4} | 1.505×10^{-4} |
| formaldehyde tropospheric air mass factor [1] | 1.40 ± 0.66 | 11463426 | 0.613 | 1.24 | 0.100 | 4.12 | 1.02 | 1.63 |
| formaldehyde tropospheric air mass factor precision [1] | 0.174 ± 0.135 | 11463426 | 0.191 | 0.123 | 9.912×10^{-3} | 1.16 | 6.434×10^{-2} | 0.255 |
| formaldehyde clear air mass factor [1] | 1.36 ± 0.59 | 11463426 | 0.259 | 1.22 | 0.603 | 3.97 | 1.08 | 1.34 |
| integrated formaldehyde profile apriori [mol m ⁻²] | $(6.015 \pm 4.763) \times 10^{-5}$ | 11463426 | 4.408×10^{-5} | 5.411×10^{-5} | 2.284×10^{-6} | 5.069×10^{-4} | 2.875×10^{-5} | 7.284×10^{-5} |
| fitted wavelength radiance shift [nm] | $(1.620 \pm 34.776) \times 10^{-4}$ | 11463426 | 2.100×10^{-3} | 7.766×10^{-5} | -5.782×10^{-2} | 4.486×10^{-2} | -8.657×10^{-4} | 1.234×10^{-3} |
| fitted wavelength radiance squeeze [1] | $(1.669 \pm 6.786) \times 10^{-5}$ | 11463426 | 8.401×10^{-5} | 1.429×10^{-5} | -1.141×10^{-2} | 8.332×10^{-4} | -2.663×10^{-5} | 5.739×10^{-5} |
| fitted root mean square win1 [1] | $(7.916 \pm 2.827) \times 10^{-4}$ | 11463426 | 2.821×10^{-4} | 7.219×10^{-4} | 2.749×10^{-4} | 6.652×10^{-3} | 6.149×10^{-4} | 8.970×10^{-4} |
| formaldehyde slant column delta [mol m ⁻²] | $(3.447 \pm 16.529) \times 10^{-6}$ | 11463426 | 1.954×10^{-5} | 2.848×10^{-6} | -8.642×10^{-5} | 1.100×10^{-4} | -5.971×10^{-6} | 1.356×10^{-5} |

Table 4: Parameterlist and basic statistics for the analysis for observations in the southern hemisphere

| Variable | mean $\pm \sigma$ | Count | IQR | Median | Minimum | Maximum | 25 % percentile | 75 % percentile |
|---|--------------------------------------|---------|------------------------|-------------------------|-------------------------|------------------------|-------------------------|------------------------|
| qa value [1] | 0.688 ± 0.345 | 8898596 | 0.680 | 0.900 | 1.000×10^{-2} | 1.000 | 0.320 | 1.000 |
| formaldehyde tropospheric vertical column [mol m ⁻²] | $(4.820 \pm 13.256) \times 10^{-5}$ | 8898596 | 1.296×10^{-4} | 3.646×10^{-5} | -2.374×10^{-3} | 5.924×10^{-3} | -2.360×10^{-5} | 1.060×10^{-4} |
| formaldehyde tropospheric vertical column precision [mol m ⁻²] | $(8.538 \pm 9.061) \times 10^{-5}$ | 8898596 | 8.594×10^{-5} | 6.136×10^{-5} | 3.765×10^{-12} | 5.428×10^{-3} | 2.791×10^{-5} | 1.139×10^{-4} |
| formaldehyde tropospheric vertical column correction [mol m ⁻²] | $(2.775 \pm 2.680) \times 10^{-5}$ | 8898596 | 3.152×10^{-5} | 2.503×10^{-5} | -5.446×10^{-6} | 6.698×10^{-4} | 9.053×10^{-6} | 4.057×10^{-5} |
| formaldehyde slant column density window1 [mol m ⁻²] | $(7.252 \pm 135.624) \times 10^{-6}$ | 8898596 | 1.732×10^{-4} | 4.048×10^{-6} | -3.206×10^{-3} | 1.937×10^{-3} | -8.122×10^{-5} | 9.197×10^{-5} |
| formaldehyde slant column density window1 precision [mol m ⁻²] | $(1.333 \pm 0.418) \times 10^{-4}$ | 8898596 | 4.169×10^{-5} | 1.238×10^{-4} | 4.825×10^{-5} | 1.525×10^{-3} | 1.073×10^{-4} | 1.490×10^{-4} |
| formaldehyde tropospheric air mass factor [1] | 1.47 ± 0.57 | 8898596 | 0.637 | 1.33 | 0.100 | 4.09 | 1.12 | 1.76 |
| formaldehyde tropospheric air mass factor precision [1] | 0.170 ± 0.117 | 8898596 | 0.184 | 0.141 | 9.181×10^{-3} | 1.60 | 6.756×10^{-2} | 0.252 |
| formaldehyde clear air mass factor [1] | 1.33 ± 0.42 | 8898596 | 0.267 | 1.27 | 0.541 | 4.08 | 1.14 | 1.41 |
| integrated formaldehyde profile apriori [mol m ⁻²] | $(5.664 \pm 10.555) \times 10^{-5}$ | 8898596 | 4.254×10^{-5} | 3.185×10^{-5} | 6.460×10^{-7} | 1.988×10^{-3} | 9.951×10^{-6} | 5.249×10^{-5} |
| fitted wavelength radiance shift [nm] | $(-3.988 \pm 32.780) \times 10^{-4}$ | 8898596 | 1.993×10^{-3} | -4.059×10^{-4} | -3.977×10^{-2} | 3.542×10^{-2} | -1.453×10^{-3} | 5.401×10^{-4} |
| fitted wavelength radiance squeeze [1] | $(1.422 \pm 6.739) \times 10^{-5}$ | 8898596 | 8.561×10^{-5} | 1.309×10^{-5} | -9.236×10^{-3} | 7.614×10^{-3} | -2.914×10^{-5} | 5.647×10^{-5} |
| fitted root mean square win1 [1] | $(7.945 \pm 2.494) \times 10^{-4}$ | 8898596 | 2.484×10^{-4} | 7.375×10^{-4} | 2.857×10^{-4} | 9.055×10^{-3} | 6.393×10^{-4} | 8.877×10^{-4} |
| formaldehyde slant column delta [mol m ⁻²] | $(1.479 \pm 1.929) \times 10^{-5}$ | 8898596 | 2.626×10^{-5} | 1.532×10^{-5} | -9.959×10^{-5} | 1.293×10^{-4} | 1.877×10^{-6} | 2.813×10^{-5} |

Table 5: Parameterlist and basic statistics for the analysis for observations over water

| Variable | mean $\pm \sigma$ | Count | IQR | Median | Minimum | Maximum | 25 % percentile | 75 % percentile |
|---|--------------------------------------|----------|------------------------|-------------------------|-------------------------|------------------------|-------------------------|------------------------|
| qa value [1] | 0.683 ± 0.343 | 14601513 | 0.680 | 0.900 | 1.000×10^{-2} | 1.000 | 0.320 | 1.000 |
| formaldehyde tropospheric vertical column [mol m ⁻²] | $(5.334 \pm 13.306) \times 10^{-5}$ | 14601513 | 1.261×10^{-4} | 4.158×10^{-5} | -2.283×10^{-3} | 5.755×10^{-3} | -1.731×10^{-5} | 1.088×10^{-4} |
| formaldehyde tropospheric vertical column precision [mol m ⁻²] | $(8.142 \pm 8.713) \times 10^{-5}$ | 14601513 | 8.156×10^{-5} | 5.933×10^{-5} | 3.765×10^{-12} | 5.428×10^{-3} | 2.709×10^{-5} | 1.087×10^{-4} |
| formaldehyde tropospheric vertical column correction [mol m ⁻²] | $(3.855 \pm 4.188) \times 10^{-5}$ | 14601513 | 3.439×10^{-5} | 3.201×10^{-5} | -3.222×10^{-6} | 7.796×10^{-4} | 1.594×10^{-5} | 5.033×10^{-5} |
| formaldehyde slant column density window1 [mol m ⁻²] | $(6.356 \pm 128.860) \times 10^{-6}$ | 14601513 | 1.637×10^{-4} | 6.189×10^{-6} | -3.206×10^{-3} | 1.937×10^{-3} | -7.582×10^{-5} | 8.791×10^{-5} |
| formaldehyde slant column density window1 precision [mol m ⁻²] | $(1.306 \pm 0.429) \times 10^{-4}$ | 14601513 | 4.359×10^{-5} | 1.199×10^{-4} | 4.688×10^{-5} | 8.842×10^{-4} | 1.035×10^{-4} | 1.471×10^{-4} |
| formaldehyde tropospheric air mass factor [1] | 1.46 \pm 0.60 | 14601513 | 0.593 | 1.31 | 0.100 | 4.09 | 1.14 | 1.73 |
| formaldehyde tropospheric air mass factor precision [1] | 0.159 \pm 0.107 | 14601513 | 0.165 | 0.122 | 1.199×10^{-2} | 1.06 | 6.722×10^{-2} | 0.232 |
| formaldehyde clear air mass factor [1] | 1.40 \pm 0.49 | 14601513 | 0.221 | 1.28 | 0.574 | 4.08 | 1.19 | 1.41 |
| integrated formaldehyde profile apriori [mol m ⁻²] | $(4.205 \pm 3.142) \times 10^{-5}$ | 14601513 | 4.408×10^{-5} | 4.424×10^{-5} | 6.478×10^{-7} | 9.594×10^{-4} | 1.437×10^{-5} | 5.845×10^{-5} |
| fitted wavelength radiance shift [nm] | $(-1.430 \pm 31.936) \times 10^{-4}$ | 14601513 | 2.096×10^{-3} | -1.718×10^{-4} | -4.138×10^{-2} | 3.997×10^{-2} | -1.220×10^{-3} | 8.762×10^{-4} |
| fitted wavelength radiance squeeze [1] | $(1.553 \pm 6.718) \times 10^{-5}$ | 14601513 | 8.391×10^{-5} | 1.344×10^{-5} | -2.106×10^{-3} | 7.614×10^{-3} | -2.758×10^{-5} | 5.633×10^{-5} |
| fitted root mean square win1 [1] | $(7.781 \pm 2.560) \times 10^{-4}$ | 14601513 | 2.597×10^{-4} | 7.147×10^{-4} | 2.764×10^{-4} | 5.244×10^{-3} | 6.165×10^{-4} | 8.762×10^{-4} |
| formaldehyde slant column delta [mol m ⁻²] | $(9.066 \pm 19.190) \times 10^{-6}$ | 14601513 | 2.530×10^{-5} | 7.832×10^{-6} | -9.550×10^{-5} | 1.293×10^{-4} | -3.375×10^{-6} | 2.193×10^{-5} |

Table 6: Parameterlist and basic statistics for the analysis for observations over land

| Variable | mean $\pm \sigma$ | Count | IQR | Median | Minimum | Maximum | 25 % percentile | 75 % percentile |
|---|--------------------------------------|---------|------------------------|-------------------------|-------------------------|------------------------|-------------------------|------------------------|
| qa value [1] | 0.707 ± 0.349 | 4012903 | 0.680 | 1.000 | 1.000×10^{-2} | 1.000 | 0.320 | 1.000 |
| formaldehyde tropospheric vertical column [mol m ⁻²] | $(1.066 \pm 1.774) \times 10^{-4}$ | 4012903 | 1.760×10^{-4} | 8.439×10^{-5} | -2.374×10^{-3} | 5.924×10^{-3} | 5.556×10^{-6} | 1.815×10^{-4} |
| formaldehyde tropospheric vertical column precision [mol m ⁻²] | $(1.144 \pm 1.235) \times 10^{-4}$ | 4012903 | 1.179×10^{-4} | 8.162×10^{-5} | 9.964×10^{-12} | 5.379×10^{-3} | 3.627×10^{-5} | 1.542×10^{-4} |
| formaldehyde tropospheric vertical column correction [mol m ⁻²] | $(5.083 \pm 3.927) \times 10^{-5}$ | 4012903 | 2.984×10^{-5} | 4.742×10^{-5} | -5.446×10^{-6} | 7.590×10^{-4} | 3.010×10^{-5} | 5.994×10^{-5} |
| formaldehyde slant column density window1 [mol m ⁻²] | $(4.727 \pm 14.485) \times 10^{-5}$ | 4012903 | 1.870×10^{-4} | 4.495×10^{-5} | -2.360×10^{-3} | 1.420×10^{-3} | -4.753×10^{-5} | 1.395×10^{-4} |
| formaldehyde slant column density window1 precision [mol m ⁻²] | $(1.382 \pm 0.509) \times 10^{-4}$ | 4012903 | 4.339×10^{-5} | 1.262×10^{-4} | 4.789×10^{-5} | 1.525×10^{-3} | 1.090×10^{-4} | 1.524×10^{-4} |
| formaldehyde tropospheric air mass factor [1] | 1.29 ± 0.62 | 4012903 | 0.579 | 1.14 | 0.100 | 4.09 | 0.913 | 1.49 |
| formaldehyde tropospheric air mass factor precision [1] | 0.203 ± 0.168 | 4012903 | 0.262 | 0.147 | 9.181×10^{-3} | 1.60 | 5.882×10^{-2} | 0.320 |
| formaldehyde clear air mass factor [1] | 1.15 ± 0.51 | 4012903 | 0.261 | 1.03 | 0.541 | 4.00 | 0.921 | 1.18 |
| integrated formaldehyde profile apriori [mol m ⁻²] | $(1.155 \pm 1.389) \times 10^{-4}$ | 4012903 | 9.970×10^{-5} | 7.143×10^{-5} | 6.732×10^{-7} | 1.988×10^{-3} | 3.809×10^{-5} | 1.378×10^{-4} |
| fitted wavelength radiance shift [nm] | $(2.539 \pm 402.552) \times 10^{-5}$ | 4012903 | 2.046×10^{-3} | -1.272×10^{-4} | -5.782×10^{-2} | 4.486×10^{-2} | -9.637×10^{-4} | 1.082×10^{-3} |
| fitted wavelength radiance squeeze [1] | $(1.353 \pm 6.748) \times 10^{-5}$ | 4012903 | 8.541×10^{-5} | 1.267×10^{-5} | -1.141×10^{-2} | 4.645×10^{-3} | -2.949×10^{-5} | 5.592×10^{-5} |
| fitted root mean square win1 [1] | $(8.234 \pm 3.034) \times 10^{-4}$ | 4012903 | 2.585×10^{-4} | 7.522×10^{-4} | 2.877×10^{-4} | 9.055×10^{-3} | 6.494×10^{-4} | 9.079×10^{-4} |
| formaldehyde slant column delta [mol m ⁻²] | $(5.147 \pm 17.140) \times 10^{-6}$ | 4012903 | 2.024×10^{-5} | 4.482×10^{-6} | -9.293×10^{-5} | 1.290×10^{-4} | -4.707×10^{-6} | 1.553×10^{-5} |

| HCHO slant column correction | | | | | | | | | | | | | | | | |
|-------------------------------|---------------------------|---------------------------|---------------------------|---------------------------|--------------------------|---------------------------|---------------------------|---------------------------|---------------------------|---------------------------|---------------------------|---------------------------|---------------------------|---------------------------|---------------------------|---------------------------|
| DOAS fit RMS (first interval) | | | | | | | | | | | | | | | | |
| DOAS fit wavelength squeeze | | | | | | | | | | | | | | | | |
| HCHO slant column corrected | | | | | | | | | | | | | | | | |
| 1.000 | -1.183 × 10 ⁻² | -1.284 × 10 ⁻² | 1.073 × 10 ⁻² | 3.761 × 10 ⁻² | 6.567 × 10 ⁻² | 3.433 × 10 ⁻³ | 7.520 × 10 ⁻³ | -5.391 × 10 ⁻² | -5.151 × 10 ⁻² | -2.201 × 10 ⁻² | 1.907 × 10 ⁻² | 6.323 × 10 ⁻³ | -8.144 × 10 ⁻³ | 6.867 × 10 ⁻³ | -1.169 × 10 ⁻² | -0.110 |
| -1.183 × 10 ⁻² | 1.000 | 4.382 × 10 ⁻² | -0.232 | -7.282 × 10 ⁻² | -0.506 | -0.158 | 0.270 | 0.363 | 0.254 | 0.402 | -0.426 | -2.878 × 10 ⁻² | 0.151 | 0.268 | -9.450 × 10 ⁻² | 0.465 |
| -1.284 × 10 ⁻² | 4.382 × 10 ⁻² | 1.000 | 7.025 × 10 ⁻² | 2.463 × 10 ⁻² | 0.167 | 5.580 × 10 ⁻² | 5.195 × 10 ⁻² | 3.962 × 10 ⁻² | 7.449 × 10 ⁻² | 0.112 | 2.303 × 10 ⁻² | 9.297 × 10 ⁻² | 6.341 × 10 ⁻² | 5.178 × 10 ⁻² | 2.633 × 10 ⁻² | -0.216 |
| 1.073 × 10 ⁻² | -0.232 | 7.025 × 10 ⁻² | 1.000 | 0.492 | 0.495 | 0.779 | -5.217 × 10 ⁻² | -0.273 | -0.162 | -0.120 | 0.294 | 0.191 | -1.245 × 10 ⁻² | -5.157 × 10 ⁻² | 0.773 | -8.018 × 10 ⁻² |
| 3.761 × 10 ⁻² | -7.282 × 10 ⁻² | 2.463 × 10 ⁻² | 0.492 | 1.000 | 0.433 | 0.212 | 9.011 × 10 ⁻² | -0.368 | -0.204 | -0.154 | 0.213 | 5.487 × 10 ⁻² | -3.143 × 10 ⁻² | 9.014 × 10 ⁻² | 0.208 | -4.065 × 10 ⁻² |
| 6.567 × 10 ⁻² | -0.506 | 0.167 | 0.495 | 0.433 | 1.000 | 0.116 | -0.181 | -0.545 | -0.341 | -0.210 | 0.277 | 3.940 × 10 ⁻² | -0.110 | -0.180 | 7.306 × 10 ⁻² | -0.315 |
| 3.433 × 10 ⁻³ | -0.158 | 5.580 × 10 ⁻² | 0.779 | 0.212 | 0.116 | 1.000 | -8.376 × 10 ⁻⁵ | -6.381 × 10 ⁻² | -3.843 × 10 ⁻² | -6.591 × 10 ⁻² | 0.258 | 0.216 | 4.670 × 10 ⁻² | 3.915 × 10 ⁻⁴ | 0.991 | -0.118 |
| 7.520 × 10 ⁻³ | 0.270 | 5.195 × 10 ⁻² | -5.217 × 10 ⁻² | 9.011 × 10 ⁻² | -0.181 | -8.376 × 10 ⁻⁵ | 1.000 | 0.134 | 2.873 × 10 ⁻² | 0.158 | -6.442 × 10 ⁻² | 2.801 × 10 ⁻² | 9.986 × 10 ⁻² | 1.000 | 1.273 × 10 ⁻² | 9.282 × 10 ⁻² |
| -5.391 × 10 ⁻² | 0.363 | 3.962 × 10 ⁻² | -0.273 | -0.368 | -0.545 | -6.381 × 10 ⁻² | 0.134 | 1.000 | 0.532 | 0.628 | -0.215 | -4.733 × 10 ⁻³ | 0.100 | 0.134 | -4.883 × 10 ⁻² | 0.112 |
| -5.151 × 10 ⁻² | 0.254 | 7.449 × 10 ⁻² | -0.162 | -0.204 | -0.341 | -3.843 × 10 ⁻² | 2.873 × 10 ⁻² | 0.532 | 1.000 | 8.408 × 10 ⁻² | -5.044 × 10 ⁻² | 1.189 × 10 ⁻² | 4.255 × 10 ⁻² | 2.849 × 10 ⁻² | -2.085 × 10 ⁻² | 0.129 |
| -2.201 × 10 ⁻² | 0.402 | 0.112 | -0.120 | -0.154 | -0.210 | -6.591 × 10 ⁻² | 0.158 | 0.628 | 8.408 × 10 ⁻² | 1.000 | -0.265 | 1.610 × 10 ⁻³ | 7.823 × 10 ⁻² | 0.159 | -5.757 × 10 ⁻² | 6.361 × 10 ⁻² |
| 1.907 × 10 ⁻² | -0.426 | 2.303 × 10 ⁻² | 0.294 | 0.213 | 0.277 | 0.258 | -6.442 × 10 ⁻² | -0.215 | -5.044 × 10 ⁻² | -0.265 | 1.000 | 1.487 × 10 ⁻² | -6.457 × 10 ⁻² | -6.462 × 10 ⁻² | 0.226 | -0.246 |
| 6.323 × 10 ⁻³ | -2.878 × 10 ⁻² | 9.297 × 10 ⁻² | 0.191 | 5.487 × 10 ⁻² | 3.940 × 10 ⁻² | 0.216 | 2.801 × 10 ⁻² | -4.733 × 10 ⁻³ | 1.189 × 10 ⁻² | 1.610 × 10 ⁻³ | 1.487 × 10 ⁻² | 1.000 | 0.151 | 2.809 × 10 ⁻² | 0.213 | -3.300 × 10 ⁻² |
| -8.144 × 10 ⁻³ | 0.151 | 6.341 × 10 ⁻² | -1.245 × 10 ⁻² | -3.143 × 10 ⁻² | -0.110 | 4.670 × 10 ⁻² | 9.986 × 10 ⁻² | 0.100 | 4.255 × 10 ⁻² | 7.823 × 10 ⁻² | -6.457 × 10 ⁻² | 0.151 | 1.000 | 9.972 × 10 ⁻² | 5.683 × 10 ⁻² | 7.109 × 10 ⁻² |
| 6.867 × 10 ⁻³ | 0.268 | 5.178 × 10 ⁻² | -5.157 × 10 ⁻² | 9.014 × 10 ⁻² | -0.180 | 3.915 × 10 ⁻⁴ | 1.000 | 0.134 | 2.849 × 10 ⁻² | 0.159 | -6.462 × 10 ⁻² | 2.809 × 10 ⁻² | 9.972 × 10 ⁻² | 1.000 | 1.325 × 10 ⁻² | 9.307 × 10 ⁻² |
| -1.169 × 10 ⁻² | -9.450 × 10 ⁻² | 2.633 × 10 ⁻² | 0.773 | 0.208 | 7.306 × 10 ⁻² | 0.991 | 1.273 × 10 ⁻² | -4.883 × 10 ⁻² | -2.085 × 10 ⁻² | -5.757 × 10 ⁻² | 0.226 | 0.213 | 5.683 × 10 ⁻² | 1.325 × 10 ⁻² | 1.000 | 1.920 × 10 ⁻² |
| -0.110 | 0.465 | -0.216 | -8.018 × 10 ⁻² | -4.065 × 10 ⁻² | -0.315 | -0.118 | 9.282 × 10 ⁻² | 0.112 | 0.129 | 6.361 × 10 ⁻² | -0.246 | -3.300 × 10 ⁻² | 7.109 × 10 ⁻² | 9.307 × 10 ⁻² | 1.920 × 10 ⁻² | 1.000 |

Table 8: Covariance matrix

| HCHO slant column correction | | | | | | | | | | | | DOAS fit RMS (first interval) | | | | |
|----------------------------------|-------------------------|--------------------------------|--------------------------|--------------------------|--------------------------|--------------------------|--------------------------|-------------------------|-------------------------|-------------------------|--------------------------|-------------------------------|--------------------------|-------------------------|-------------------------|--------------------------|
| HCHO slant column corrected | | | | | | | | | | | | | | | | |
| Integrated a priori HCHO profile | | | | | | | | | | | | DOAS fit wavelength squeeze | | | | |
| Airmass factor total | Airmass factor clear | Airmass factor total precision | Airmass factor clear | Airmass factor total | Airmass factor clear | Airmass factor total | Airmass factor clear | Airmass factor total | Airmass factor clear | Airmass factor total | Airmass factor clear | Airmass factor total | Airmass factor clear | Airmass factor total | | |
| 380 | -3.72 | -10.0 | 3.111×10^{-5} | 7.345×10^{-5} | 5.283×10^{-5} | 9.102×10^{-6} | 6.600×10^{-6} | -0.654 | -0.128 | -0.225 | 2.916×10^{-5} | 4.195×10^{-4} | -1.074×10^{-5} | 3.596×10^{-5} | -3.078×10^{-5} | -3.989×10^{-5} |
| -3.72 | 261 | 28.4 | -5.577×10^{-4} | -1.178×10^{-4} | -3.370×10^{-4} | -3.463×10^{-4} | 1.962×10^{-4} | 3.65 | 0.522 | 3.41 | -5.400×10^{-4} | -1.582×10^{-3} | 1.645×10^{-4} | 1.163×10^{-3} | -2.061×10^{-4} | 1.402×10^{-4} |
| -10.0 | 28.4 | 1.607×10^3 | 4.189×10^{-4} | 9.893×10^{-5} | 2.757×10^{-4} | 3.043×10^{-4} | 9.378×10^{-5} | 0.988 | 0.381 | 2.35 | 7.239×10^{-5} | 1.268×10^{-2} | 1.720×10^{-4} | 5.577×10^{-4} | -1.617×10^{-4} | 1.426×10^{-4} |
| 3.111×10^{-5} | -5.577×10^{-4} | 4.189×10^{-4} | 2.213×10^{-8} | 7.336×10^{-9} | 3.038×10^{-9} | 1.575×10^{-8} | -3.495×10^{-10} | -2.522×10^{-5} | -3.067×10^{-6} | -9.350×10^{-6} | 3.425×10^{-9} | 9.679×10^{-8} | -1.254×10^{-10} | -2.061×10^{-9} | 1.553×10^{-8} | -2.225×10^{-10} |
| 7.345×10^{-5} | -1.178×10^{-4} | 9.893×10^{-5} | 7.336×10^{-9} | 1.004×10^{-8} | 1.789×10^{-9} | 2.893×10^{-9} | 4.065×10^{-10} | -2.293×10^{-5} | -2.599×10^{-6} | -8.113×10^{-6} | 1.670×10^{-9} | 1.871×10^{-8} | -2.131×10^{-10} | 2.426×10^{-9} | 2.817×10^{-9} | -7.596×10^{-11} |
| 5.283×10^{-5} | -3.370×10^{-4} | 2.757×10^{-4} | 3.038×10^{-9} | 1.789×10^{-9} | 1.703×10^{-9} | 6.495×10^{-10} | -3.357×10^{-10} | -1.399×10^{-5} | -1.791×10^{-6} | -4.553×10^{-6} | 8.963×10^{-10} | 5.534×10^{-9} | -3.066×10^{-10} | -1.998×10^{-9} | 4.073×10^{-10} | -2.422×10^{-10} |
| 9.102×10^{-6} | -3.463×10^{-4} | 3.043×10^{-4} | 1.575×10^{-8} | 2.893×10^{-9} | 6.495×10^{-10} | 1.850×10^{-8} | -5.130×10^{-13} | -5.397×10^{-6} | -6.661×10^{-7} | -4.705×10^{-6} | 2.750×10^{-9} | 1.001×10^{-7} | 4.298×10^{-10} | 1.431×10^{-11} | 1.820×10^{-8} | -2.996×10^{-10} |
| 6.600×10^{-6} | 1.962×10^{-4} | 9.378×10^{-5} | -3.495×10^{-10} | 4.065×10^{-10} | -3.357×10^{-10} | -5.130×10^{-13} | 2.028×10^{-9} | 3.749×10^{-6} | 1.649×10^{-7} | 3.726×10^{-6} | -2.275×10^{-10} | 4.293×10^{-9} | 3.043×10^{-10} | 1.209×10^{-8} | 7.745×10^{-11} | 7.797×10^{-11} |
| -0.654 | 365 | 0.988 | -2.522×10^{-5} | -2.293×10^{-5} | -1.399×10^{-5} | -5.397×10^{-6} | 3.749×10^{-6} | 0.387 | 0.205 | -0.1048 | -1.002×10^{-5} | 4.226×10^{-6} | 2.246×10^{-5} | -4.102×10^{-6} | 1.295×10^{-6} | 1.295×10^{-6} |
| -0.128 | 0.522 | 0.381 | -3.067×10^{-6} | -2.599×10^{-6} | -1.791×10^{-6} | -6.661×10^{-7} | 1.649×10^{-7} | 4.220×10^{-2} | 1.624×10^{-2} | 5.624×10^{-3} | -5.041×10^{-7} | 5.157×10^{-6} | 3.669×10^{-7} | 9.756×10^{-7} | -3.590×10^{-7} | 3.071×10^{-7} |
| -0.225 | 3.41 | 2.35 | -9.350×10^{-6} | -8.113×10^{-6} | -4.553×10^{-6} | -4.705×10^{-6} | 3.726×10^{-6} | 0.205 | 0.275 | -1.091×10^{-5} | 2.876×10^{-6} | 2.778×10^{-6} | 2.236×10^{-5} | -4.082×10^{-6} | 6.227×10^{-7} | |
| 2.916×10^{-5} | -5.400×10^{-4} | 7.239×10^{-5} | 3.425×10^{-9} | 1.670×10^{-9} | 8.963×10^{-10} | 2.750×10^{-9} | -2.275×10^{-10} | -1.048×10^{-5} | -5.041×10^{-7} | -1.091×10^{-5} | 6.149×10^{-9} | 3.969×10^{-9} | -3.426×10^{-10} | -1.361×10^{-9} | 2.390×10^{-9} | -3.599×10^{-10} |
| 4.195×10^{-4} | -1.582×10^{-3} | 1.268×10^{-2} | 9.679×10^{-8} | 1.871×10^{-8} | 5.534×10^{-9} | 1.001×10^{-7} | 4.293×10^{-9} | -1.002×10^{-5} | 5.157×10^{-6} | 2.876×10^{-6} | 3.969×10^{-9} | 1.158×10^{-8} | 3.470×10^{-8} | 2.568×10^{-8} | 9.803×10^{-8} | -2.095×10^{-9} |
| -1.074×10^{-5} | 1.645×10^{-4} | 1.720×10^{-4} | -1.254×10^{-10} | -2.131×10^{-10} | -3.066×10^{-10} | 4.298×10^{-10} | 3.043×10^{-8} | 4.226×10^{-6} | 3.669×10^{-7} | 2.778×10^{-6} | -3.426×10^{-10} | 3.479×10^{-9} | 1.813×10^{-9} | 5.195×10^{-10} | 8.973×10^{-11} | 8.973×10^{-10} |
| 3.596×10^{-5} | 1.163×10^{-3} | 5.577×10^{-4} | -2.061×10^{-9} | 2.426×10^{-9} | -1.998×10^{-9} | 1.431×10^{-11} | 1.209×10^{-8} | 2.246×10^{-5} | 9.756×10^{-7} | 2.236×10^{-5} | -1.361×10^{-9} | 2.568×10^{-8} | 1.813×10^{-9} | 7.218×10^{-8} | 4.808×10^{-10} | 4.664×10^{-10} |
| -3.989×10^{-5} | -2.061×10^{-4} | 1.426×10^{-4} | 1.553×10^{-8} | 2.817×10^{-9} | 4.073×10^{-10} | 1.820×10^{-8} | 7.745×10^{-11} | -4.102×10^{-6} | -3.590×10^{-7} | -4.082×10^{-6} | 2.390×10^{-9} | 5.195×10^{-10} | 4.808×10^{-10} | 1.825×10^{-8} | 4.837×10^{-11} | |
| -3.989×10^{-5} | 1.402×10^{-4} | -1.617×10^{-4} | -2.225×10^{-10} | -7.596×10^{-11} | -2.422×10^{-10} | -2.996×10^{-10} | 7.797×10^{-11} | 1.295×10^{-6} | 3.071×10^{-7} | 6.227×10^{-7} | -3.599×10^{-10} | -2.095×10^{-9} | 8.973×10^{-11} | 4.664×10^{-10} | 4.837×10^{-11} | 3.480×10^{-10} |

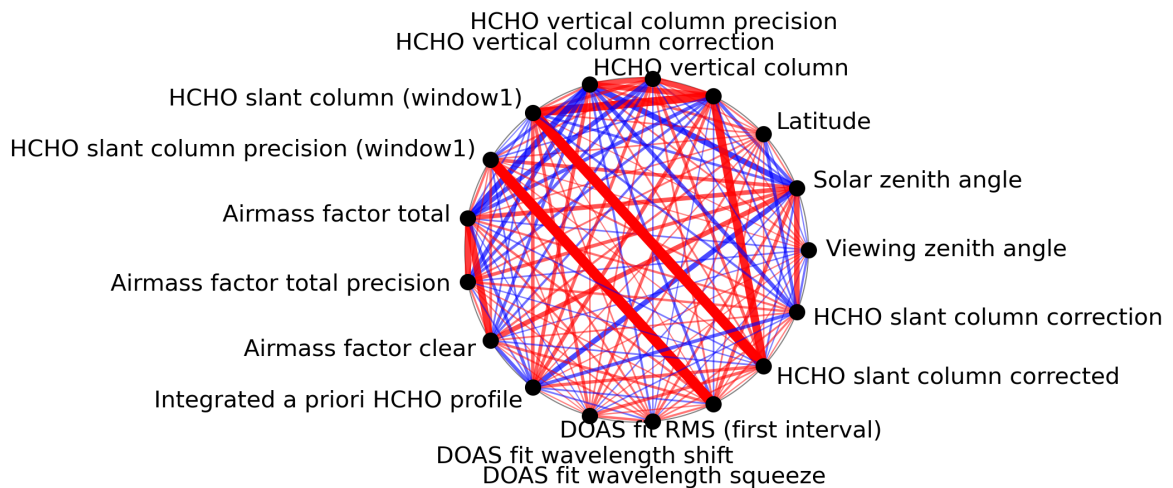


Figure 1: Map of correlation graph for 2023-09-11 to 2023-09-13.

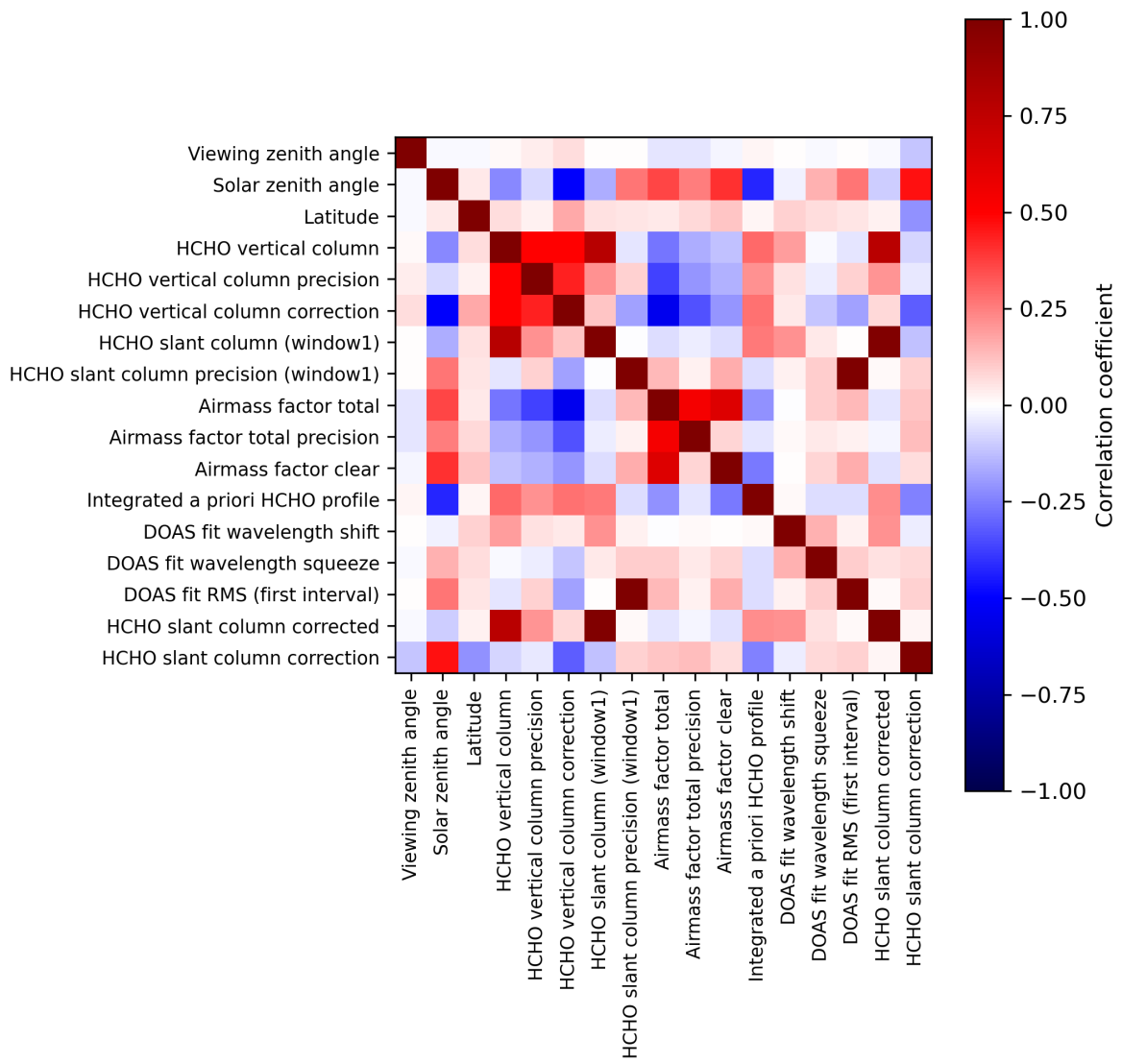


Figure 2: Map of correlation matrix for 2023-09-11 to 2023-09-13.

3 Granule outlines

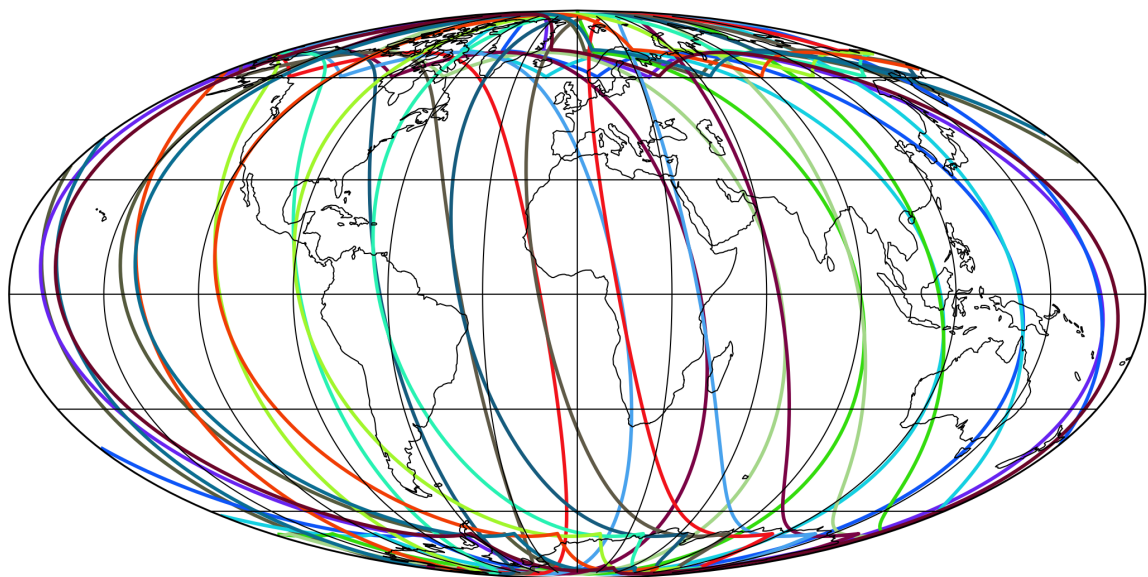


Figure 3: Outline of the granules.

4 Input data monitoring

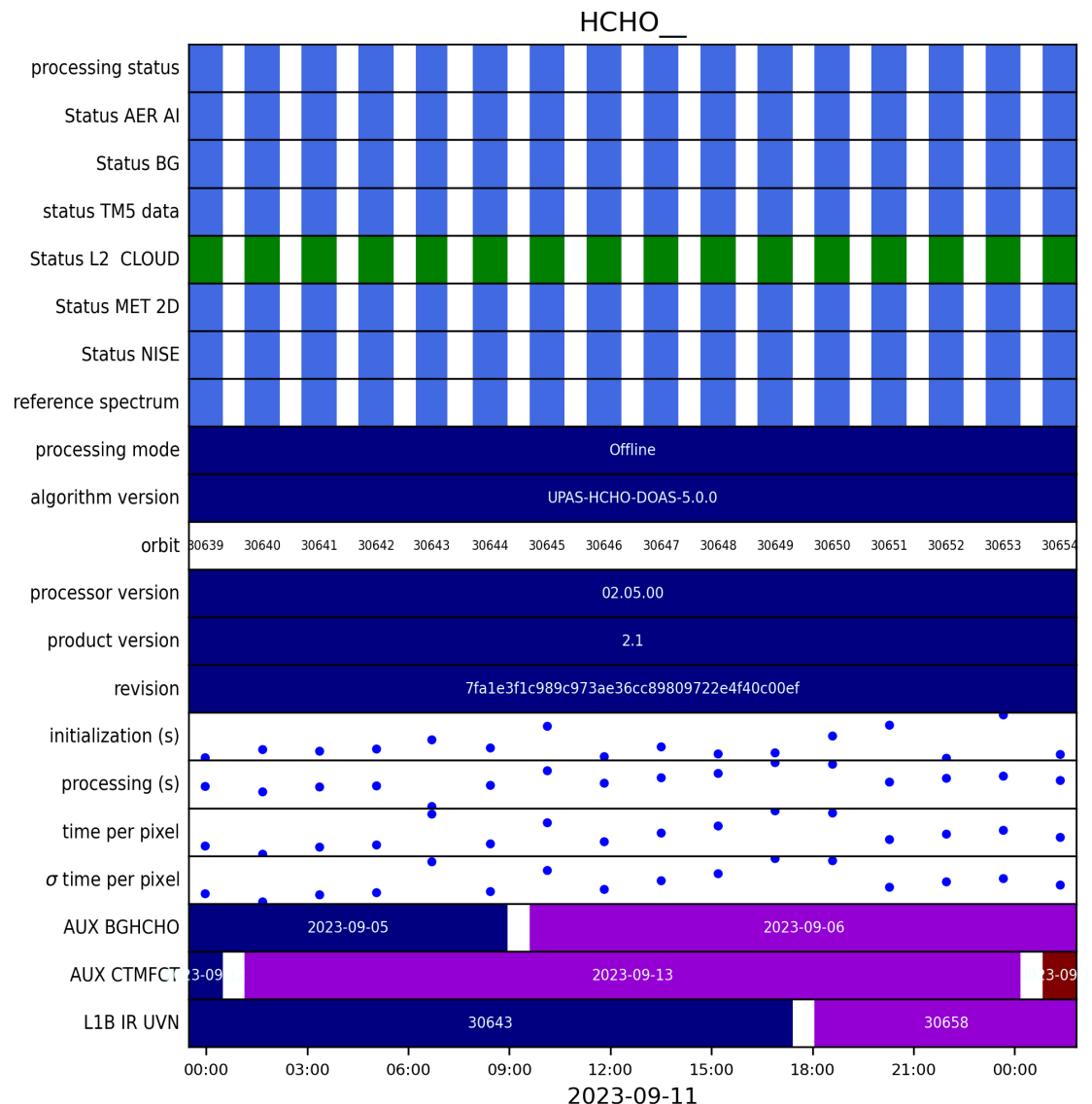


Figure 4: Input data per granule

5 Warnings and errors

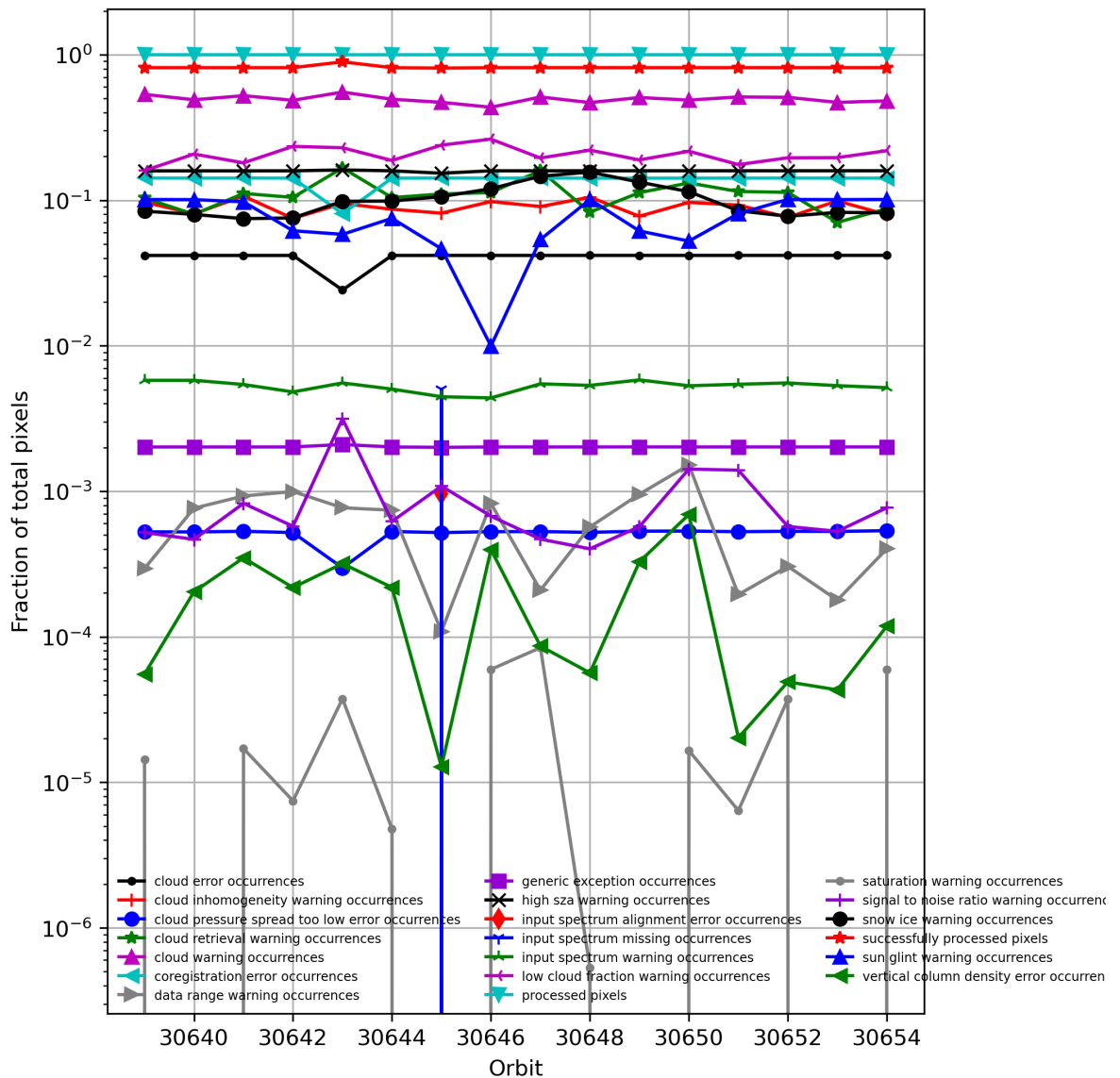


Figure 5: Fraction of pixels with specific warnings and errors during processing

6 World maps

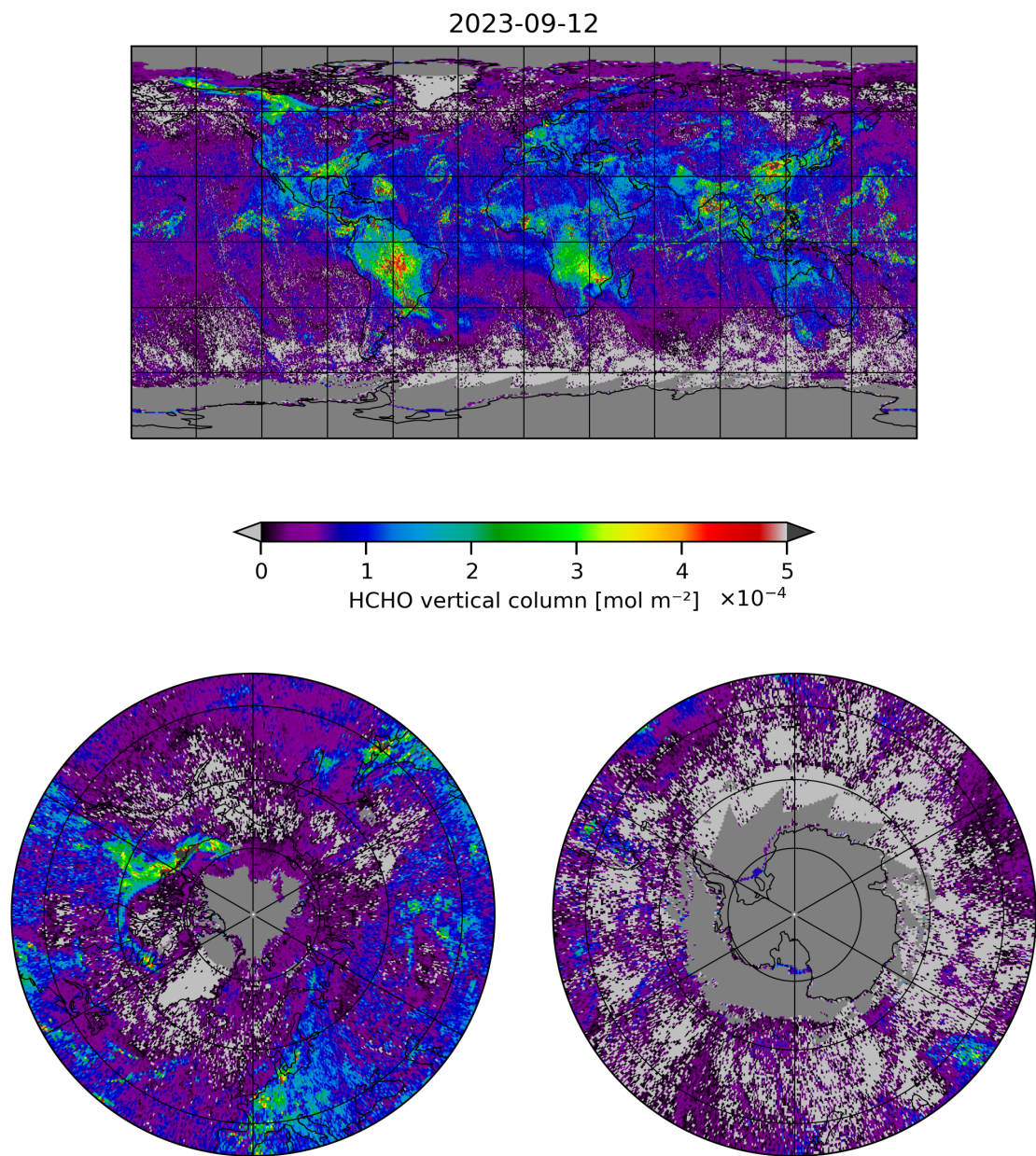


Figure 6: Map of “HCHO vertical column” for 2023-09-11 to 2023-09-13

2023-09-12

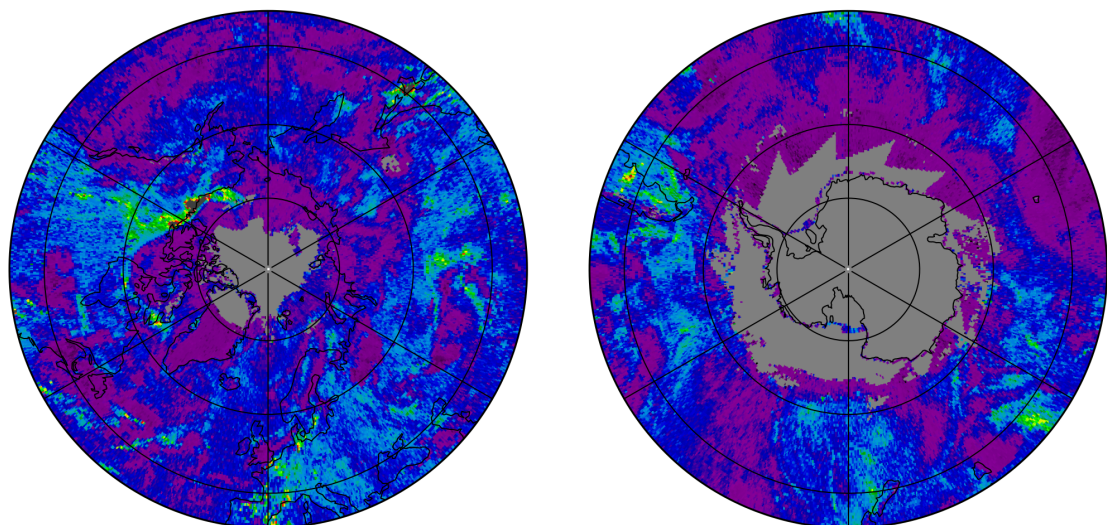
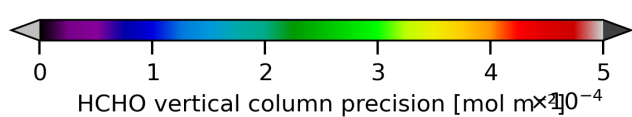
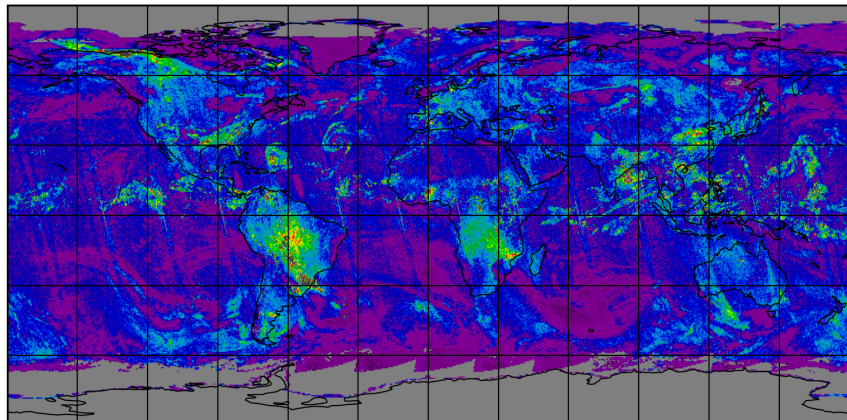


Figure 7: Map of “HCHO vertical column precision” for 2023-09-11 to 2023-09-13

2023-09-12

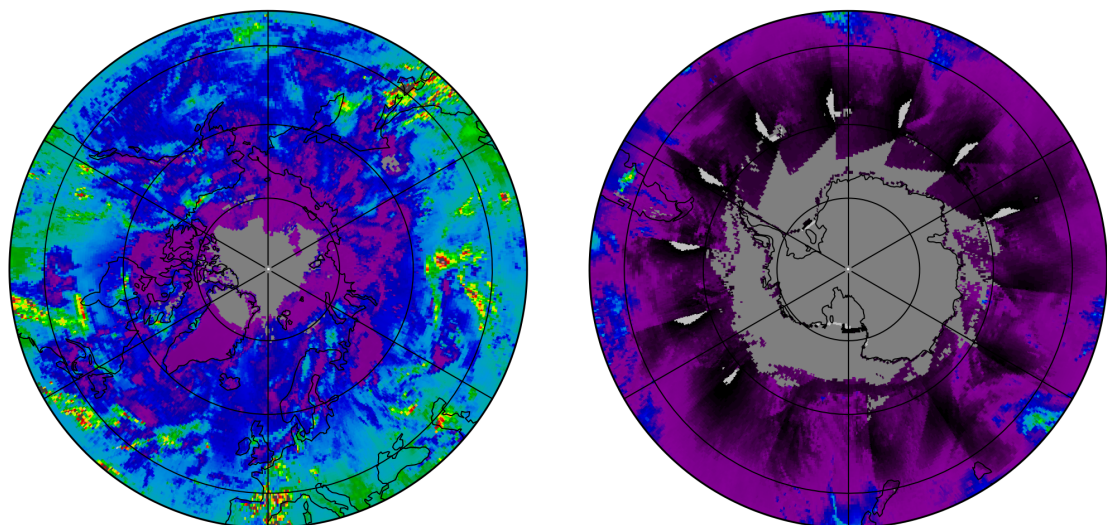
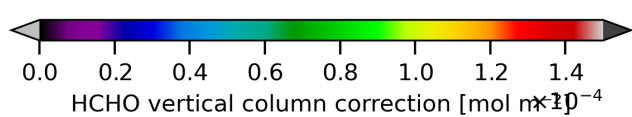
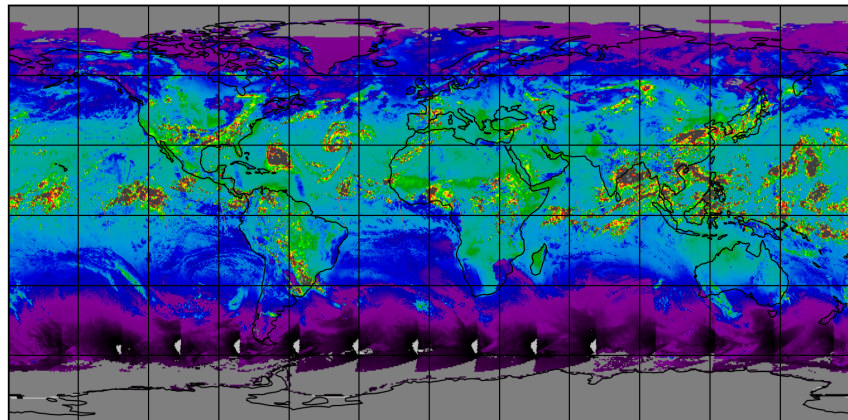


Figure 8: Map of “HCHO vertical column correction” for 2023-09-11 to 2023-09-13

2023-09-12

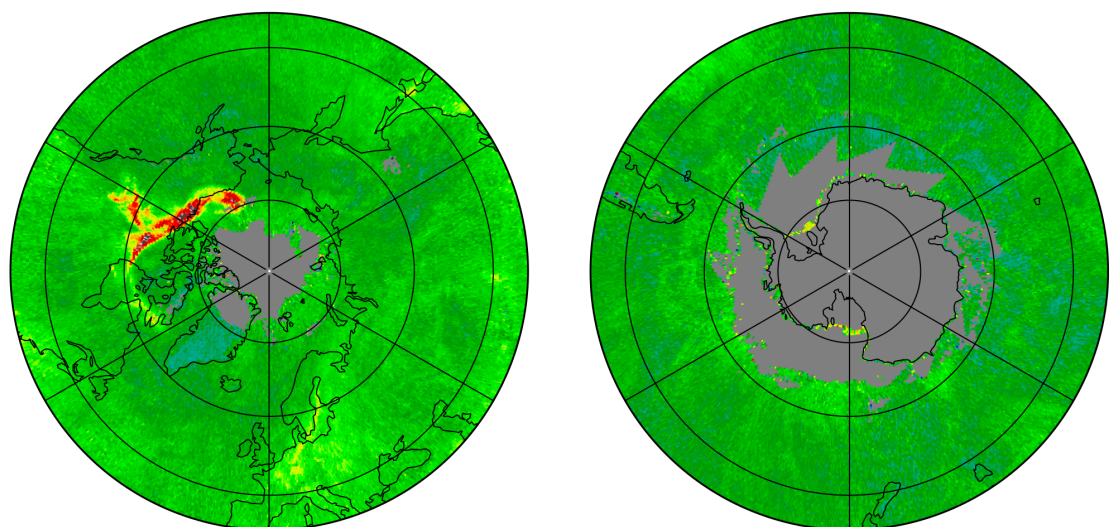
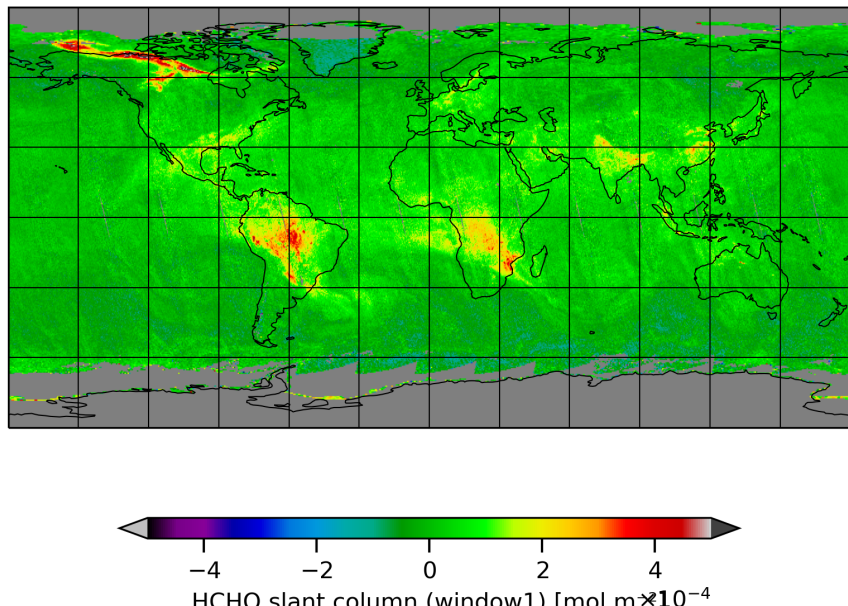


Figure 9: Map of “HCHO slant column (window1)” for 2023-09-11 to 2023-09-13

2023-09-12

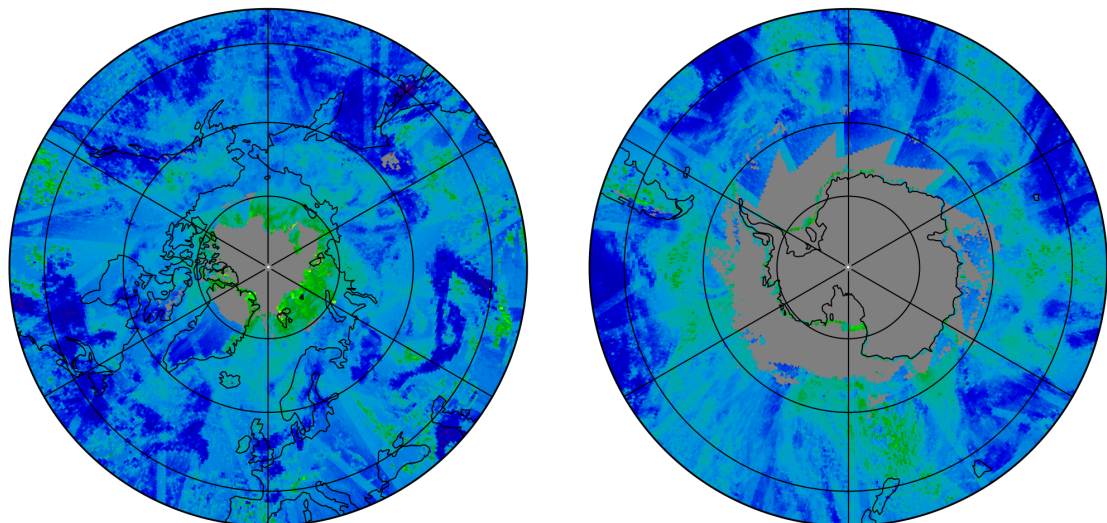
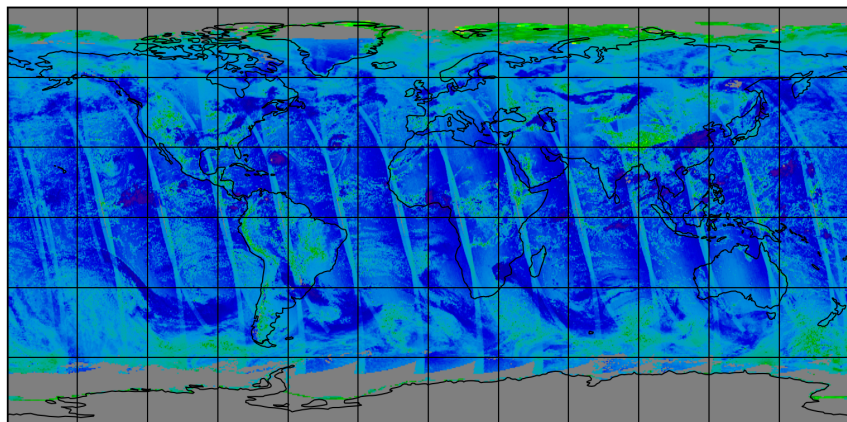


Figure 10: Map of “HCHO slant column precision (window1)” for 2023-09-11 to 2023-09-13

2023-09-12

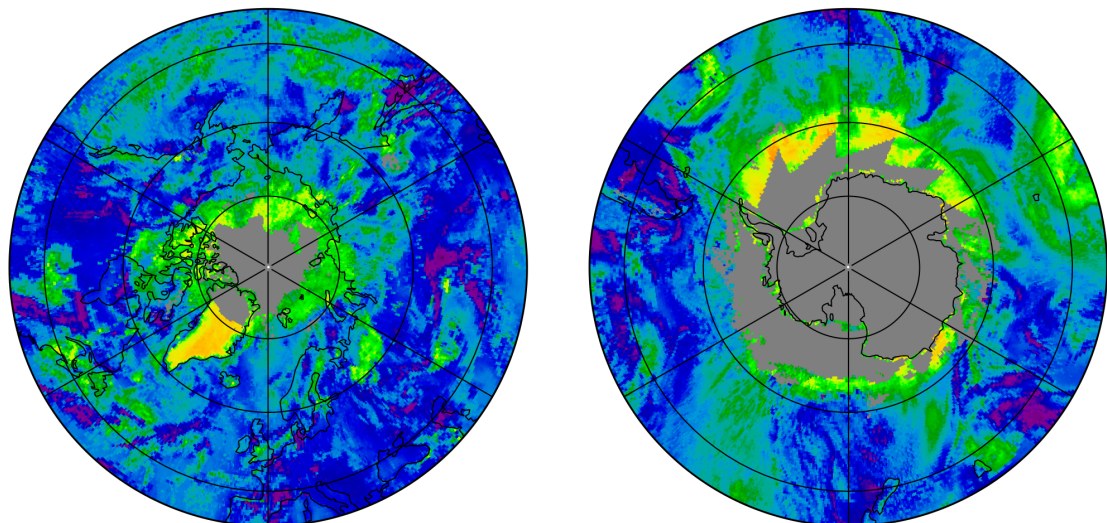
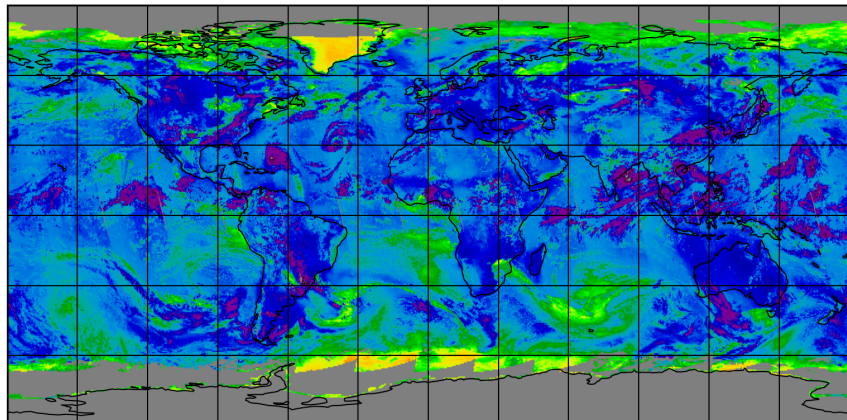


Figure 11: Map of “Airmass factor total” for 2023-09-11 to 2023-09-13

2023-09-12

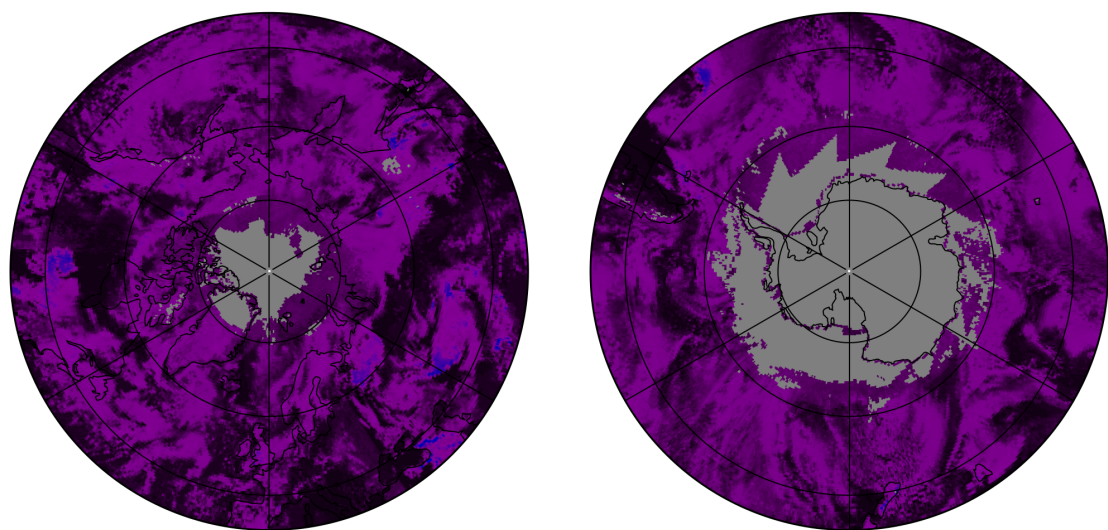
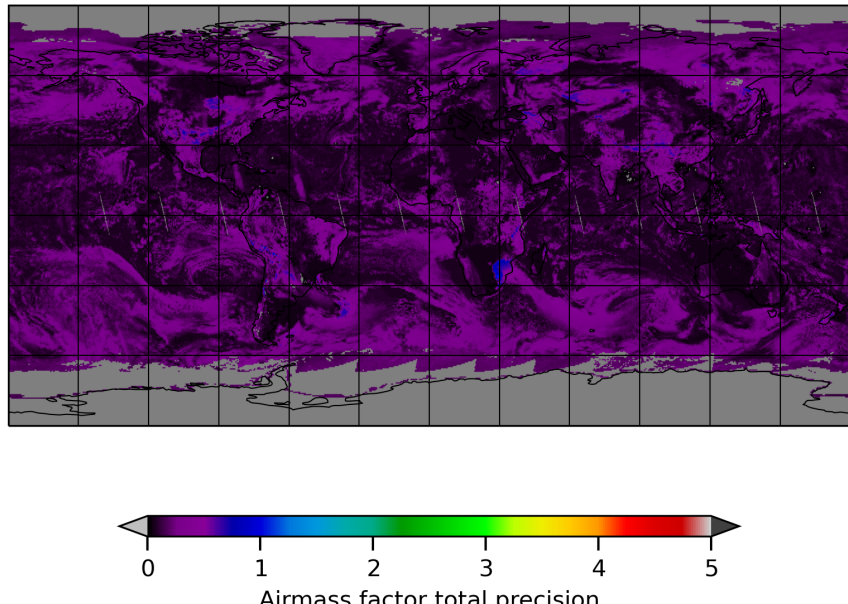


Figure 12: Map of “Airmass factor total precision” for 2023-09-11 to 2023-09-13

2023-09-12

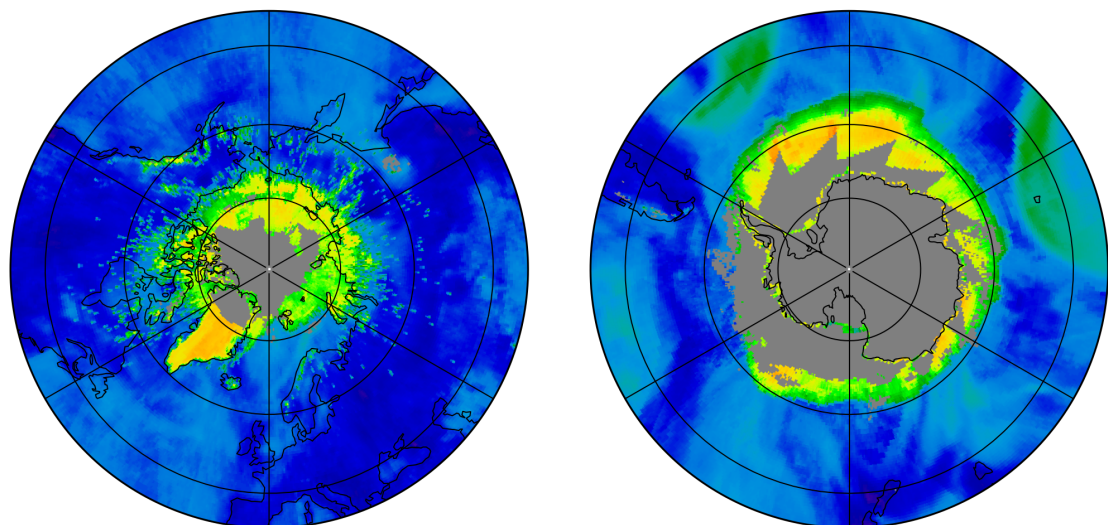
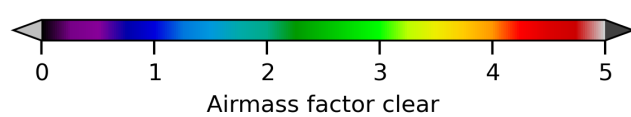
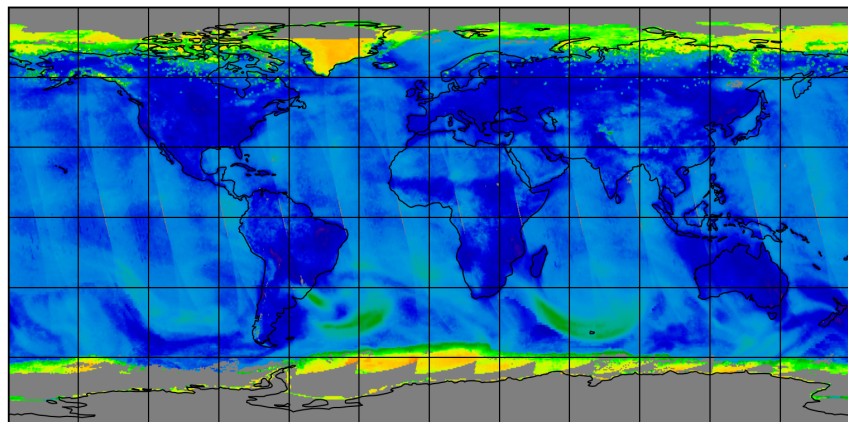


Figure 13: Map of “Airmass factor clear” for 2023-09-11 to 2023-09-13

2023-09-12

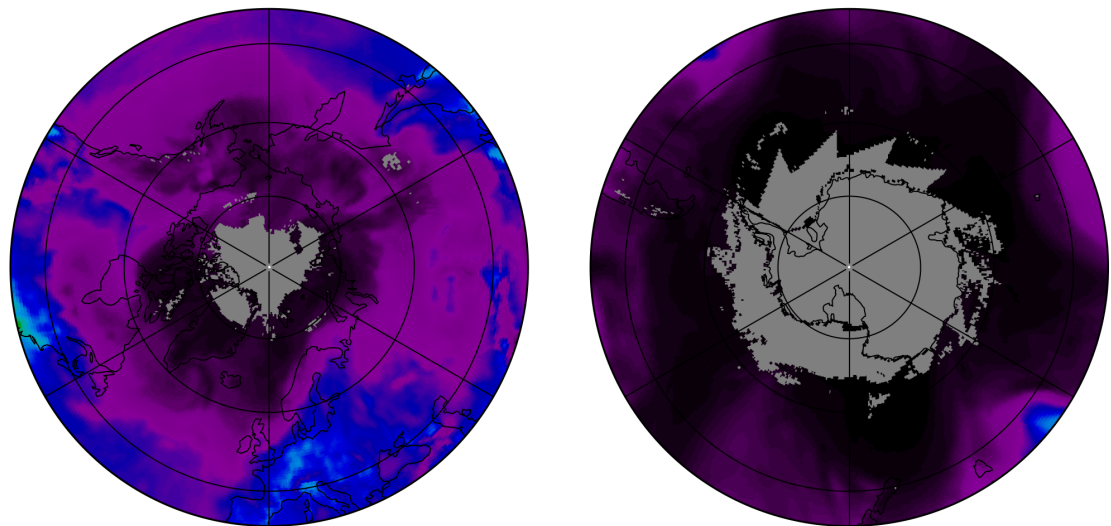
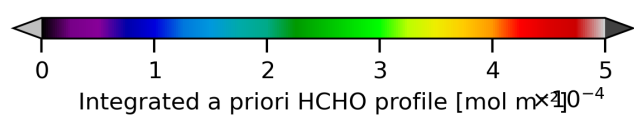
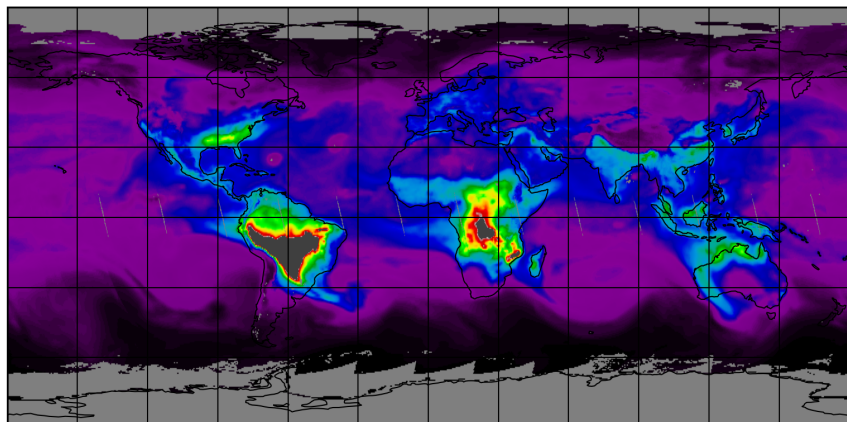


Figure 14: Map of “Integrated a priori HCHO profile” for 2023-09-11 to 2023-09-13

2023-09-12

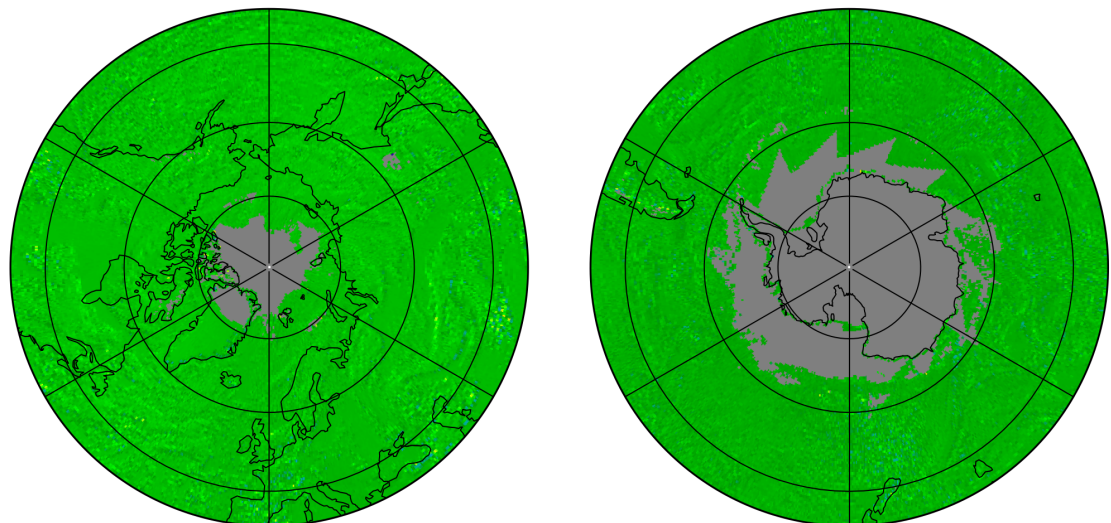
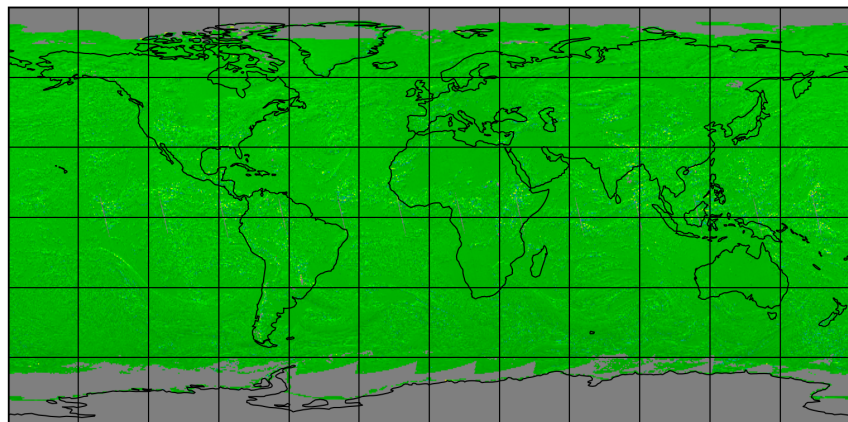


Figure 15: Map of “DOAS fit wavelength shift” for 2023-09-11 to 2023-09-13

2023-09-12

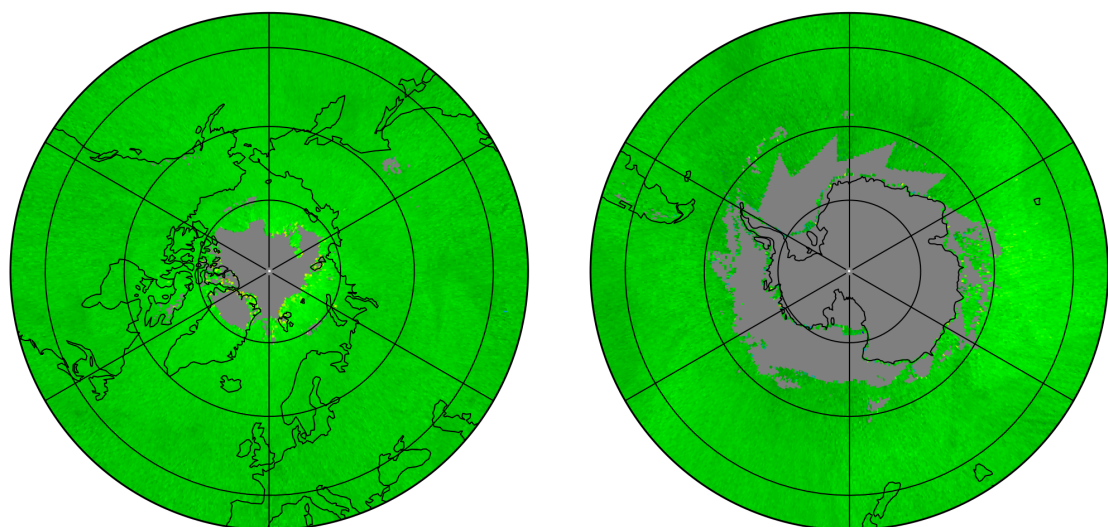
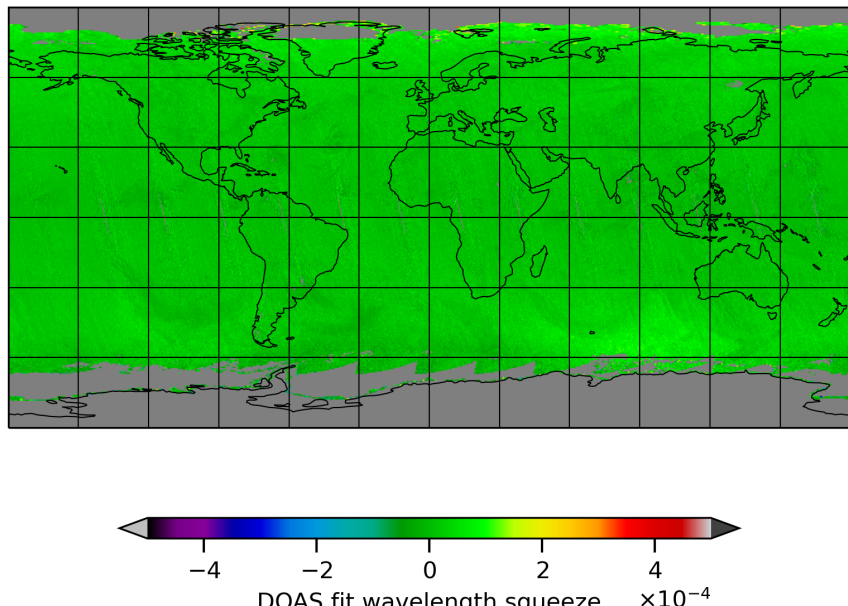


Figure 16: Map of “DOAS fit wavelength squeeze” for 2023-09-11 to 2023-09-13

2023-09-12

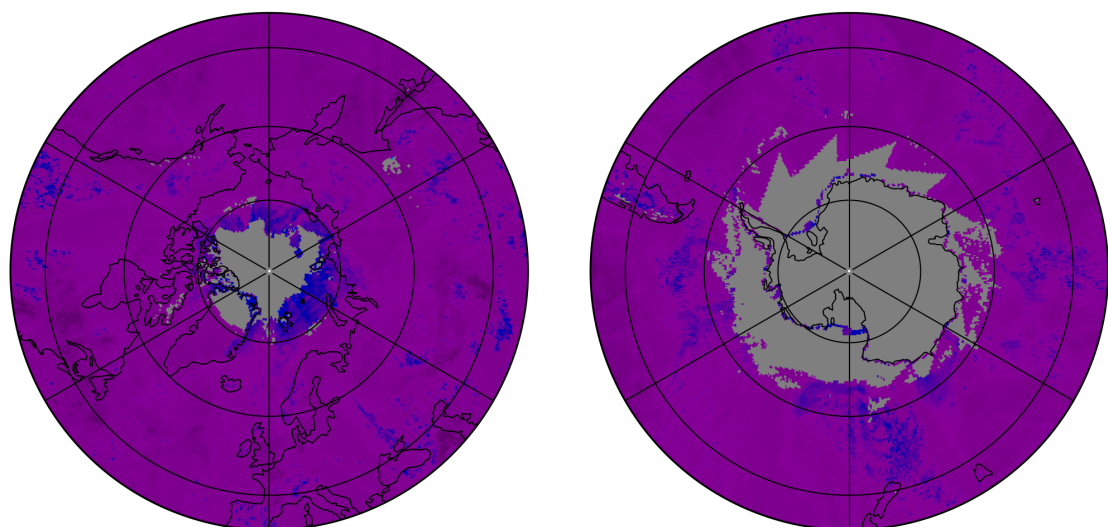
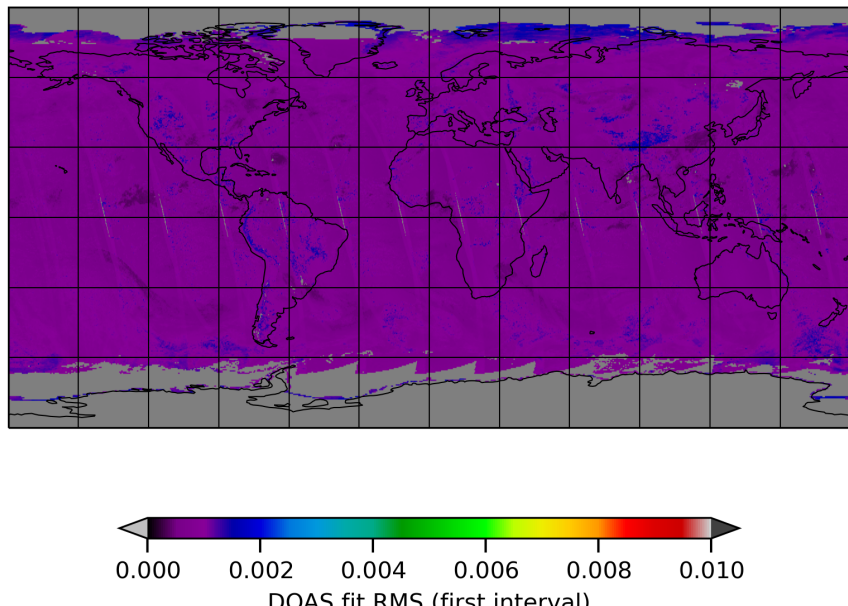


Figure 17: Map of “DOAS fit RMS (first interval)” for 2023-09-11 to 2023-09-13

2023-09-12

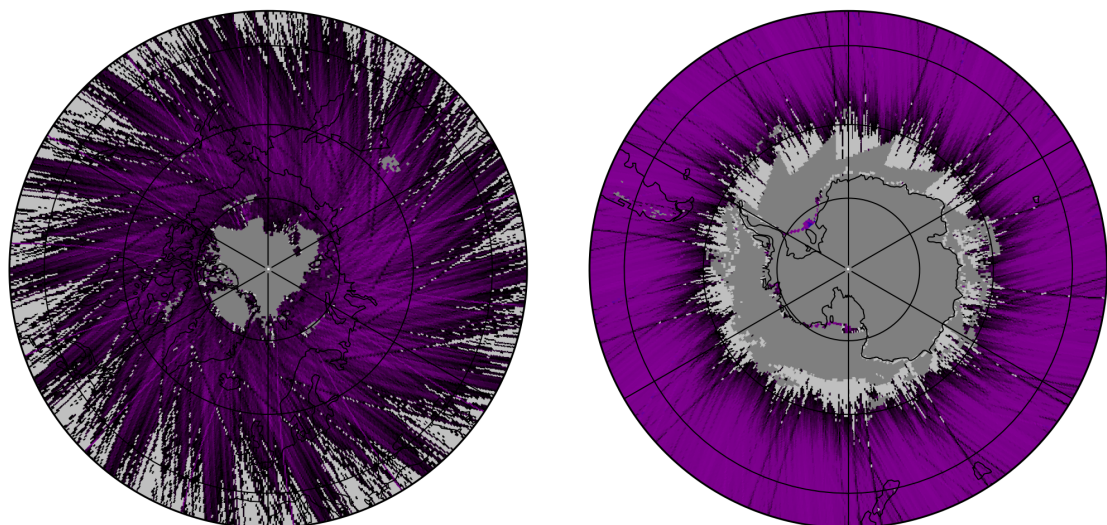
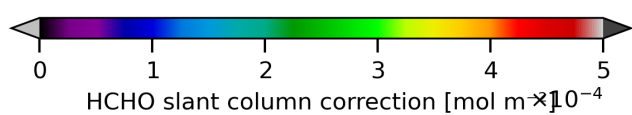
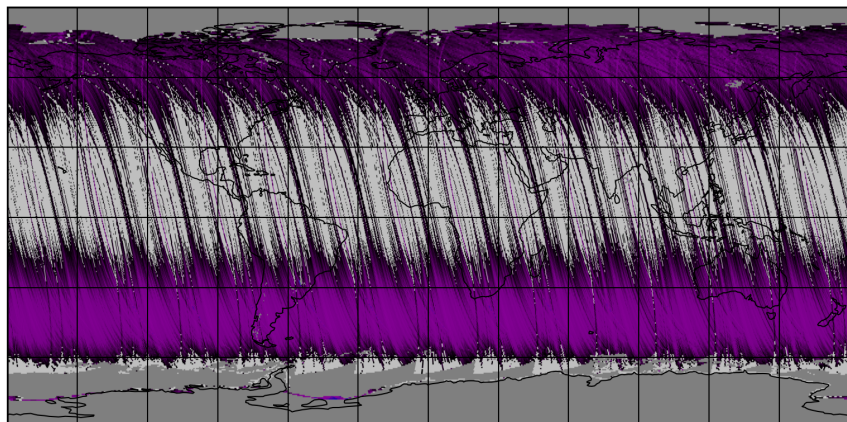


Figure 18: Map of “HCHO slant column correction” for 2023-09-11 to 2023-09-13

2023-09-12

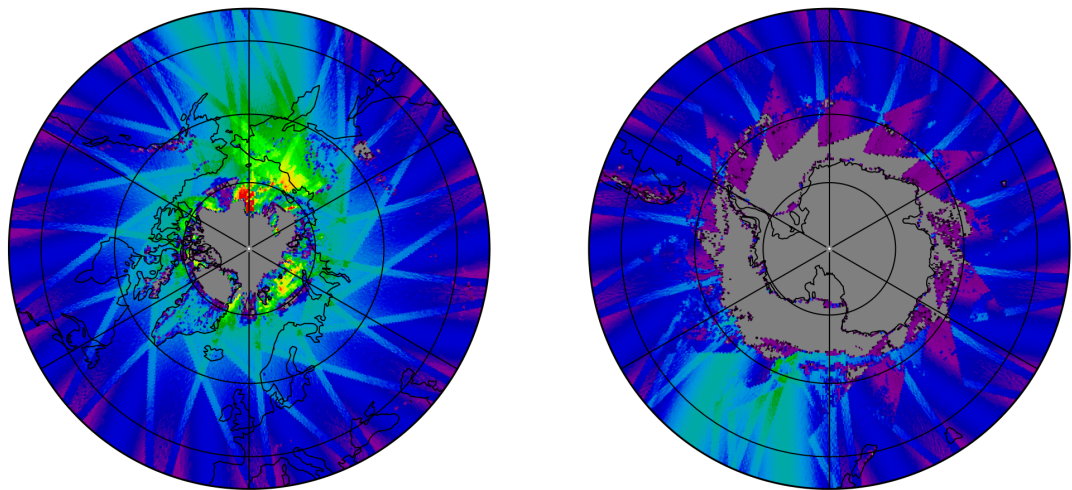
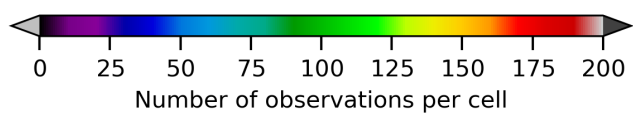
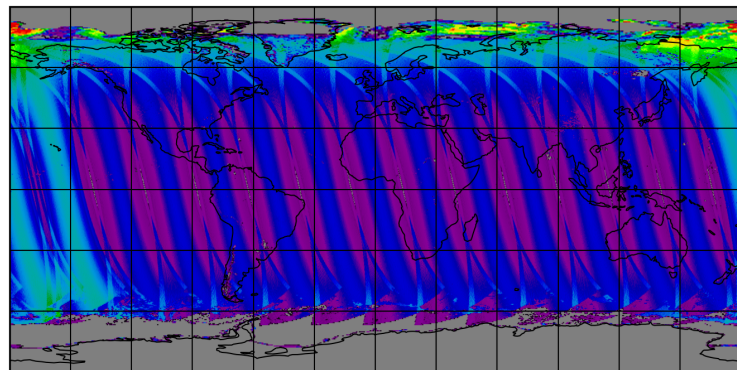


Figure 19: Map of the number of observations for 2023-09-11 to 2023-09-13

7 Zonal average

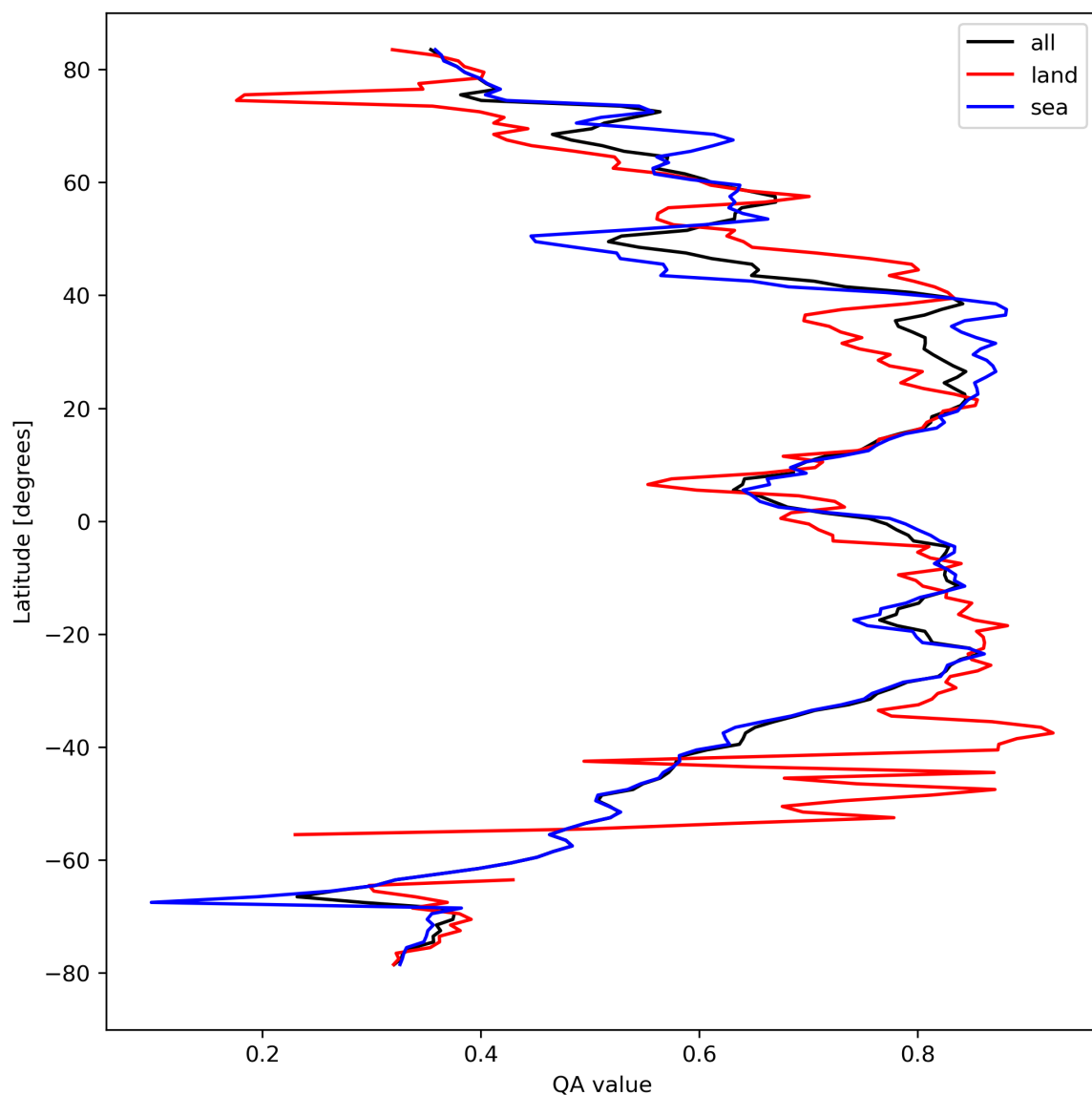


Figure 20: Zonal average of “QA value” for 2023-09-11 to 2023-09-13.

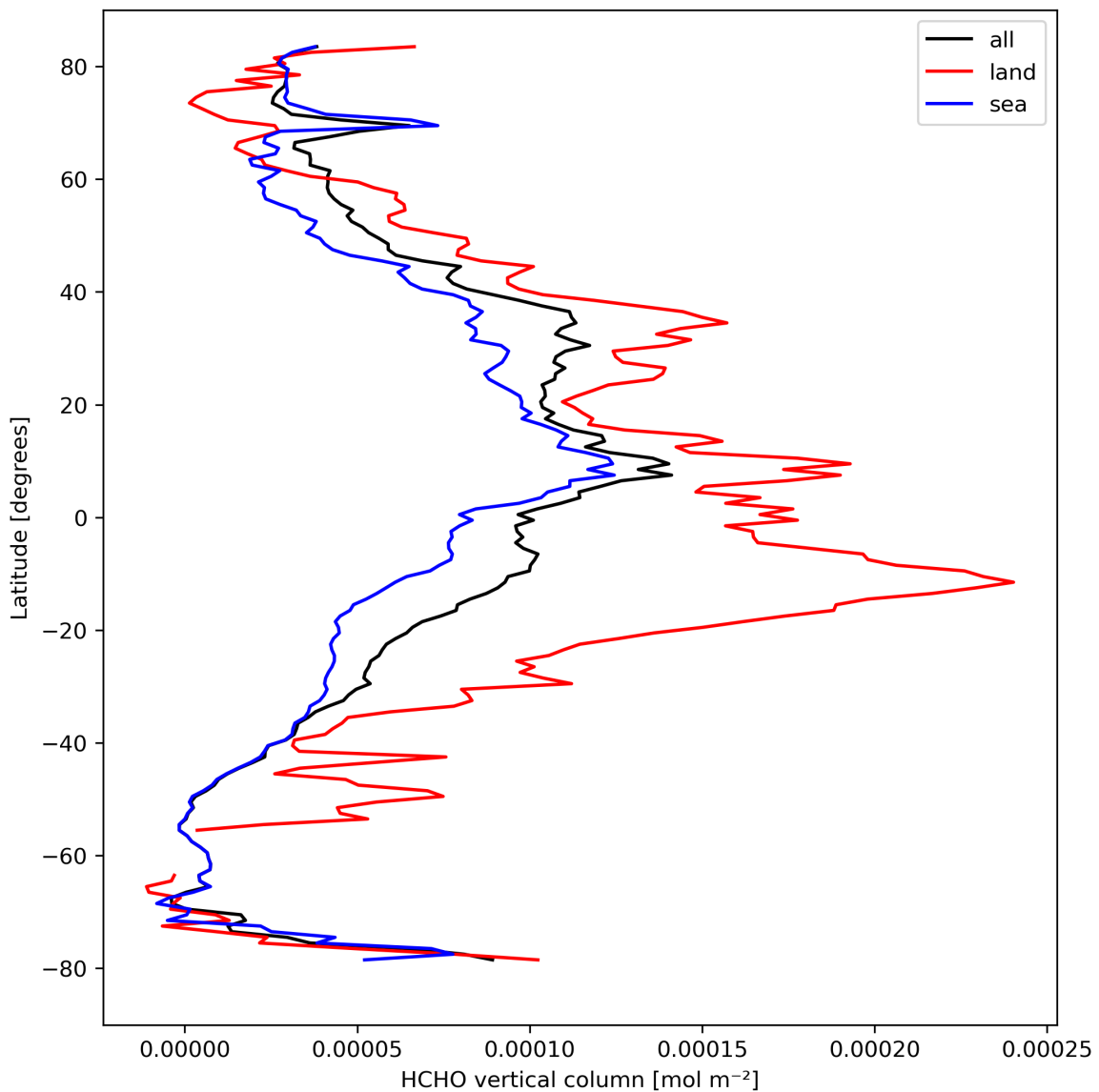


Figure 21: Zonal average of “HCHO vertical column” for 2023-09-11 to 2023-09-13.

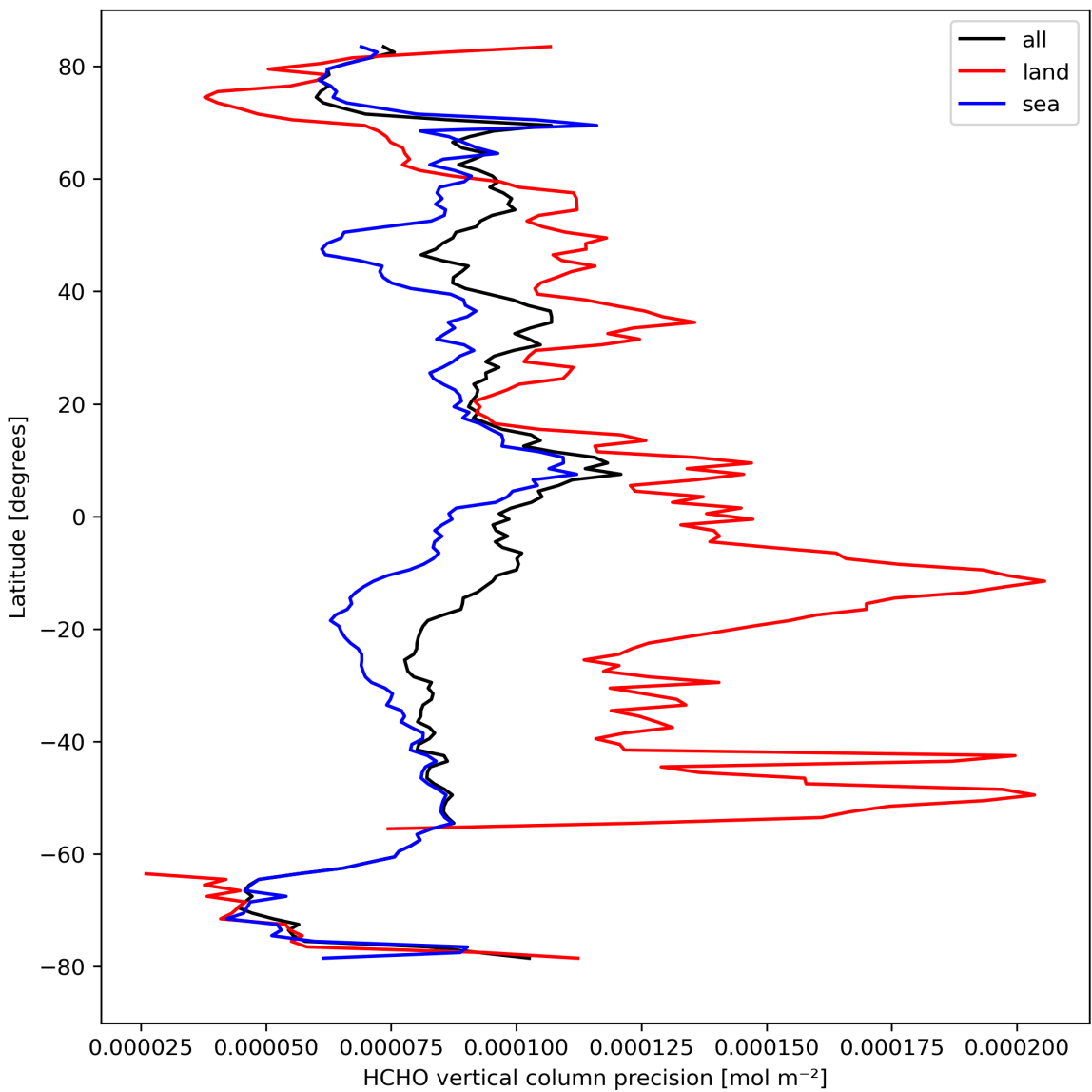


Figure 22: Zonal average of “HCHO vertical column precision” for 2023-09-11 to 2023-09-13.

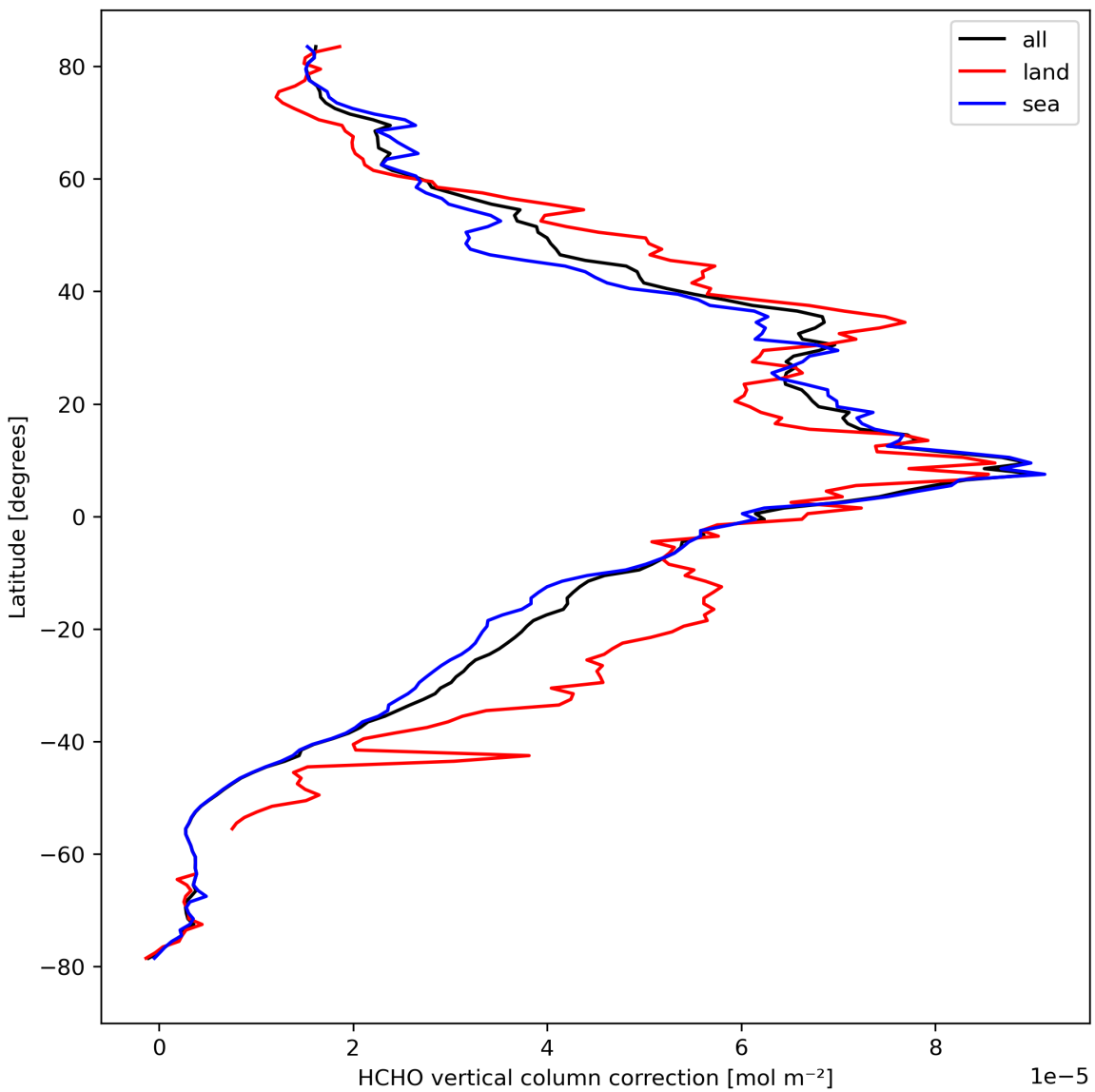


Figure 23: Zonal average of “HCHO vertical column correction” for 2023-09-11 to 2023-09-13.

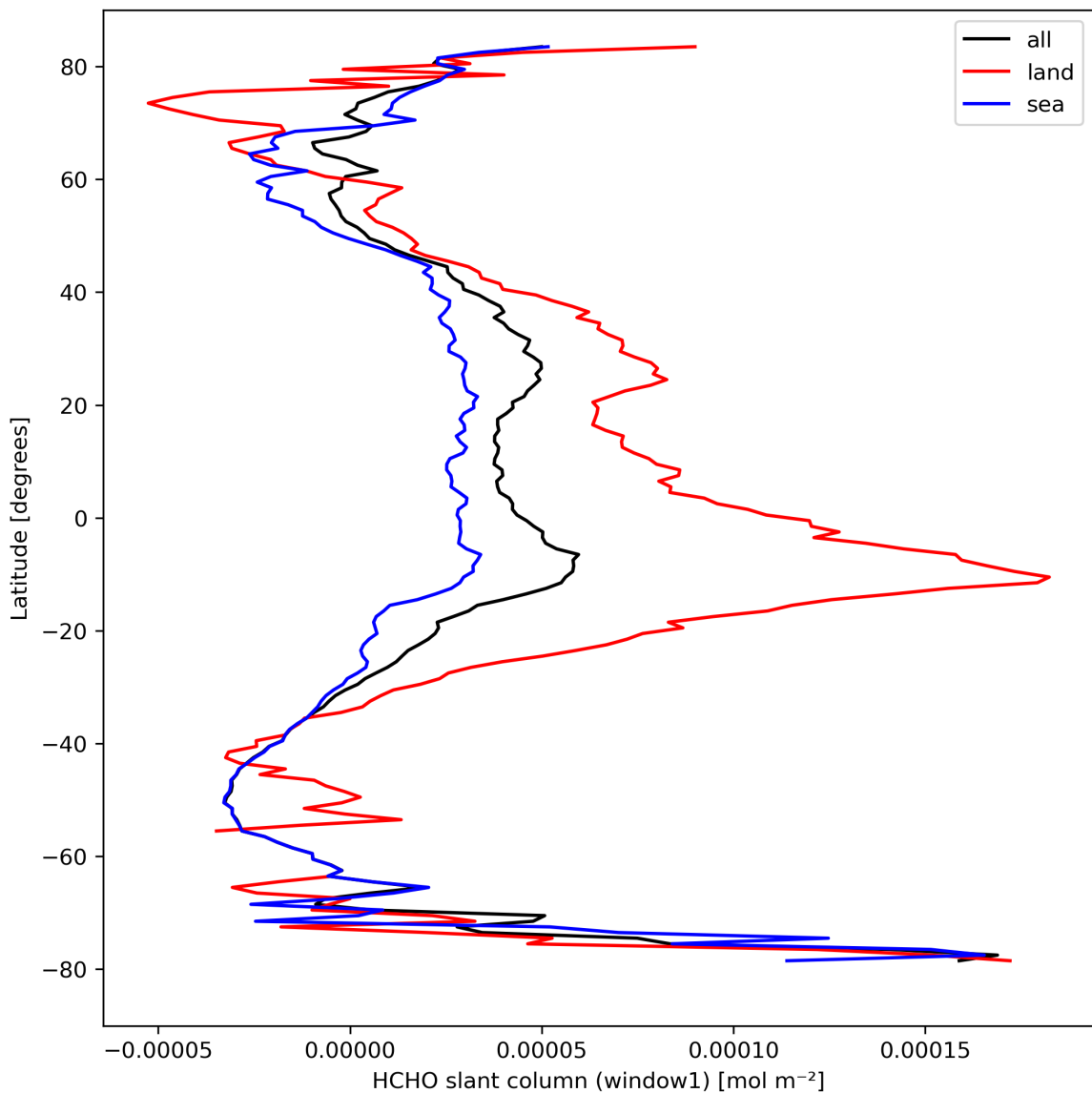


Figure 24: Zonal average of “HCHO slant column (window1)” for 2023-09-11 to 2023-09-13.

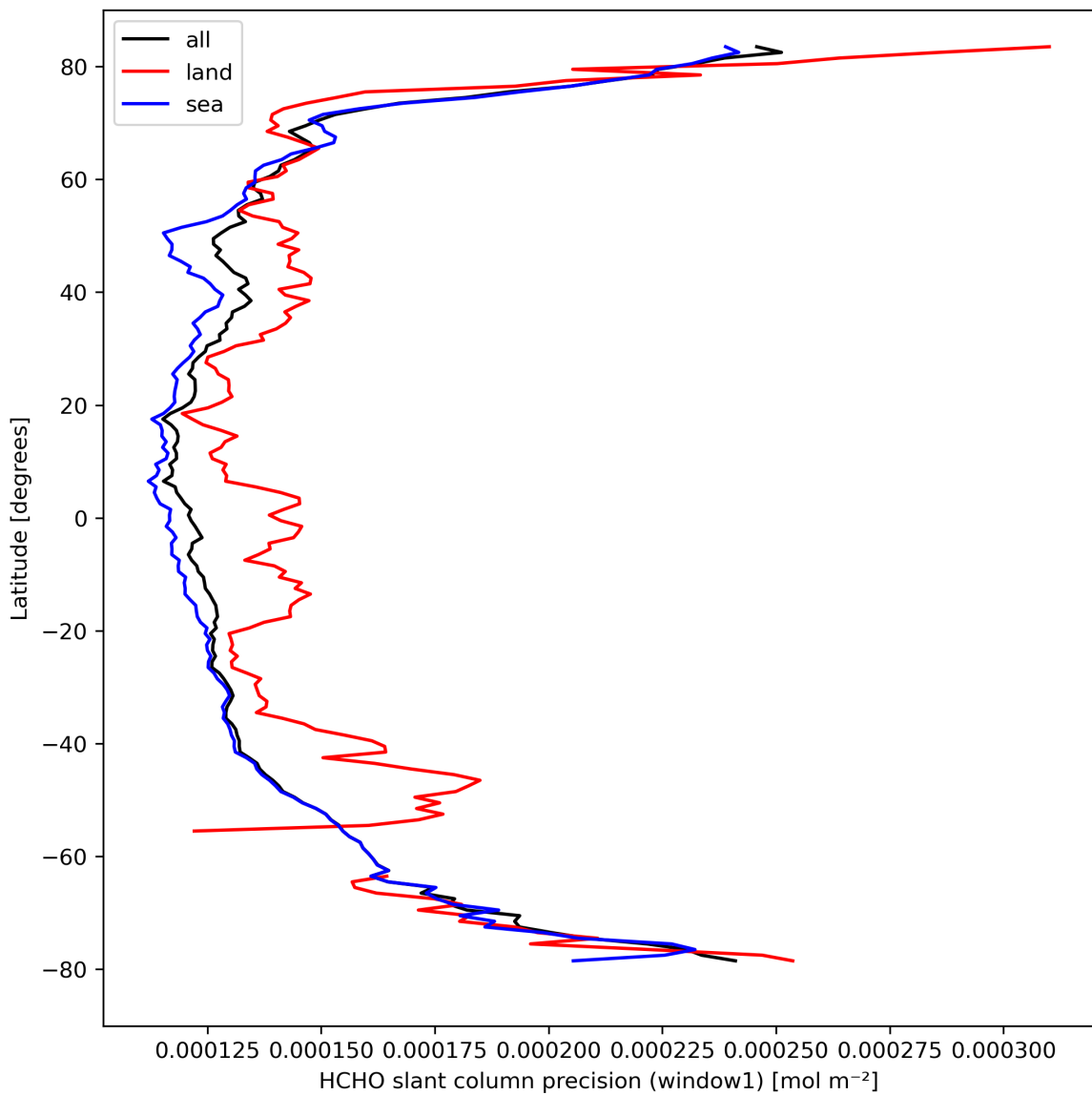


Figure 25: Zonal average of “HCHO slant column precision (window1)” for 2023-09-11 to 2023-09-13.

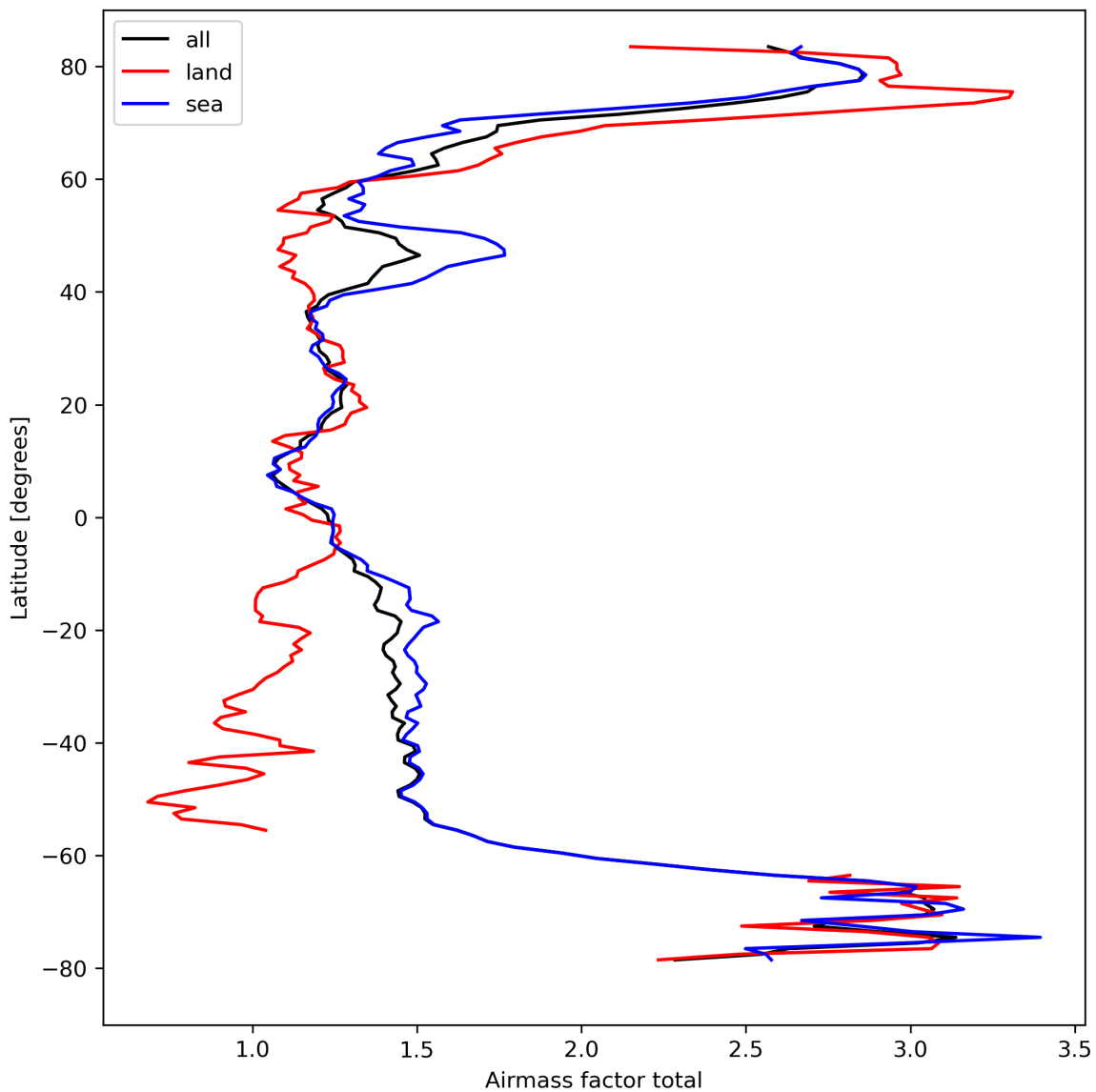


Figure 26: Zonal average of “Airmass factor total” for 2023-09-11 to 2023-09-13.

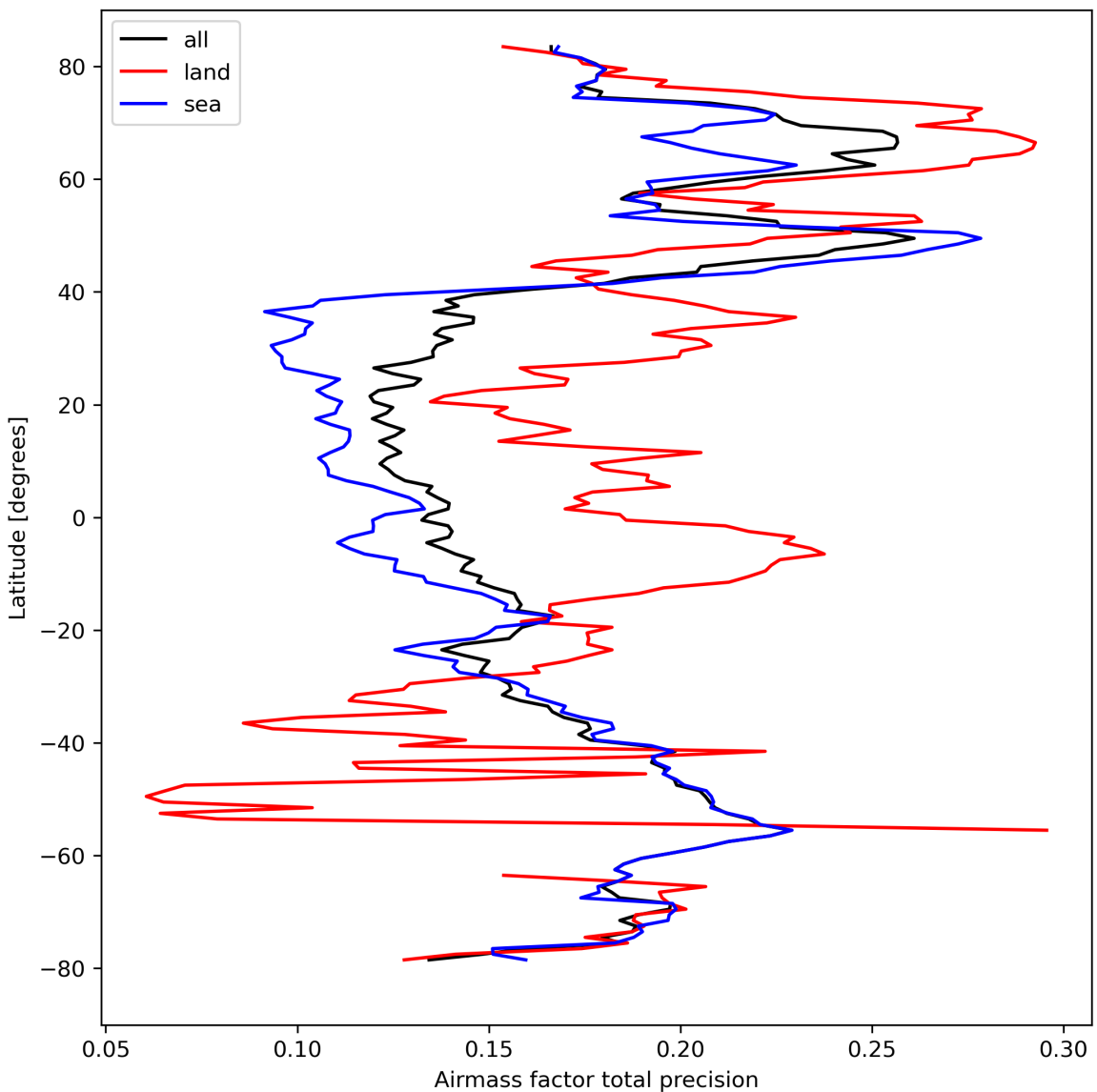


Figure 27: Zonal average of “Airmass factor total precision” for 2023-09-11 to 2023-09-13.

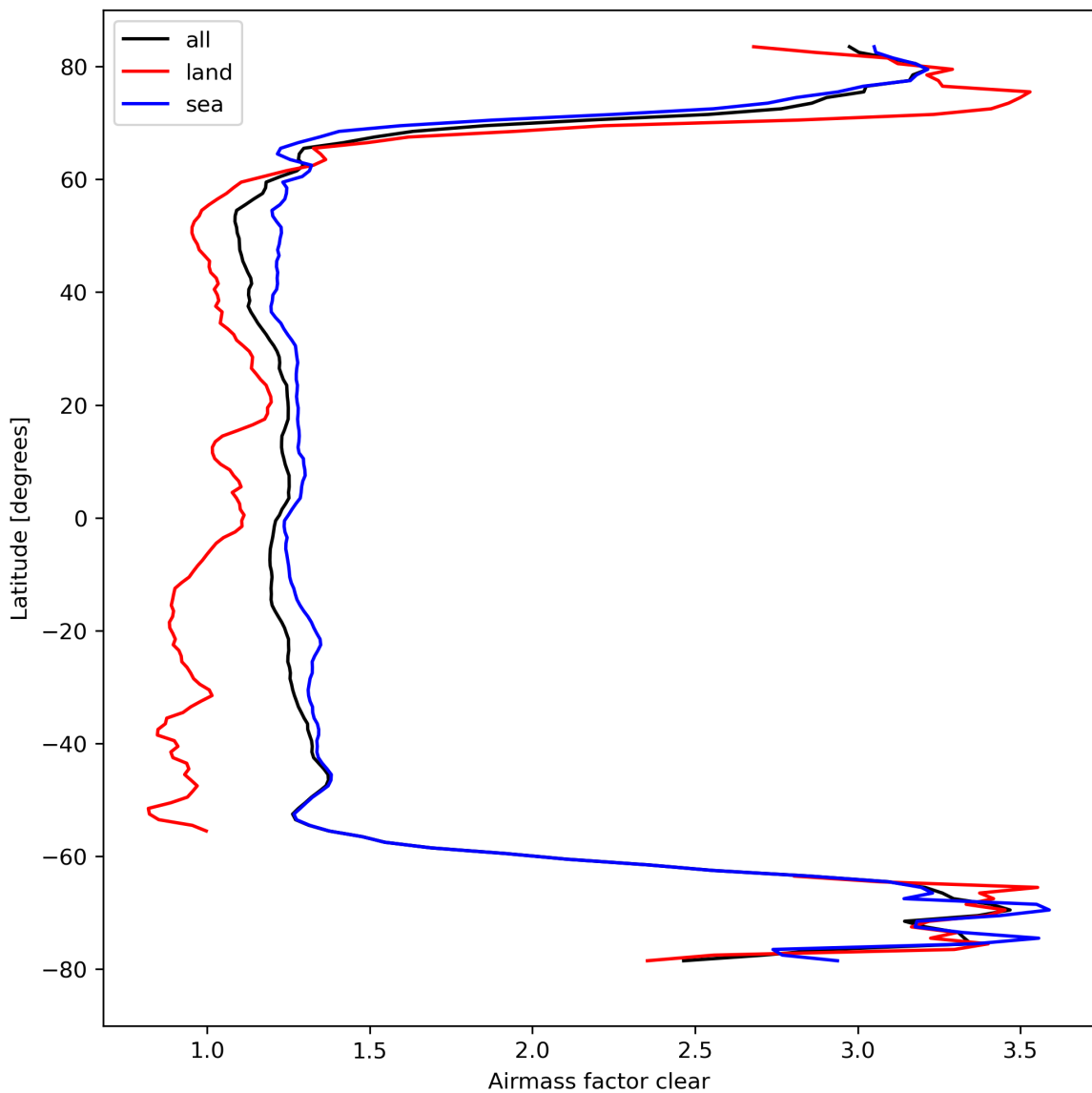


Figure 28: Zonal average of “Airmass factor clear” for 2023-09-11 to 2023-09-13.

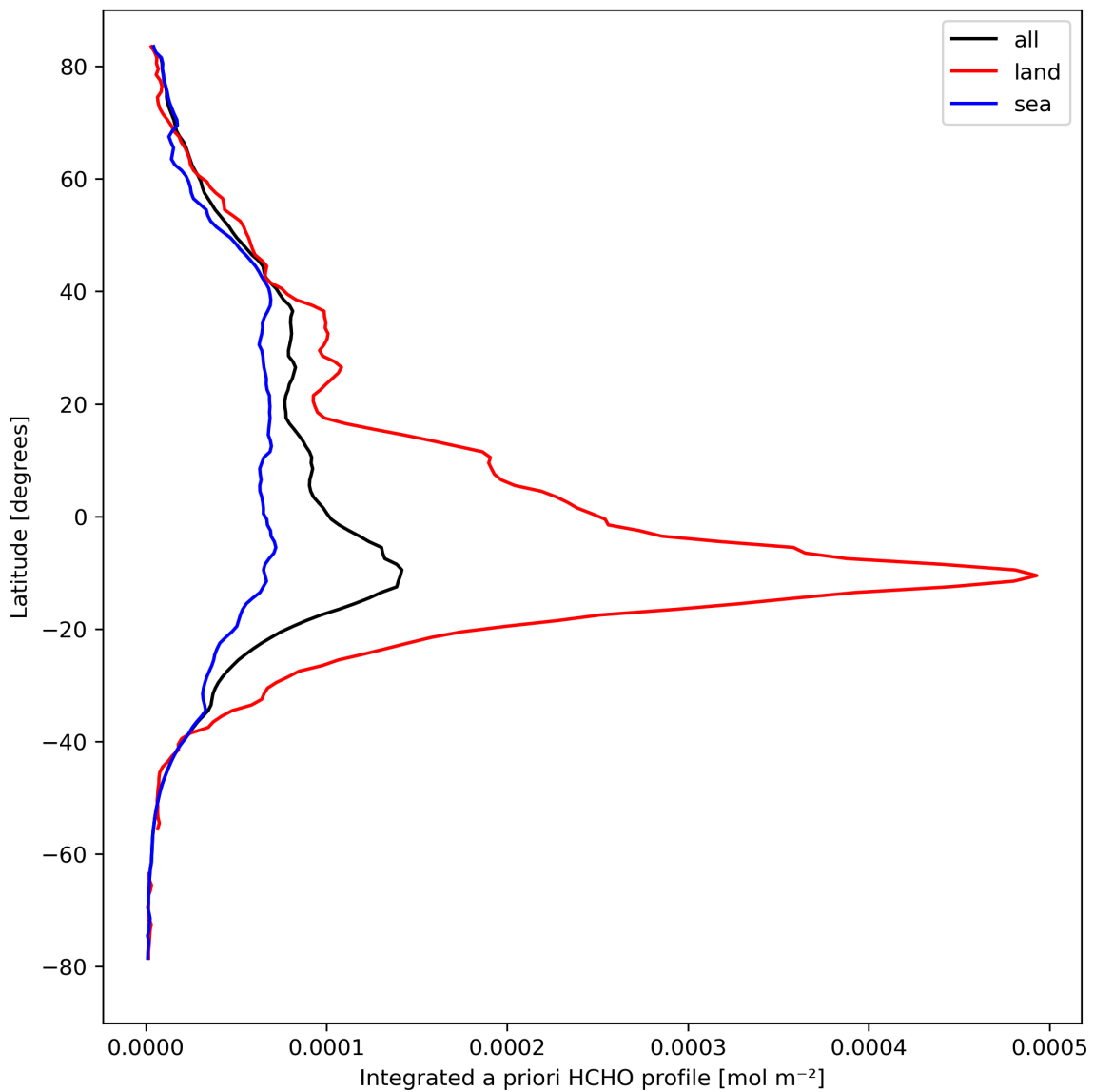


Figure 29: Zonal average of “Integrated a priori HCHO profile” for 2023-09-11 to 2023-09-13.

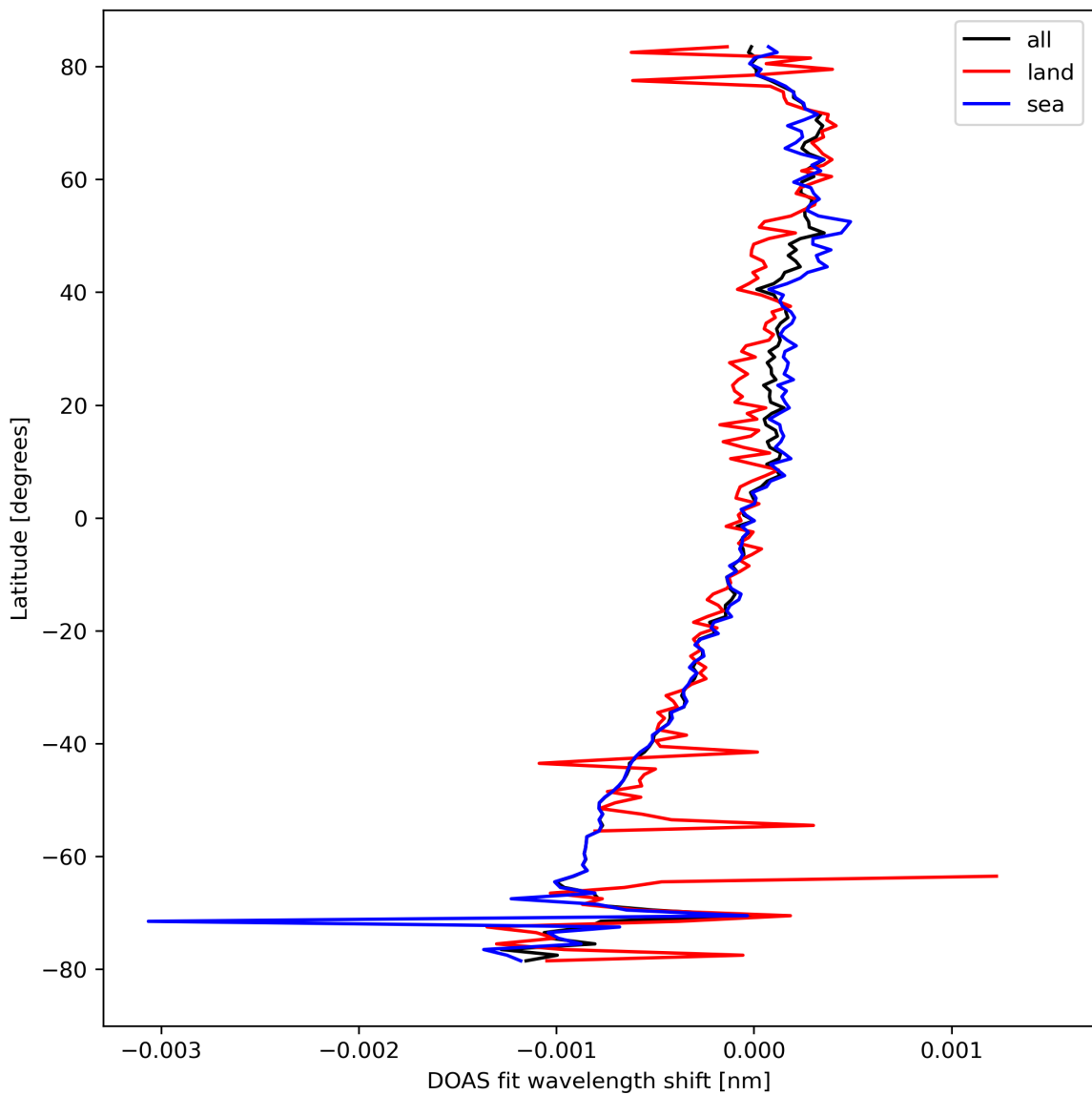


Figure 30: Zonal average of “DOAS fit wavelength shift” for 2023-09-11 to 2023-09-13.

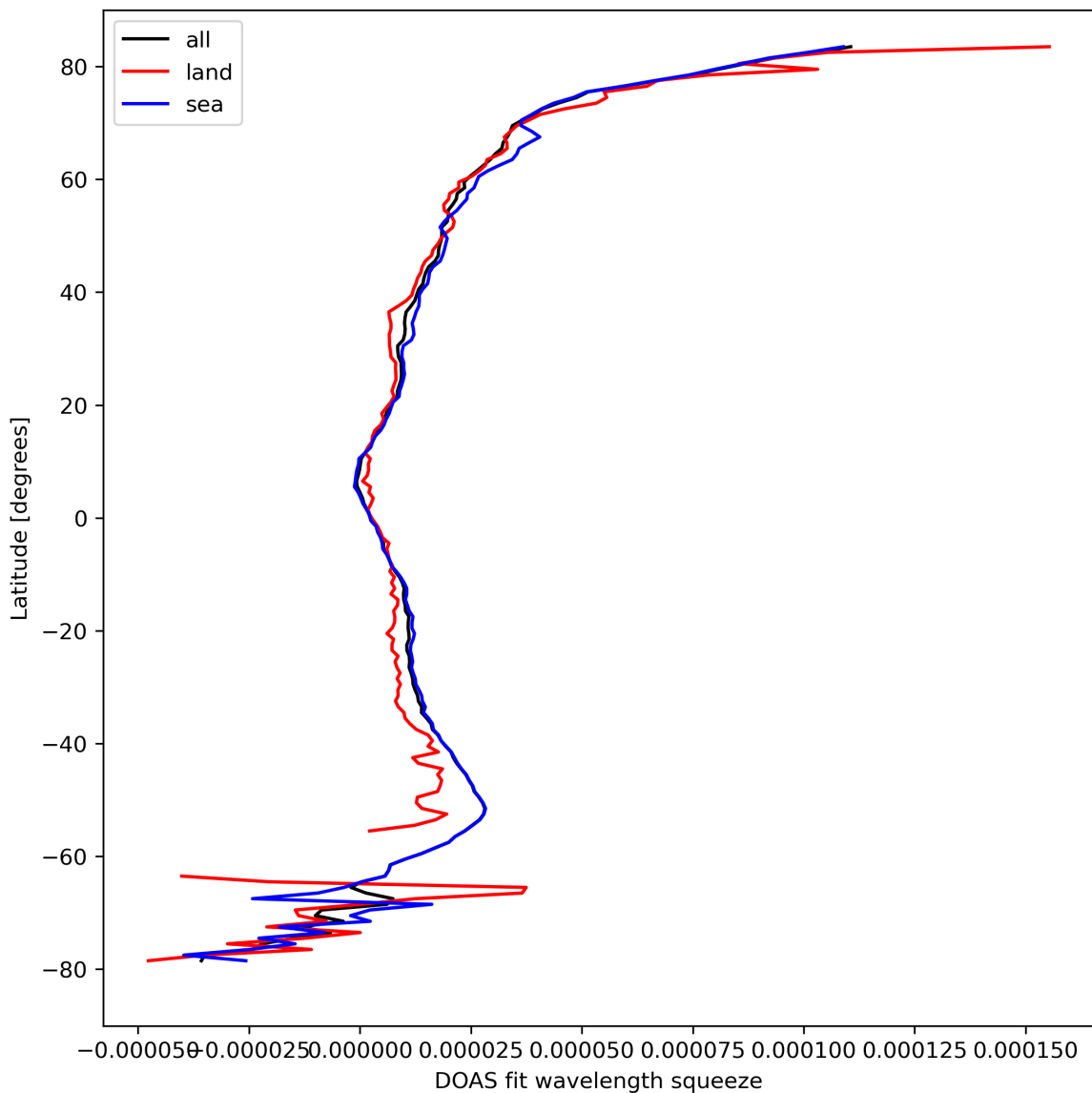


Figure 31: Zonal average of “DOAS fit wavelength squeeze” for 2023-09-11 to 2023-09-13.

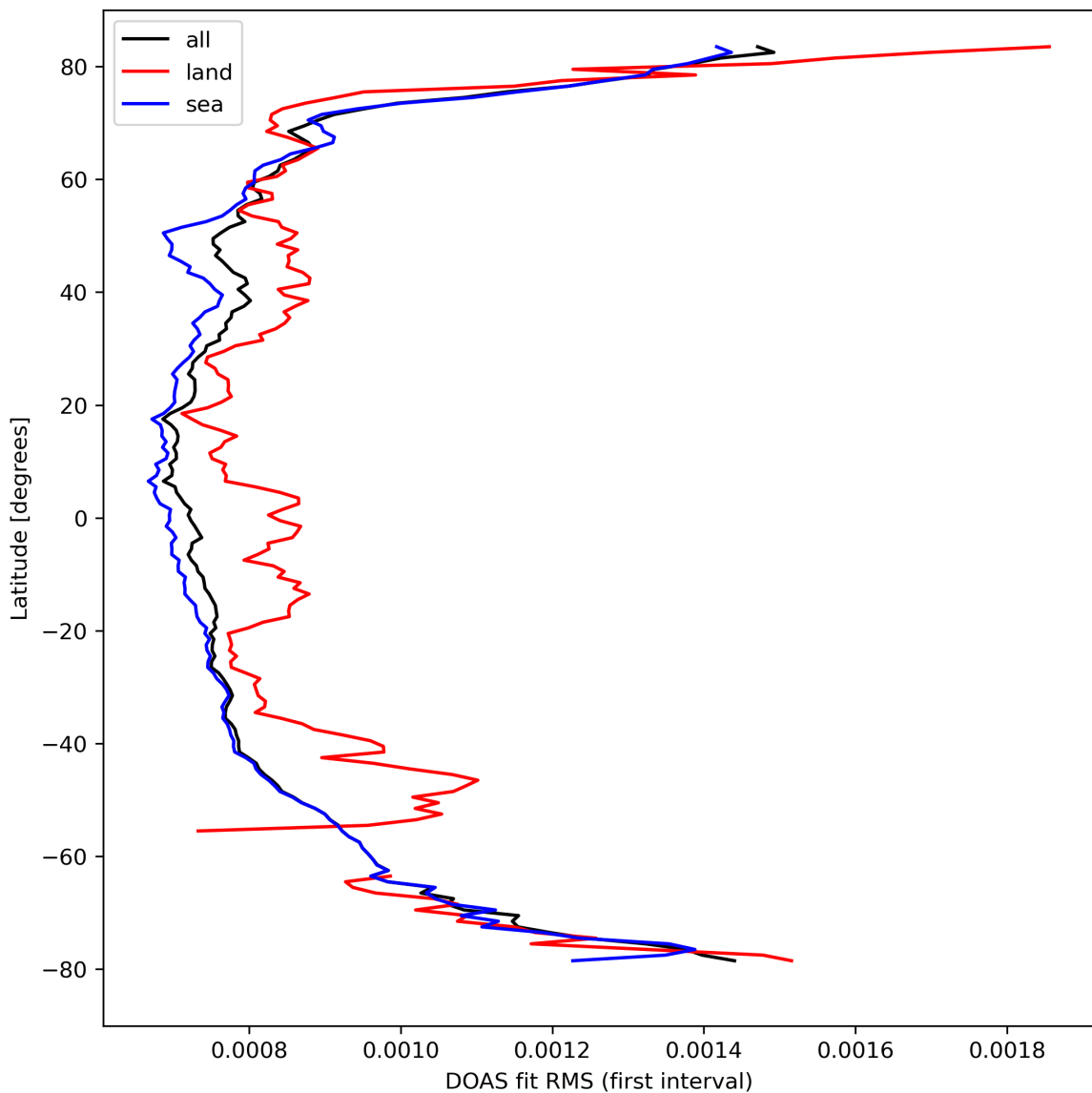


Figure 32: Zonal average of “DOAS fit RMS (first interval)” for 2023-09-11 to 2023-09-13.

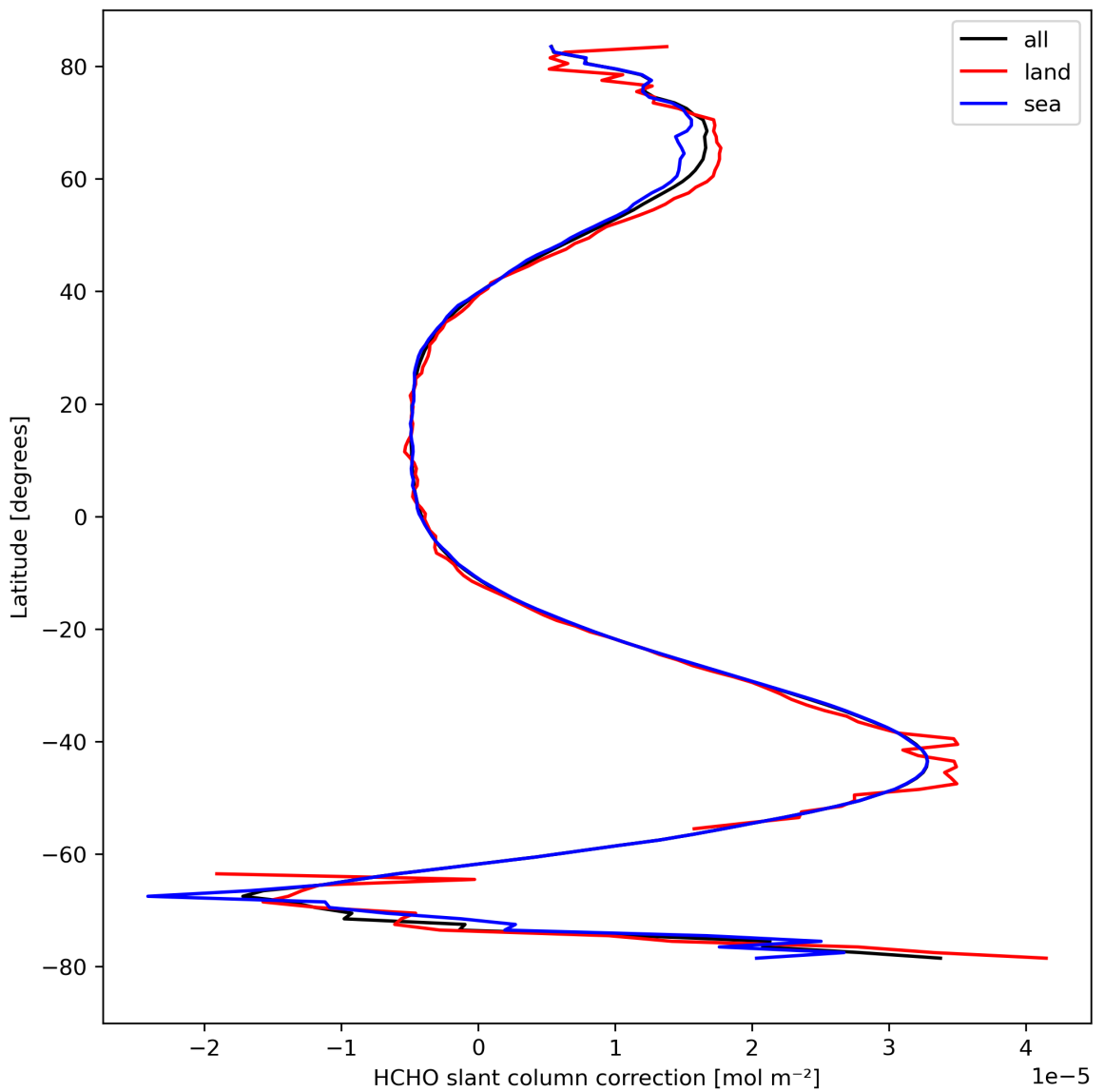


Figure 33: Zonal average of “HCHO slant column correction” for 2023-09-11 to 2023-09-13.

8 Histograms

The definitions of the parameters given in this section can be found in section 2.

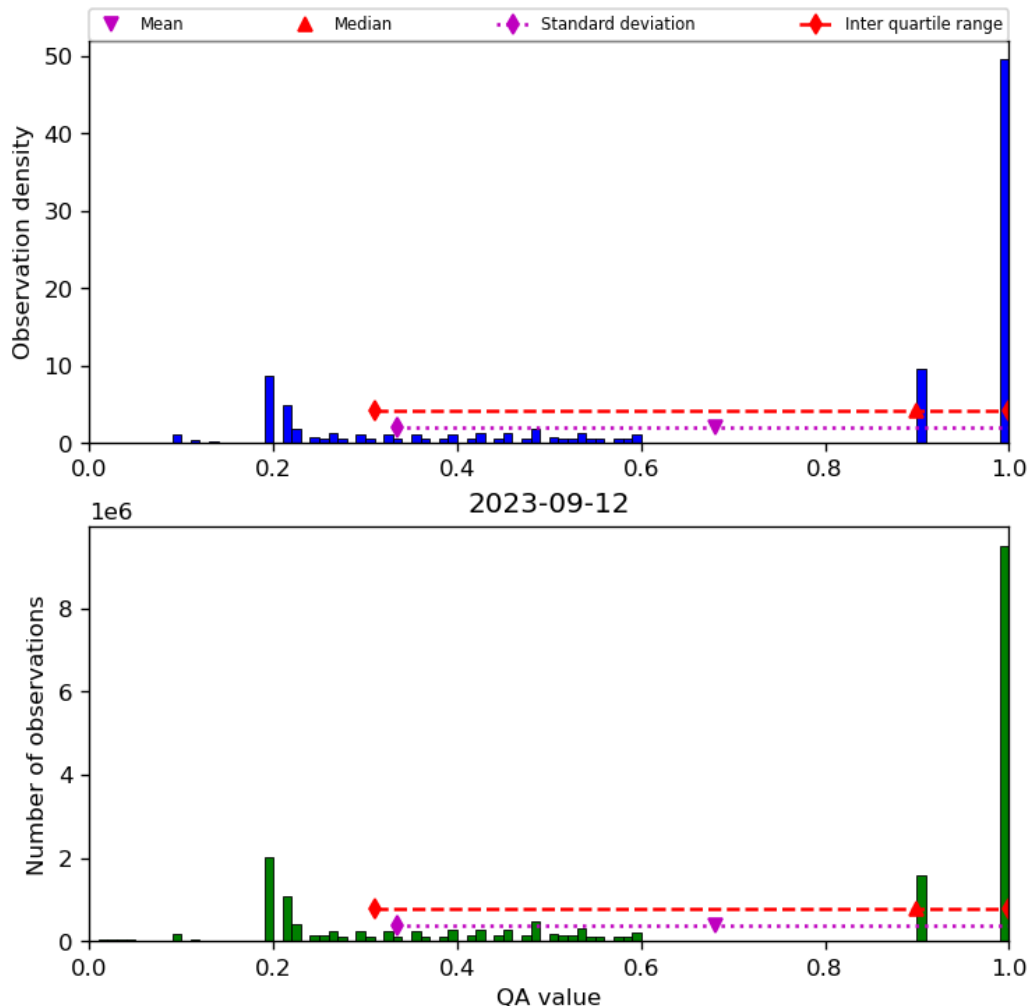


Figure 34: Histogram of “QA value” for 2023-09-11 to 2023-09-13

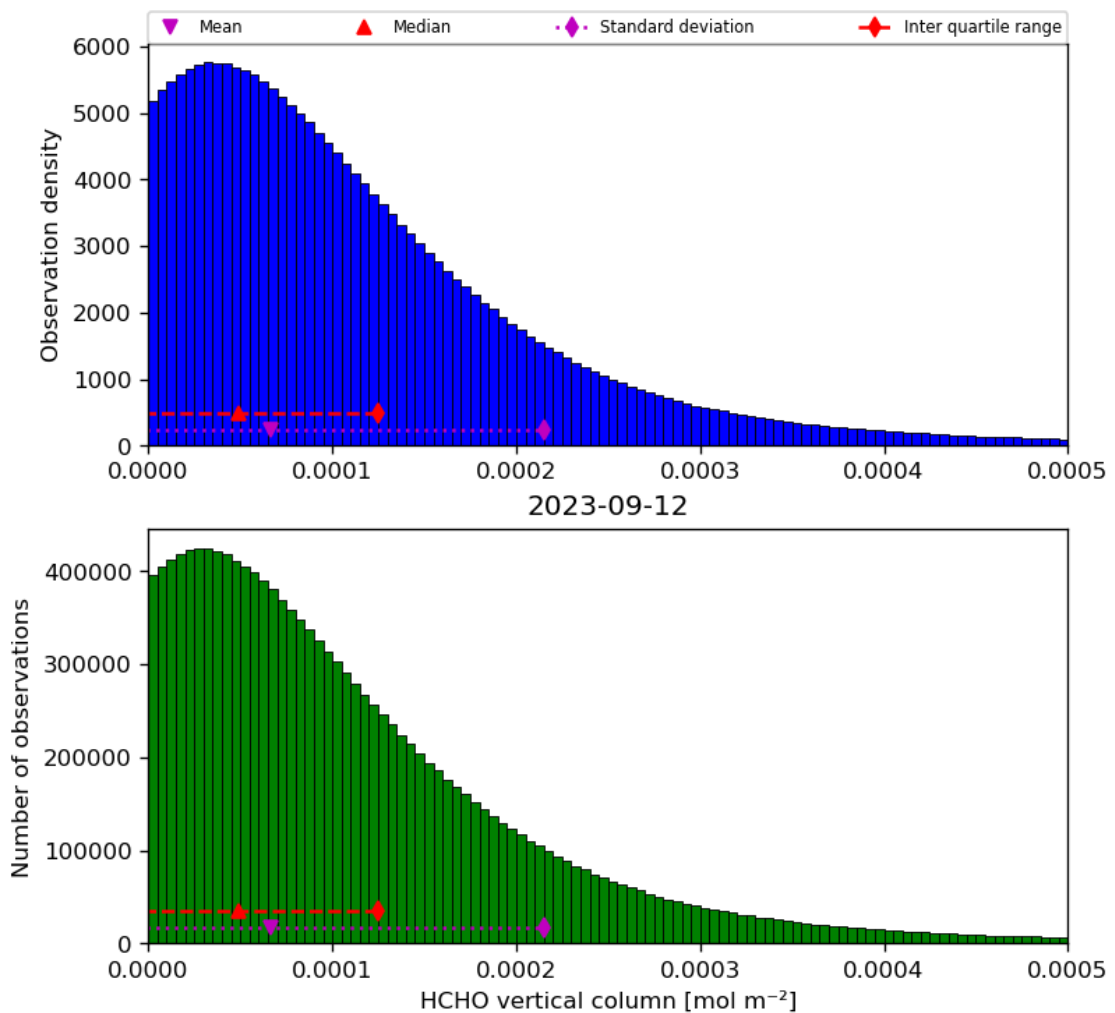


Figure 35: Histogram of “HCHO vertical column” for 2023-09-11 to 2023-09-13

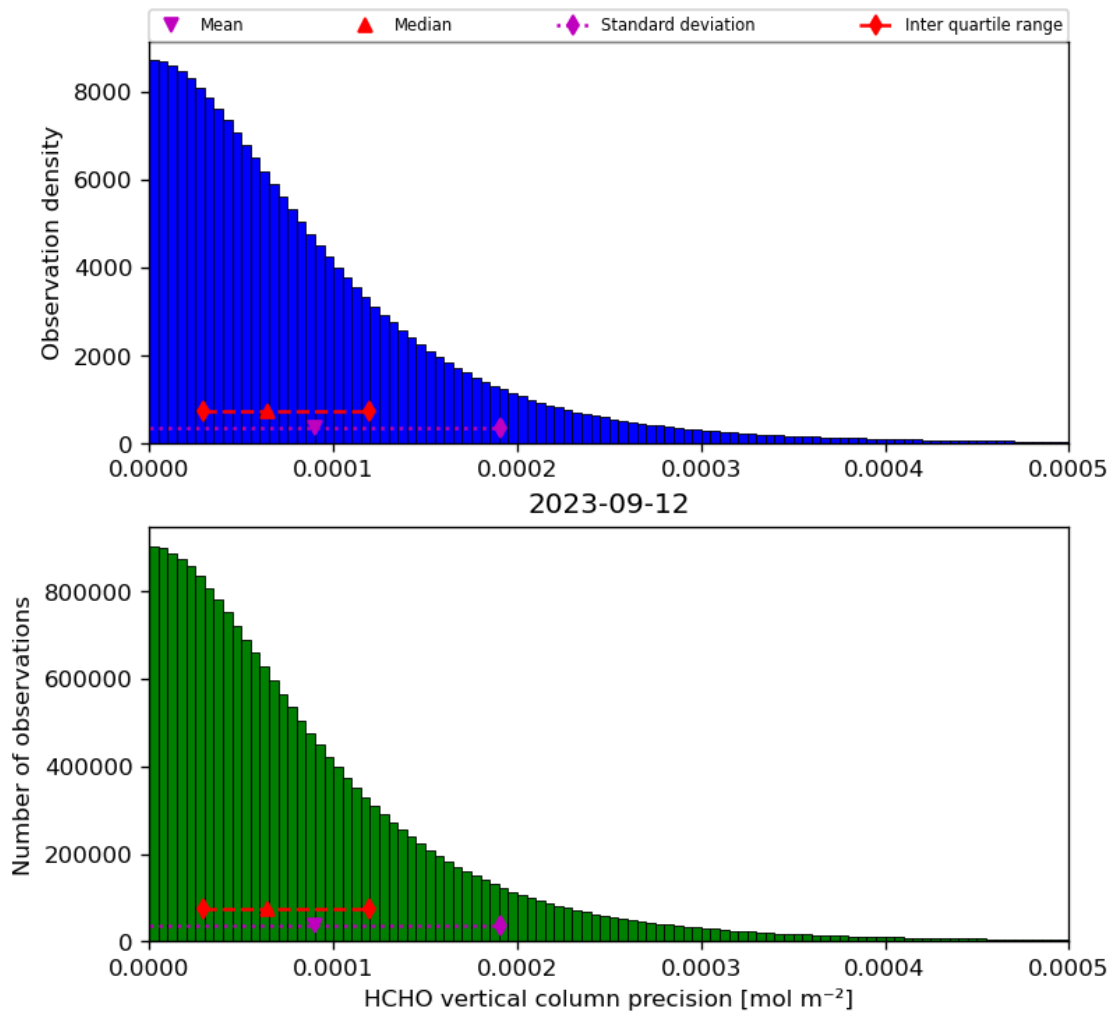


Figure 36: Histogram of “HCHO vertical column precision” for 2023-09-11 to 2023-09-13

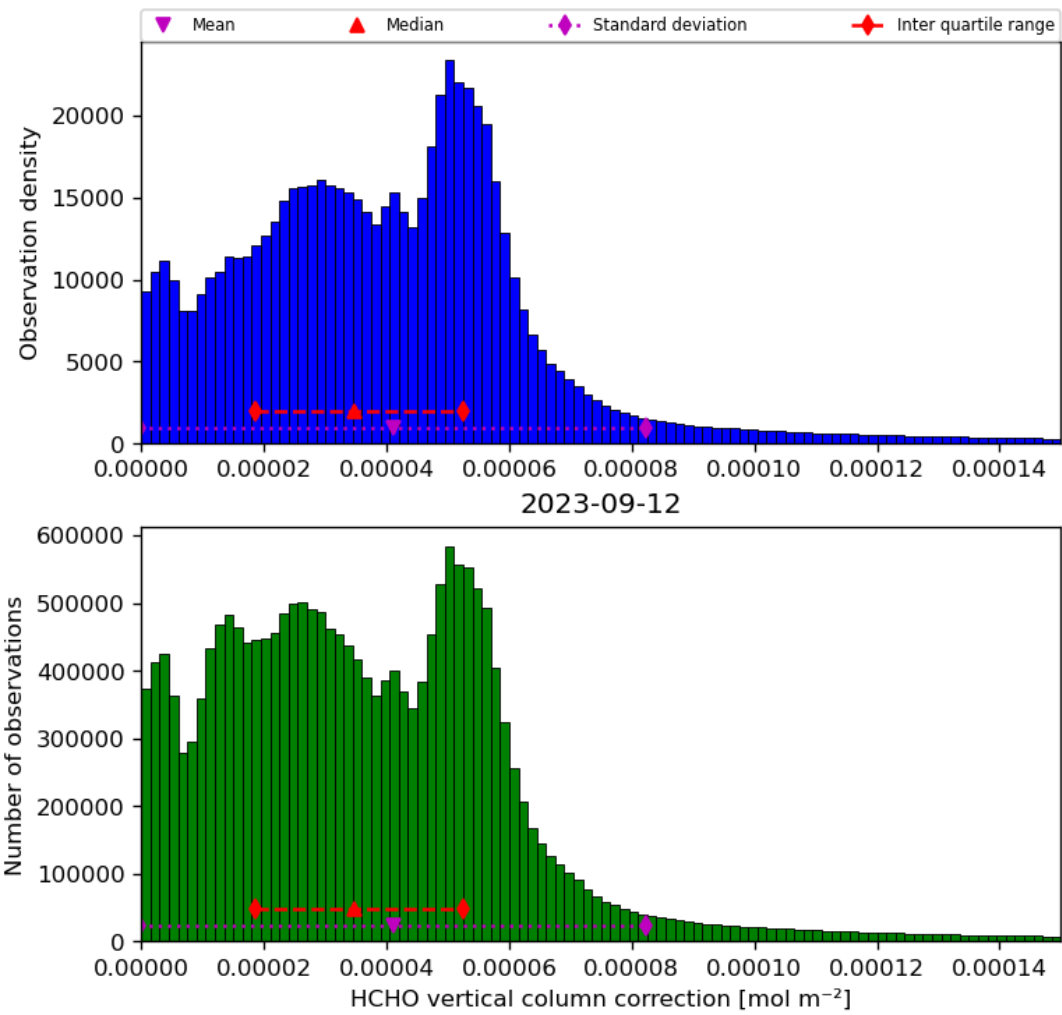


Figure 37: Histogram of “HCHO vertical column correction” for 2023-09-11 to 2023-09-13

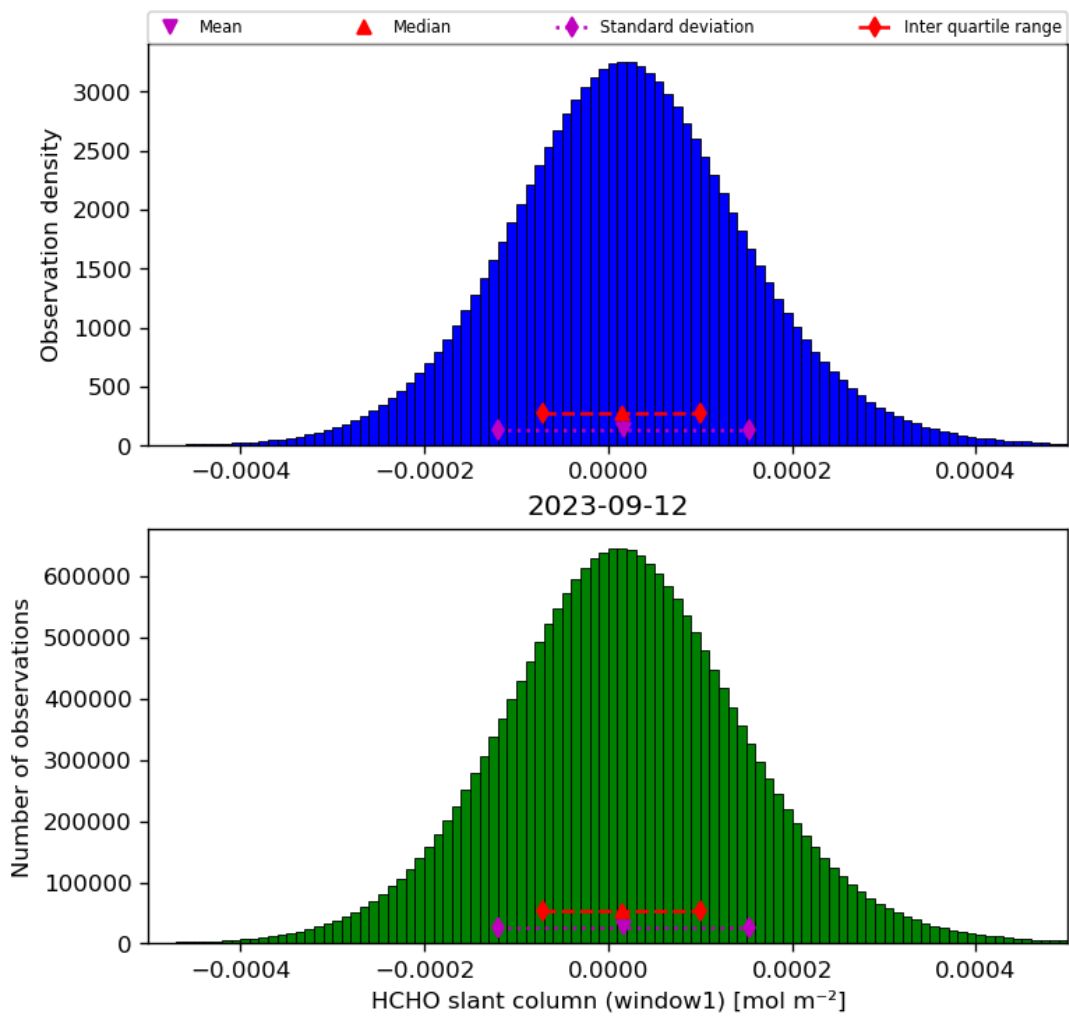


Figure 38: Histogram of “HCHO slant column (window1)” for 2023-09-11 to 2023-09-13

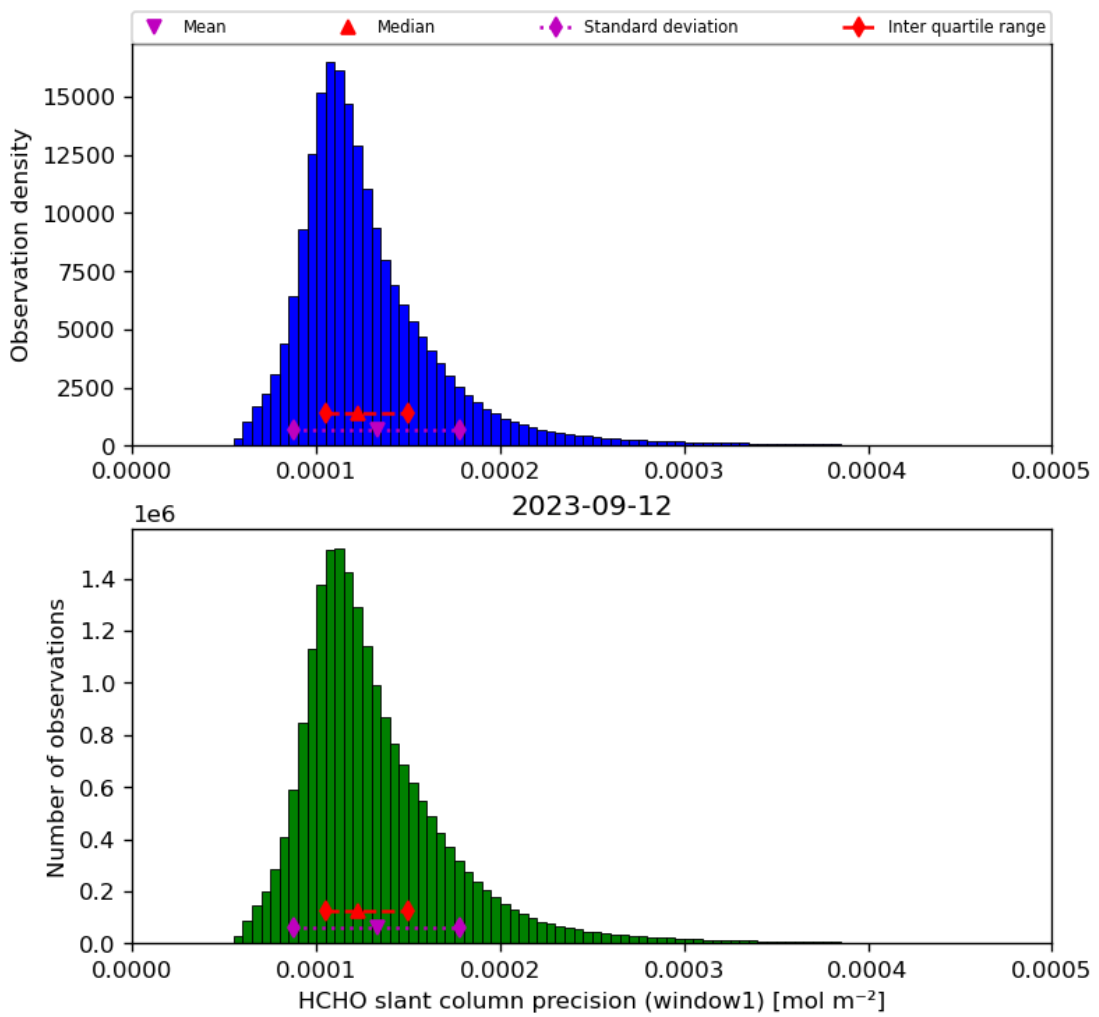


Figure 39: Histogram of “HCHO slant column precision (window1)” for 2023-09-11 to 2023-09-13

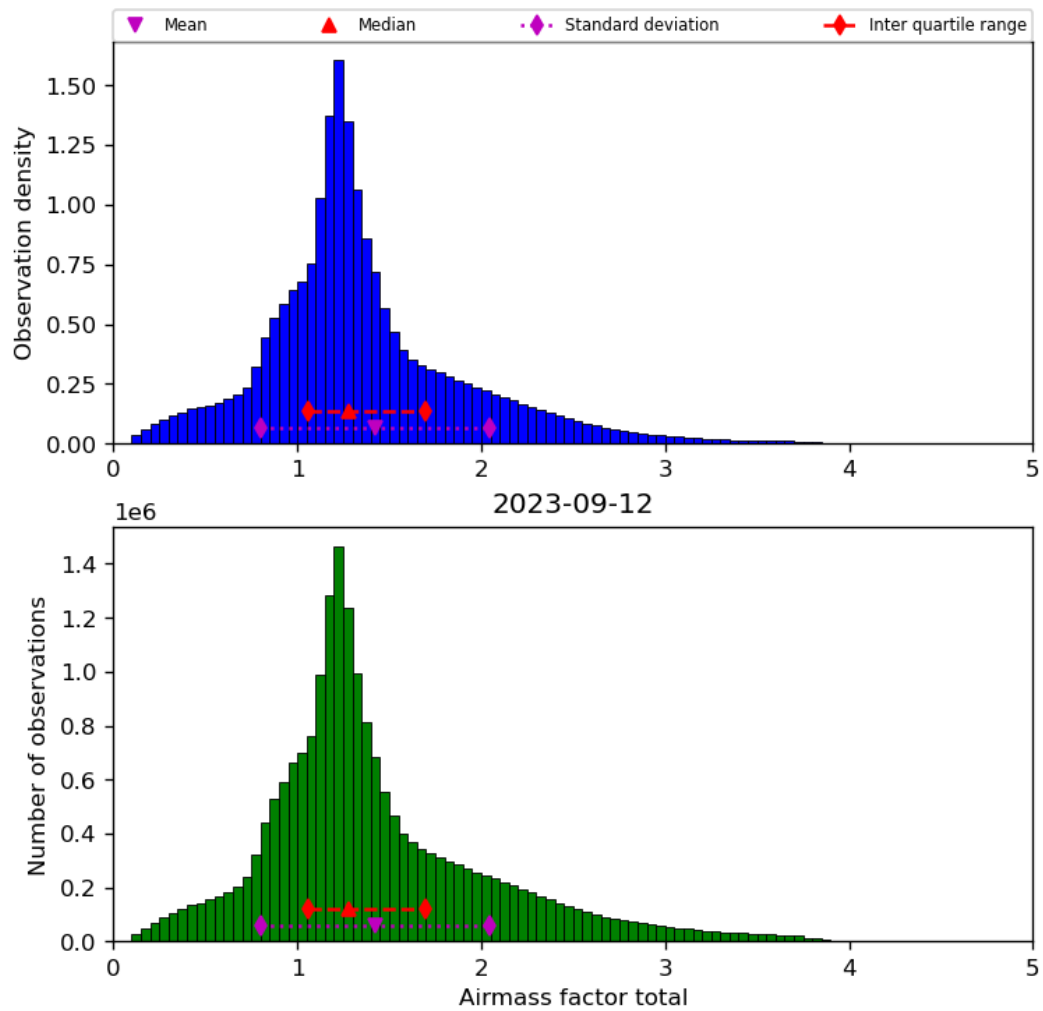


Figure 40: Histogram of “Airmass factor total” for 2023-09-11 to 2023-09-13

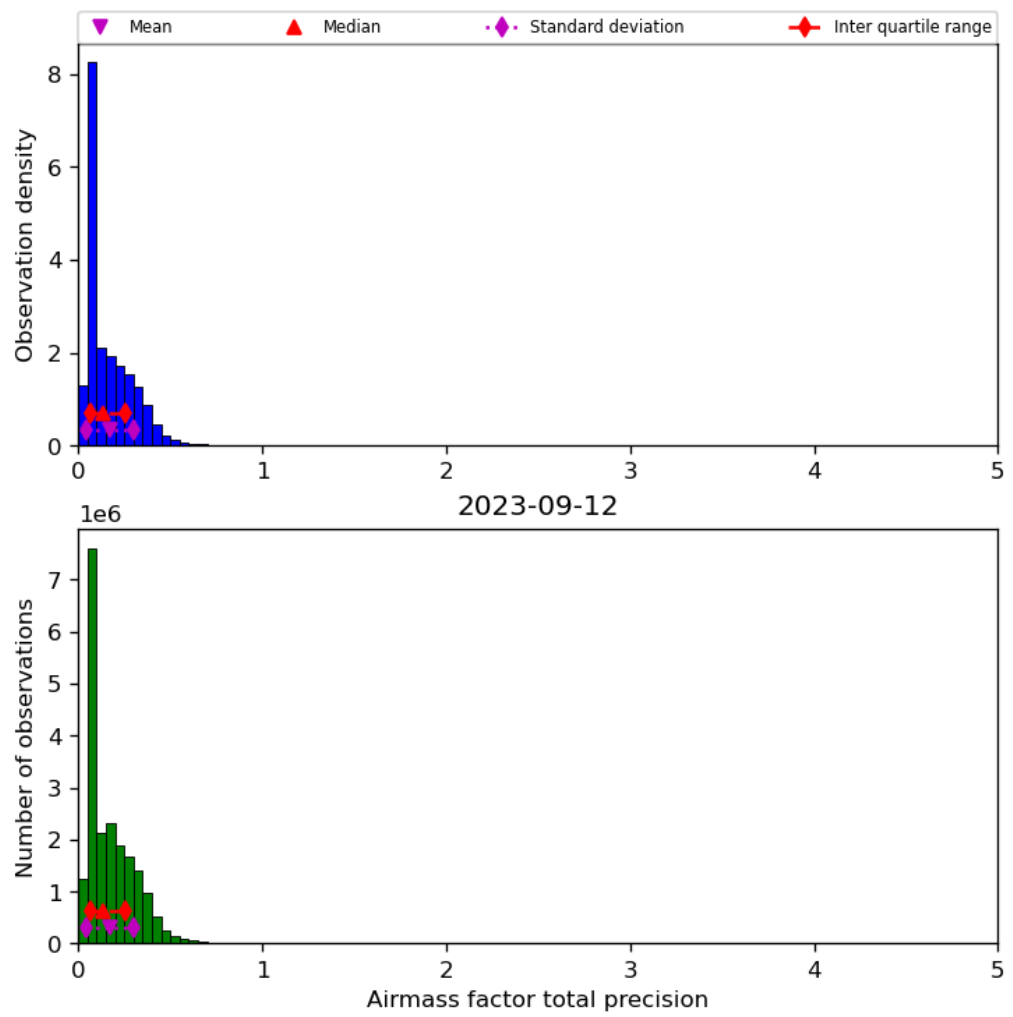


Figure 41: Histogram of “Airmass factor total precision” for 2023-09-11 to 2023-09-13

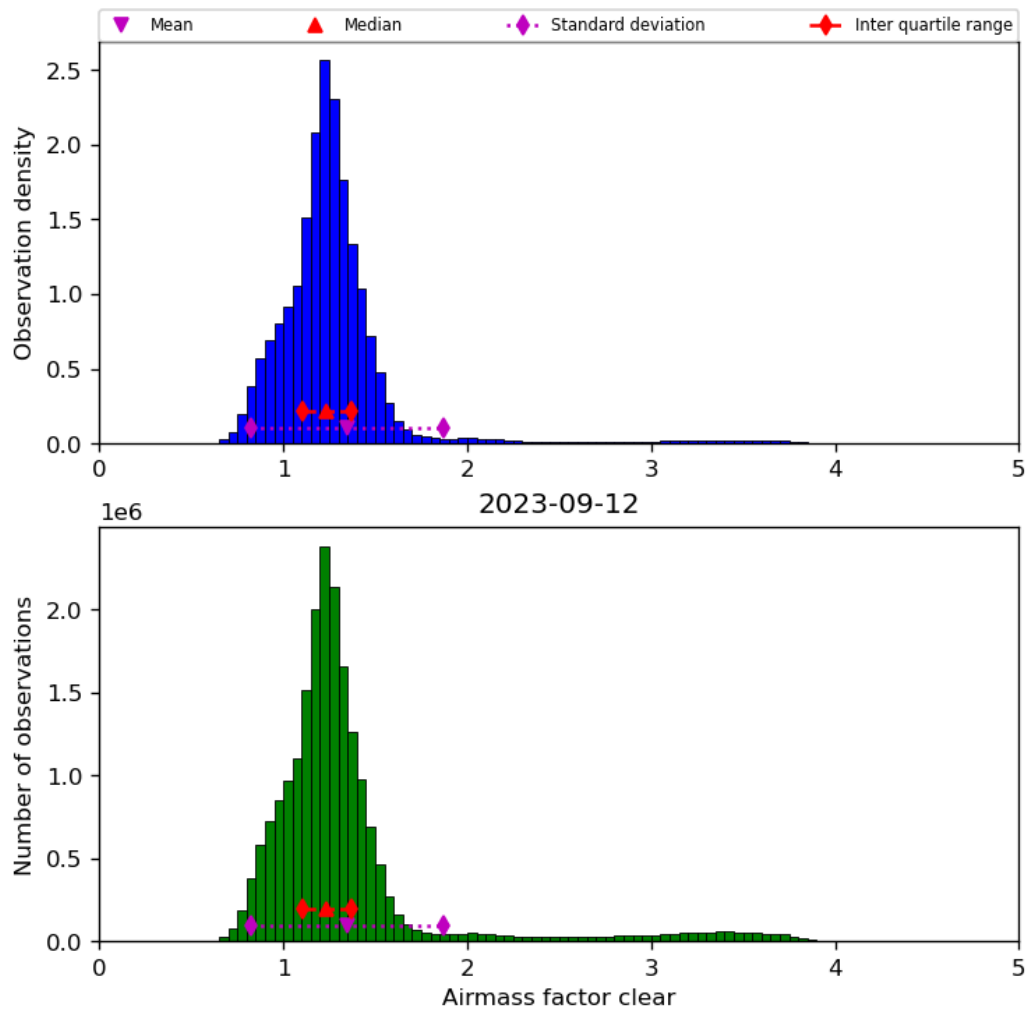


Figure 42: Histogram of “Airmass factor clear” for 2023-09-11 to 2023-09-13

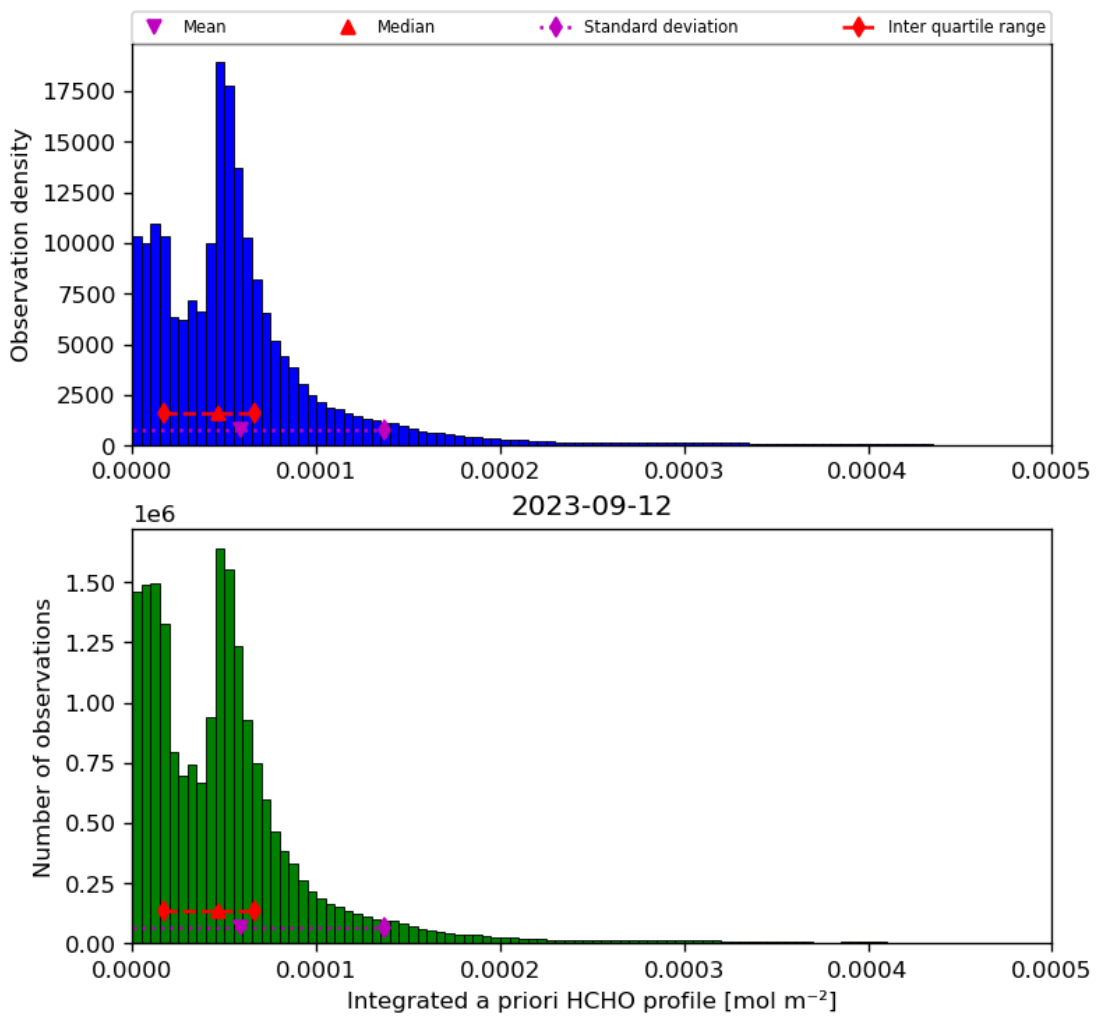


Figure 43: Histogram of “Integrated a priori HCHO profile” for 2023-09-11 to 2023-09-13

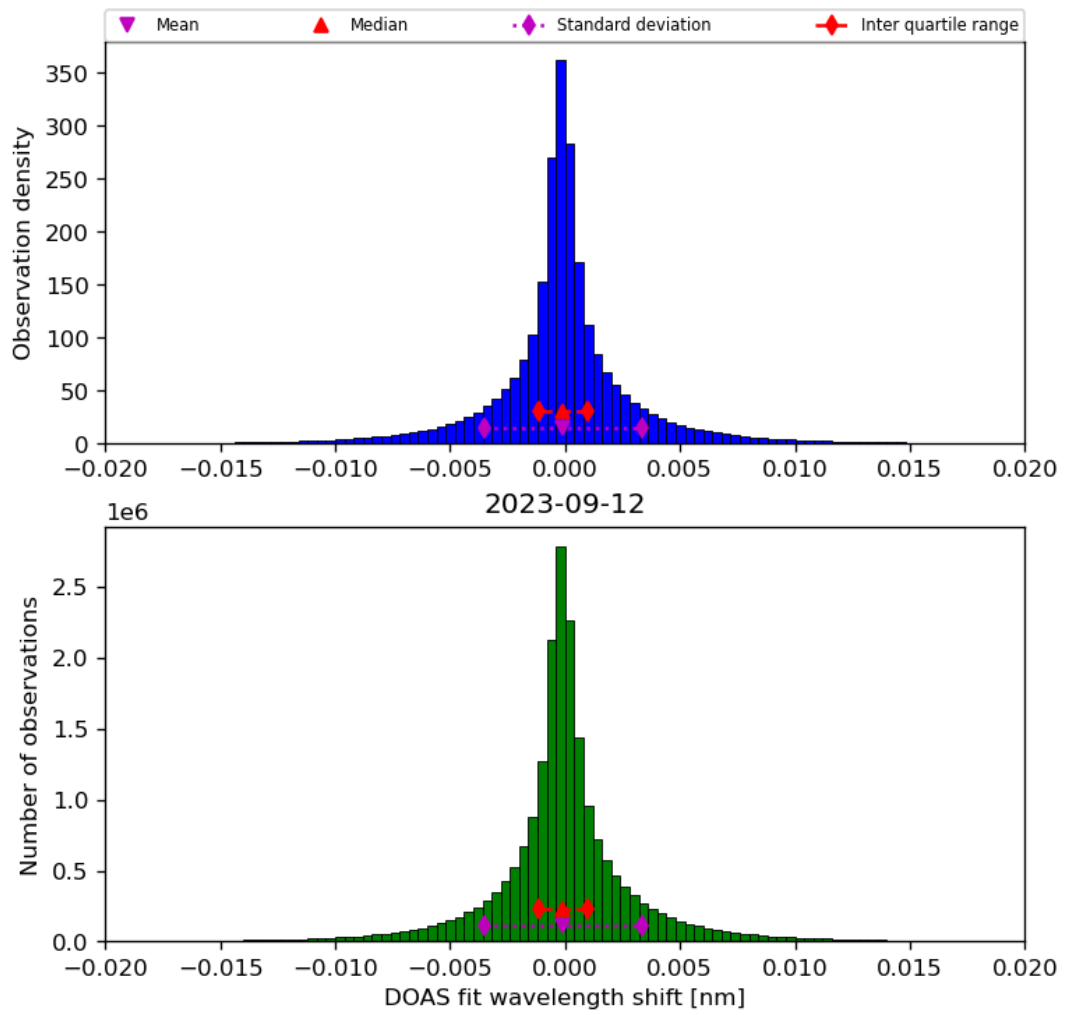


Figure 44: Histogram of “DOAS fit wavelength shift” for 2023-09-11 to 2023-09-13

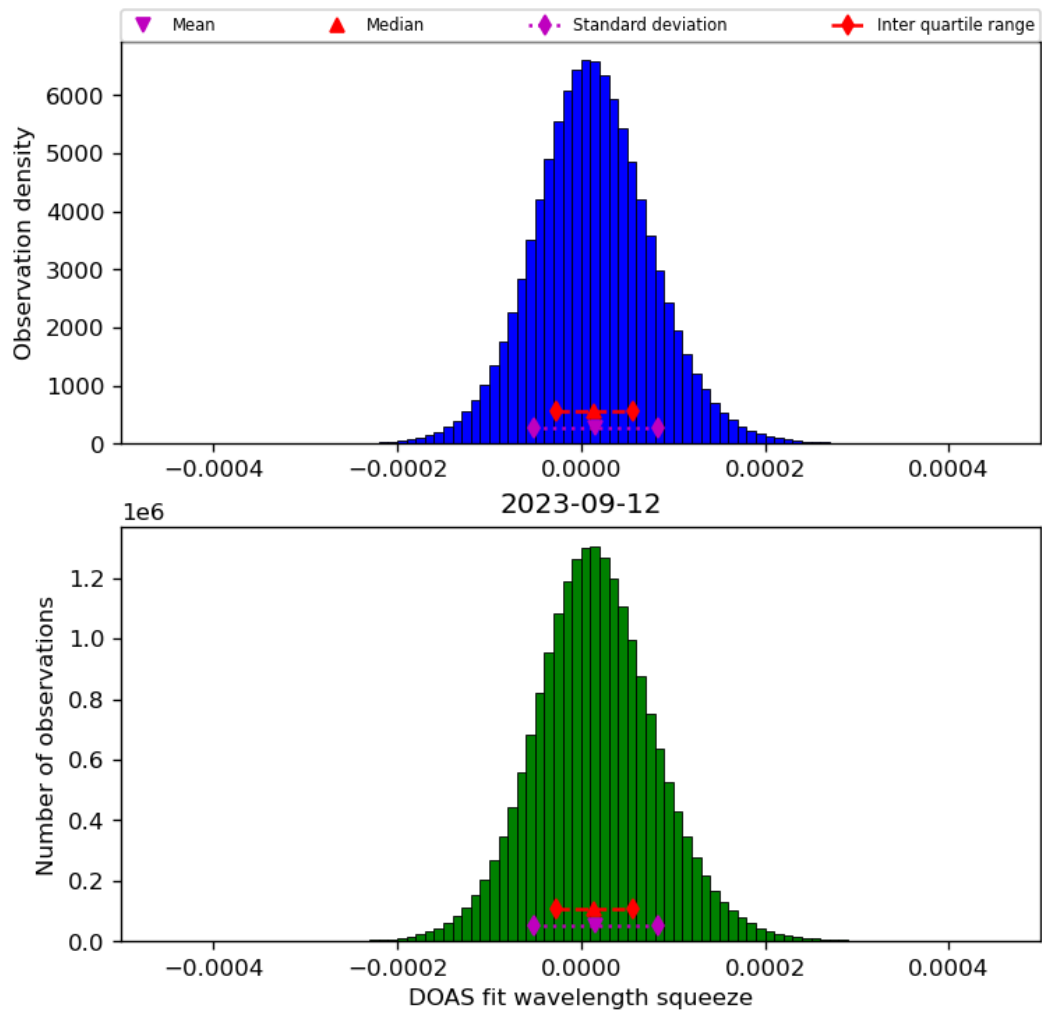


Figure 45: Histogram of “DOAS fit wavelength squeeze” for 2023-09-11 to 2023-09-13

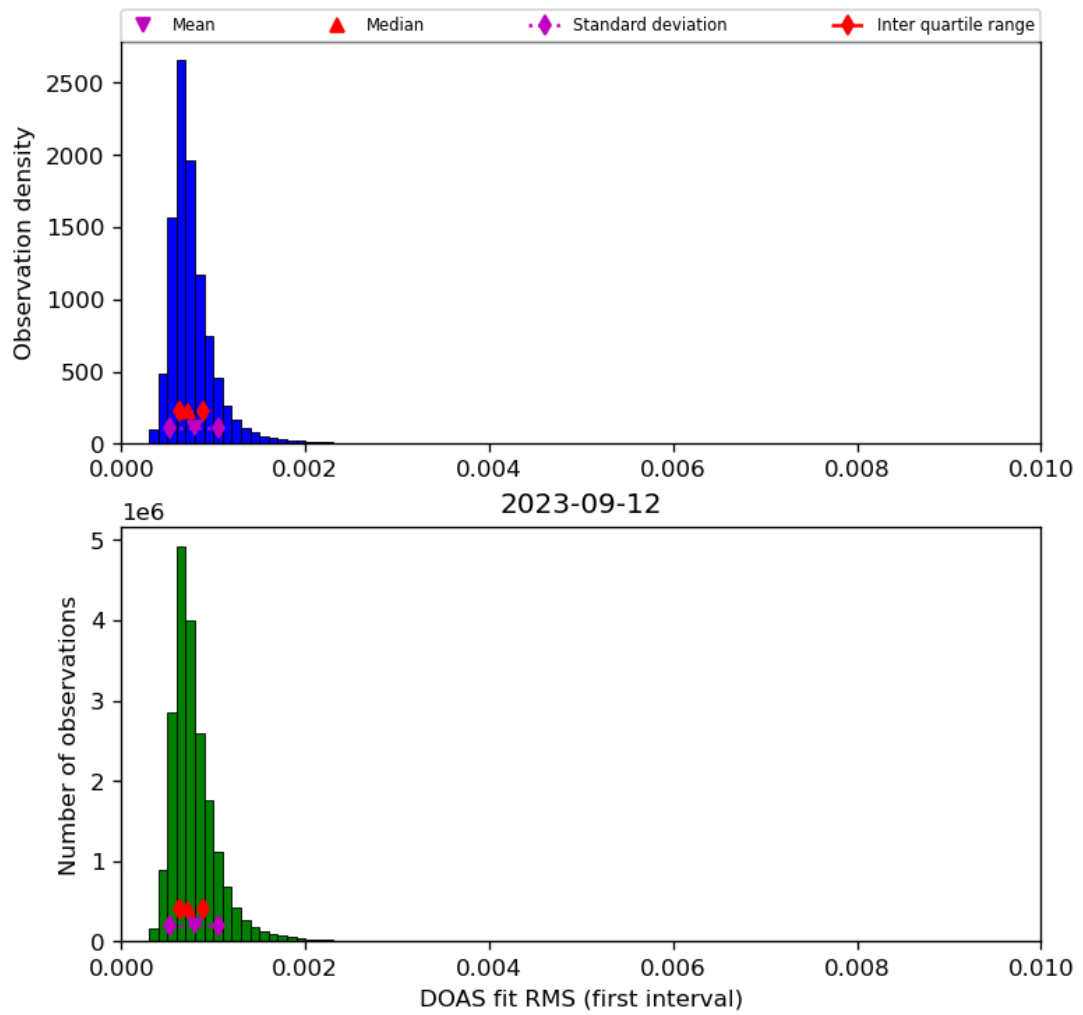


Figure 46: Histogram of “DOAS fit RMS (first interval)” for 2023-09-11 to 2023-09-13

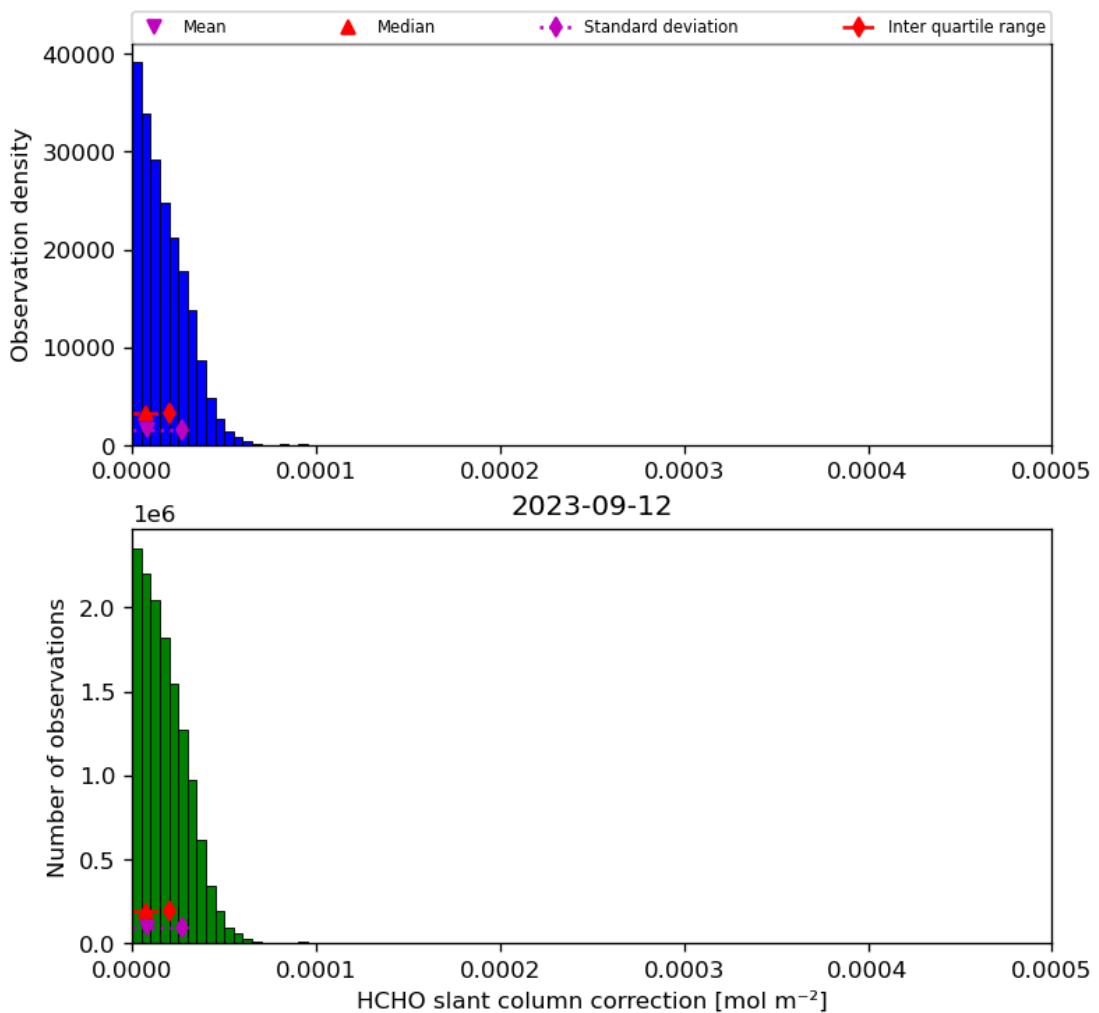


Figure 47: Histogram of “HCHO slant column correction” for 2023-09-11 to 2023-09-13

9 Along track statistics

The TROPOMI instrument uses different binned detector rows for different viewing directions. In this section statistics are presented for each of the binned rows in the instrument.

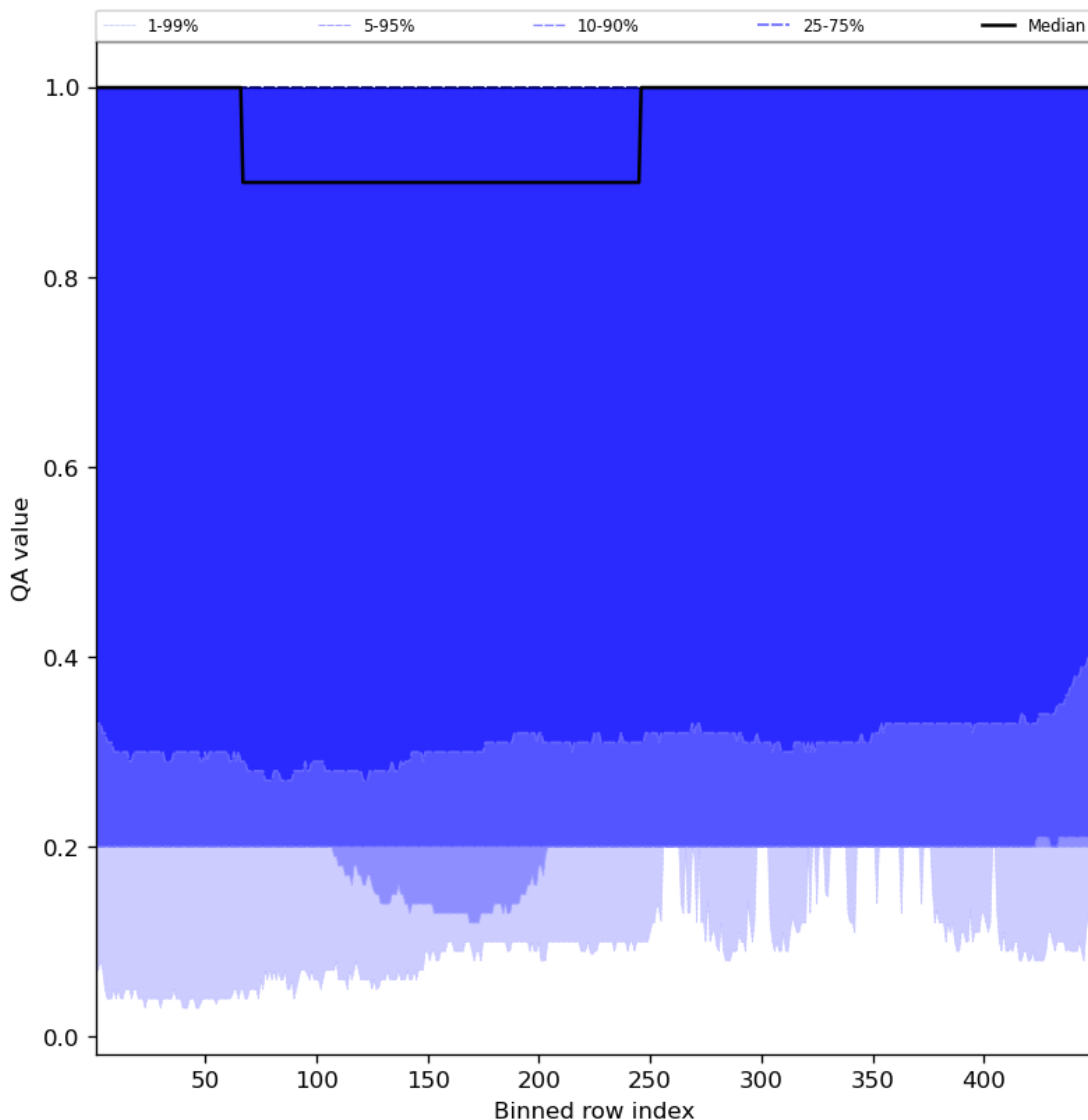


Figure 48: Along track statistics of “QA value” for 2023-09-11 to 2023-09-13

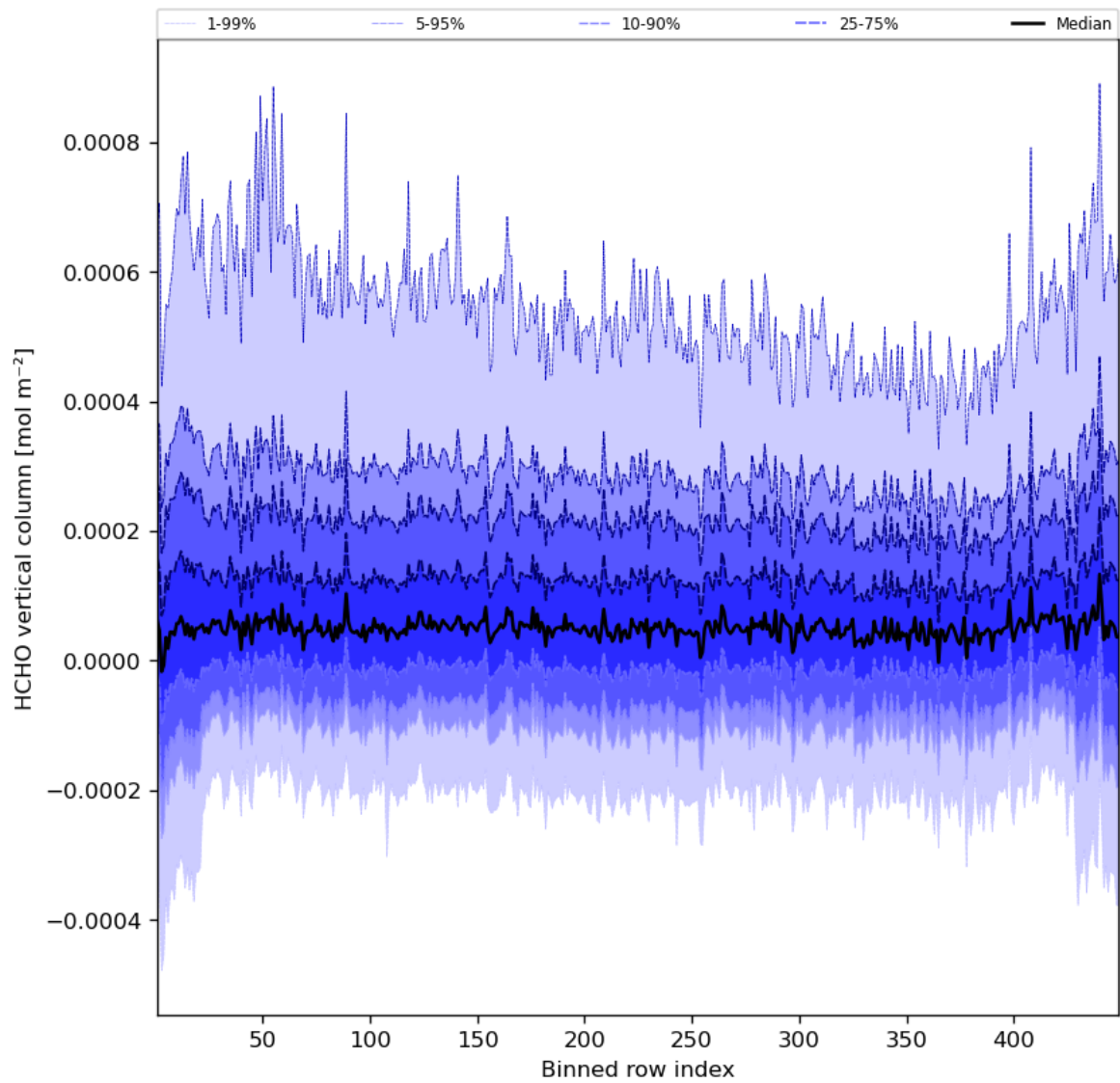


Figure 49: Along track statistics of “HCHO vertical column” for 2023-09-11 to 2023-09-13

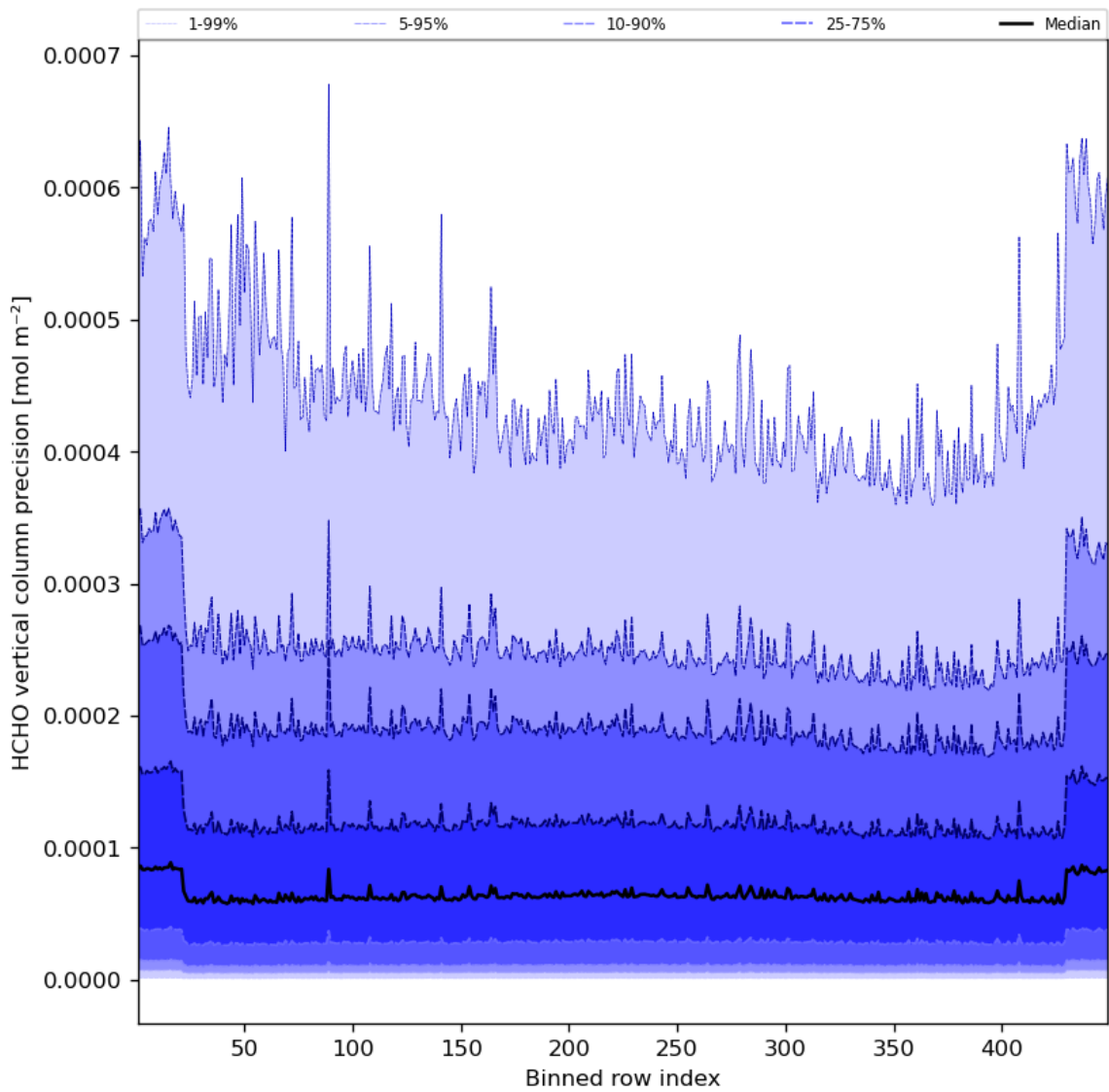


Figure 50: Along track statistics of “HCHO vertical column precision” for 2023-09-11 to 2023-09-13

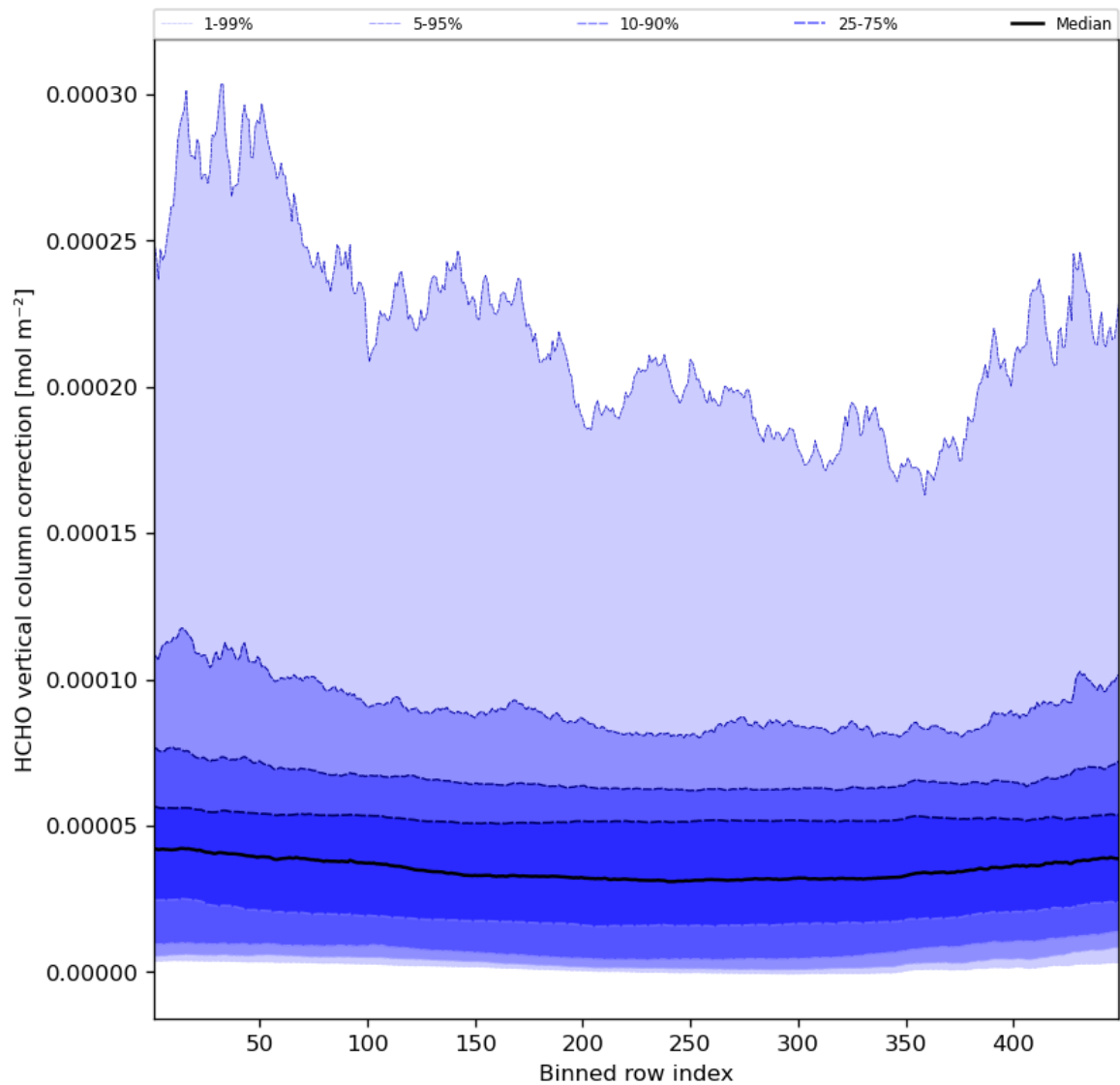


Figure 51: Along track statistics of “HCHO vertical column correction” for 2023-09-11 to 2023-09-13

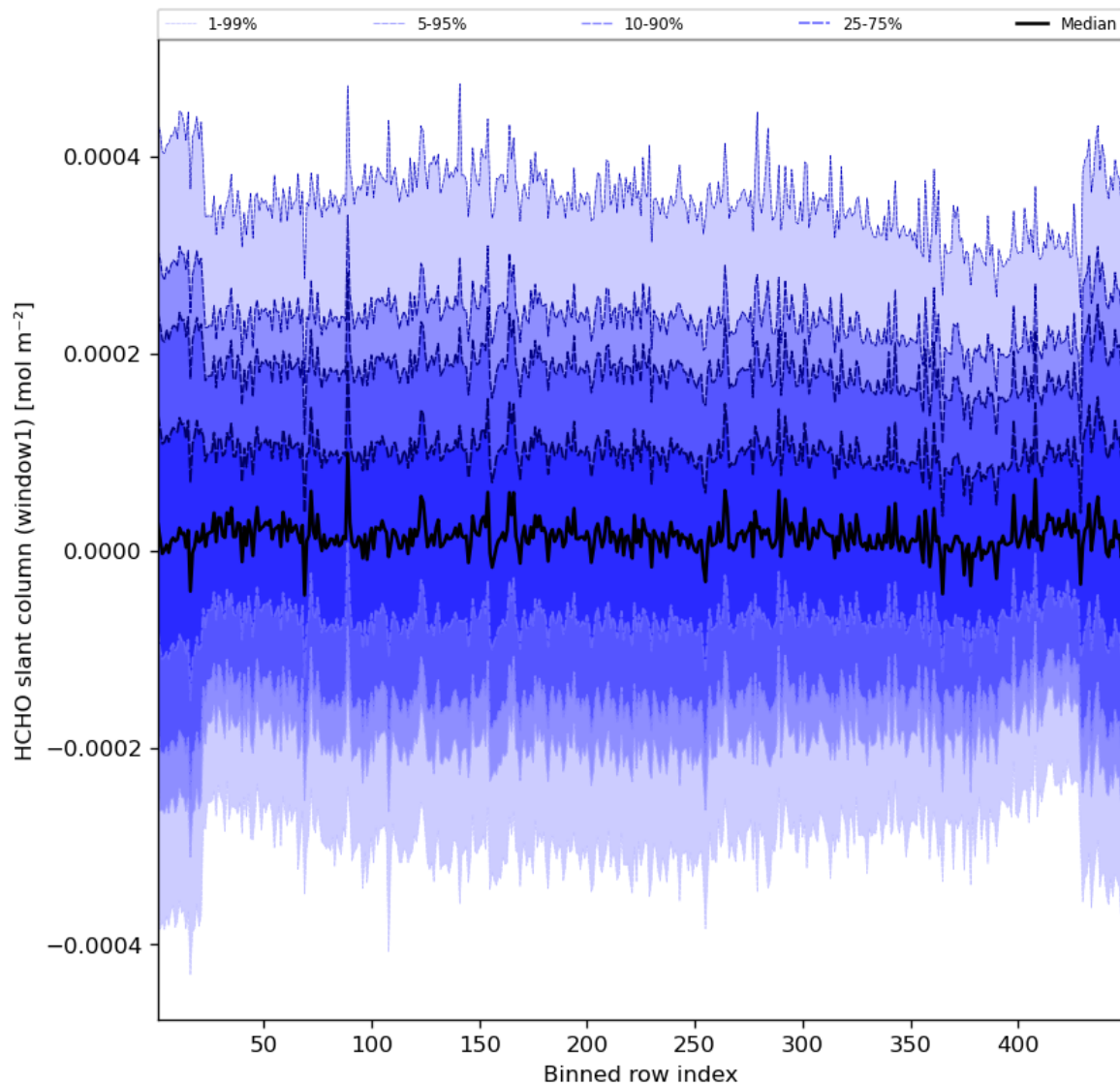


Figure 52: Along track statistics of “HCHO slant column (window1)” for 2023-09-11 to 2023-09-13

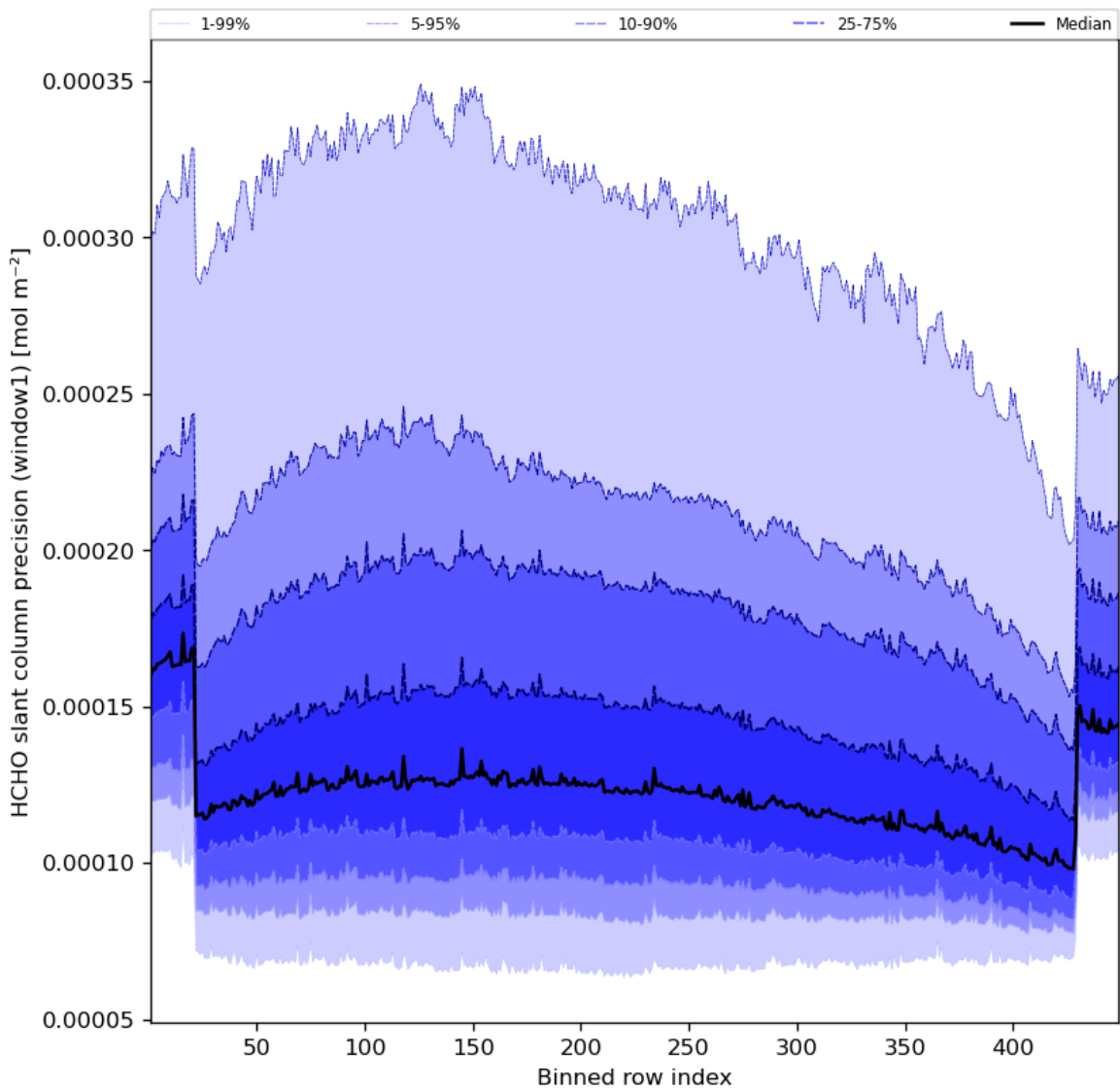


Figure 53: Along track statistics of “HCHO slant column precision (window1)” for 2023-09-11 to 2023-09-13

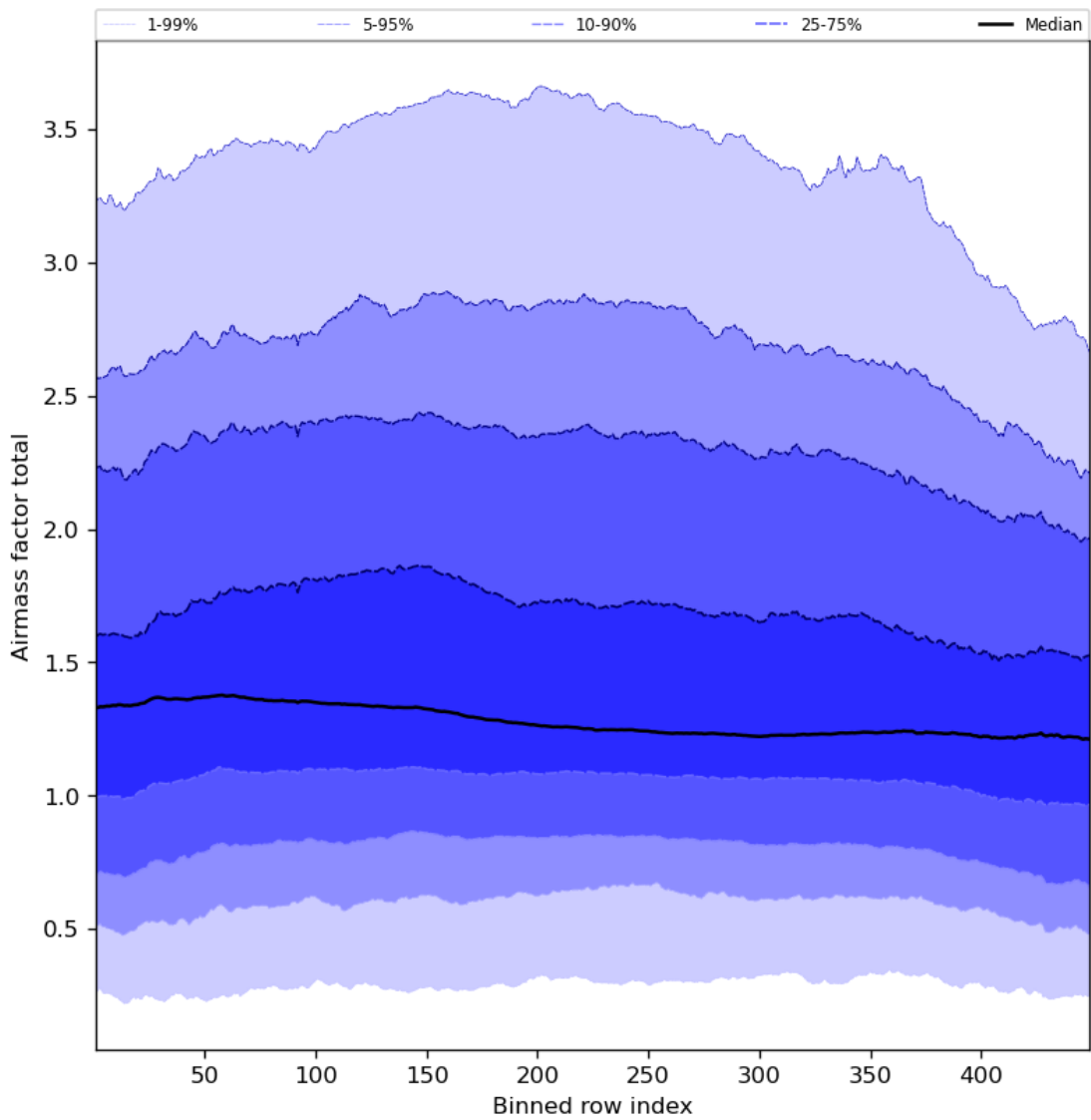


Figure 54: Along track statistics of “Airmass factor total” for 2023-09-11 to 2023-09-13

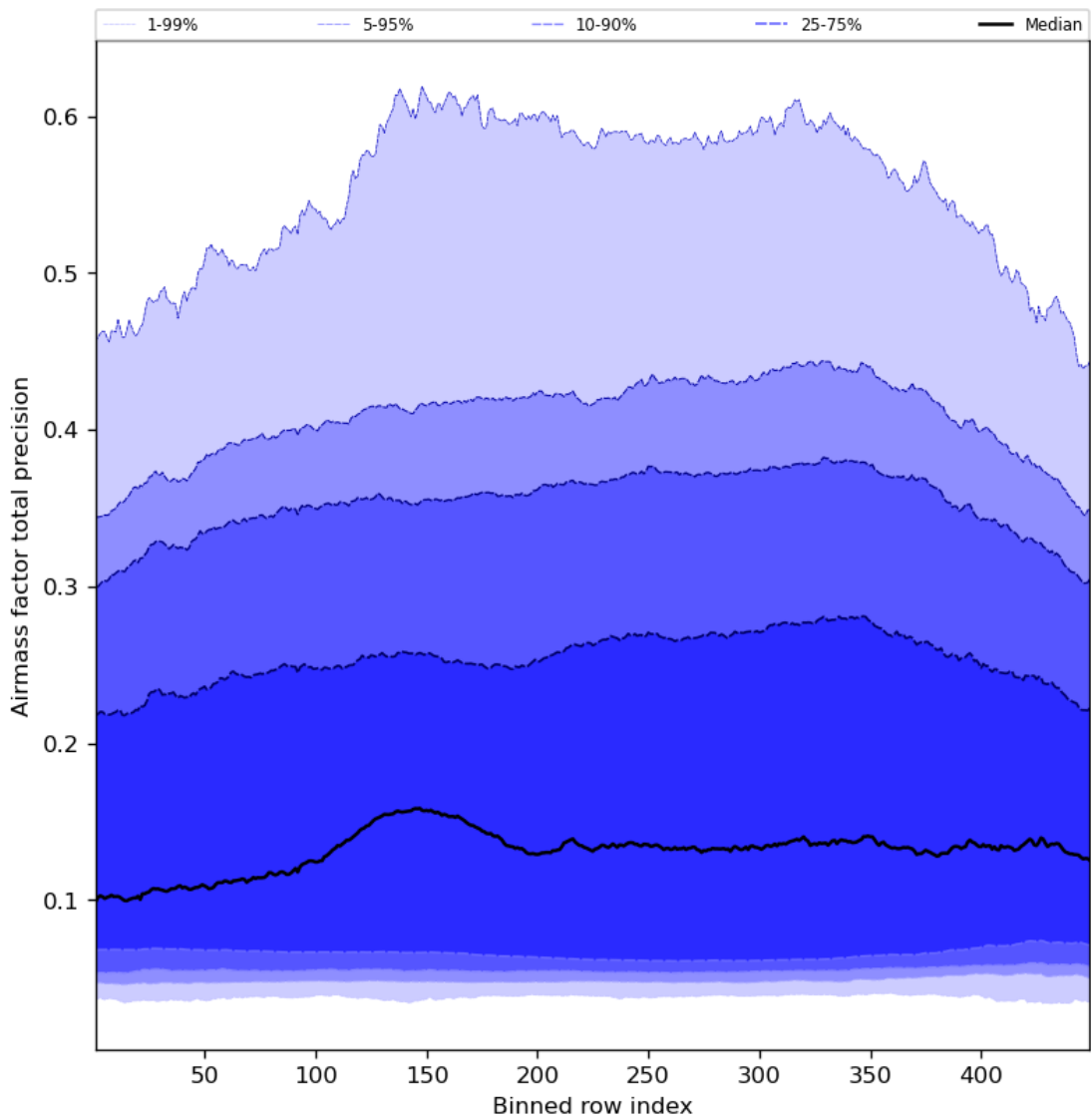


Figure 55: Along track statistics of “Airmass factor total precision” for 2023-09-11 to 2023-09-13

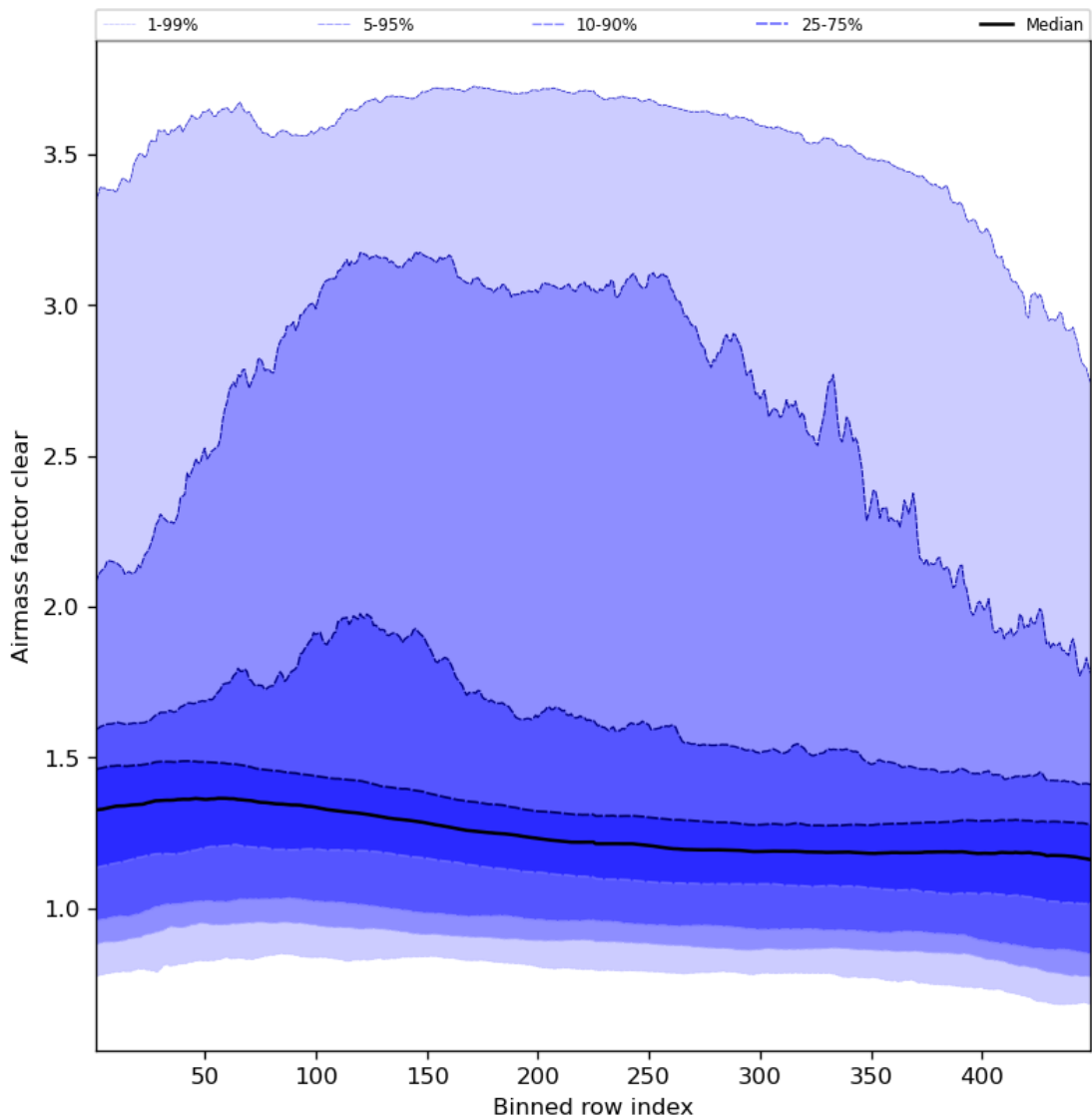


Figure 56: Along track statistics of “Airmass factor clear” for 2023-09-11 to 2023-09-13

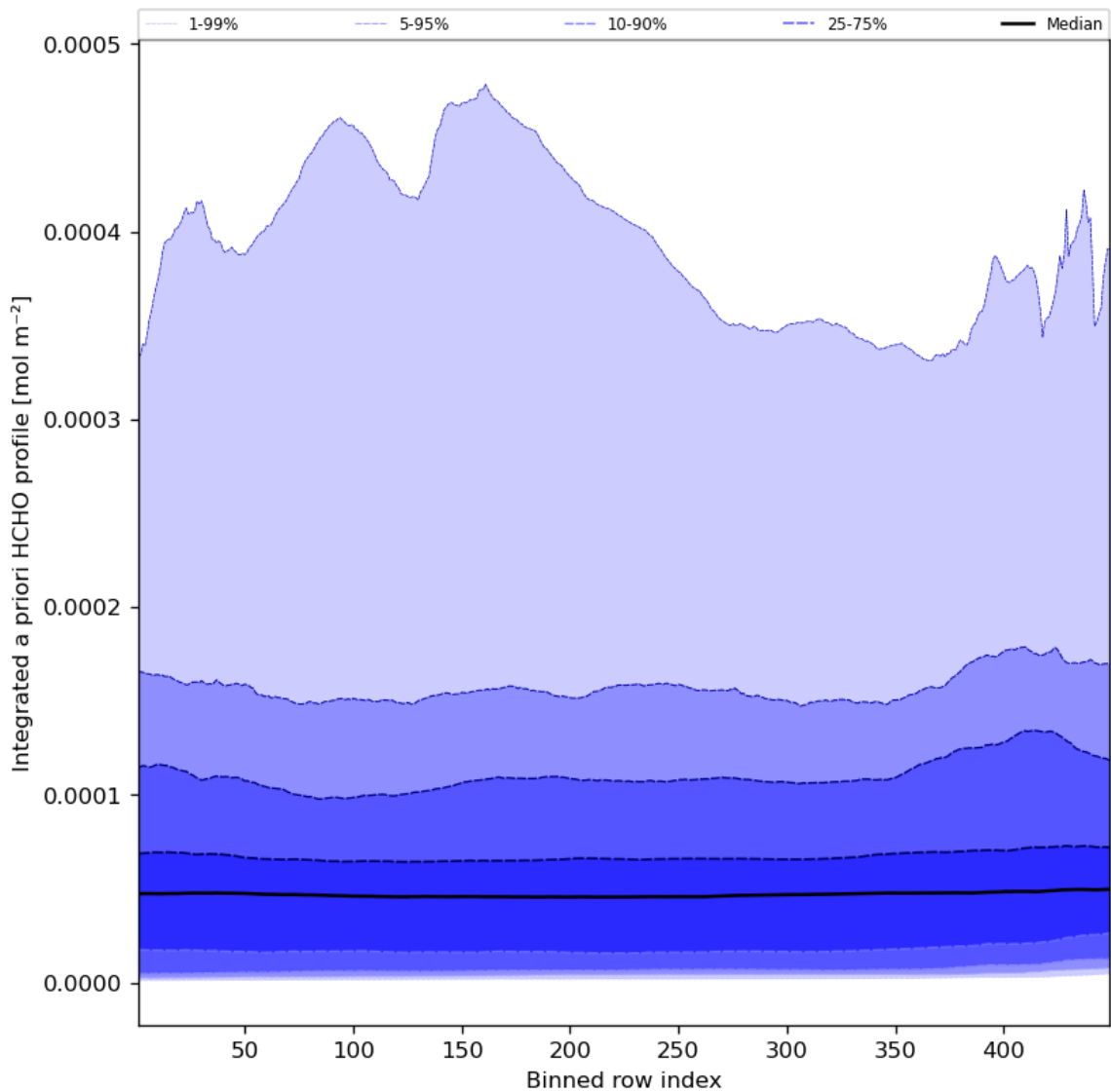


Figure 57: Along track statistics of “Integrated a priori HCHO profile” for 2023-09-11 to 2023-09-13

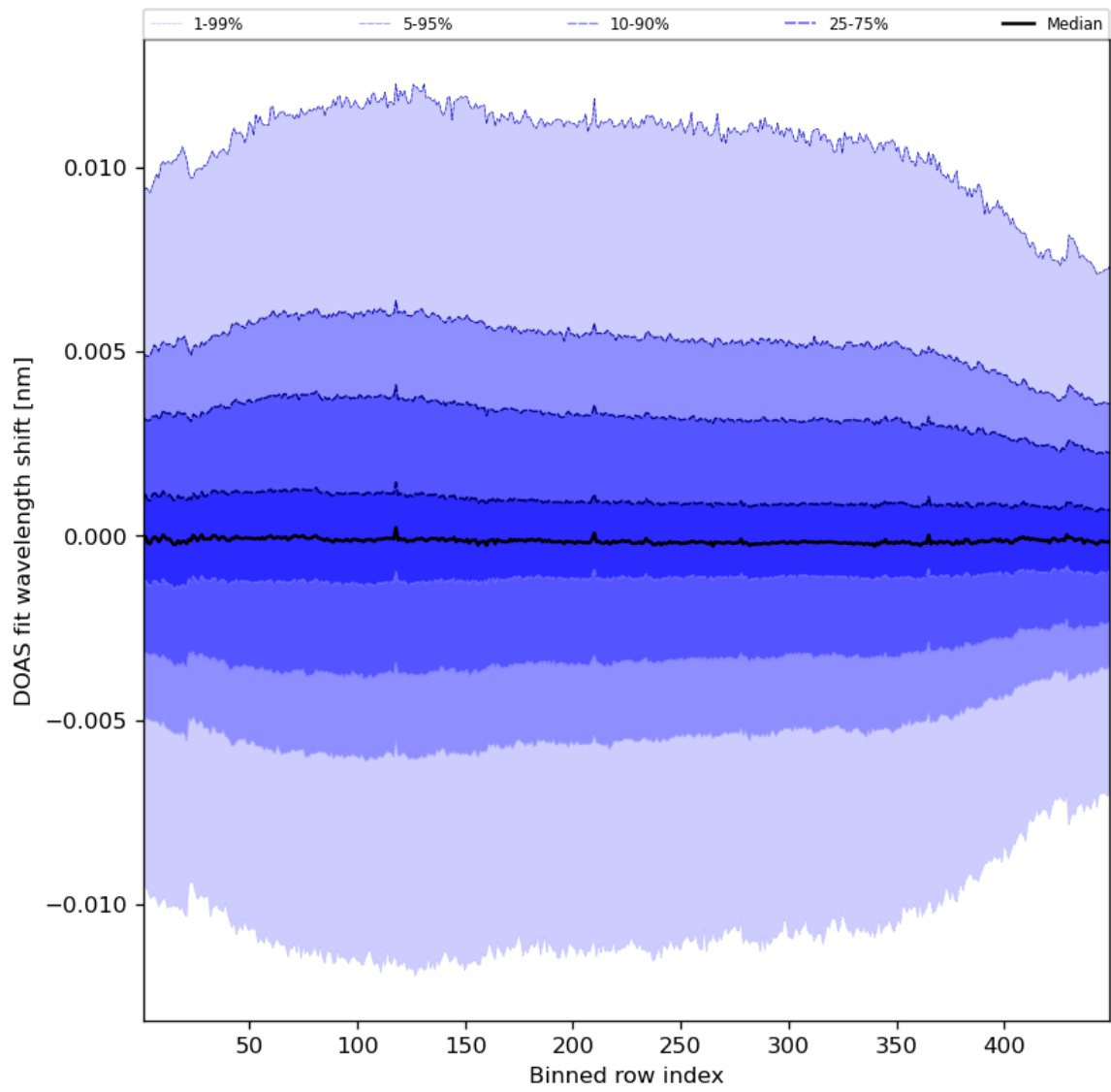


Figure 58: Along track statistics of “DOAS fit wavelength shift” for 2023-09-11 to 2023-09-13

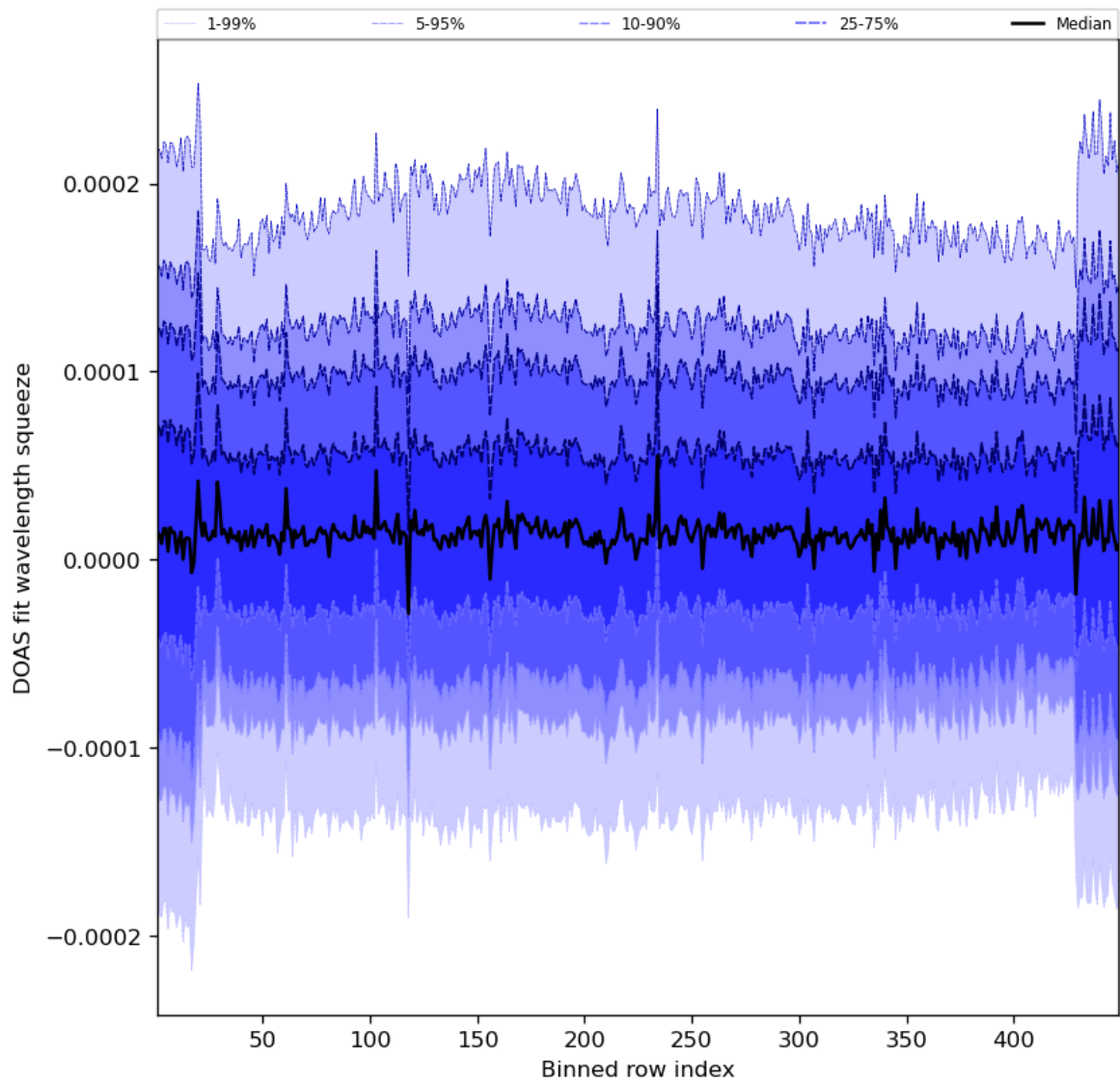


Figure 59: Along track statistics of “DOAS fit wavelength squeeze” for 2023-09-11 to 2023-09-13

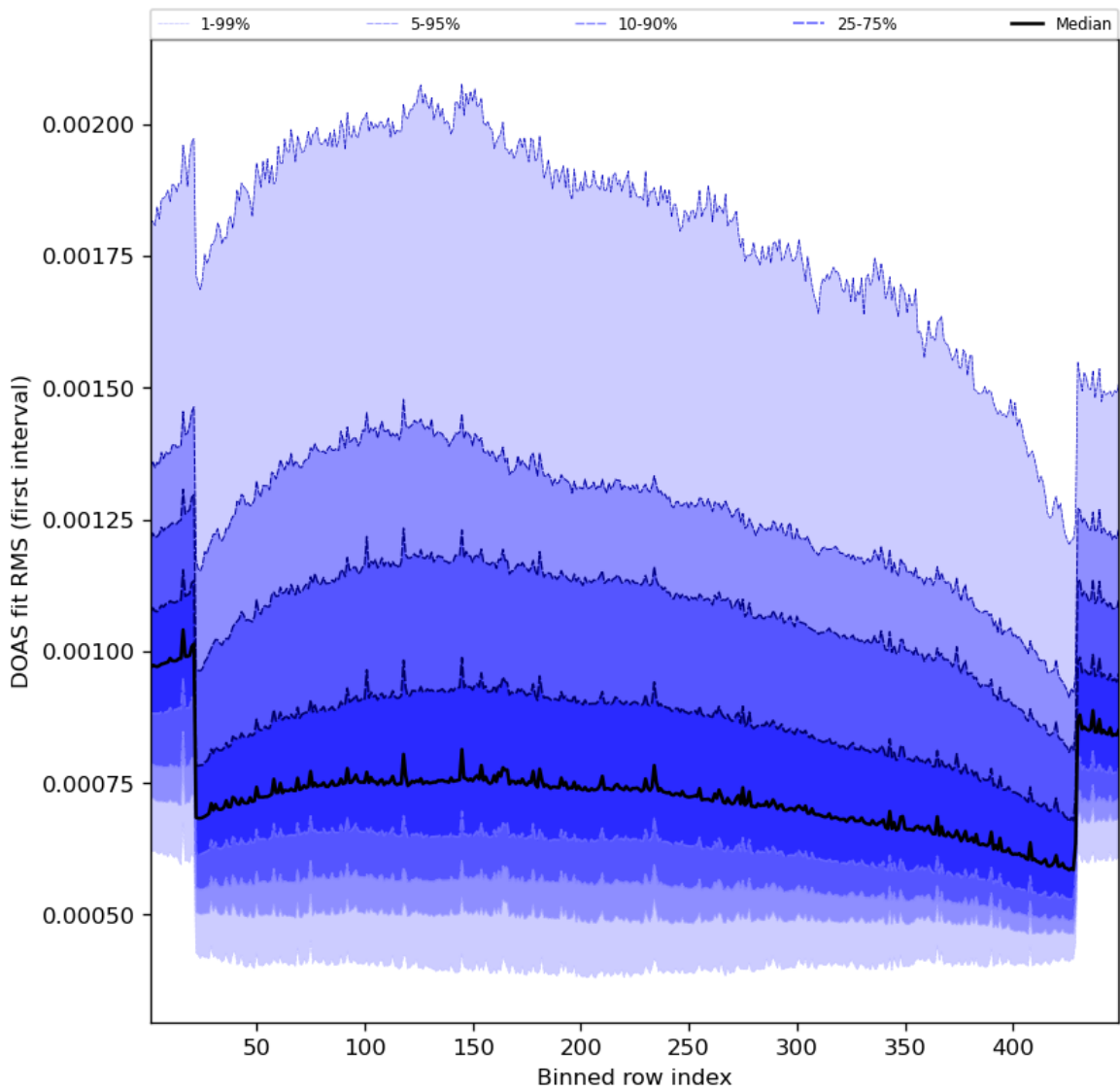


Figure 60: Along track statistics of “DOAS fit RMS (first interval)” for 2023-09-11 to 2023-09-13

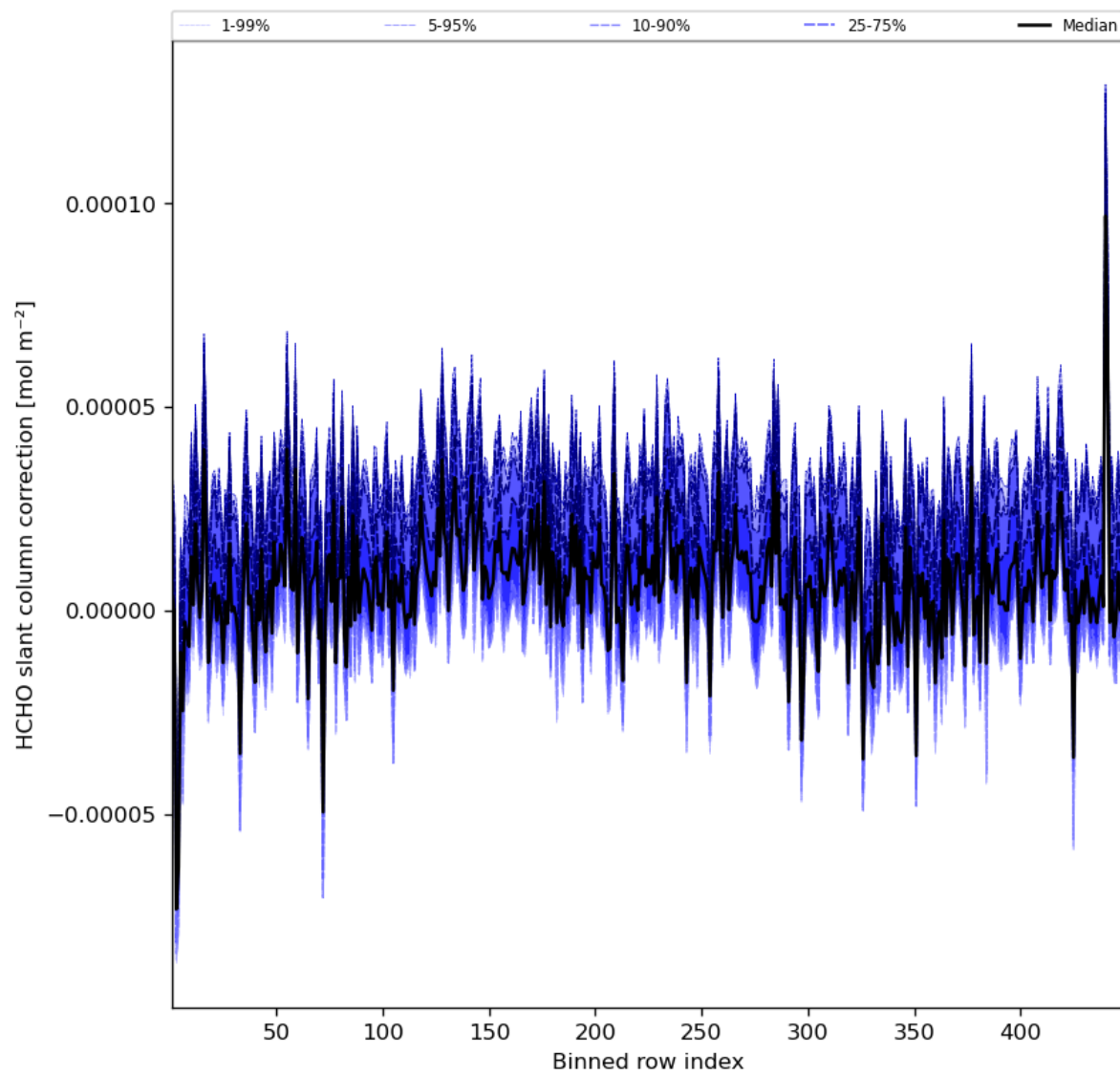


Figure 61: Along track statistics of “HCHO slant column correction” for 2023-09-11 to 2023-09-13

10 Coincidence density

To investigate the relation between parameters scatter density plots are produced. These include some ‘hidden’ parameters, latitude and the solar- and viewing geometries, in addition to all configured parameters. All combinations of pairs of parameters are included *once*, in one direction alone.

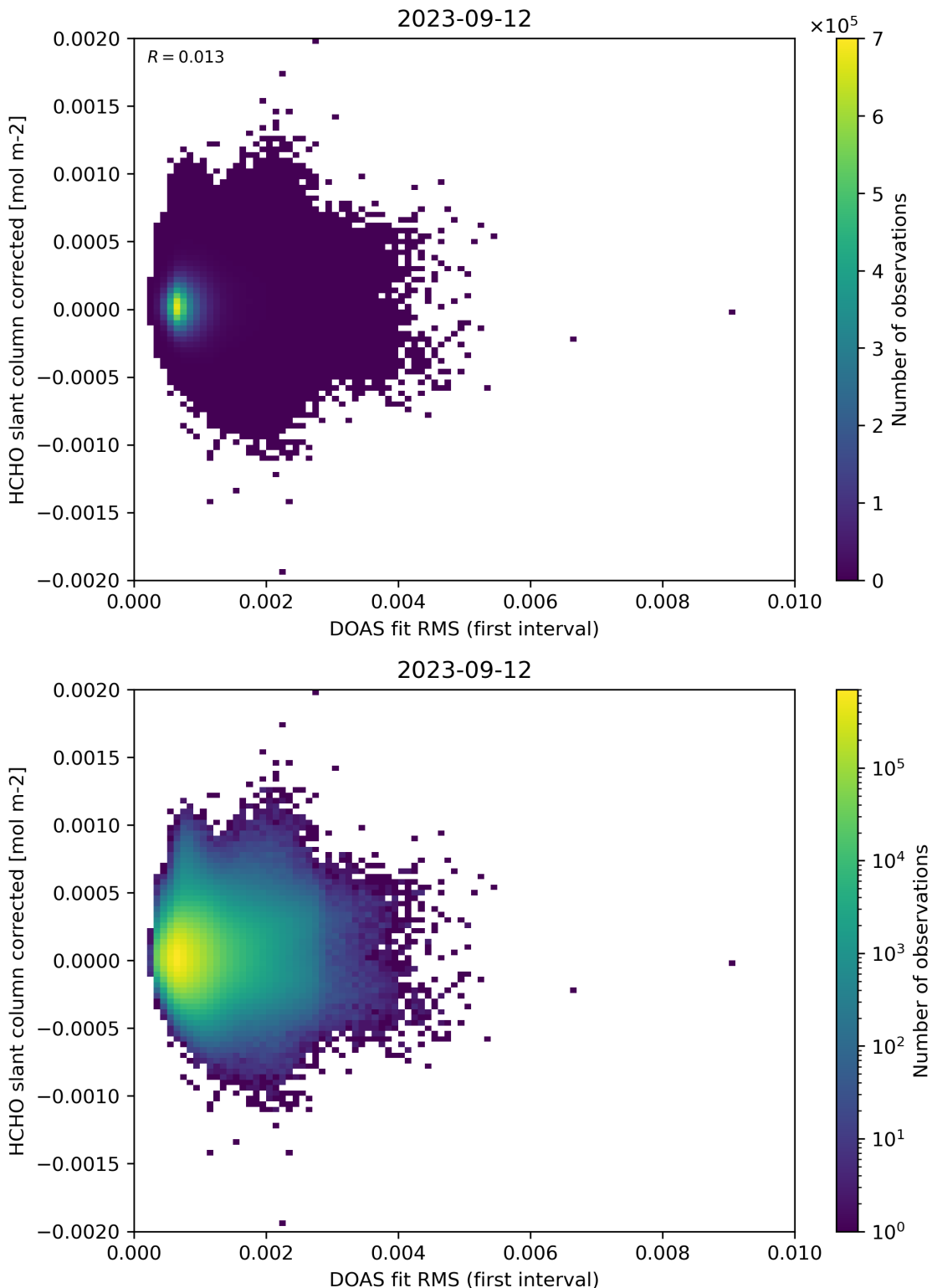


Figure 62: Scatter density plot of “DOAS fit RMS (first interval)” against “HCHO slant column corrected” for 2023-09-11 to 2023-09-13.

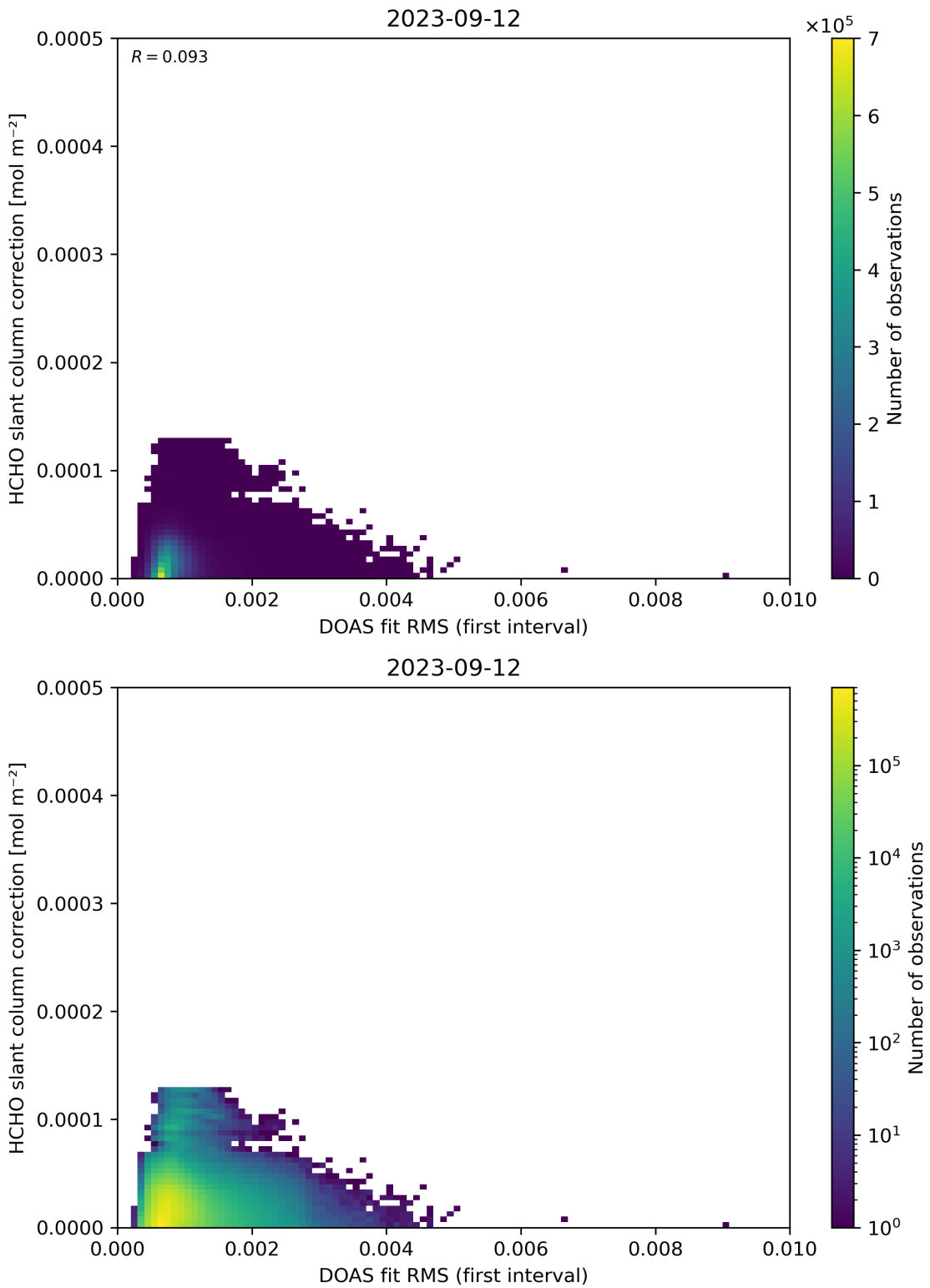


Figure 63: Scatter density plot of “DOAS fit RMS (first interval)” against “HCHO slant column correction” for 2023-09-11 to 2023-09-13.

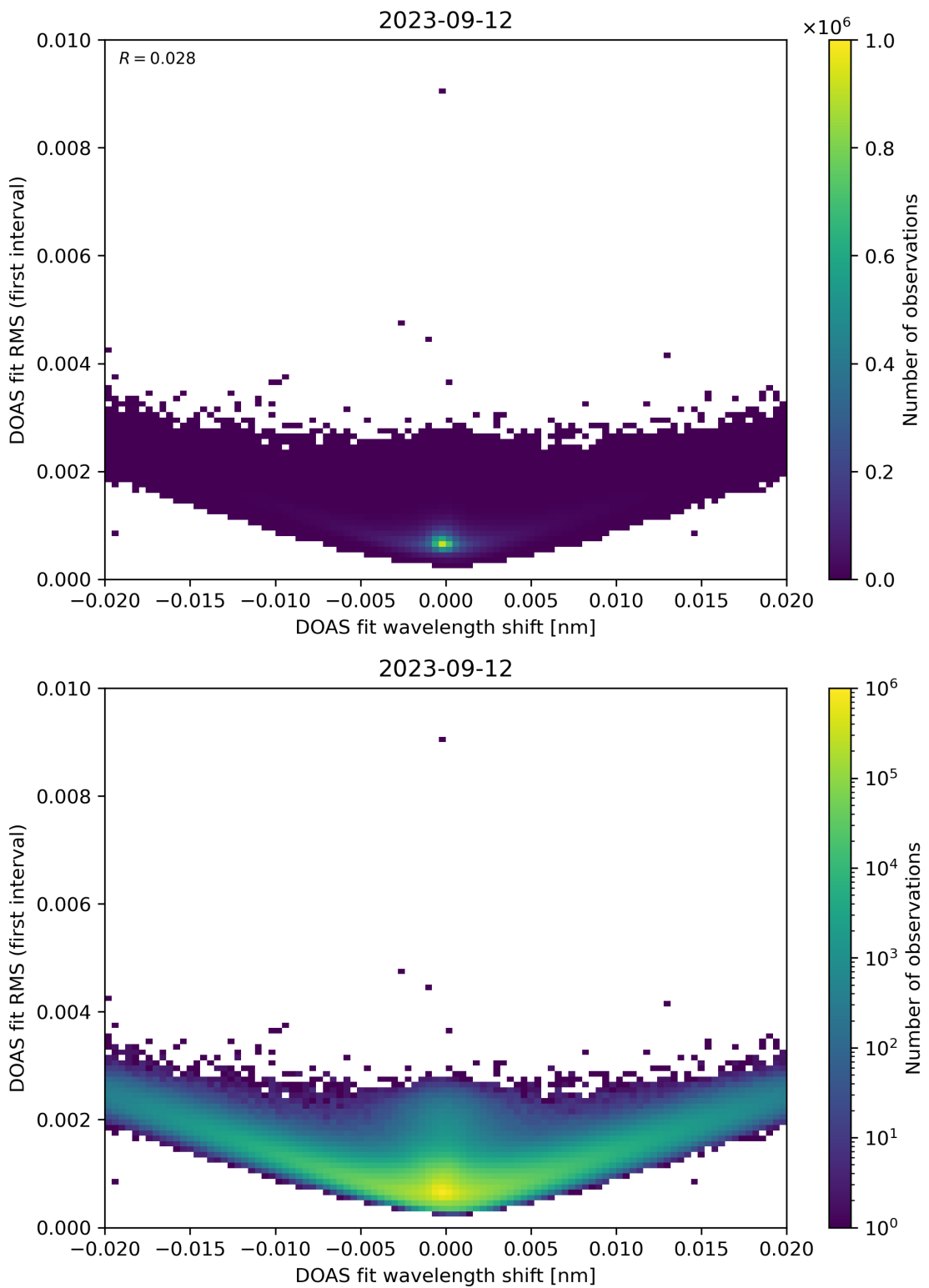


Figure 64: Scatter density plot of “DOAS fit wavelength shift” against “DOAS fit RMS (first interval)” for 2023-09-11 to 2023-09-13.

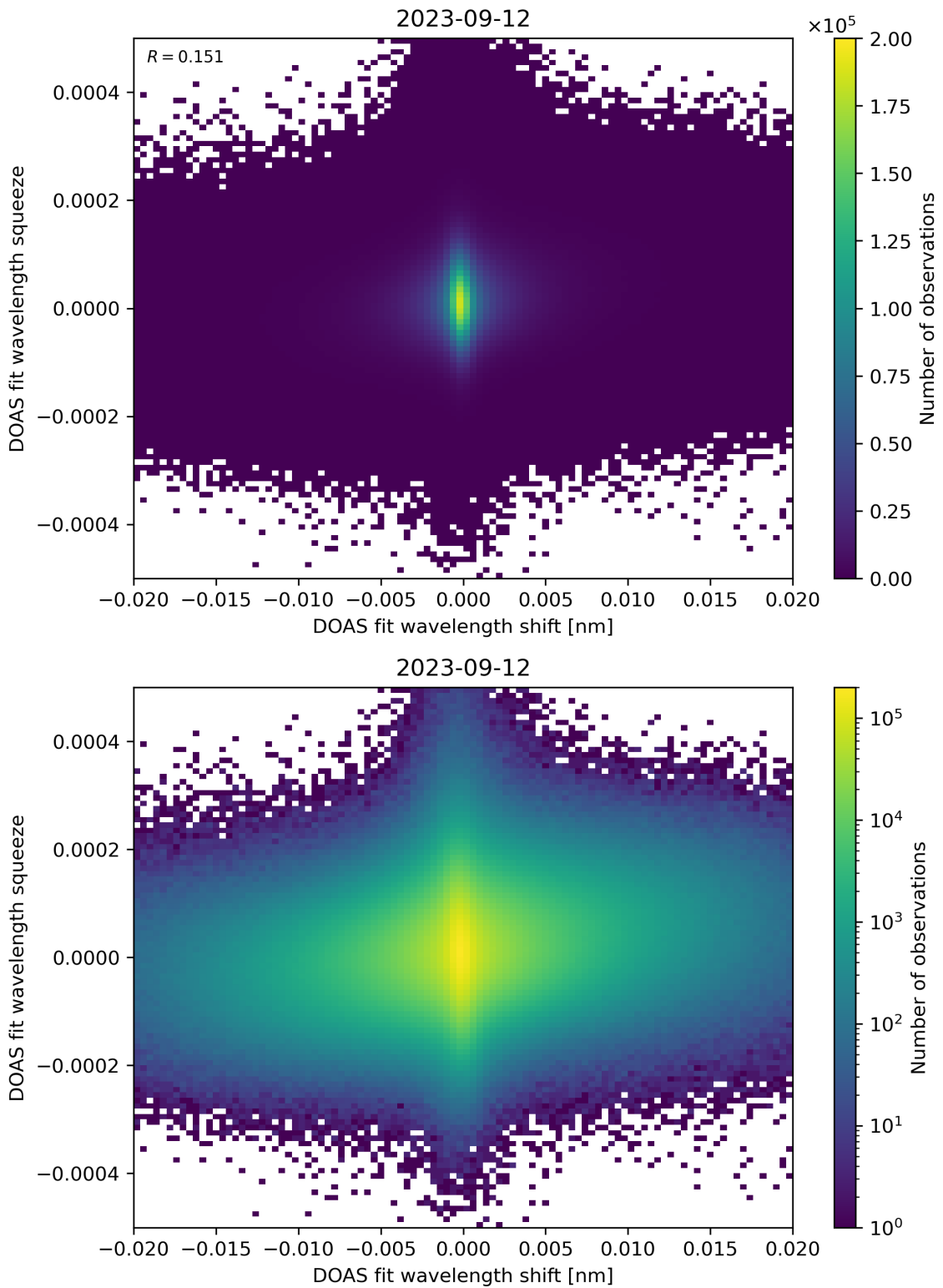


Figure 65: Scatter density plot of “DOAS fit wavelength shift” against “DOAS fit wavelength squeeze” for 2023-09-11 to 2023-09-13.

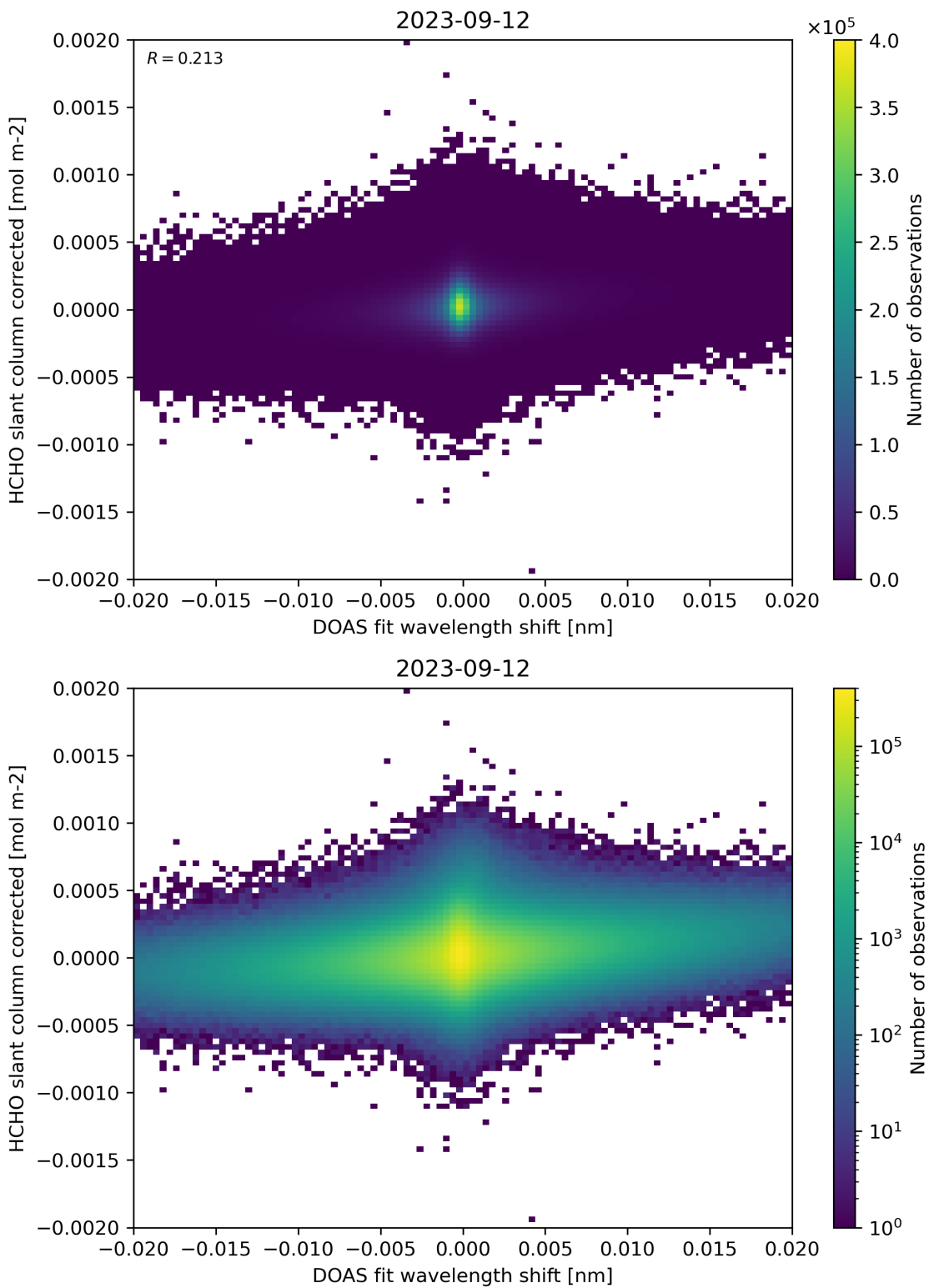


Figure 66: Scatter density plot of “DOAS fit wavelength shift” against “HCHO slant column corrected” for 2023-09-11 to 2023-09-13.

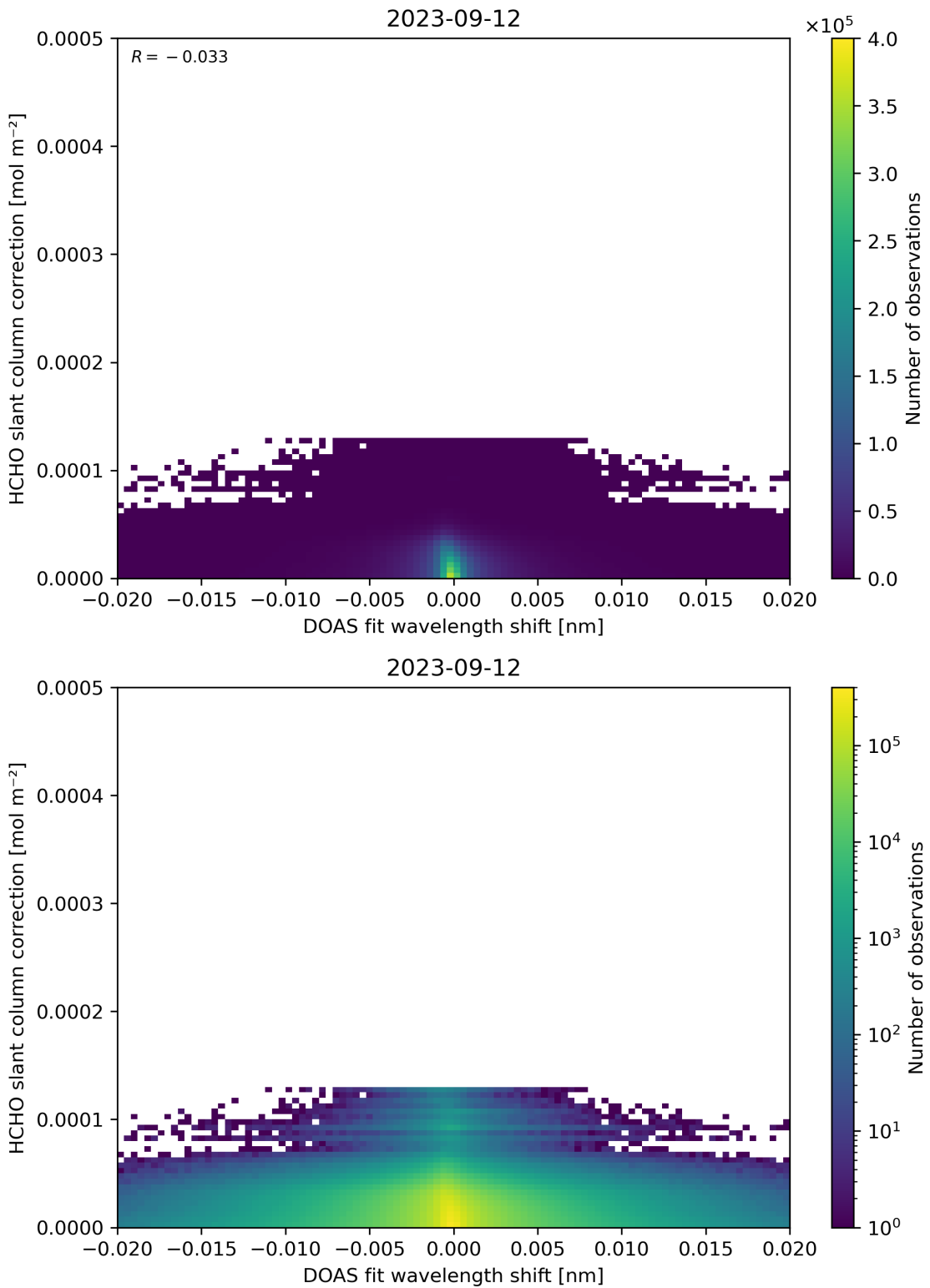


Figure 67: Scatter density plot of “DOAS fit wavelength shift” against “HCHO slant column correction” for 2023-09-11 to 2023-09-13.

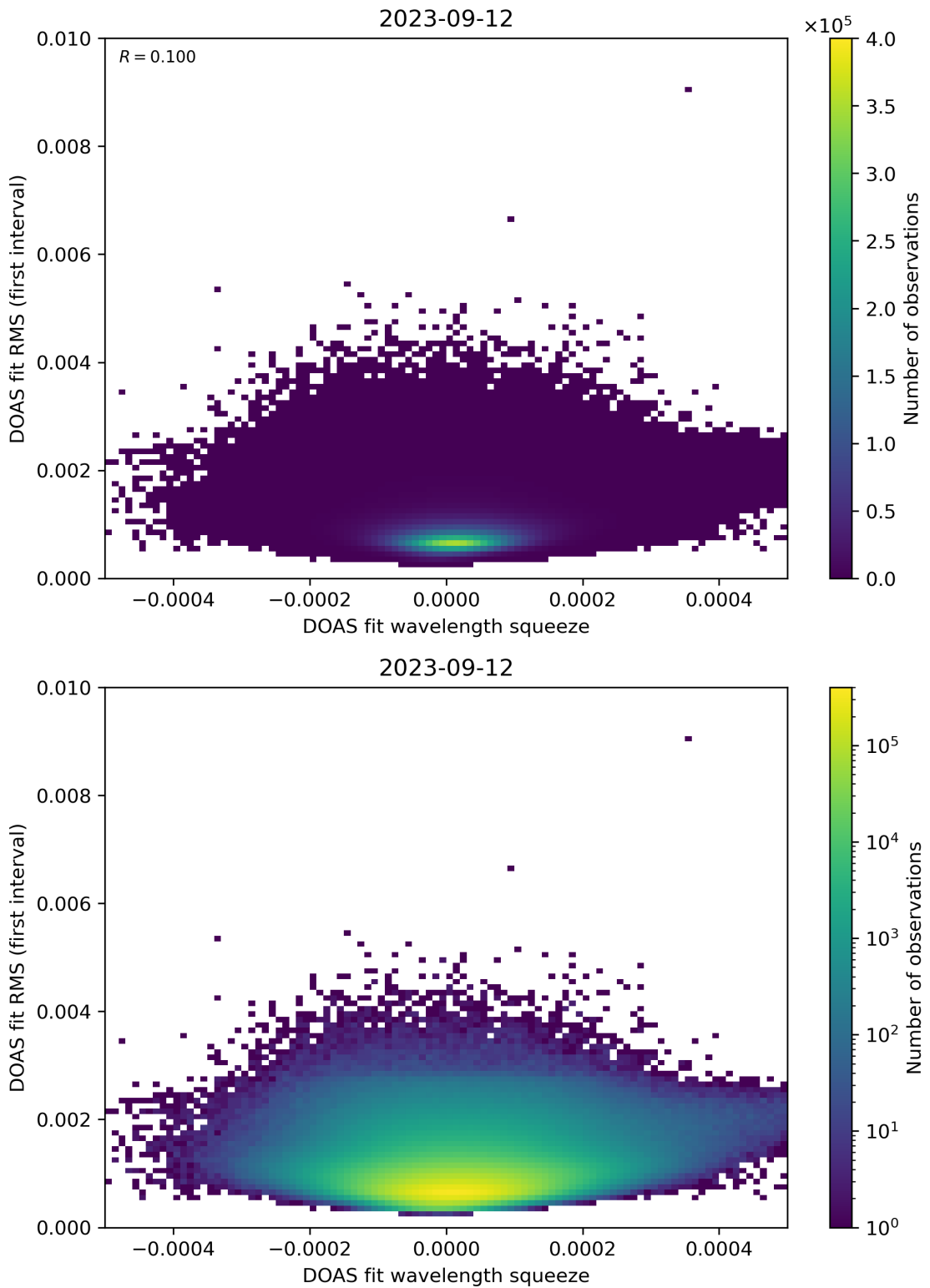


Figure 68: Scatter density plot of “DOAS fit wavelength squeeze” against “DOAS fit RMS (first interval)” for 2023-09-11 to 2023-09-13.

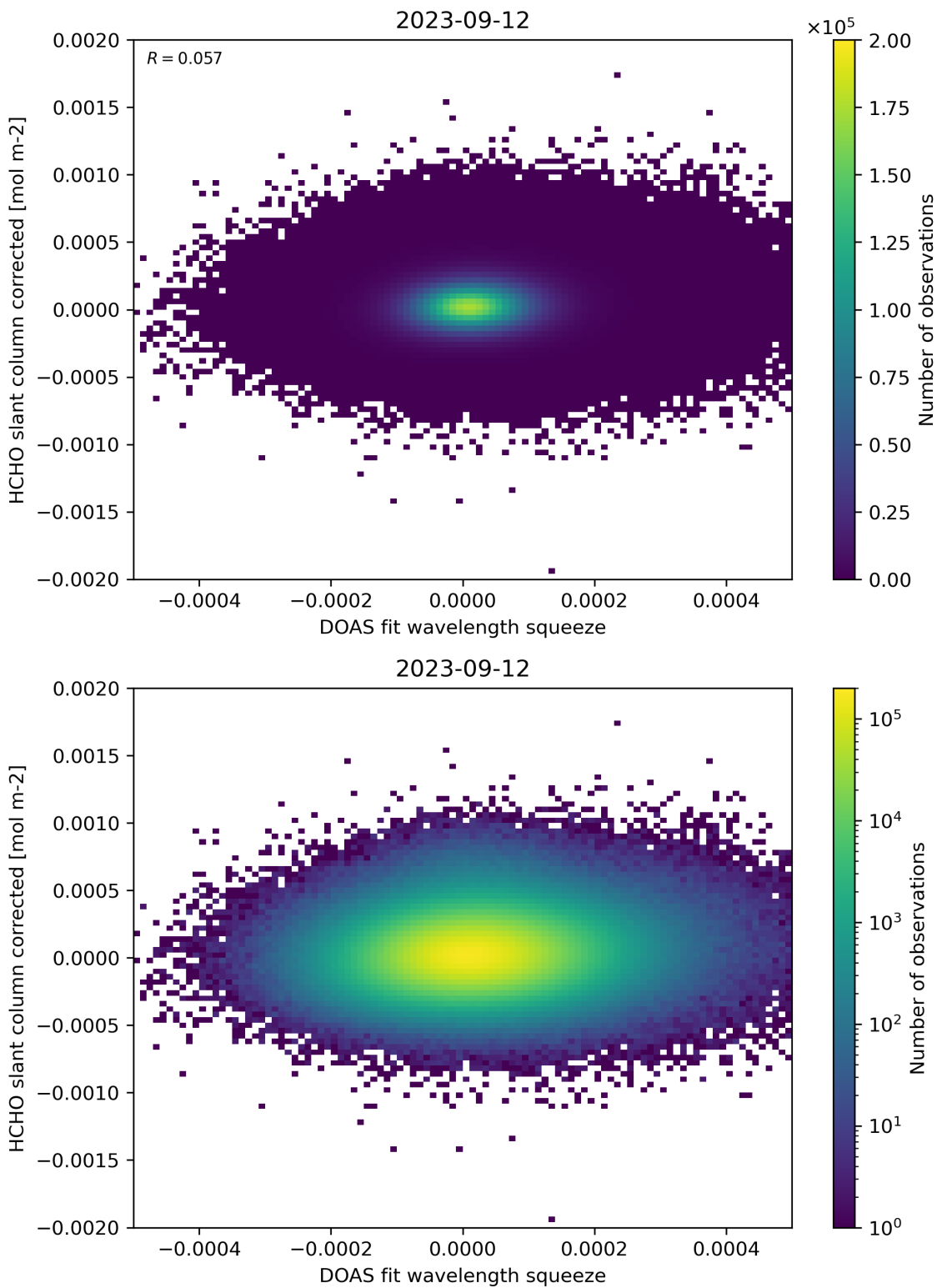


Figure 69: Scatter density plot of “DOAS fit wavelength squeeze” against “HCHO slant column corrected” for 2023-09-11 to 2023-09-13.

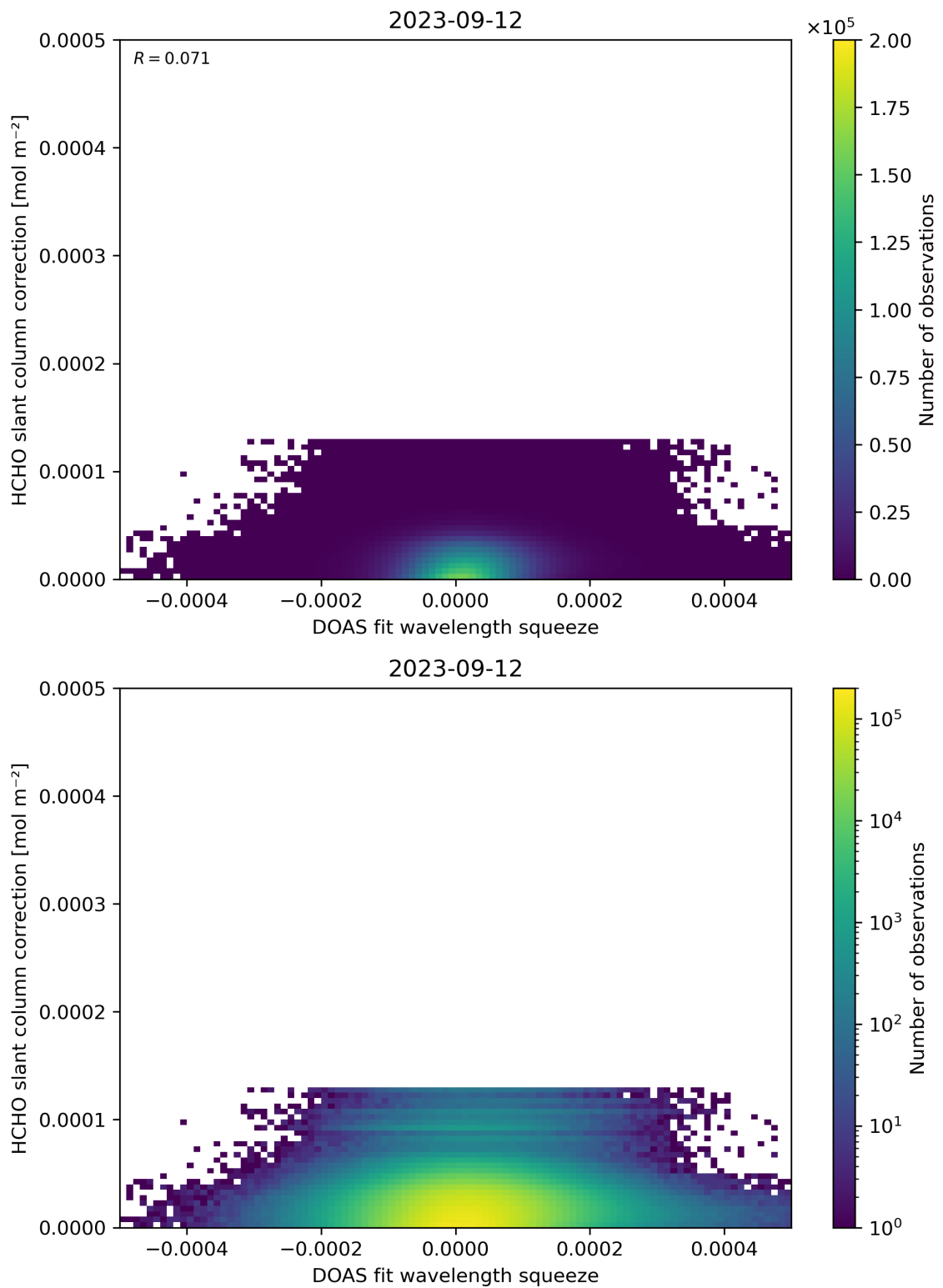


Figure 70: Scatter density plot of “DOAS fit wavelength squeeze” against “HCHO slant column correction” for 2023-09-11 to 2023-09-13.

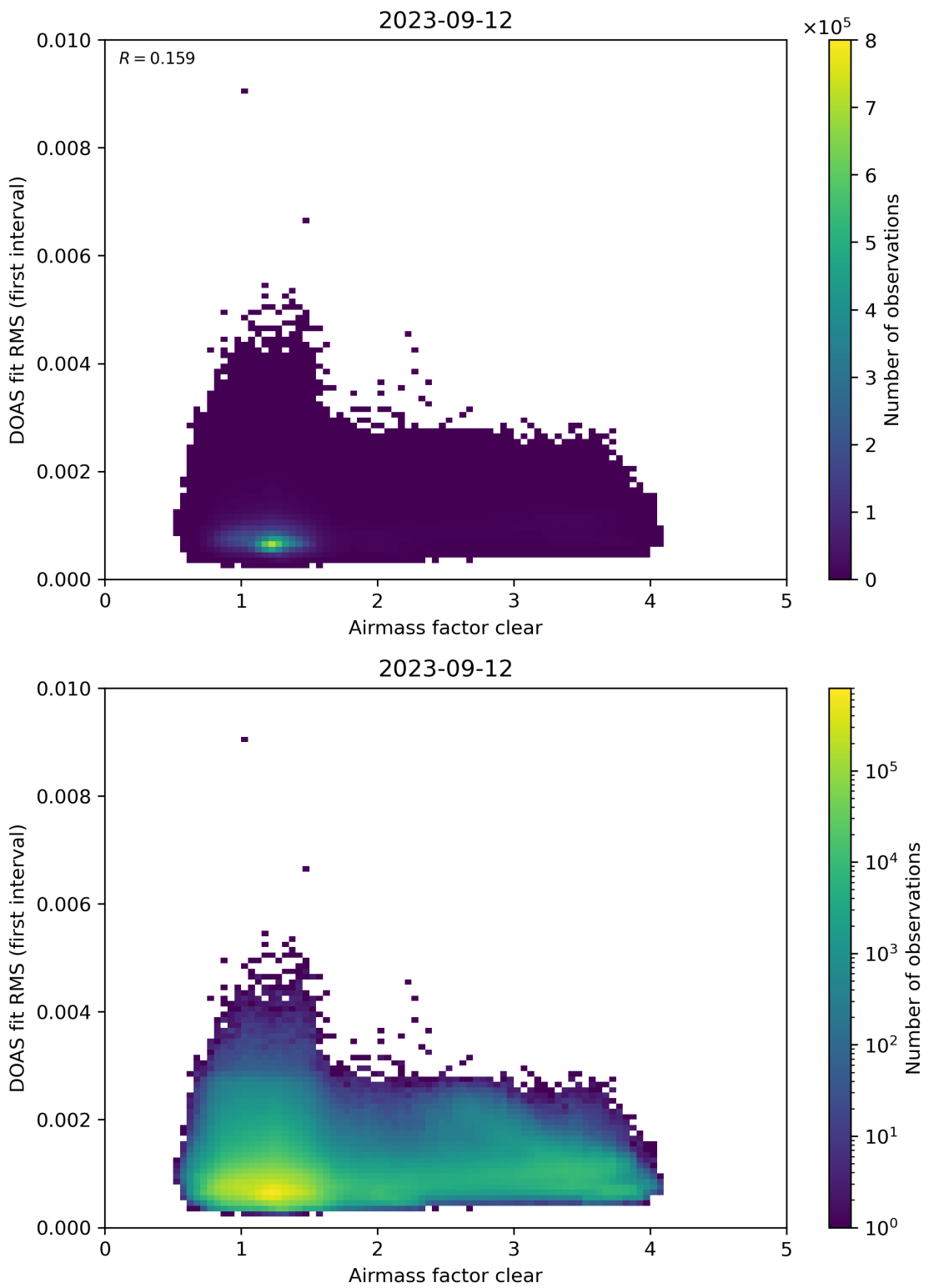


Figure 71: Scatter density plot of “Airmass factor clear” against “DOAS fit RMS (first interval)” for 2023-09-11 to 2023-09-13.

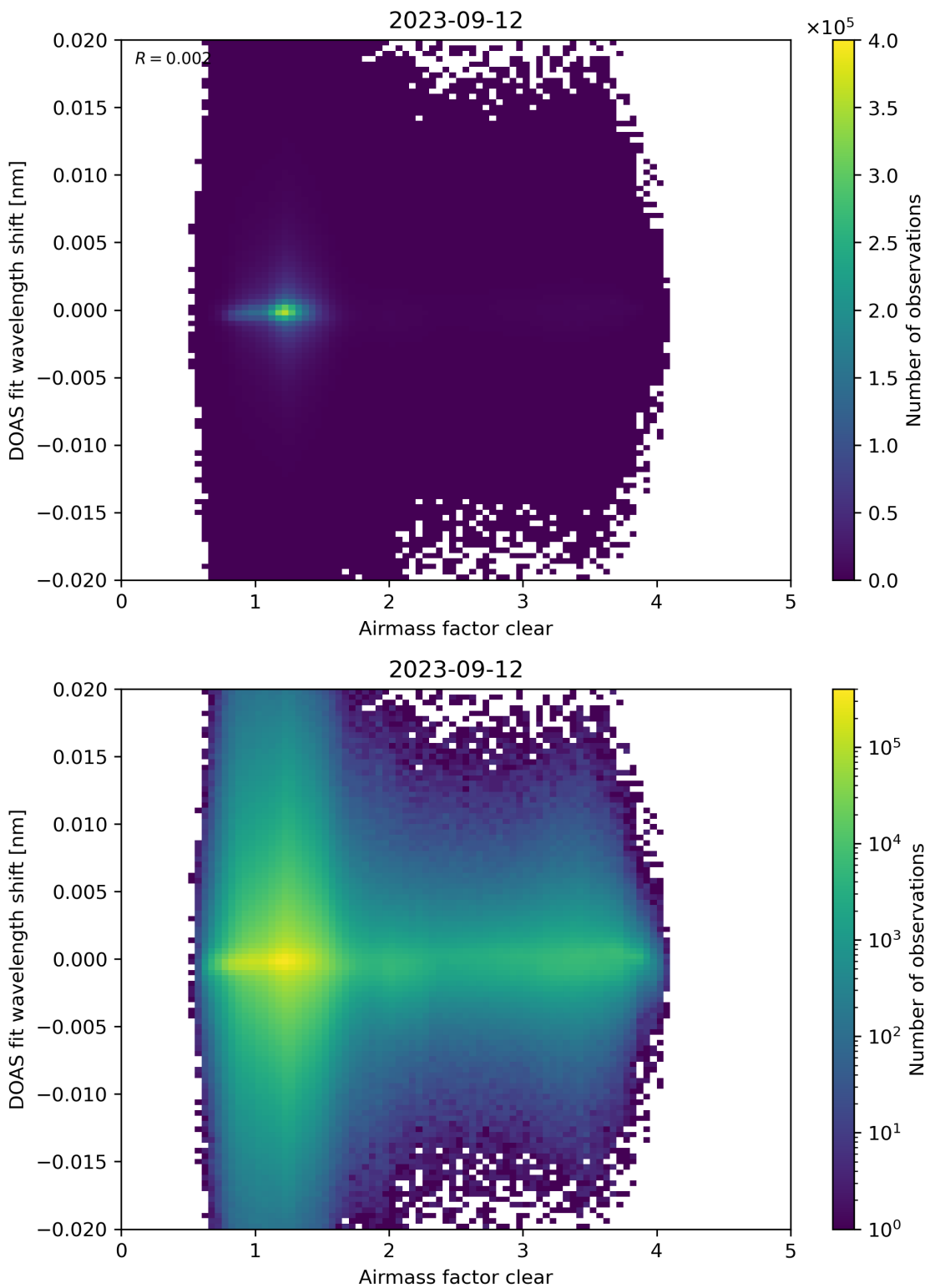


Figure 72: Scatter density plot of “Airmass factor clear” against “DOAS fit wavelength shift” for 2023-09-11 to 2023-09-13.

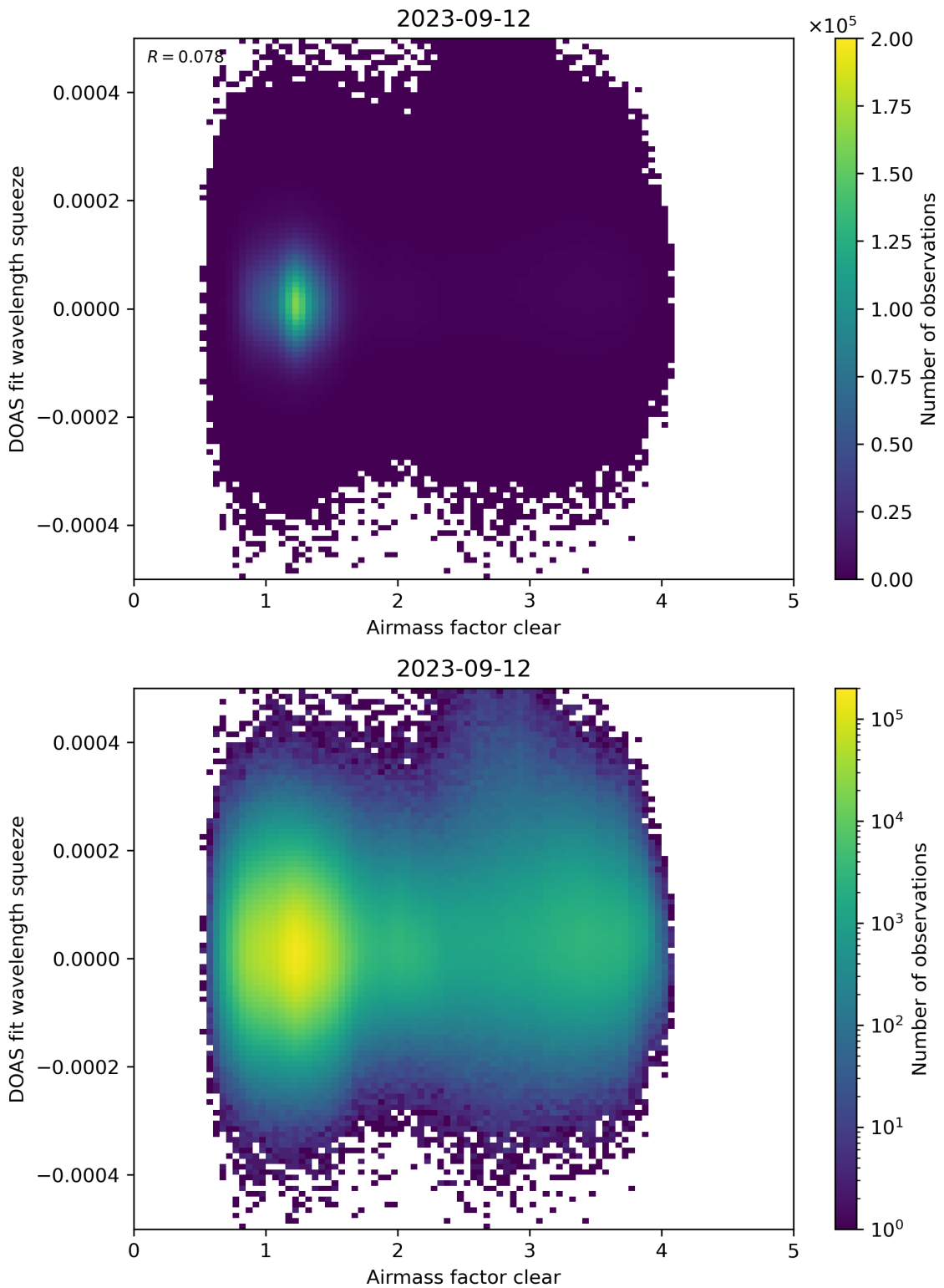


Figure 73: Scatter density plot of “Airmass factor clear” against “DOAS fit wavelength squeeze” for 2023-09-11 to 2023-09-13.

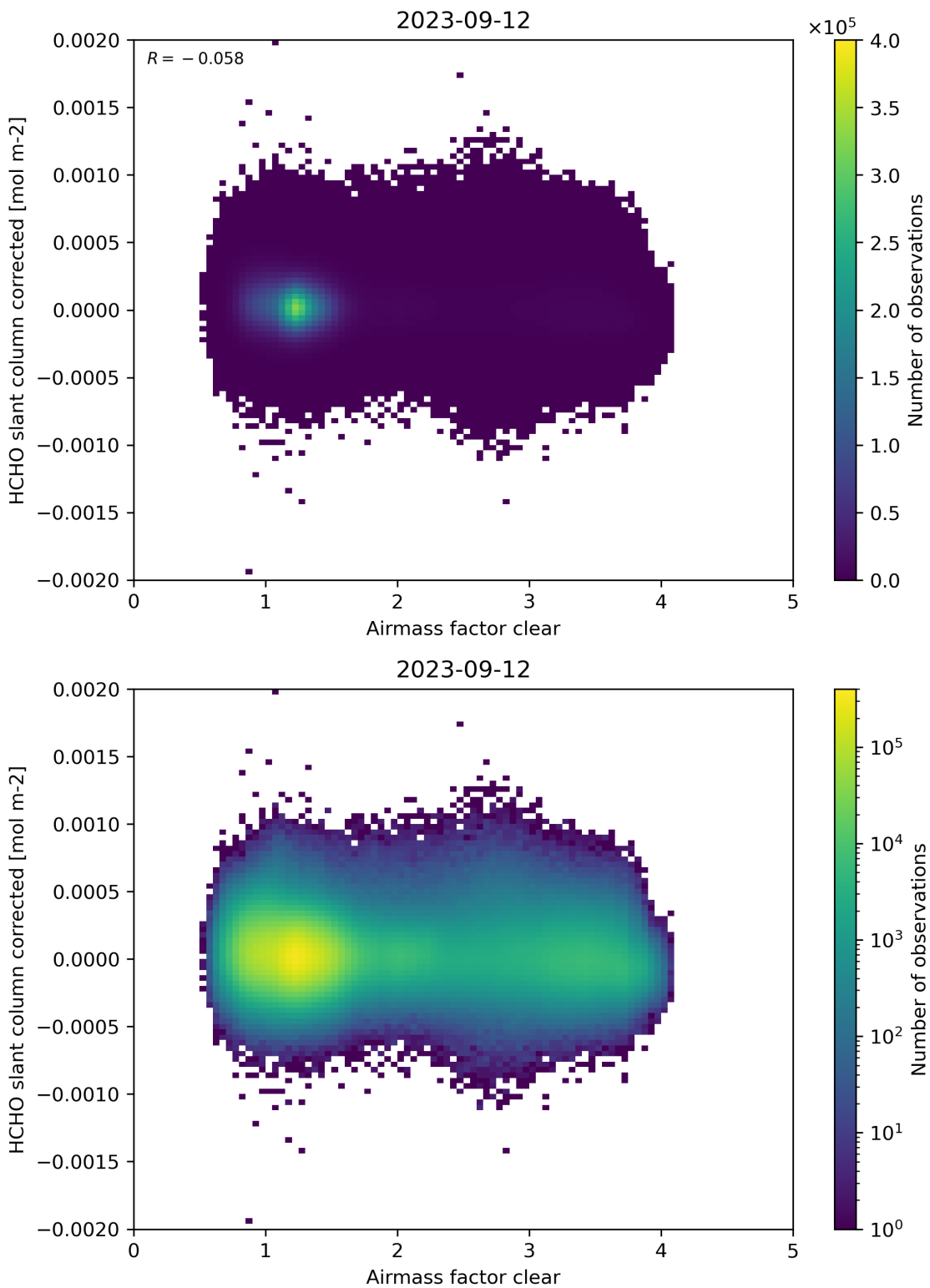


Figure 74: Scatter density plot of “Airmass factor clear” against “HCHO slant column corrected” for 2023-09-11 to 2023-09-13.

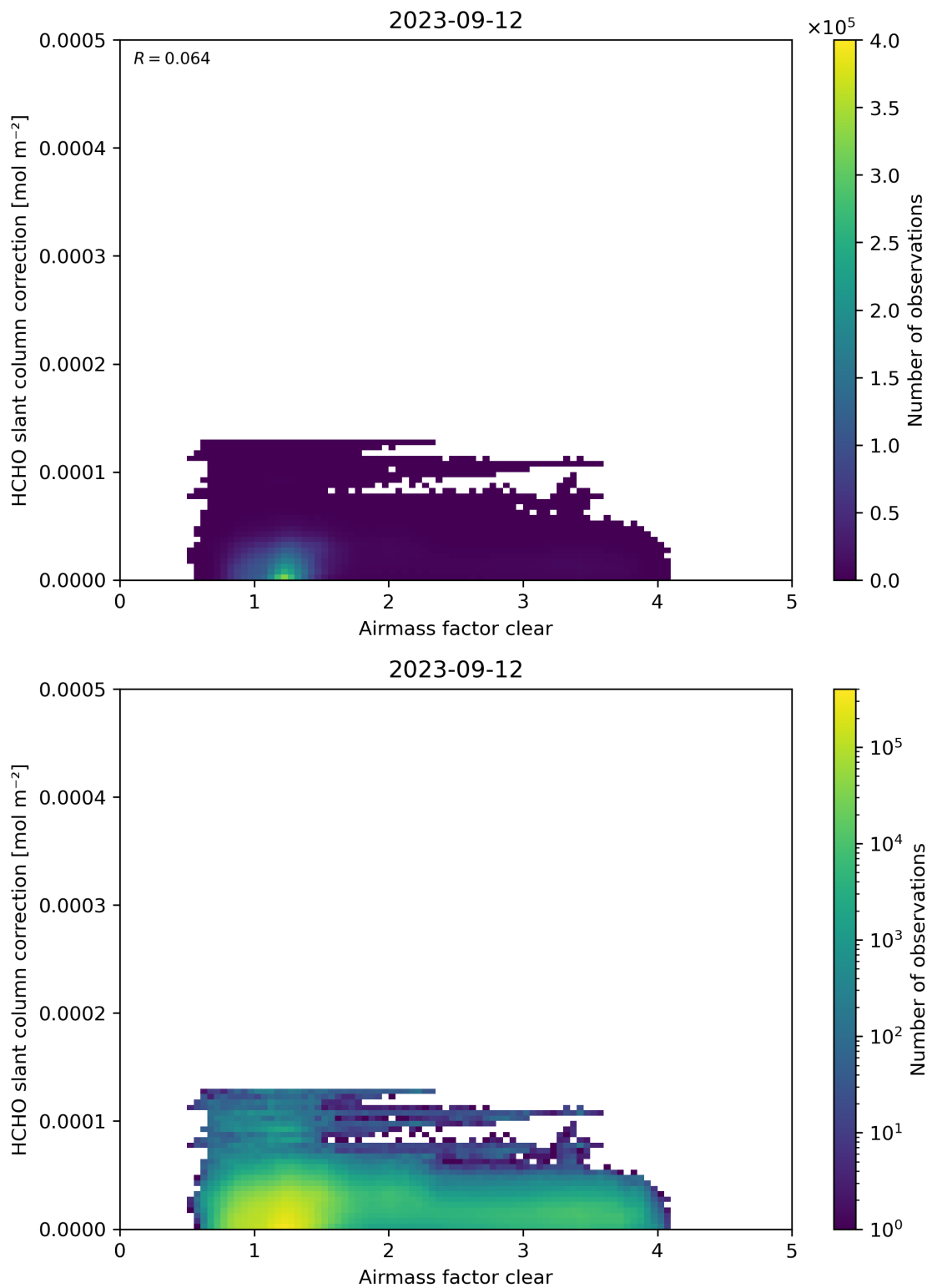


Figure 75: Scatter density plot of “Airmass factor clear” against “HCHO slant column correction” for 2023-09-11 to 2023-09-13.

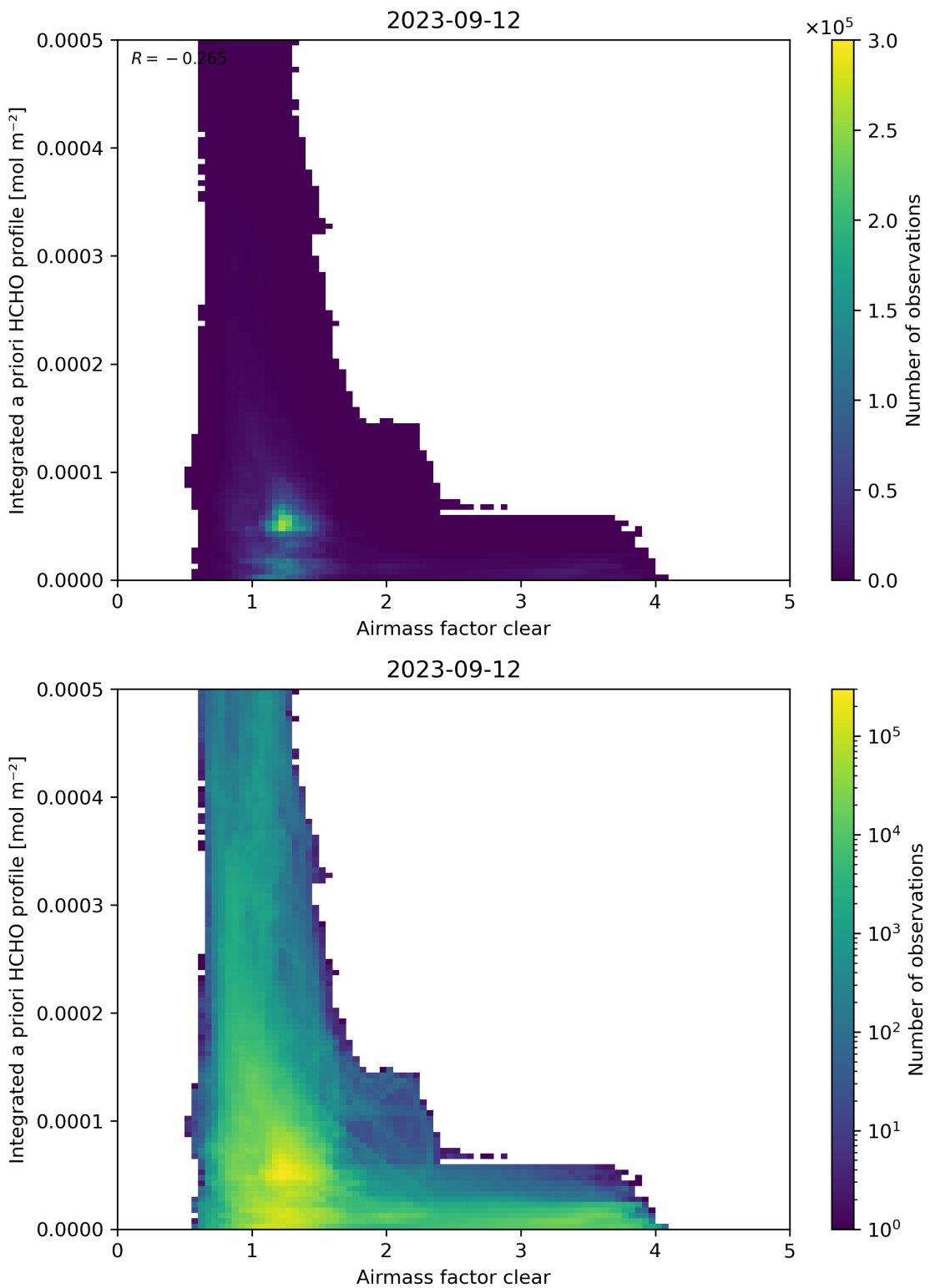


Figure 76: Scatter density plot of “Airmass factor clear” against “Integrated a priori HCHO profile” for 2023-09-11 to 2023-09-13.

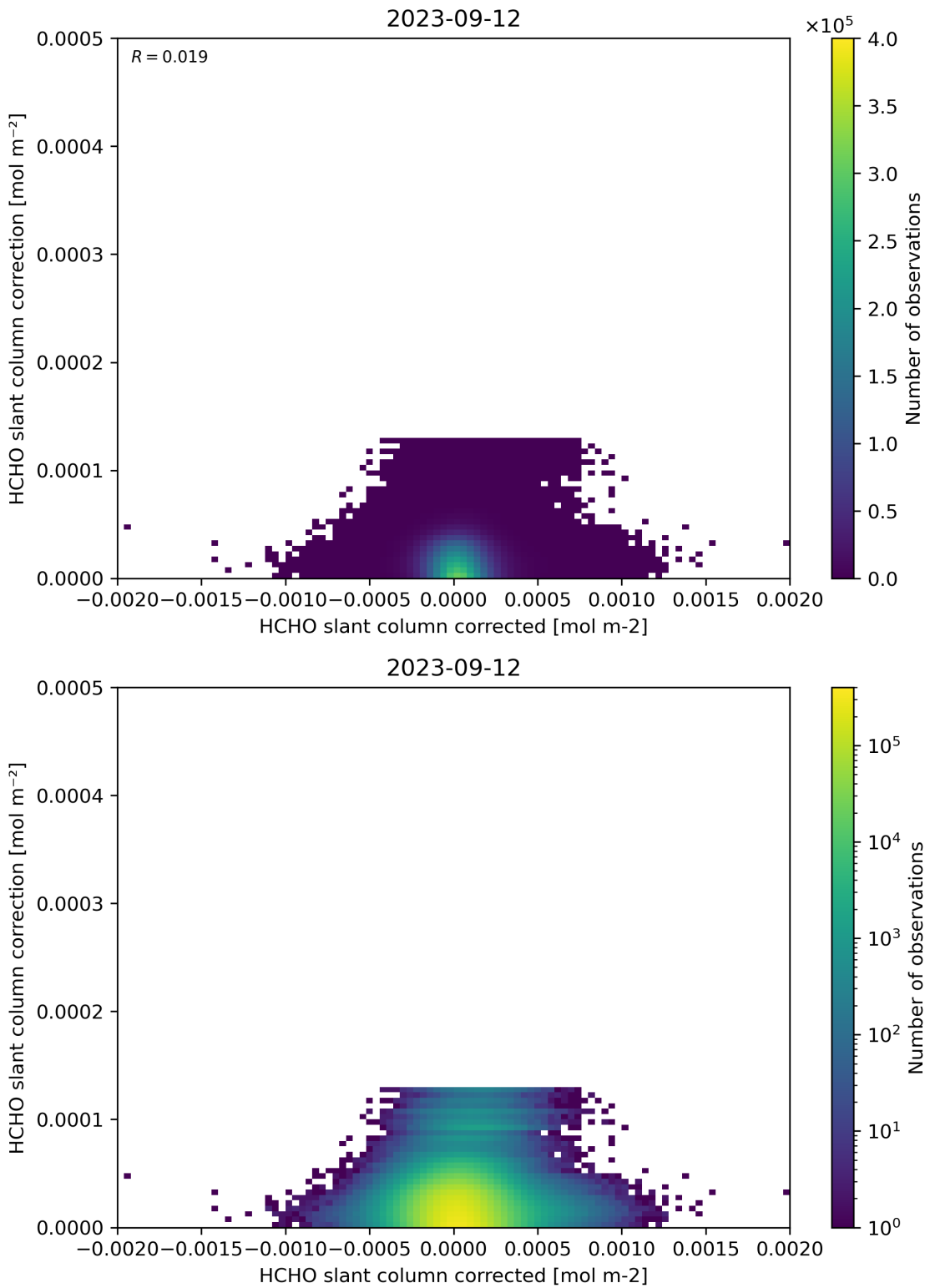


Figure 77: Scatter density plot of “HCHO slant column corrected” against “HCHO slant column correction” for 2023-09-11 to 2023-09-13.

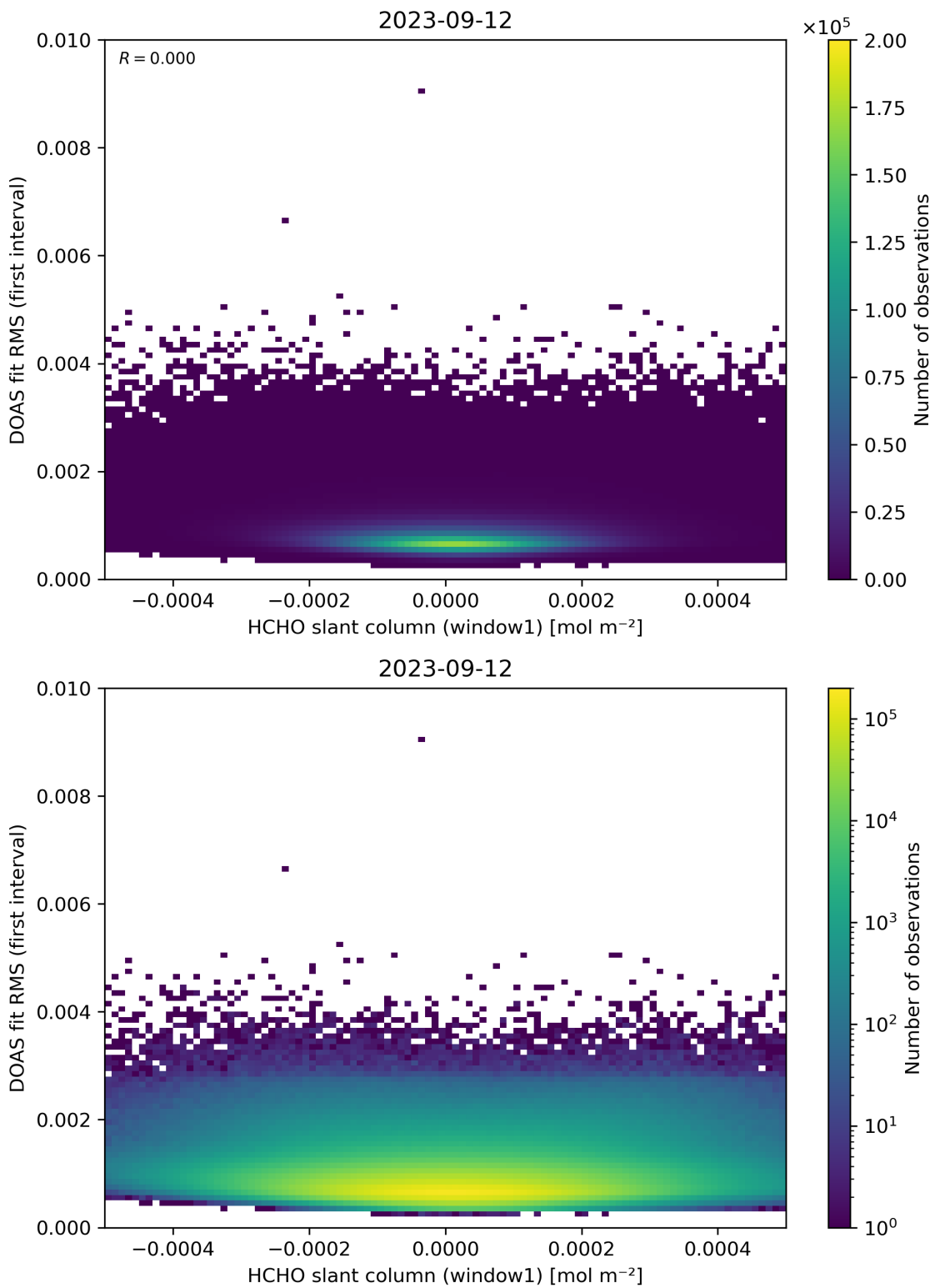


Figure 78: Scatter density plot of “HCHO slant column (window1)” against “DOAS fit RMS (first interval)” for 2023-09-11 to 2023-09-13.

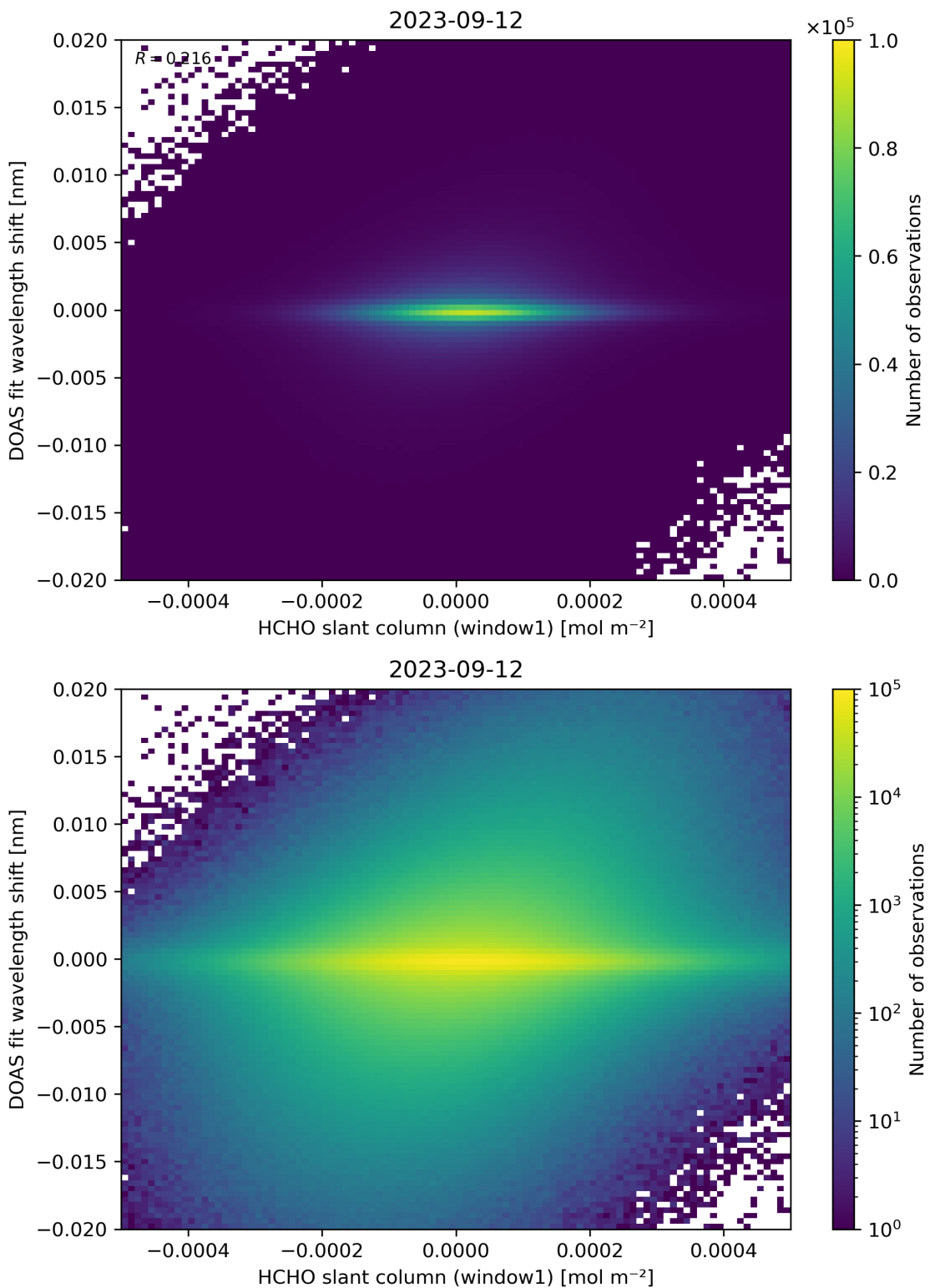


Figure 79: Scatter density plot of “HCHO slant column (window1)” against “DOAS fit wavelength shift” for 2023-09-11 to 2023-09-13.

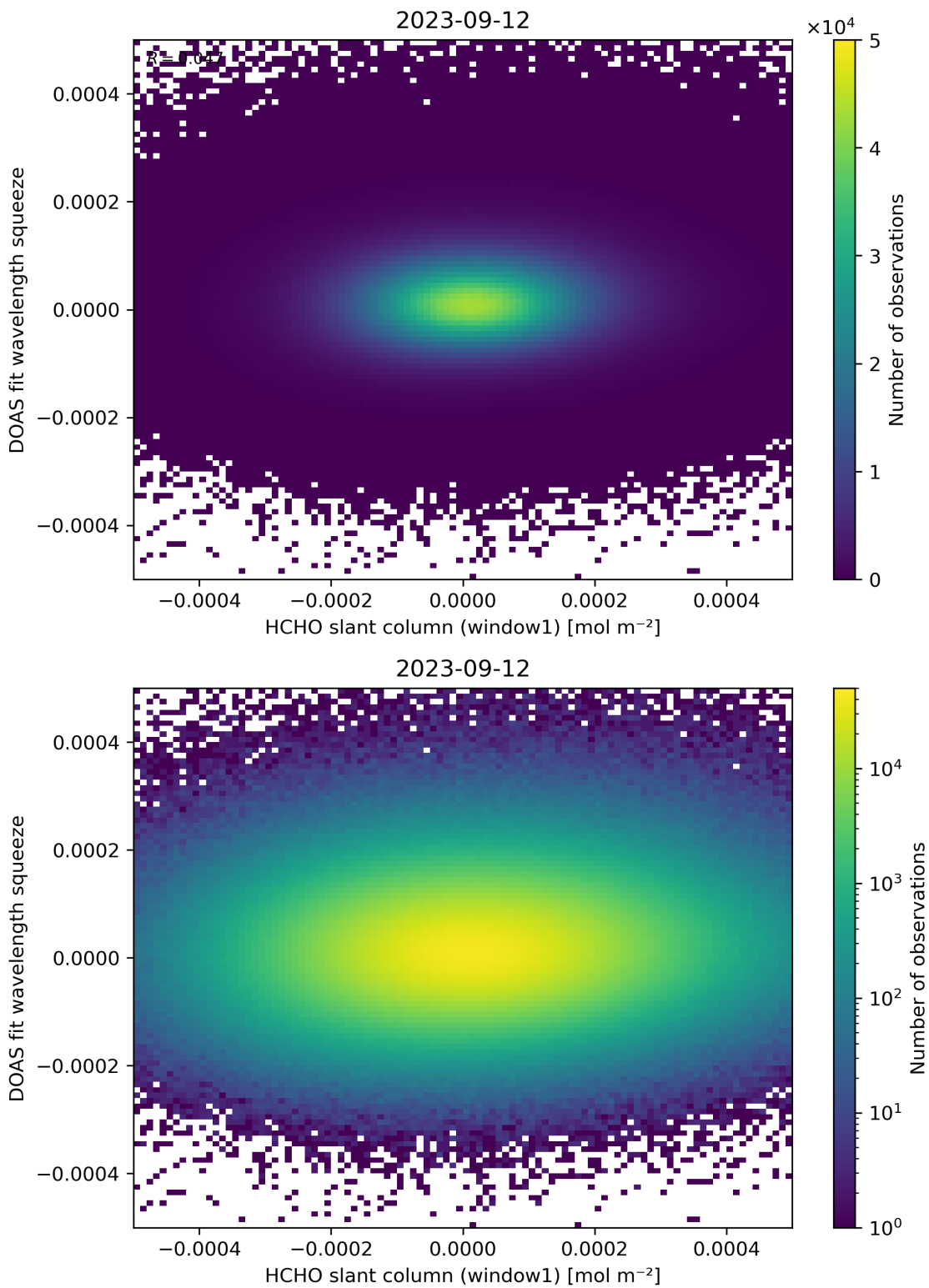


Figure 80: Scatter density plot of “HCHO slant column (window1)” against “DOAS fit wavelength squeeze” for 2023-09-11 to 2023-09-13.

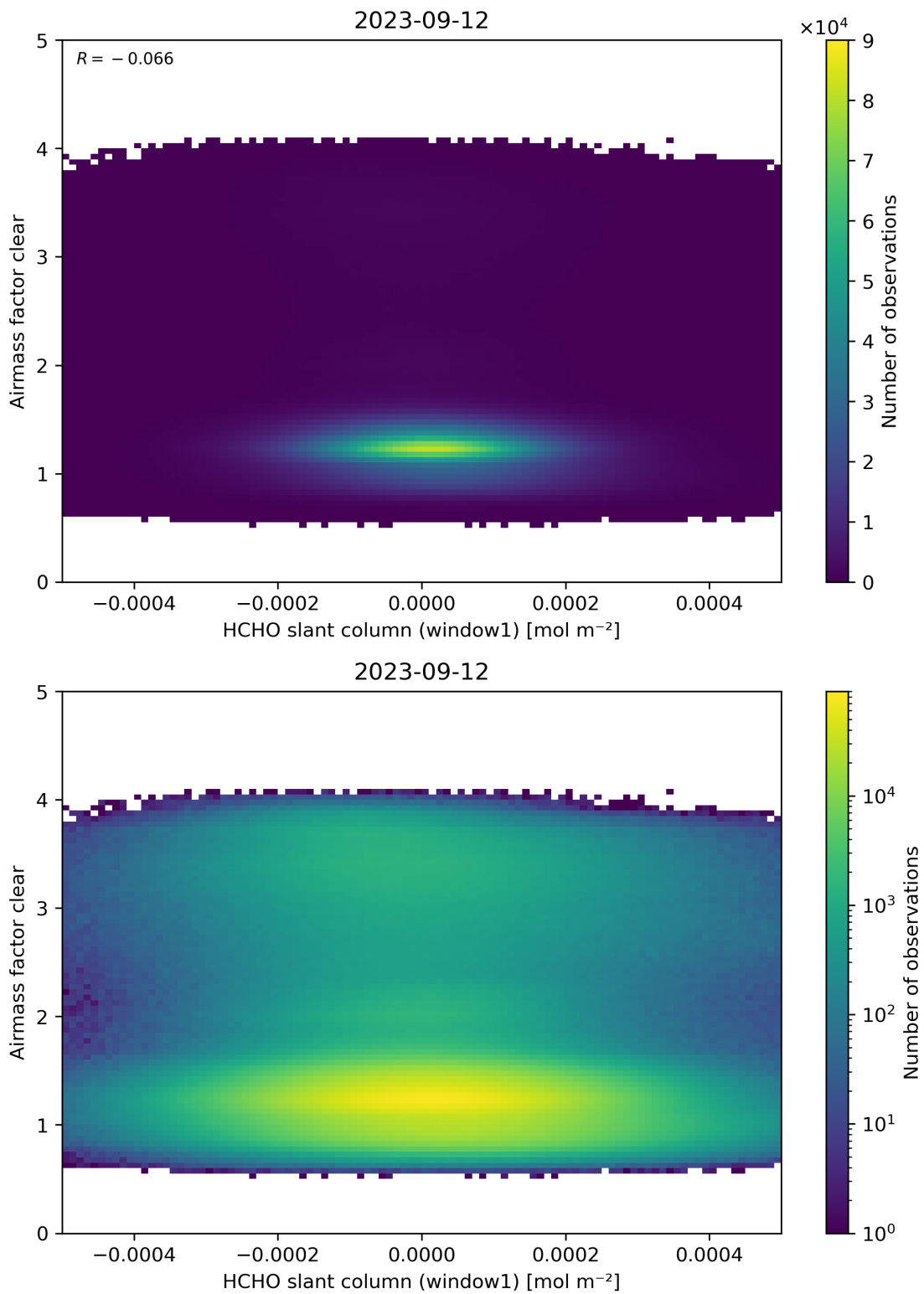


Figure 81: Scatter density plot of “HCHO slant column (window1)” against “Airmass factor clear” for 2023-09-11 to 2023-09-13.

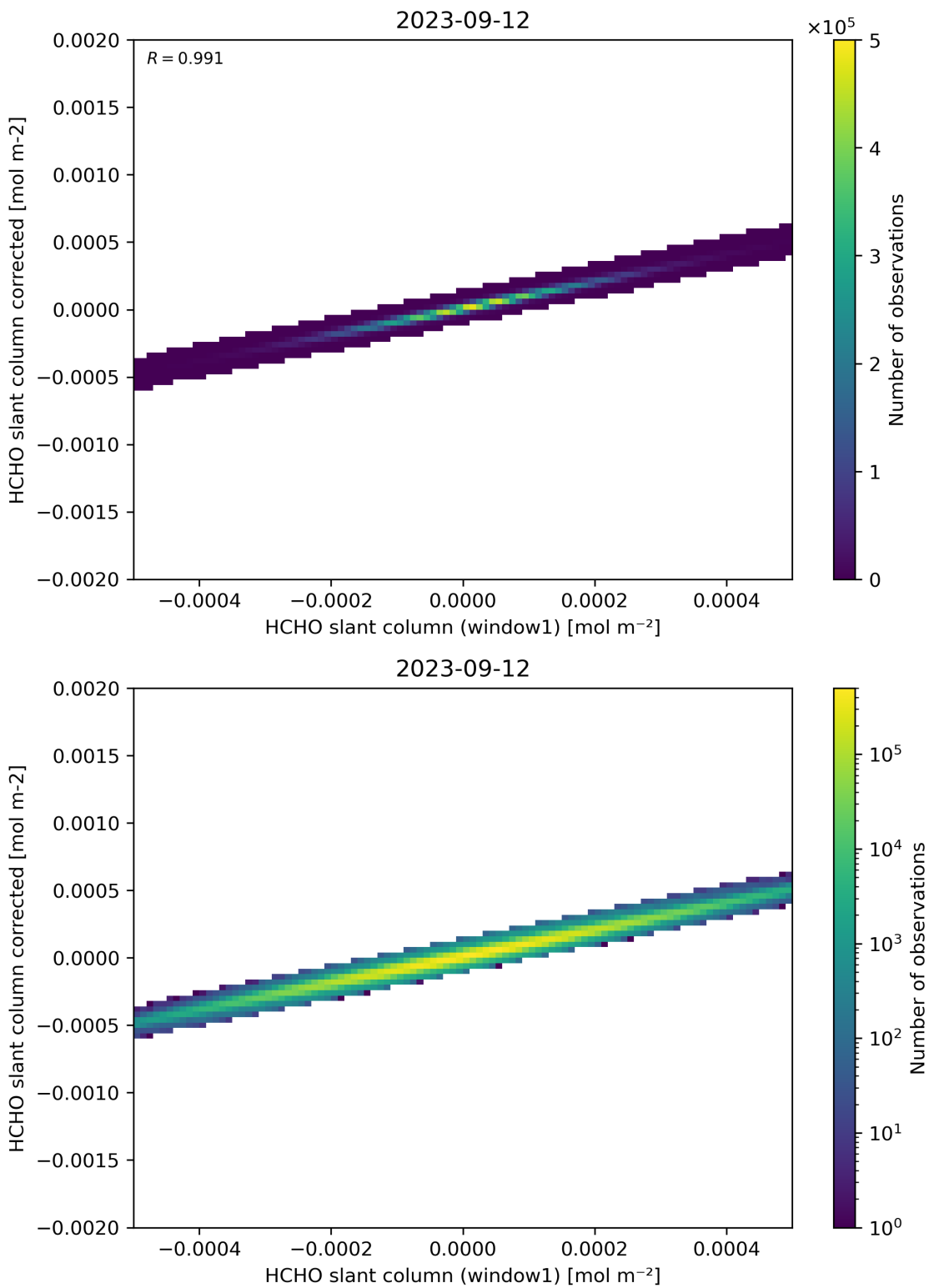


Figure 82: Scatter density plot of “HCHO slant column (window1)” against “HCHO slant column corrected” for 2023-09-11 to 2023-09-13.

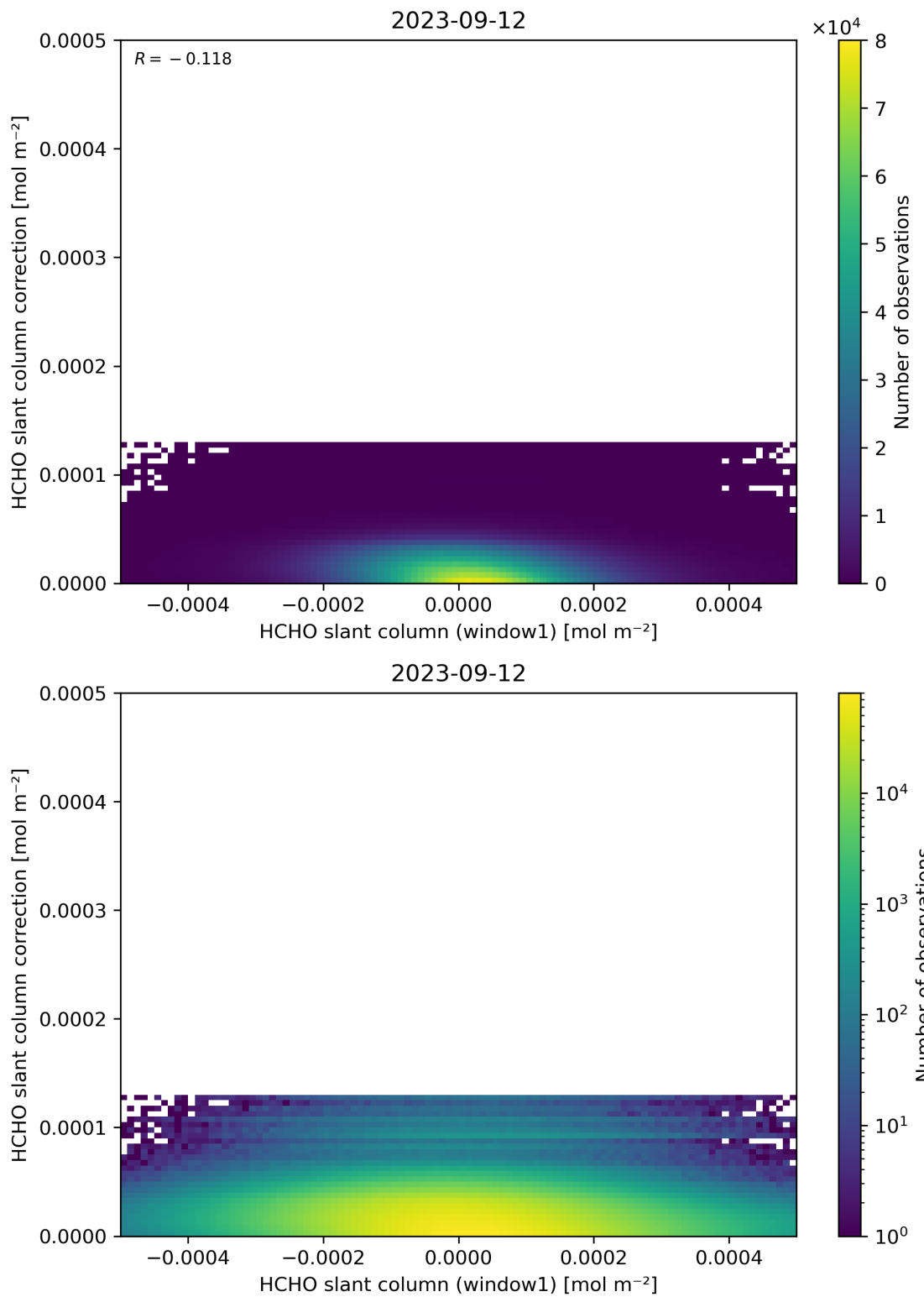


Figure 83: Scatter density plot of “HCHO slant column (window1)” against “HCHO slant column correction” for 2023-09-11 to 2023-09-13.

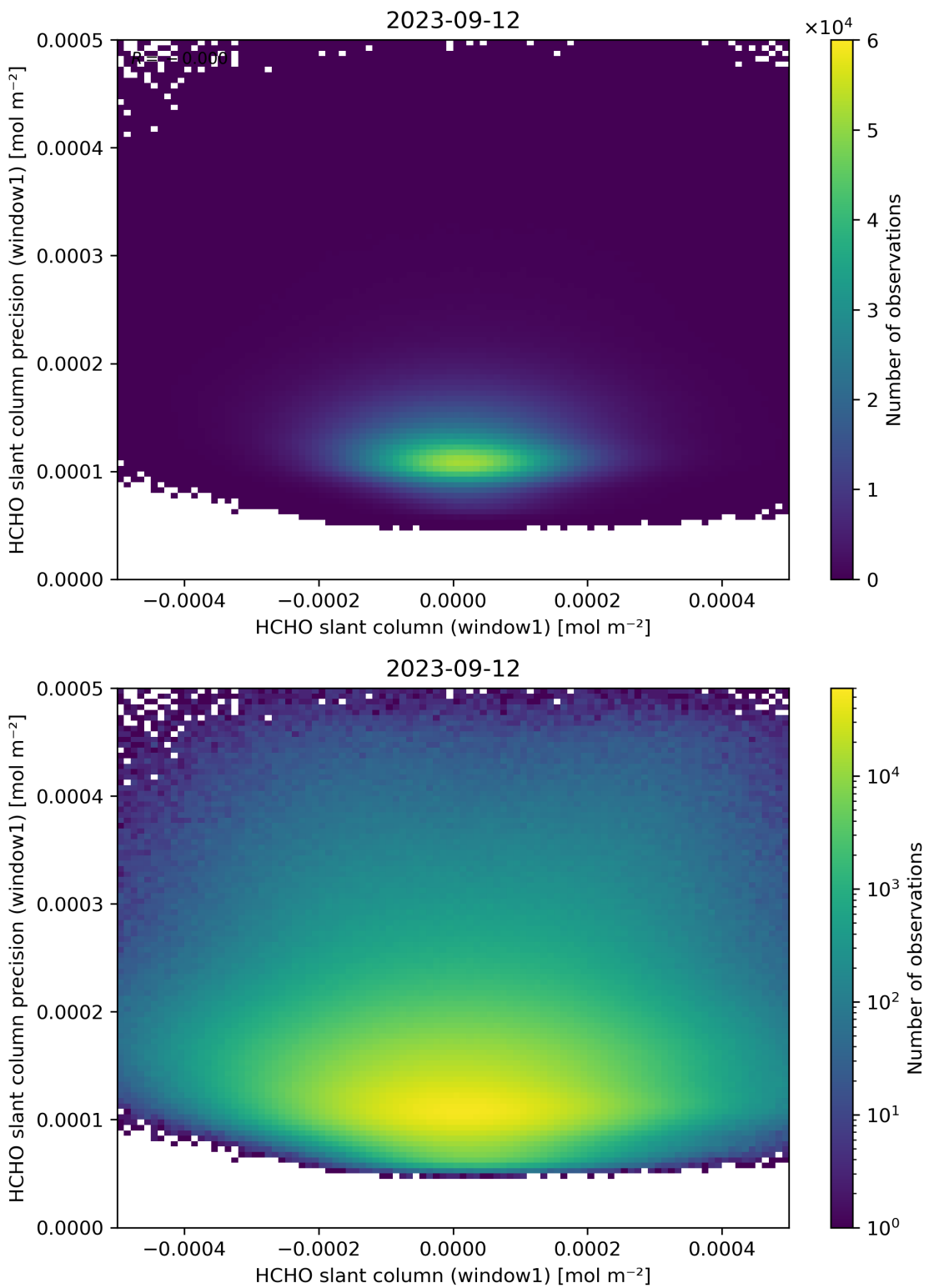


Figure 84: Scatter density plot of “HCHO slant column (window1)” against “HCHO slant column precision (window1)” for 2023-09-11 to 2023-09-13.

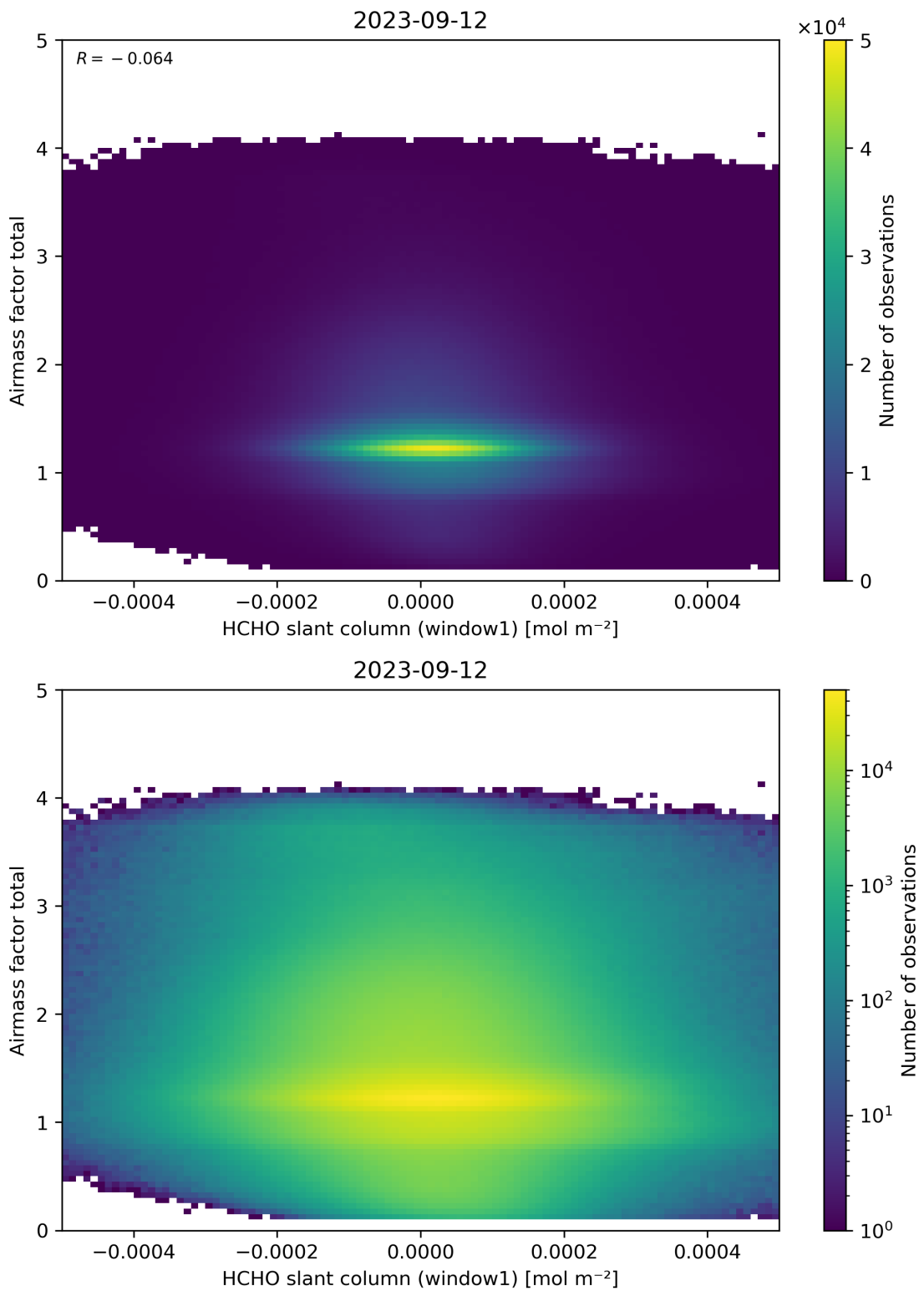


Figure 85: Scatter density plot of “HCHO slant column (window1)” against “Airmass factor total” for 2023-09-11 to 2023-09-13.

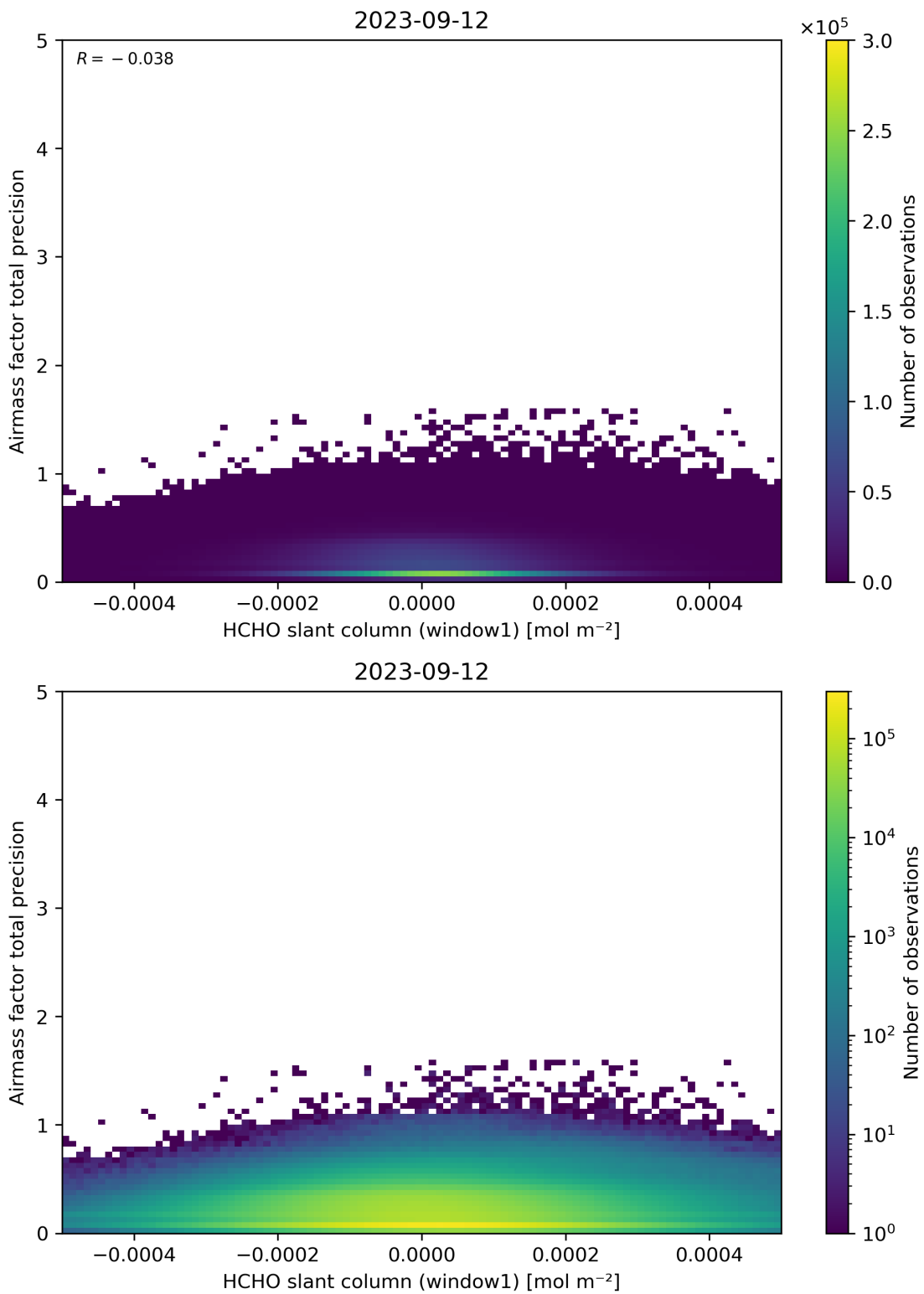


Figure 86: Scatter density plot of “HCHO slant column (window1)” against “Airmass factor total precision” for 2023-09-11 to 2023-09-13.

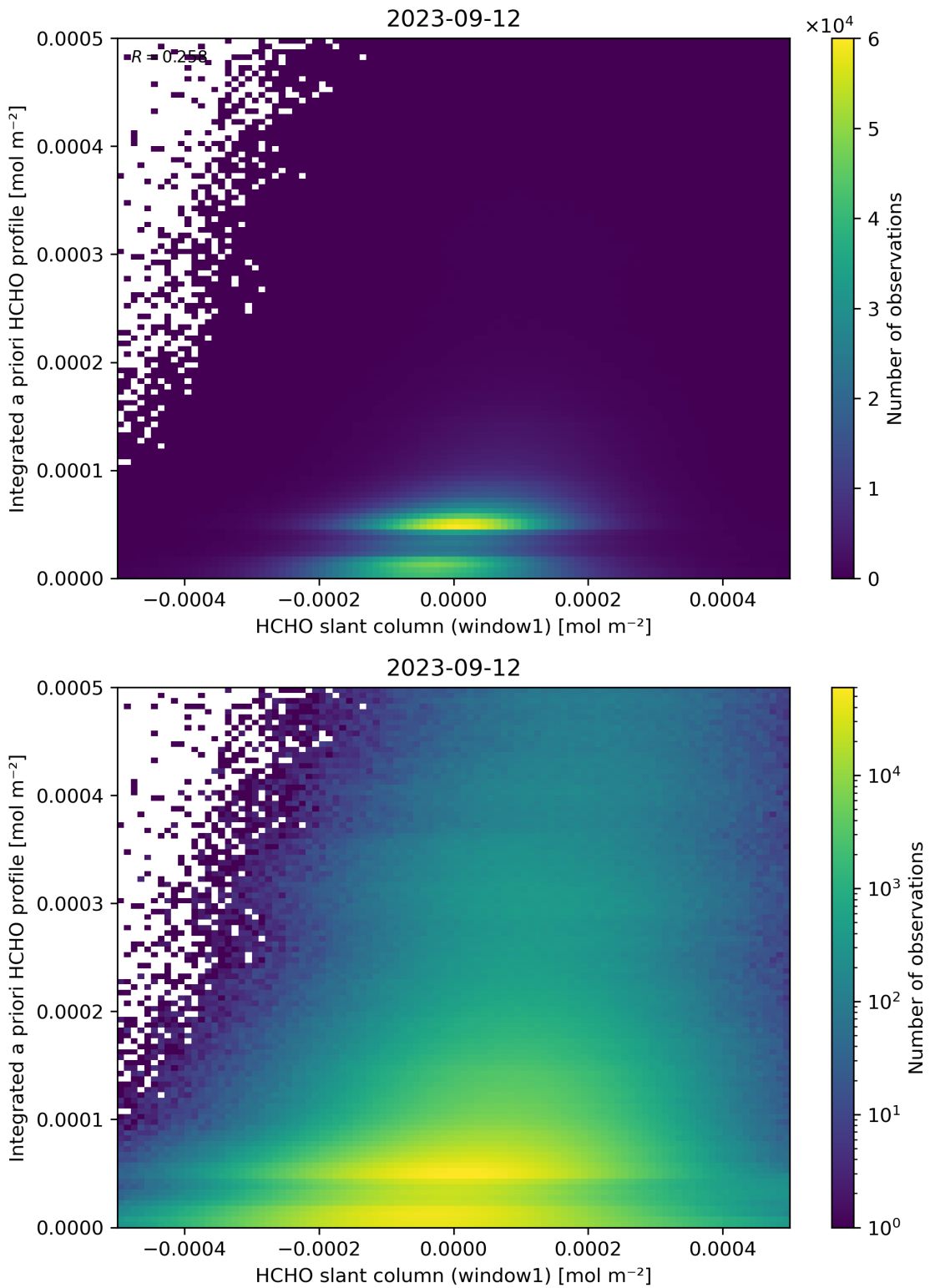


Figure 87: Scatter density plot of “HCHO slant column (window1)” against “Integrated a priori HCHO profile” for 2023-09-11 to 2023-09-13.

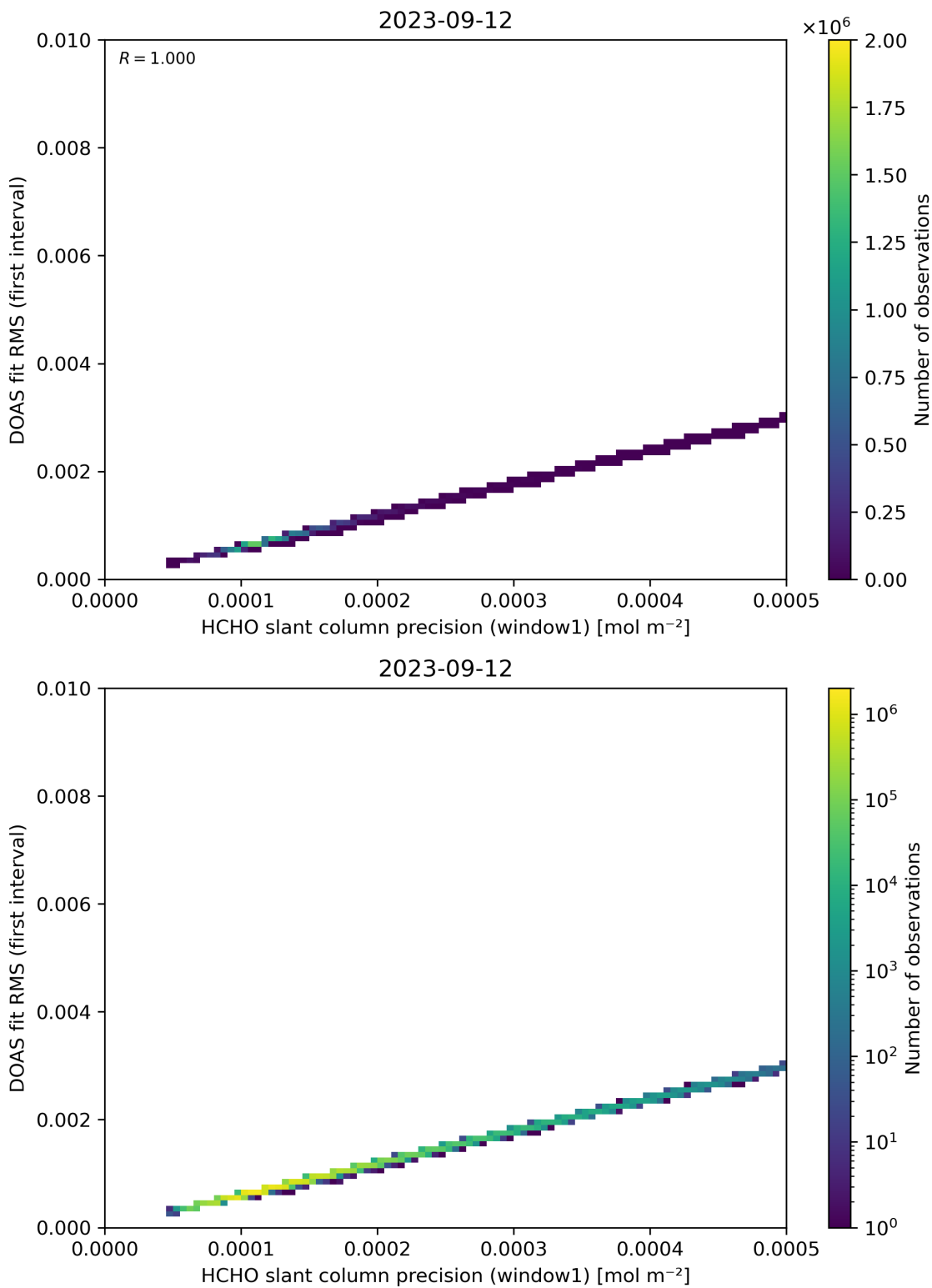


Figure 88: Scatter density plot of “HCHO slant column precision (window1)” against “DOAS fit RMS (first interval)” for 2023-09-11 to 2023-09-13.

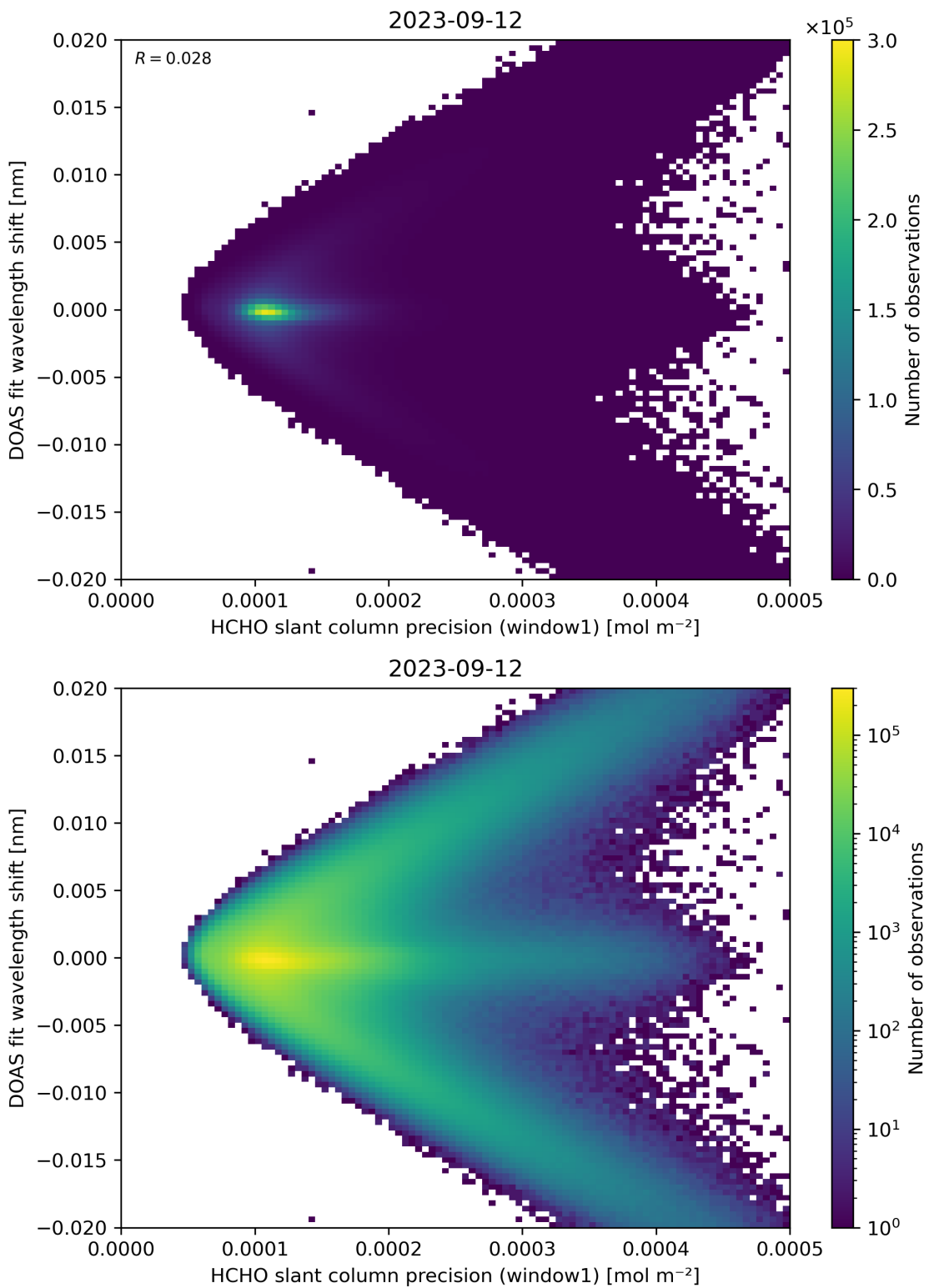


Figure 89: Scatter density plot of “HCHO slant column precision (window1)” against “DOAS fit wavelength shift” for 2023-09-11 to 2023-09-13.

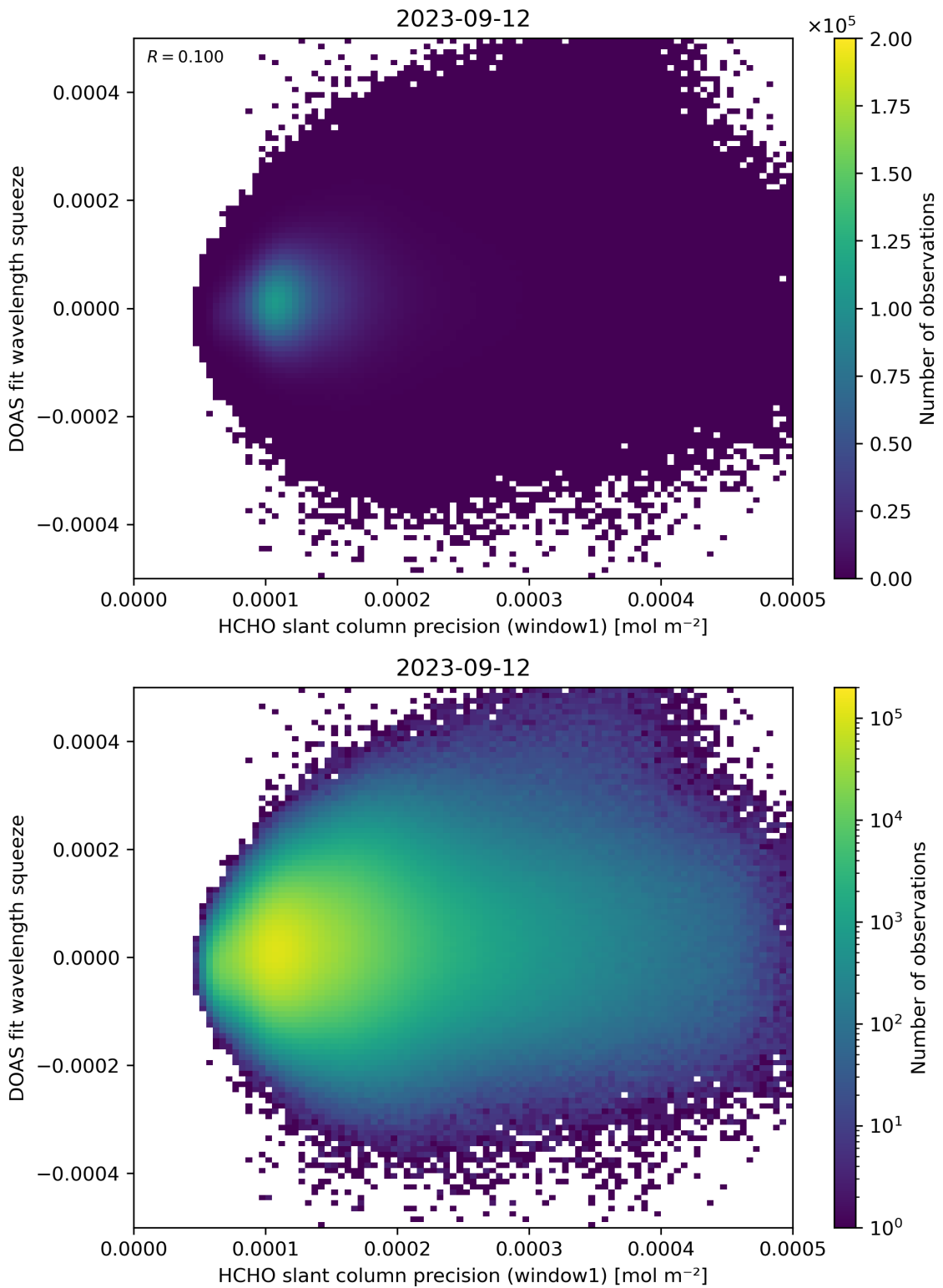


Figure 90: Scatter density plot of “HCHO slant column precision (window1)” against “DOAS fit wavelength squeeze” for 2023-09-11 to 2023-09-13.

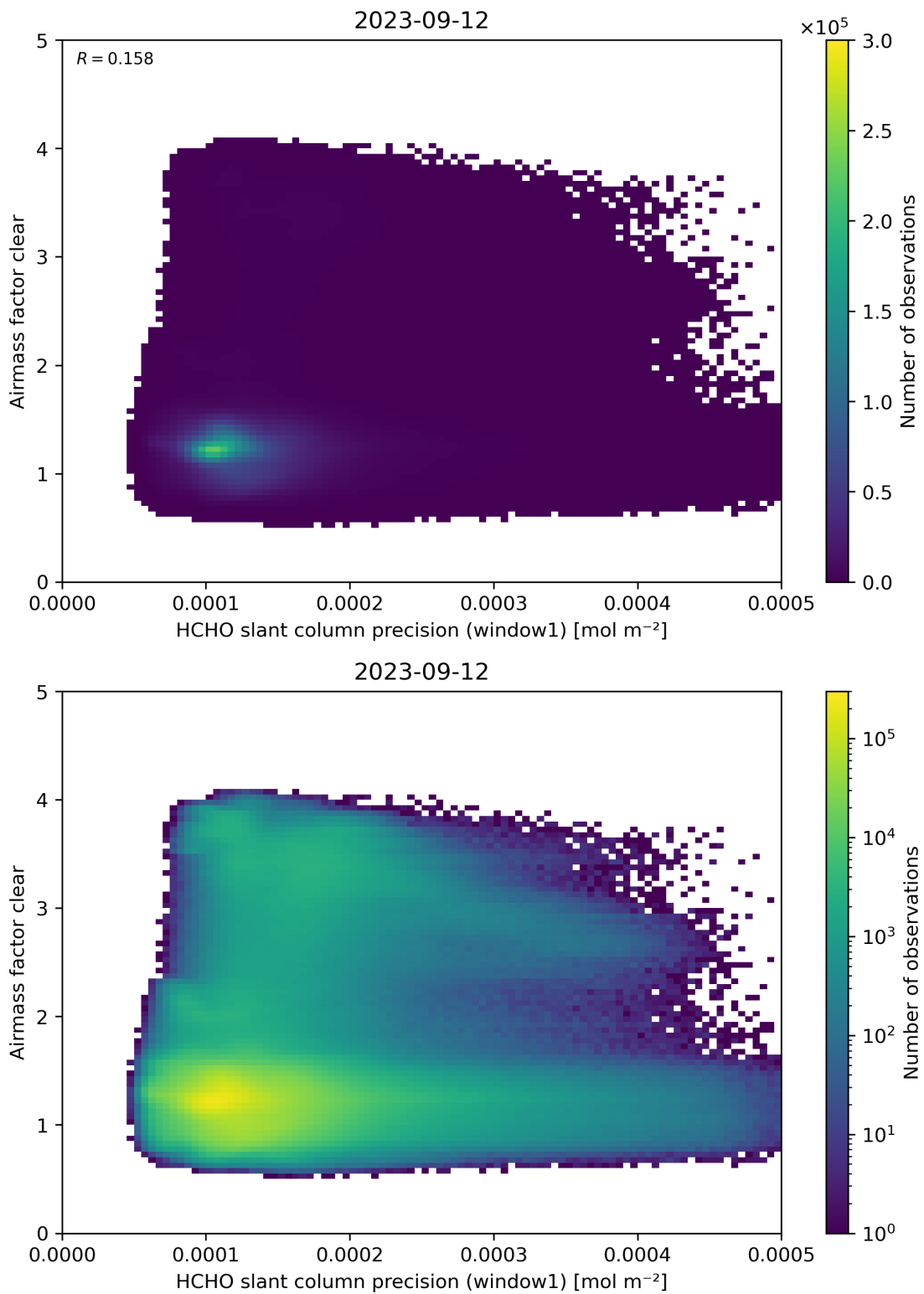


Figure 91: Scatter density plot of “HCHO slant column precision (window1)” against “Airmass factor clear” for 2023-09-11 to 2023-09-13.

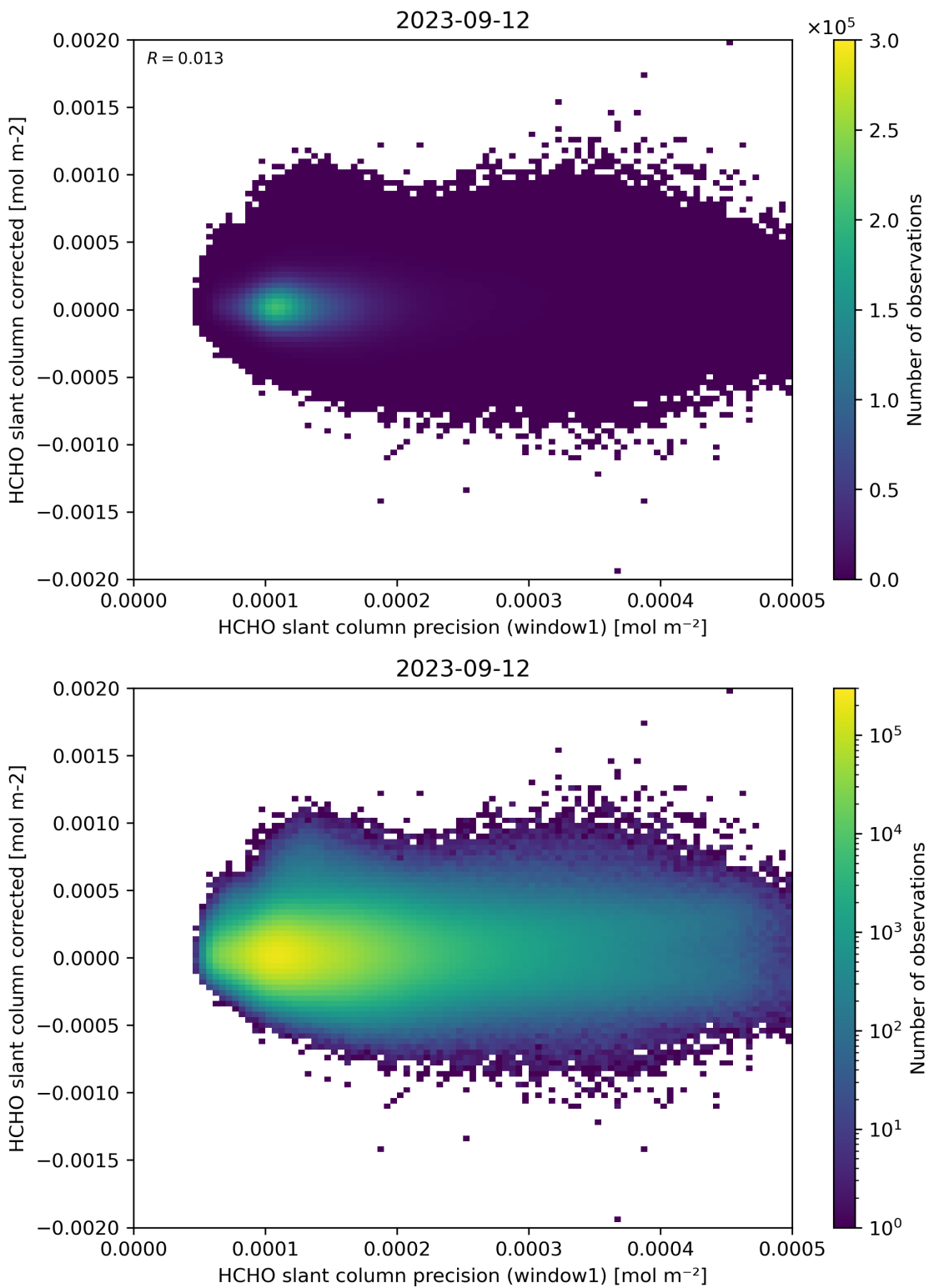


Figure 92: Scatter density plot of “HCHO slant column precision (window1)” against “HCHO slant column corrected” for 2023-09-11 to 2023-09-13.

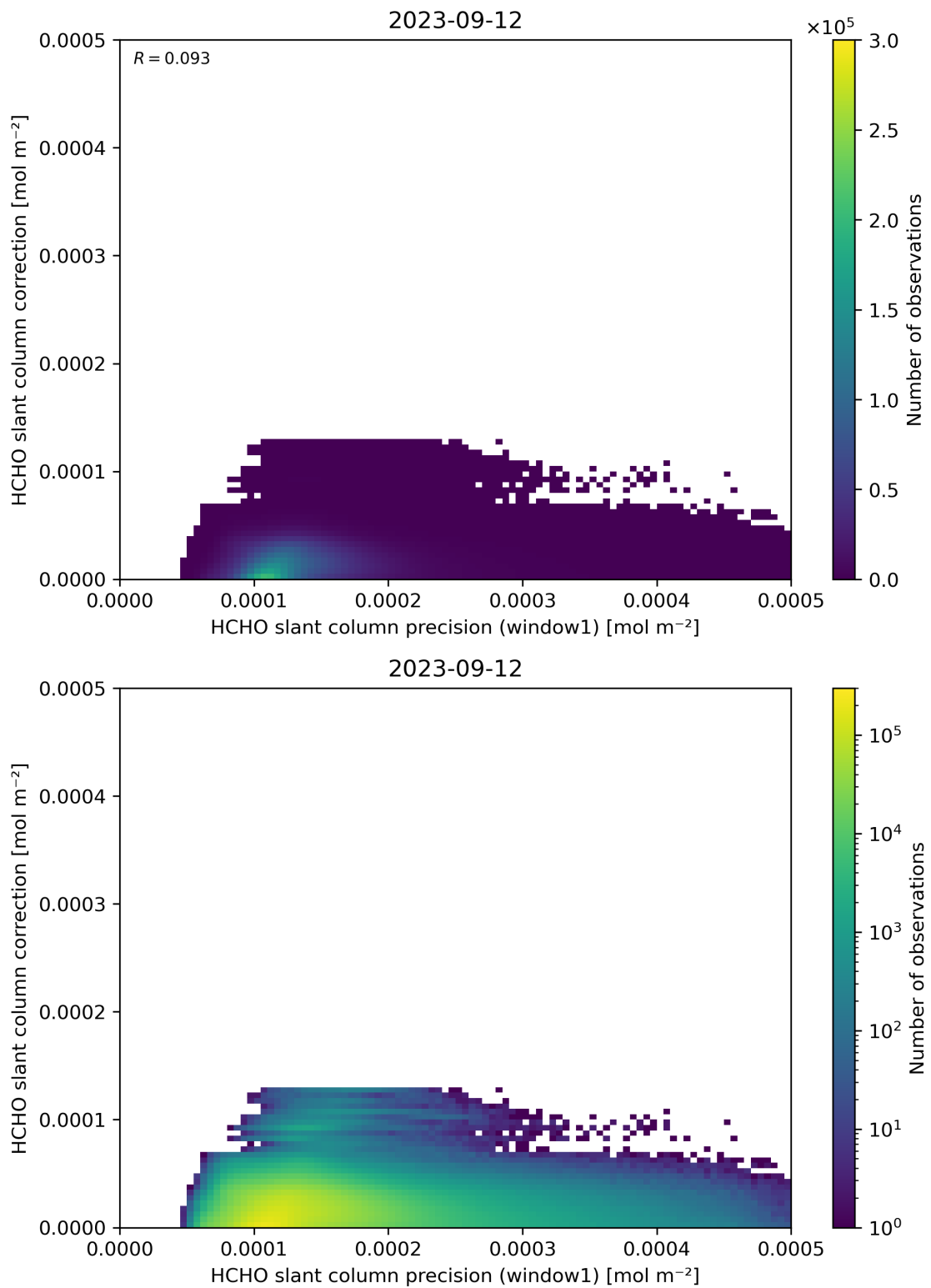


Figure 93: Scatter density plot of “HCHO slant column precision (window1)” against “HCHO slant column correction” for 2023-09-11 to 2023-09-13.

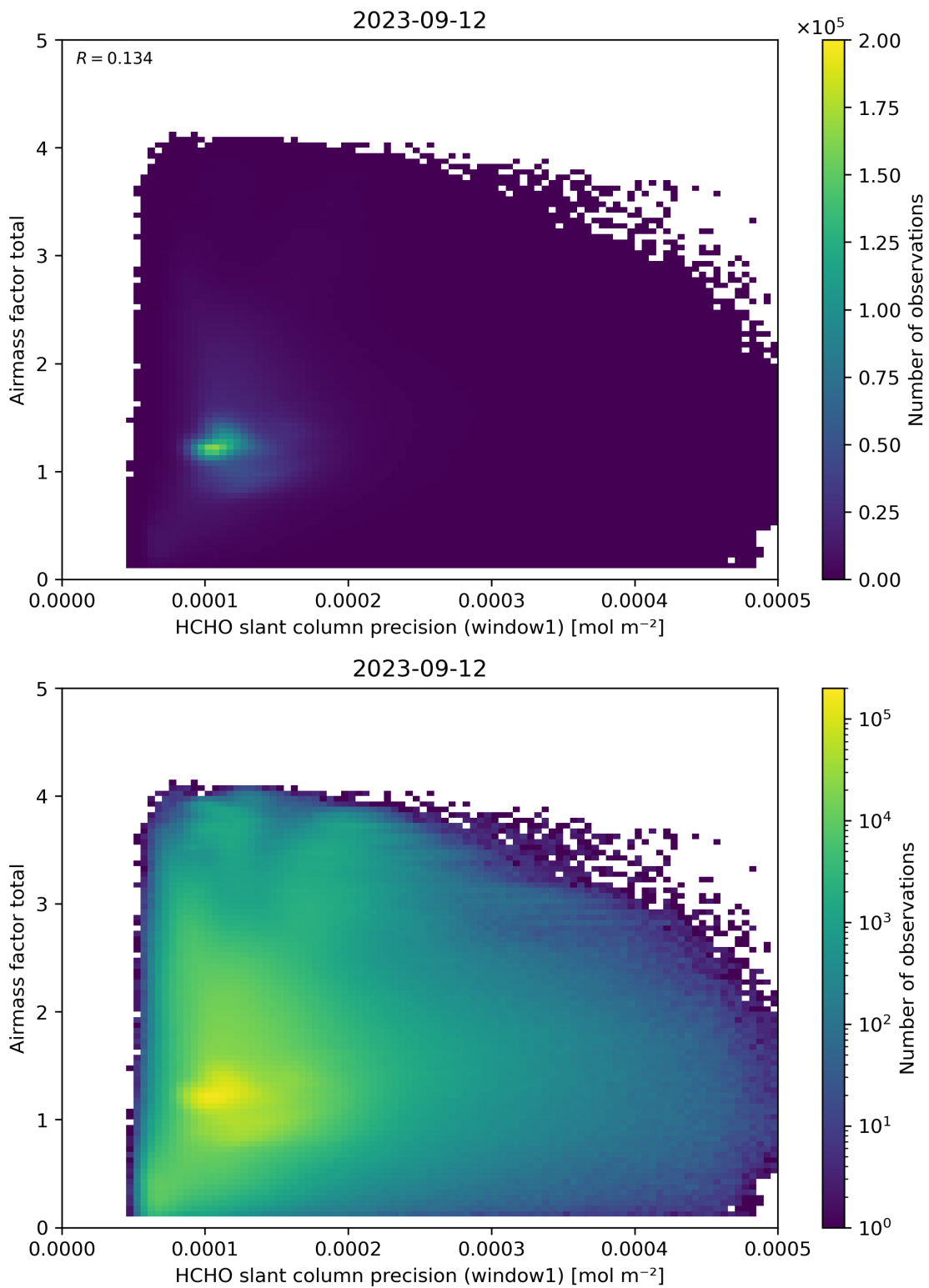


Figure 94: Scatter density plot of “HCHO slant column precision (window1)” against “Airmass factor total” for 2023-09-11 to 2023-09-13.

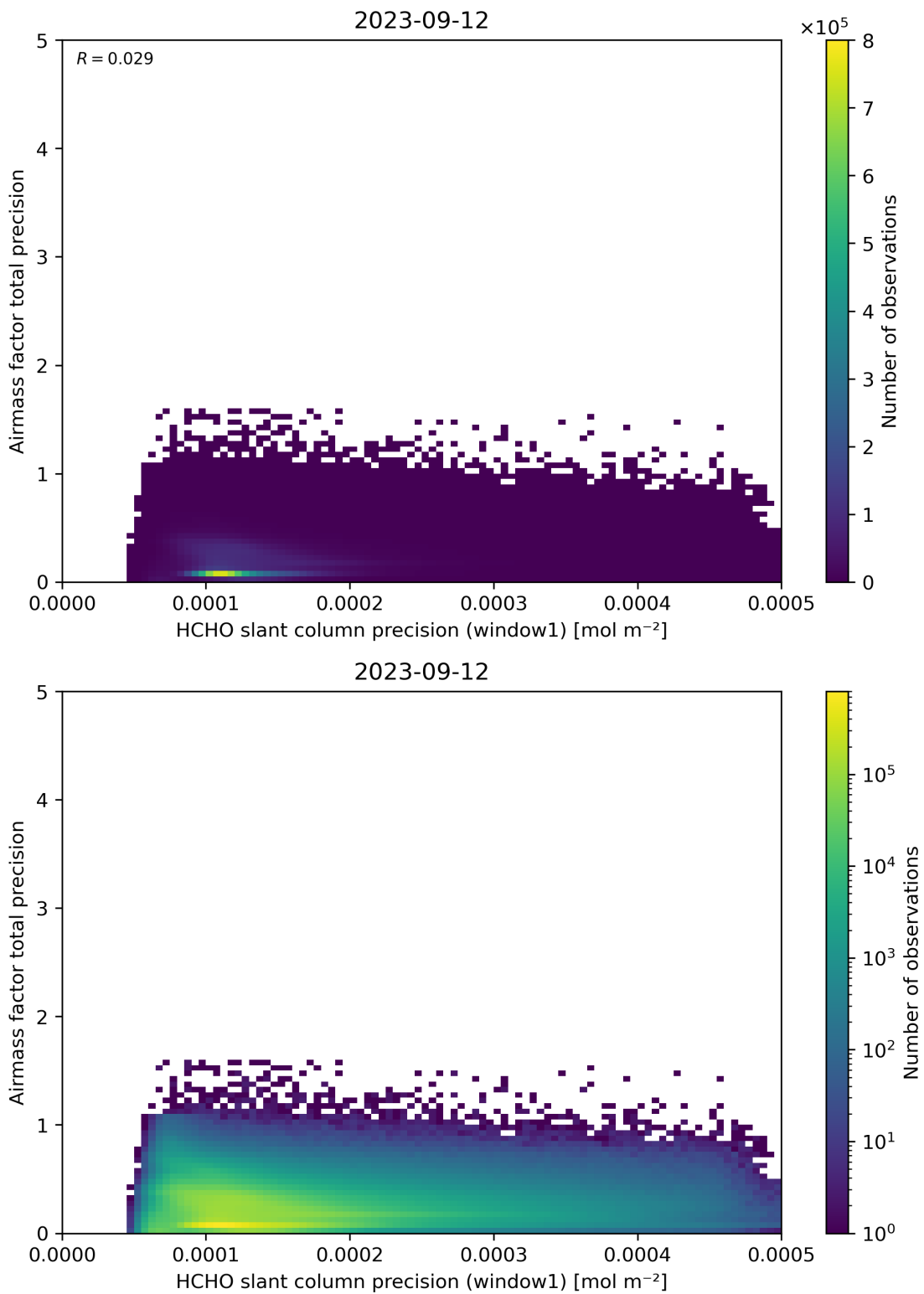


Figure 95: Scatter density plot of “HCHO slant column precision (window1)” against “Airmass factor total precision” for 2023-09-11 to 2023-09-13.

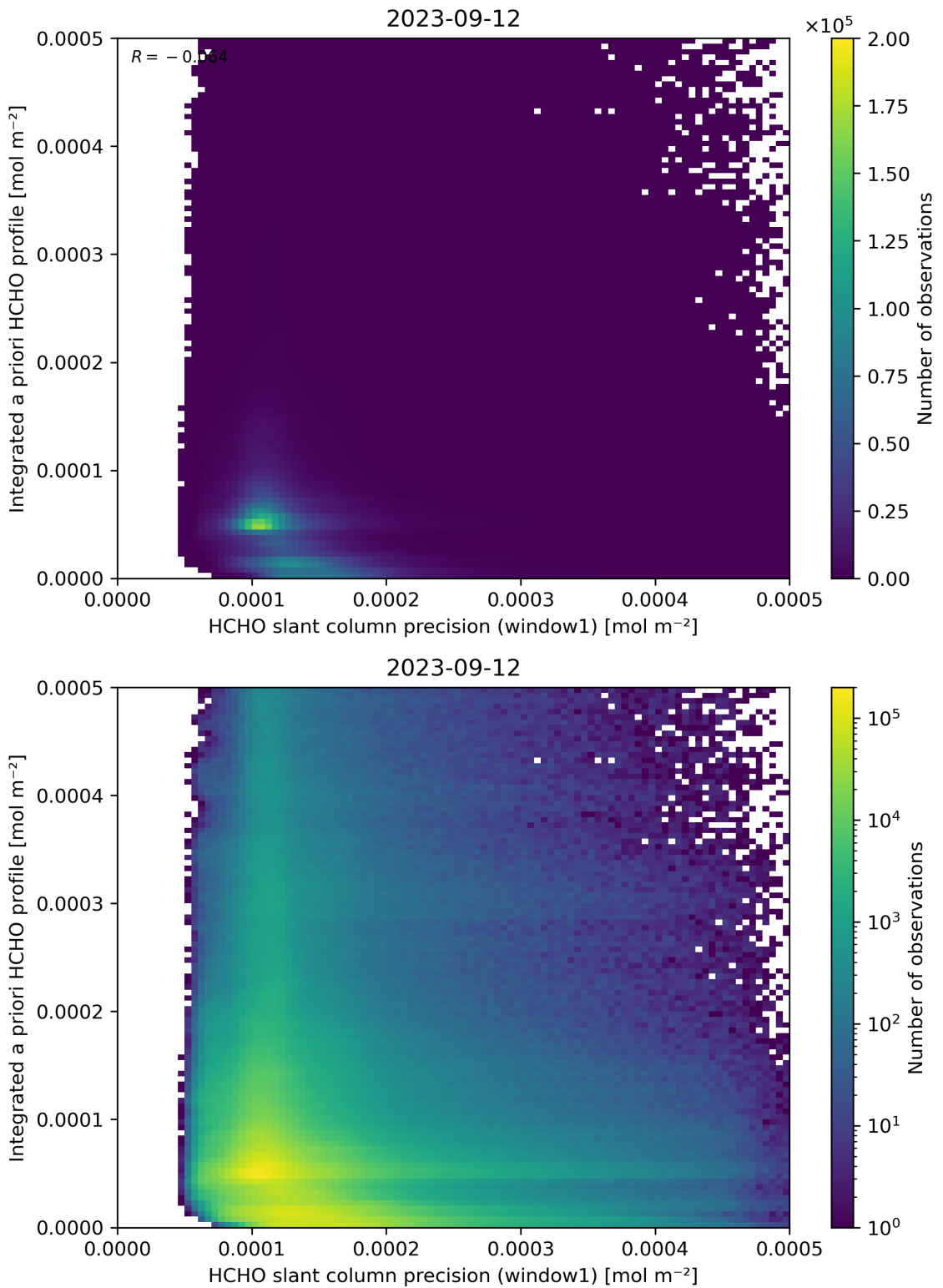


Figure 96: Scatter density plot of “HCHO slant column precision (window1)” against “Integrated a priori HCHO profile” for 2023-09-11 to 2023-09-13.

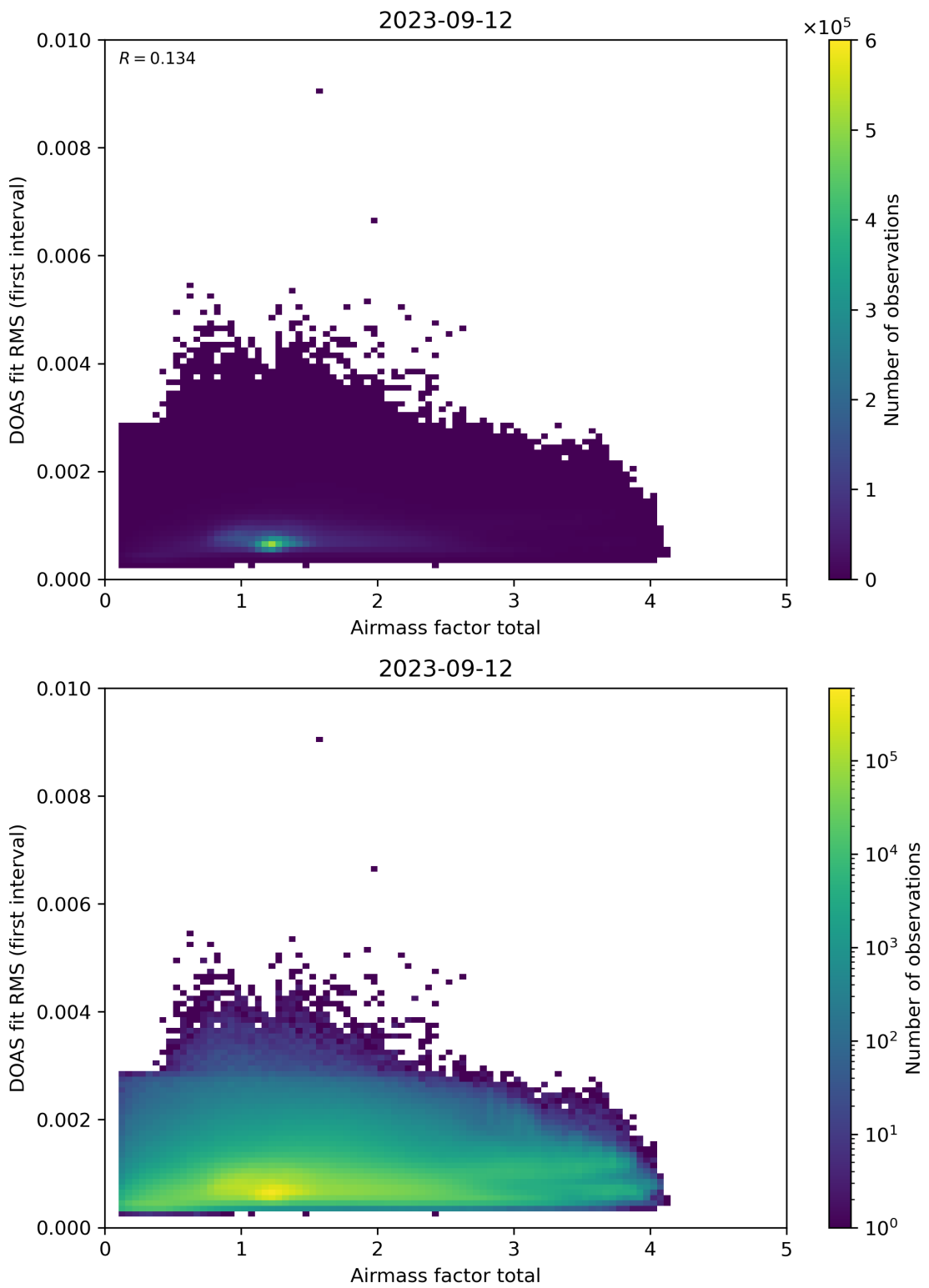


Figure 97: Scatter density plot of “Airmass factor total” against “DOAS fit RMS (first interval)” for 2023-09-11 to 2023-09-13.

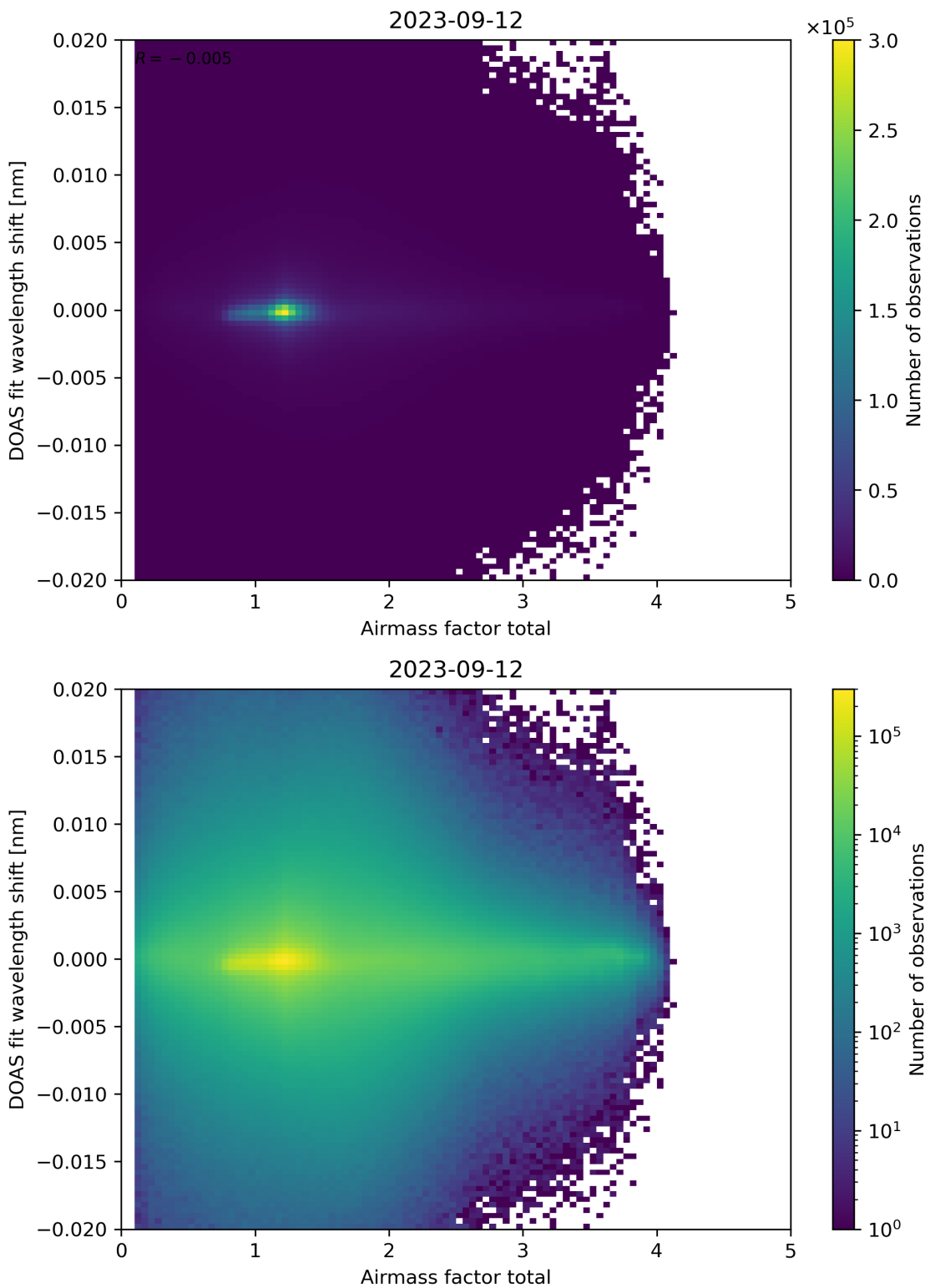


Figure 98: Scatter density plot of “Airmass factor total” against “DOAS fit wavelength shift” for 2023-09-11 to 2023-09-13.

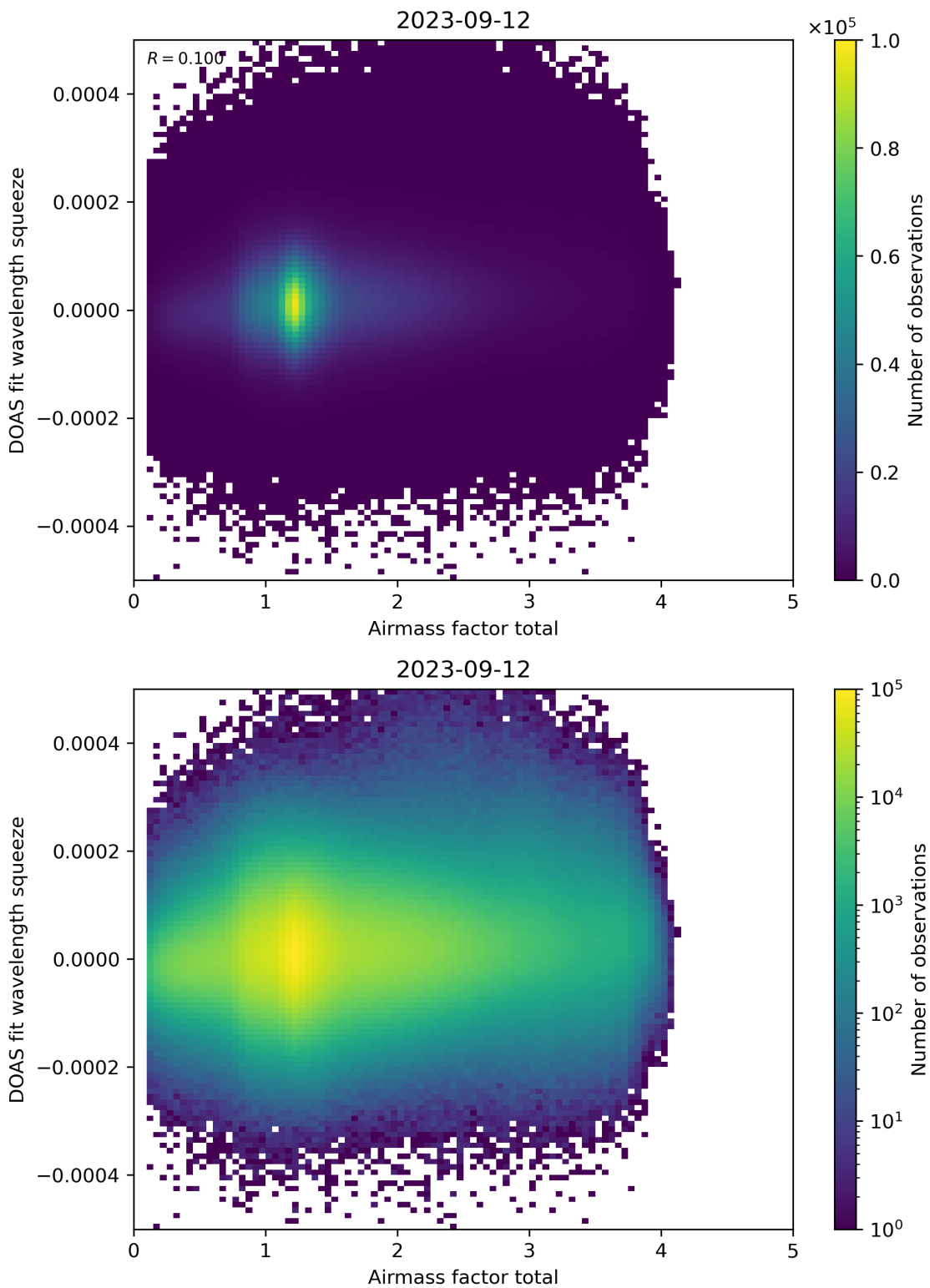


Figure 99: Scatter density plot of “Airmass factor total” against “DOAS fit wavelength squeeze” for 2023-09-11 to 2023-09-13.

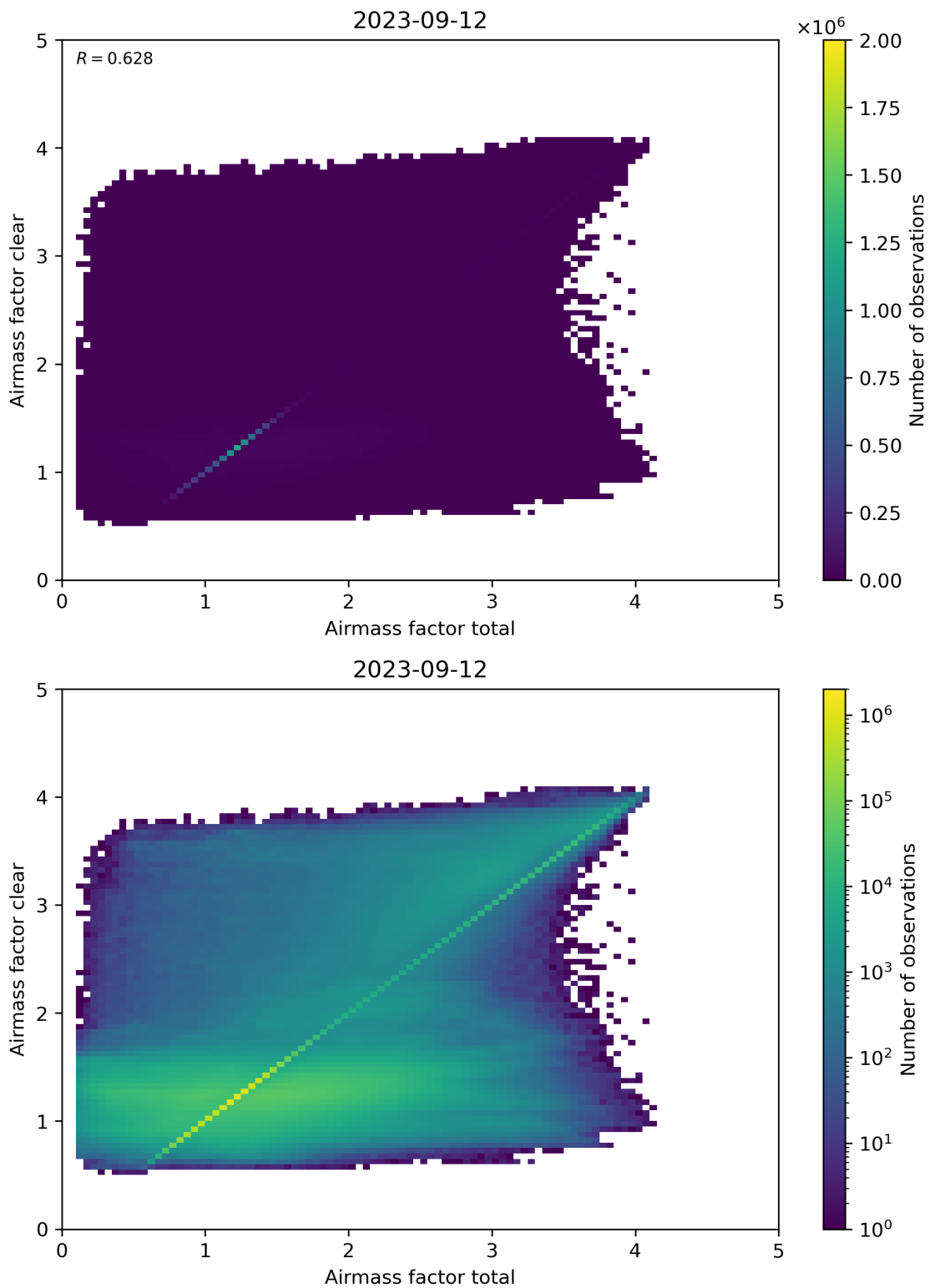


Figure 100: Scatter density plot of “Airmass factor total” against “Airmass factor clear” for 2023-09-11 to 2023-09-13.

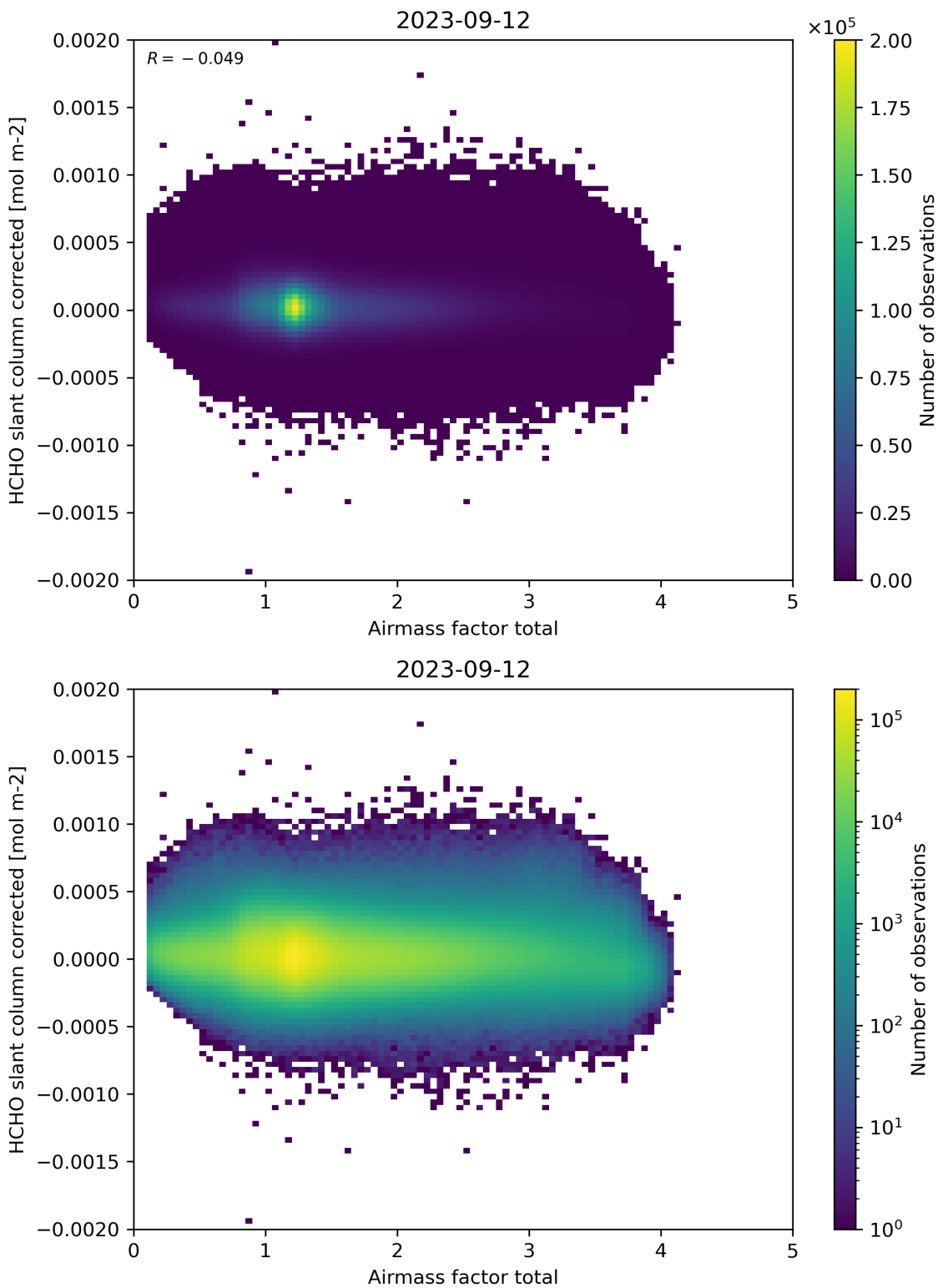


Figure 101: Scatter density plot of “Airmass factor total” against “HCHO slant column corrected” for 2023-09-11 to 2023-09-13.

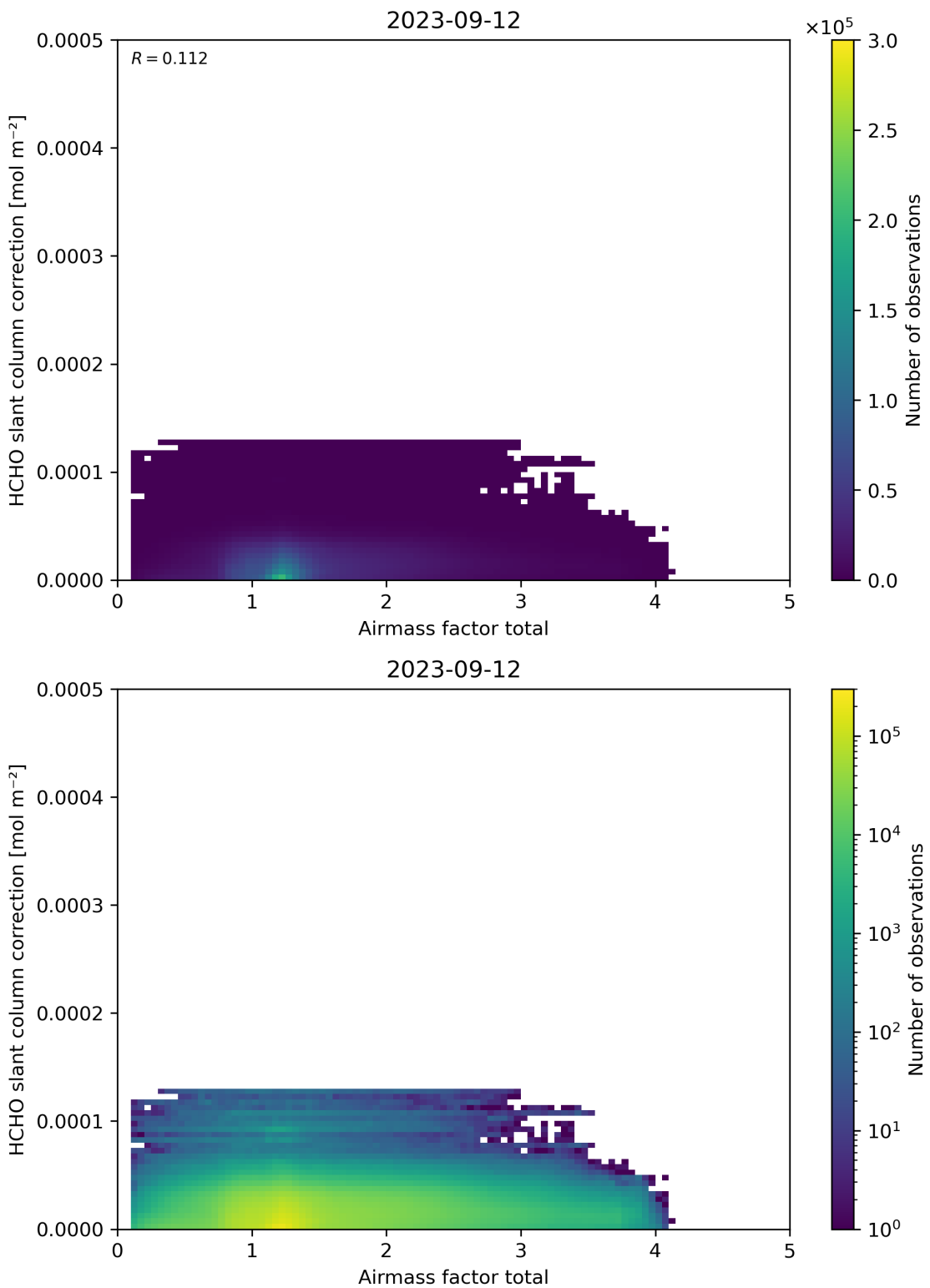


Figure 102: Scatter density plot of “Airmass factor total” against “HCHO slant column correction” for 2023-09-11 to 2023-09-13.

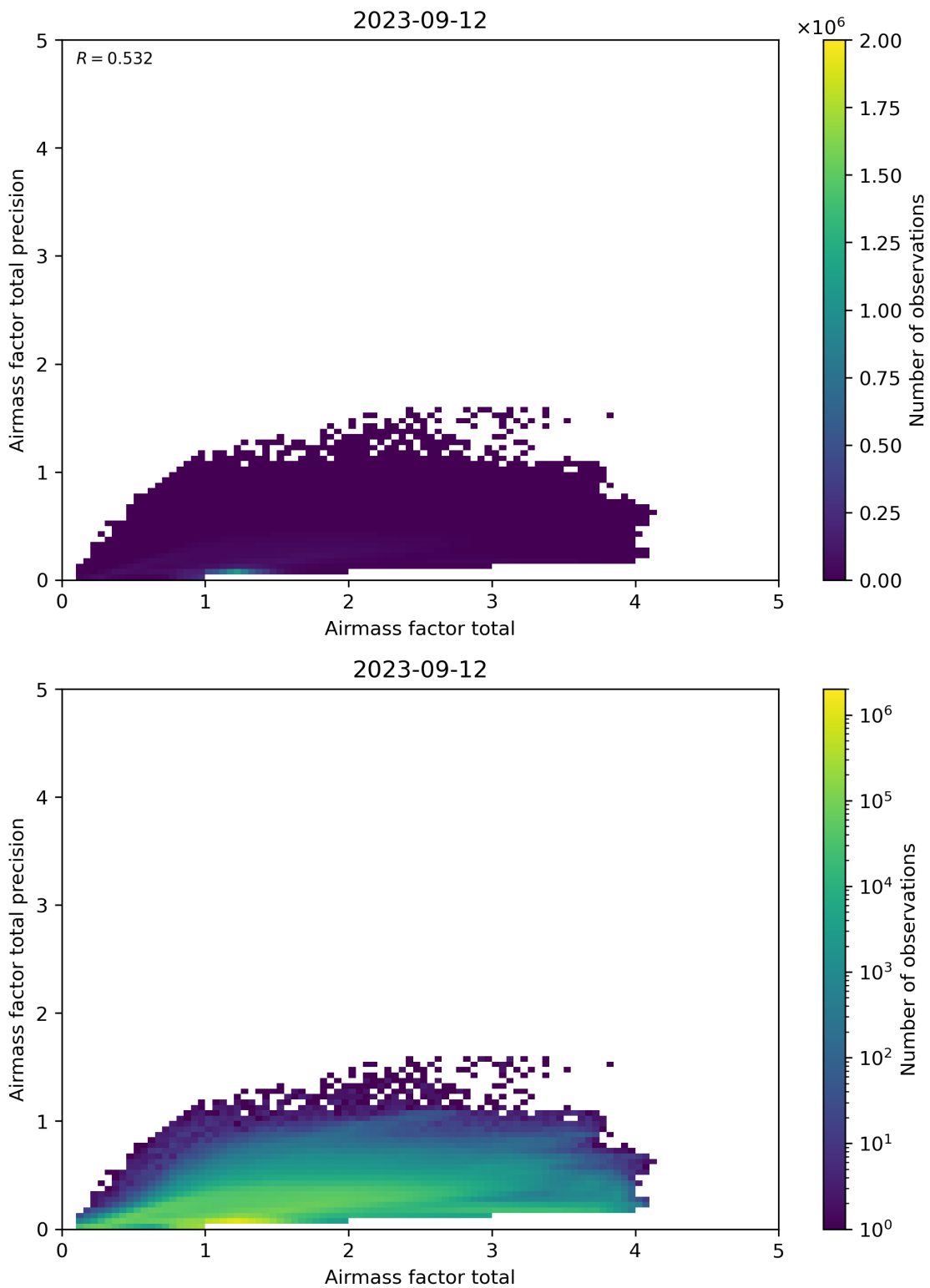


Figure 103: Scatter density plot of “Airmass factor total” against “Airmass factor total precision” for 2023-09-11 to 2023-09-13.

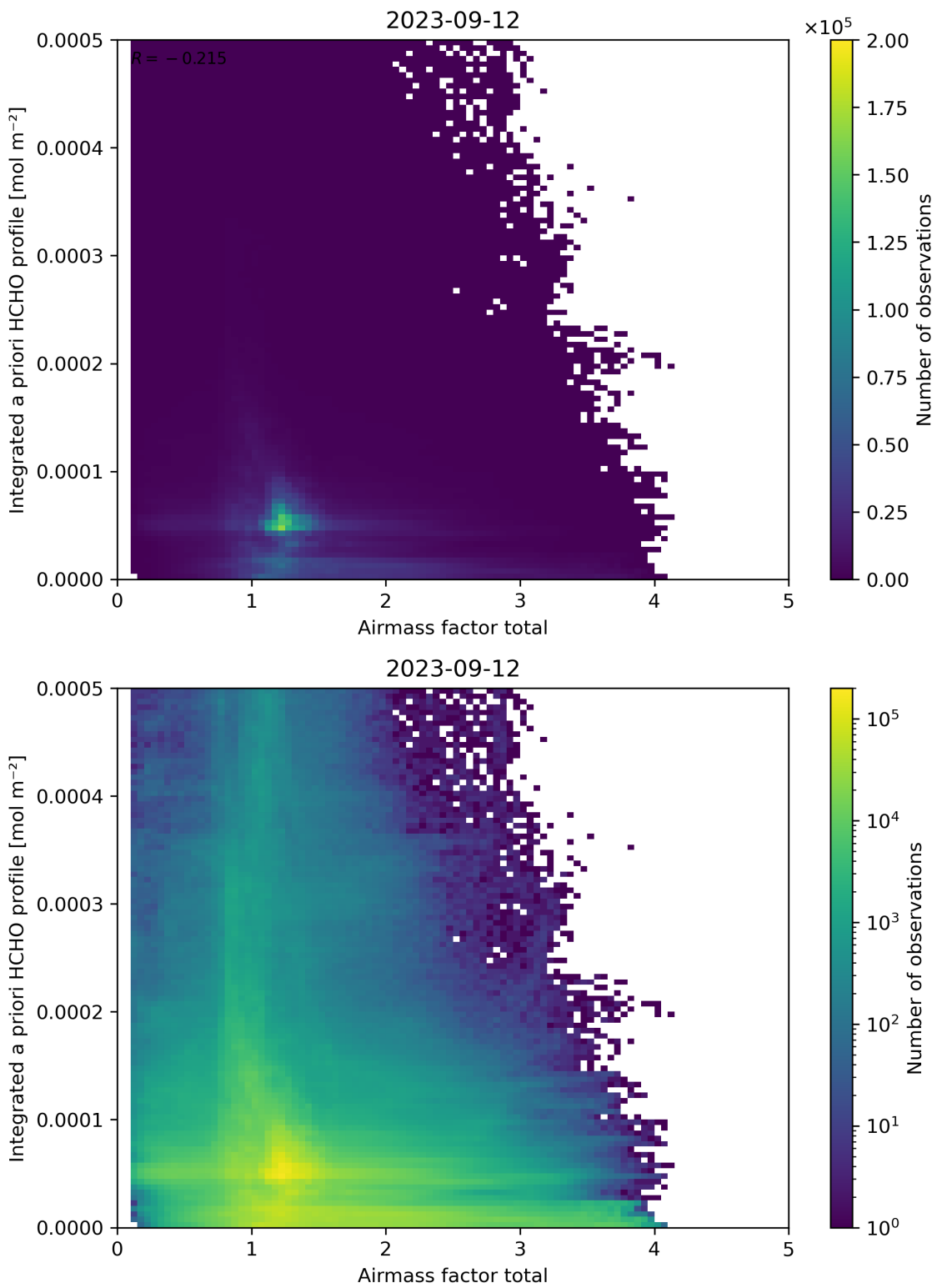


Figure 104: Scatter density plot of “Airmass factor total” against “Integrated a priori HCHO profile” for 2023-09-11 to 2023-09-13.

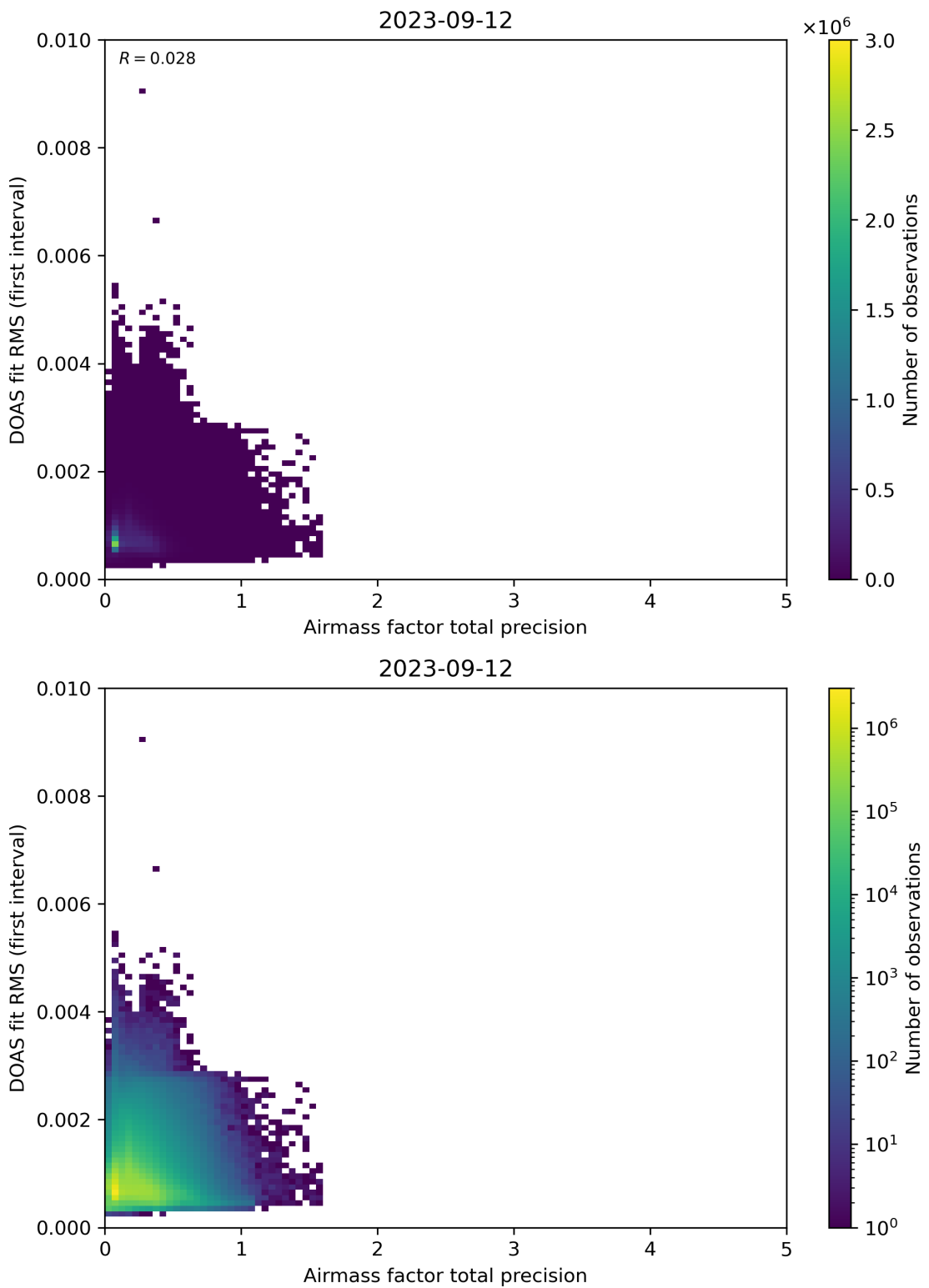


Figure 105: Scatter density plot of “Airmass factor total precision” against “DOAS fit RMS (first interval)” for 2023-09-11 to 2023-09-13.

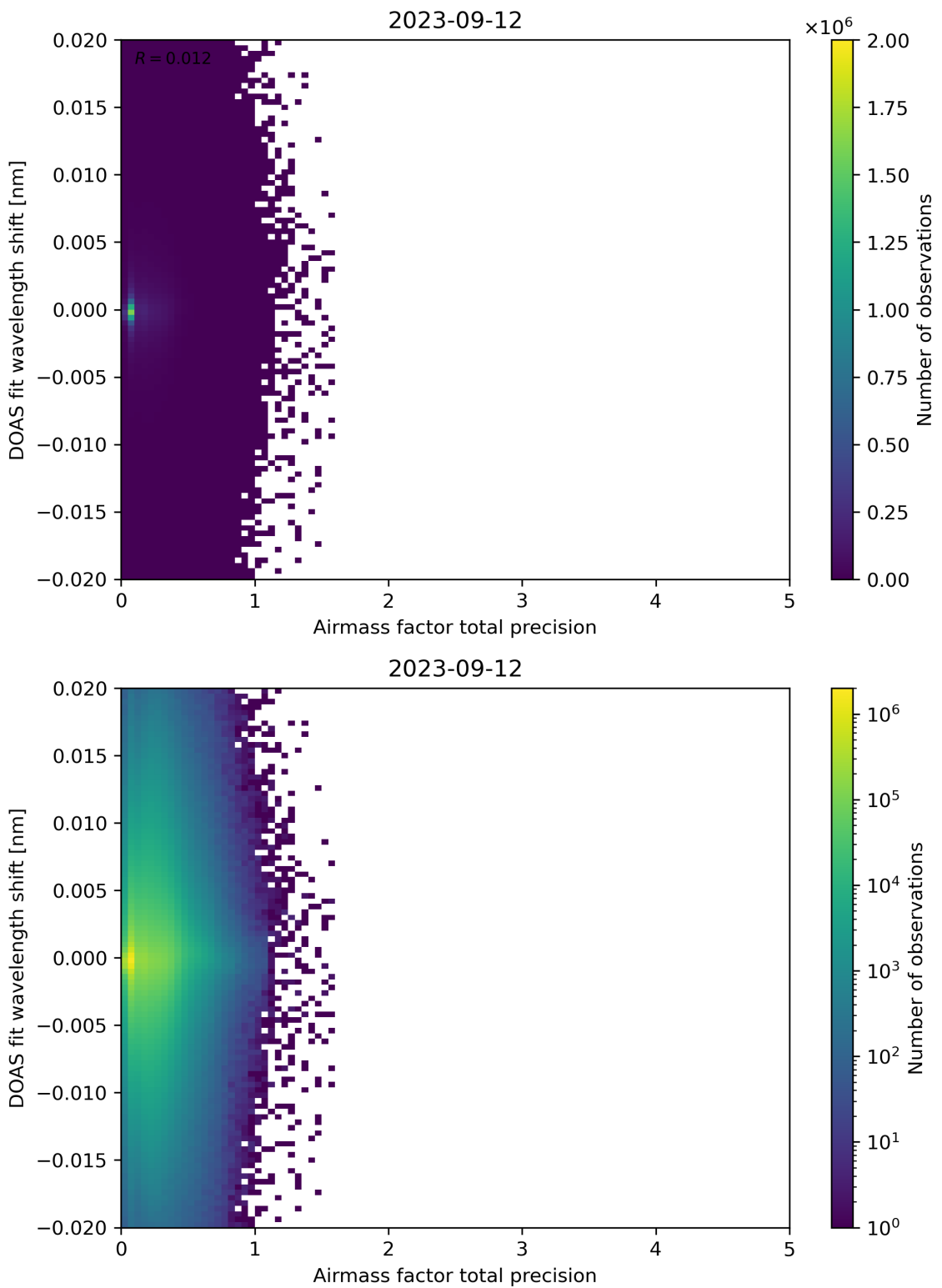


Figure 106: Scatter density plot of “Airmass factor total precision” against “DOAS fit wavelength shift” for 2023-09-11 to 2023-09-13.

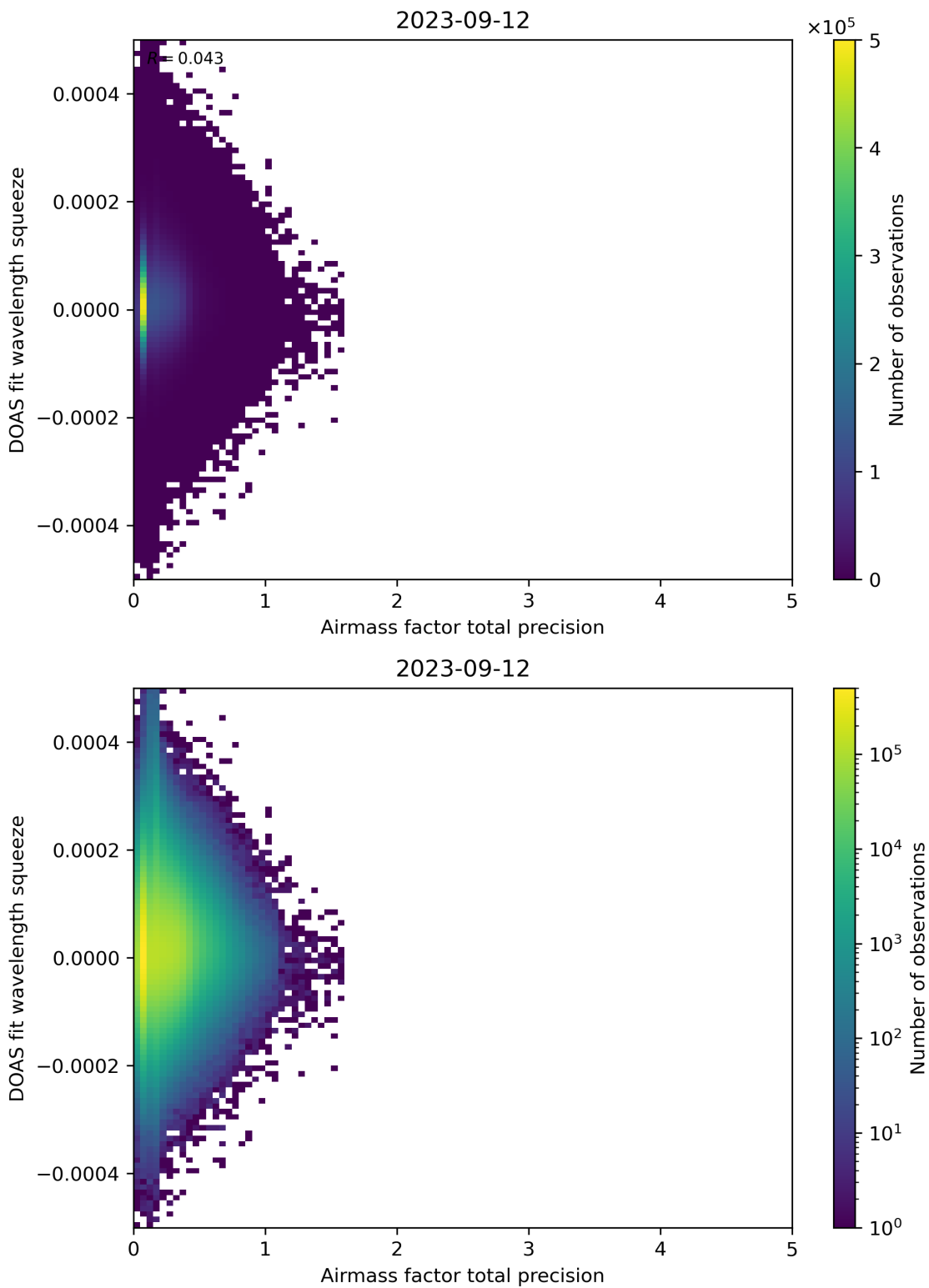


Figure 107: Scatter density plot of “Airmass factor total precision” against “DOAS fit wavelength squeeze” for 2023-09-11 to 2023-09-13.

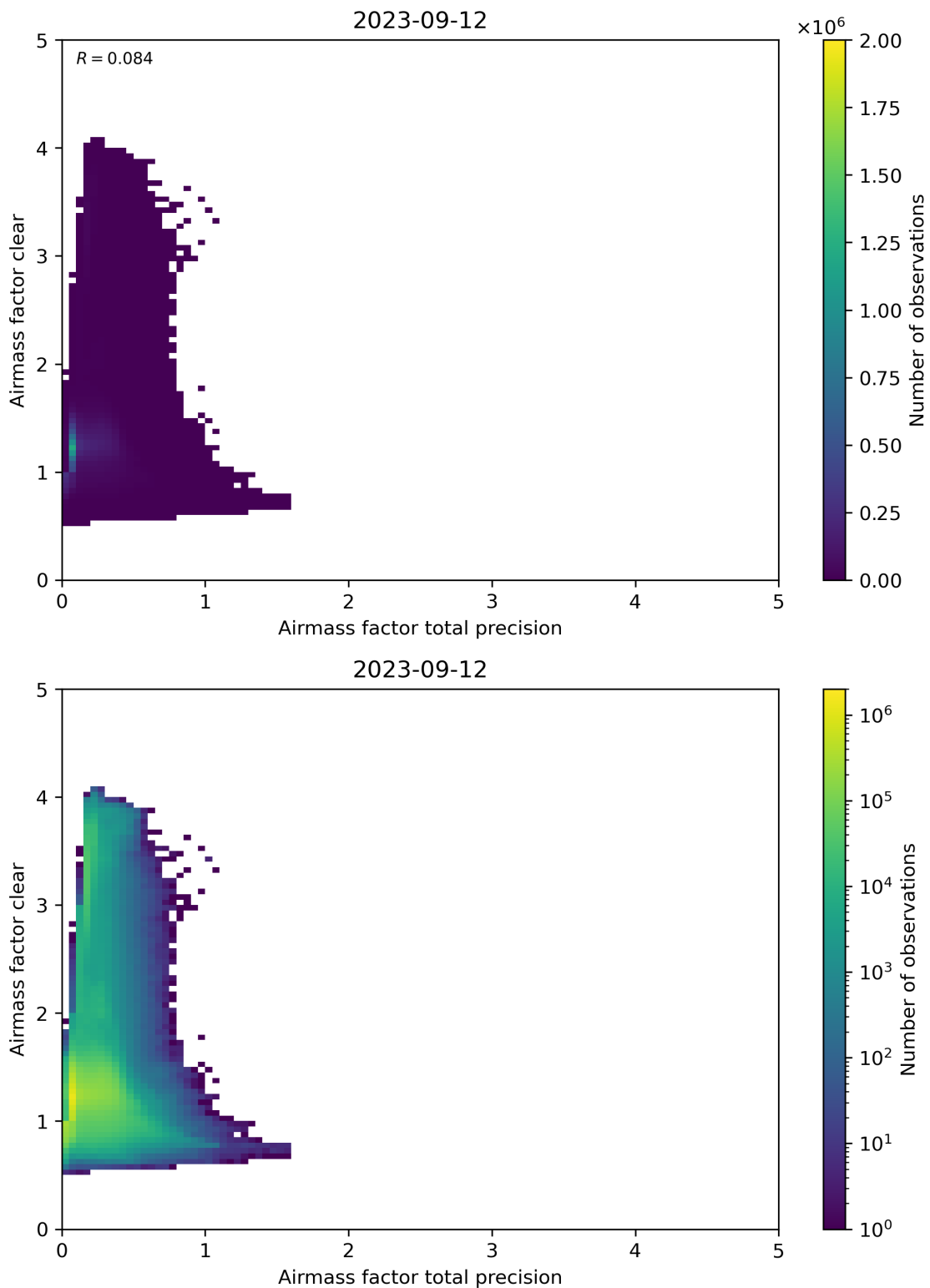


Figure 108: Scatter density plot of “Airmass factor total precision” against “Airmass factor clear” for 2023-09-11 to 2023-09-13.

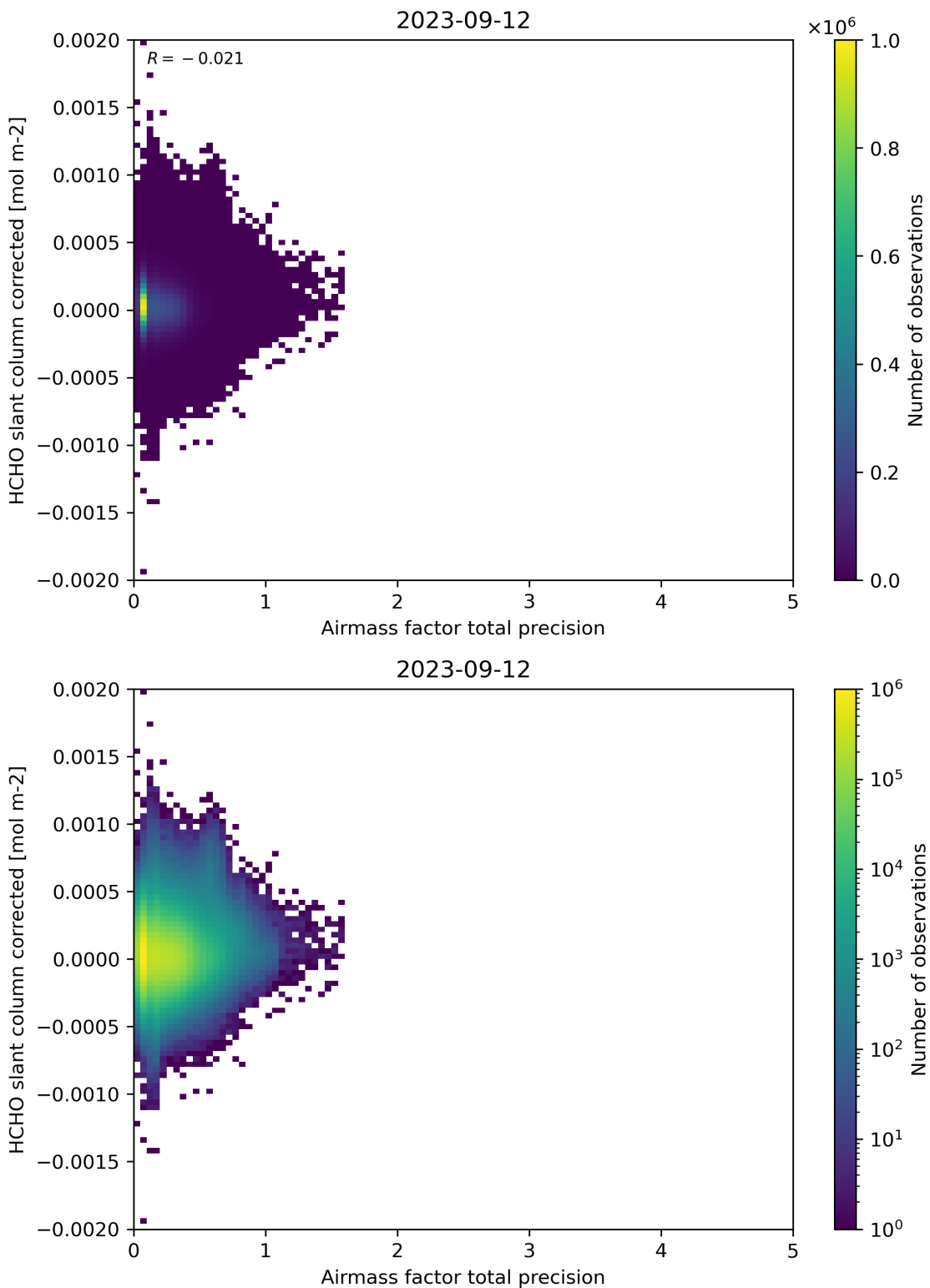


Figure 109: Scatter density plot of “Airmass factor total precision” against “HCHO slant column corrected” for 2023-09-11 to 2023-09-13.

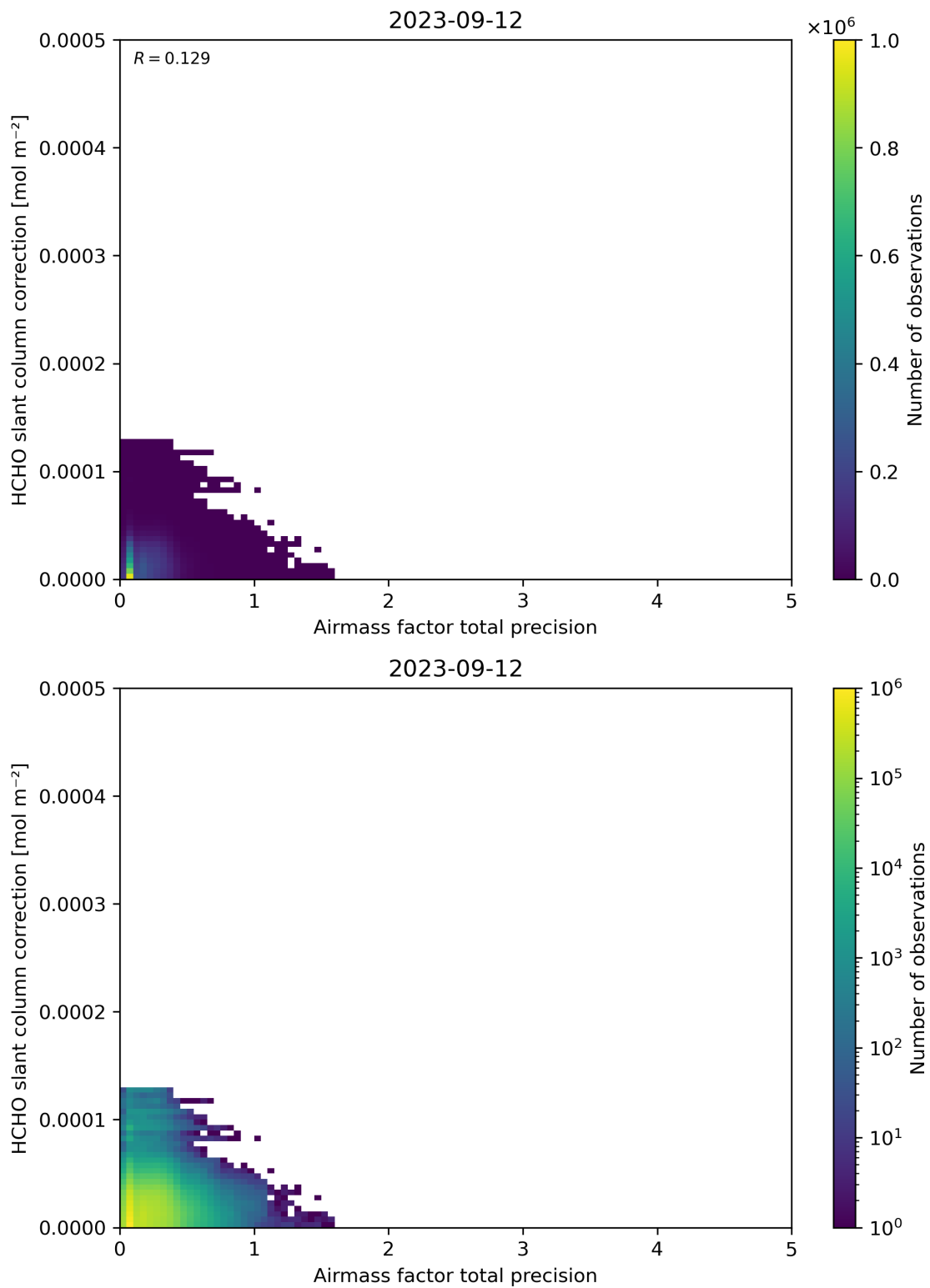


Figure 110: Scatter density plot of “Airmass factor total precision” against “HCHO slant column correction” for 2023-09-11 to 2023-09-13.

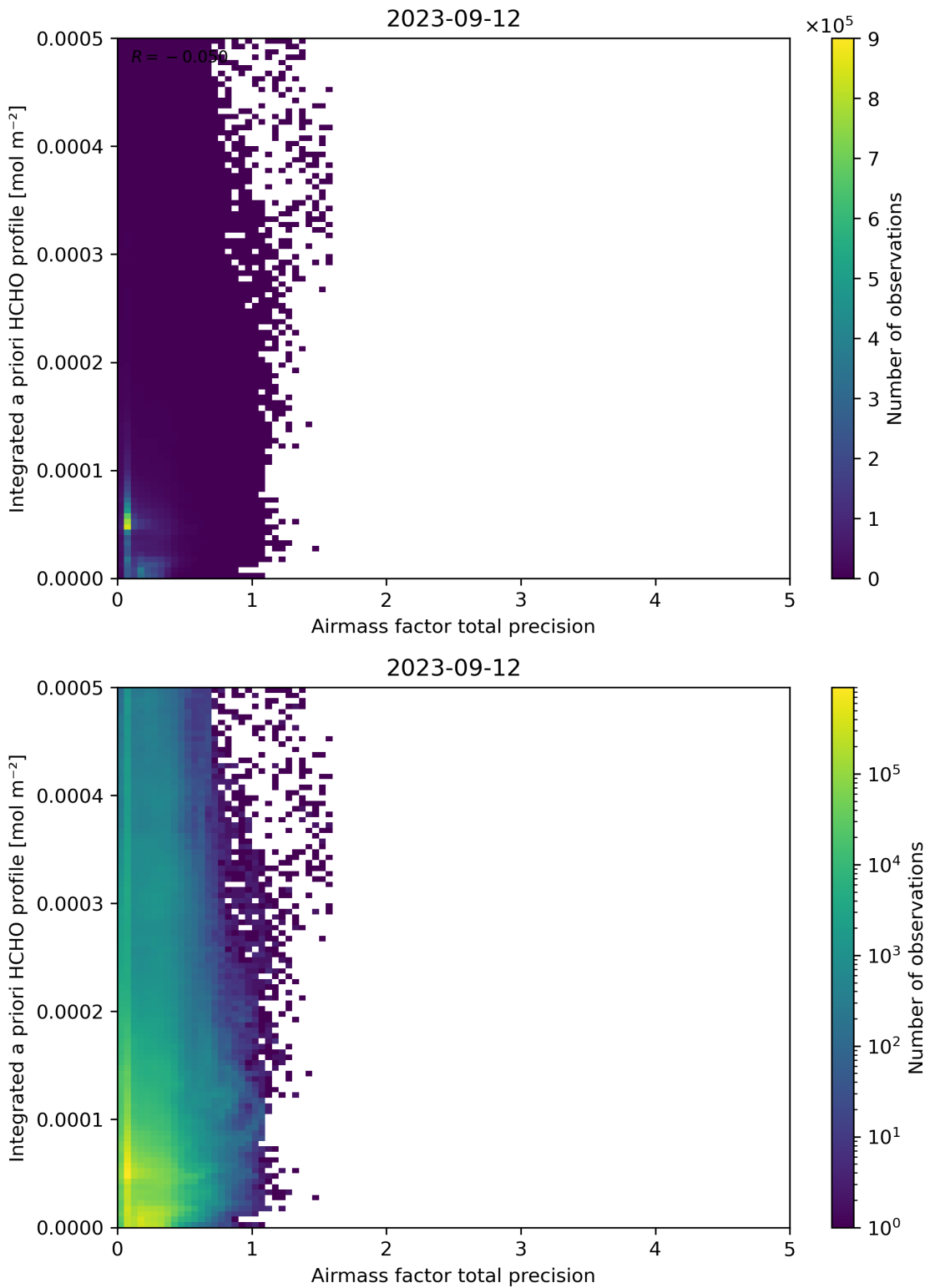


Figure 111: Scatter density plot of “Airmass factor total precision” against “Integrated a priori HCHO profile” for 2023-09-11 to 2023-09-13.

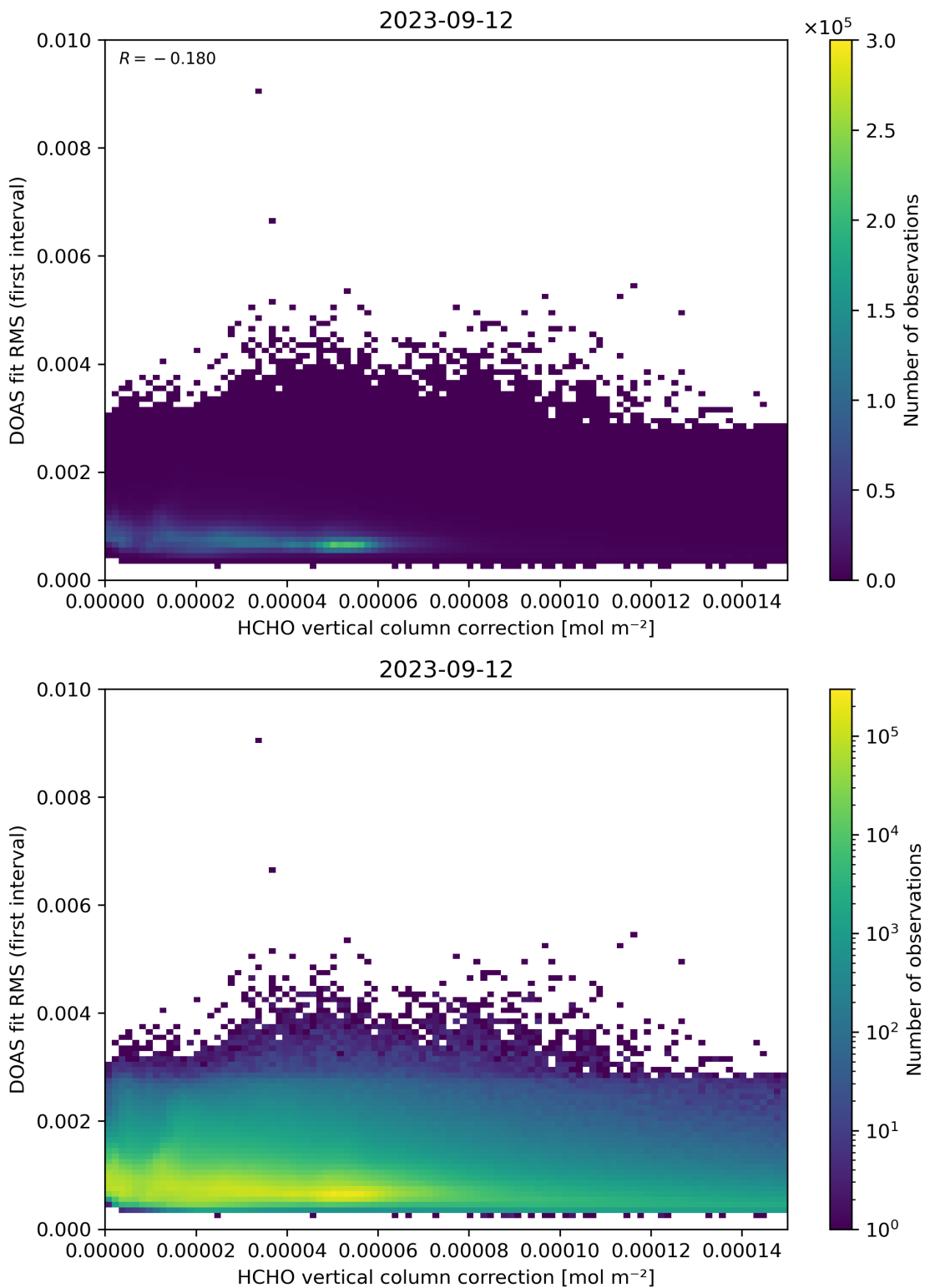


Figure 112: Scatter density plot of “HCHO vertical column correction” against “DOAS fit RMS (first interval)” for 2023-09-11 to 2023-09-13.

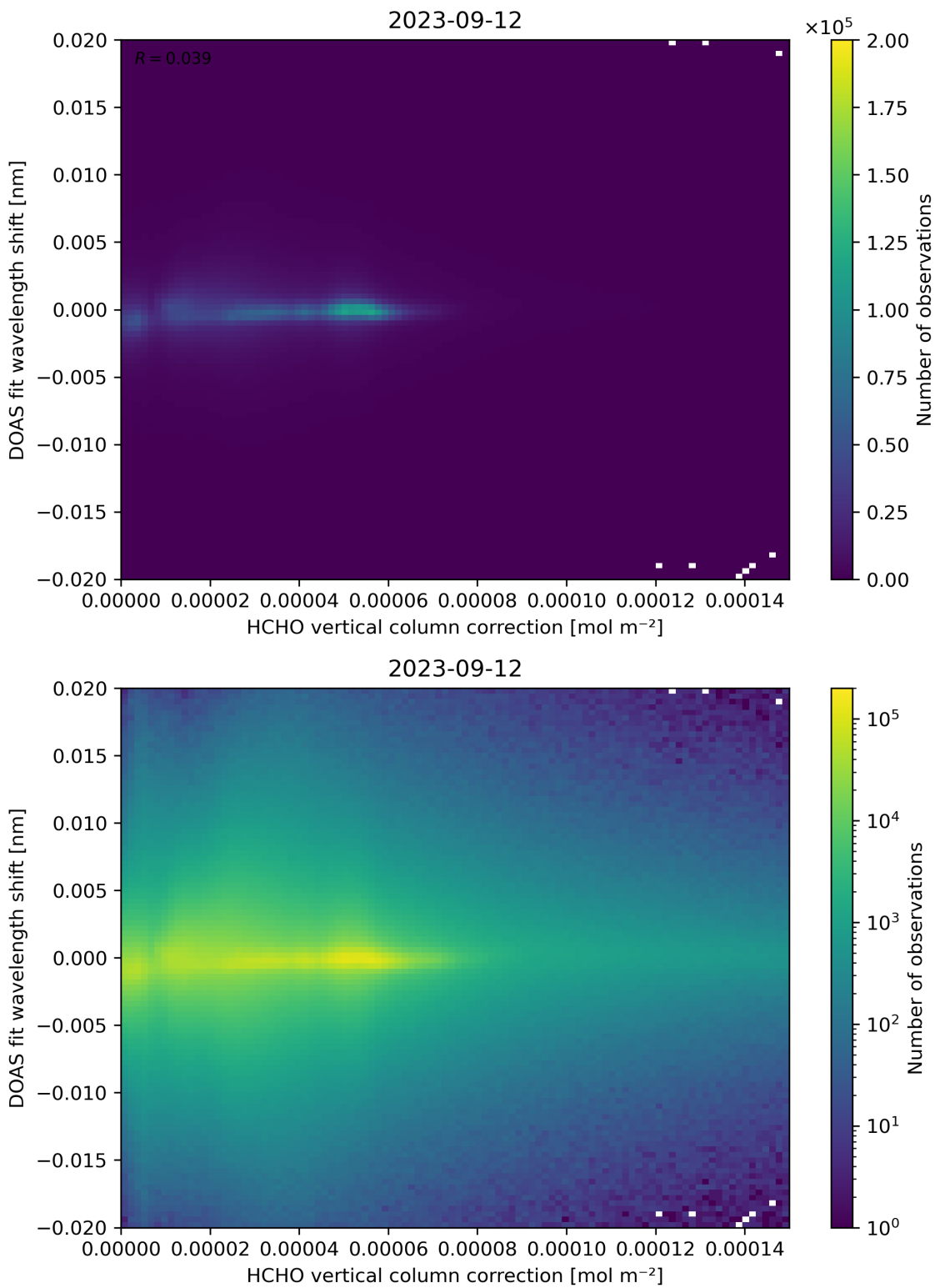


Figure 113: Scatter density plot of “HCHO vertical column correction” against “DOAS fit wavelength shift” for 2023-09-11 to 2023-09-13.

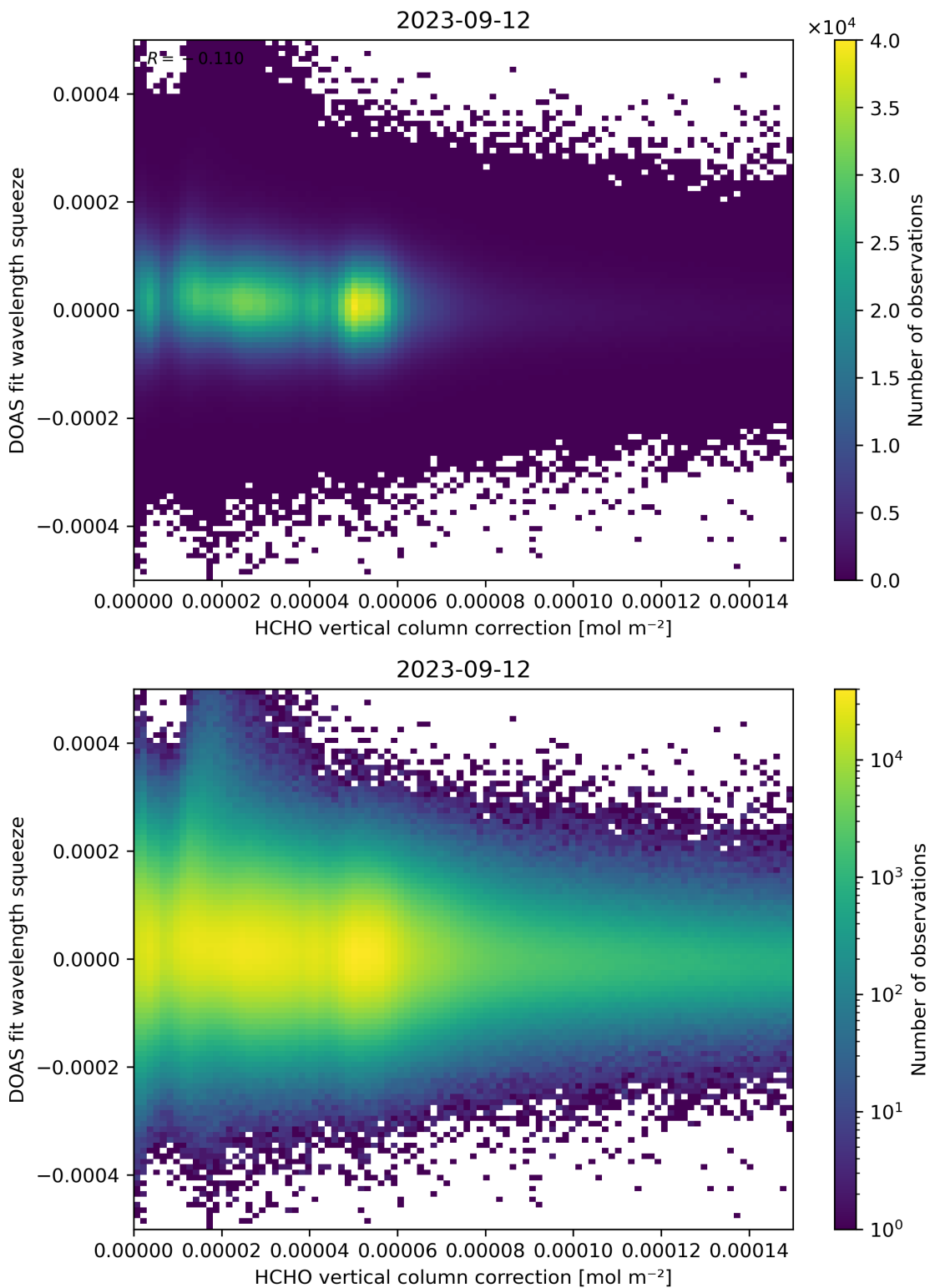


Figure 114: Scatter density plot of “HCHO vertical column correction” against “DOAS fit wavelength squeeze” for 2023-09-11 to 2023-09-13.

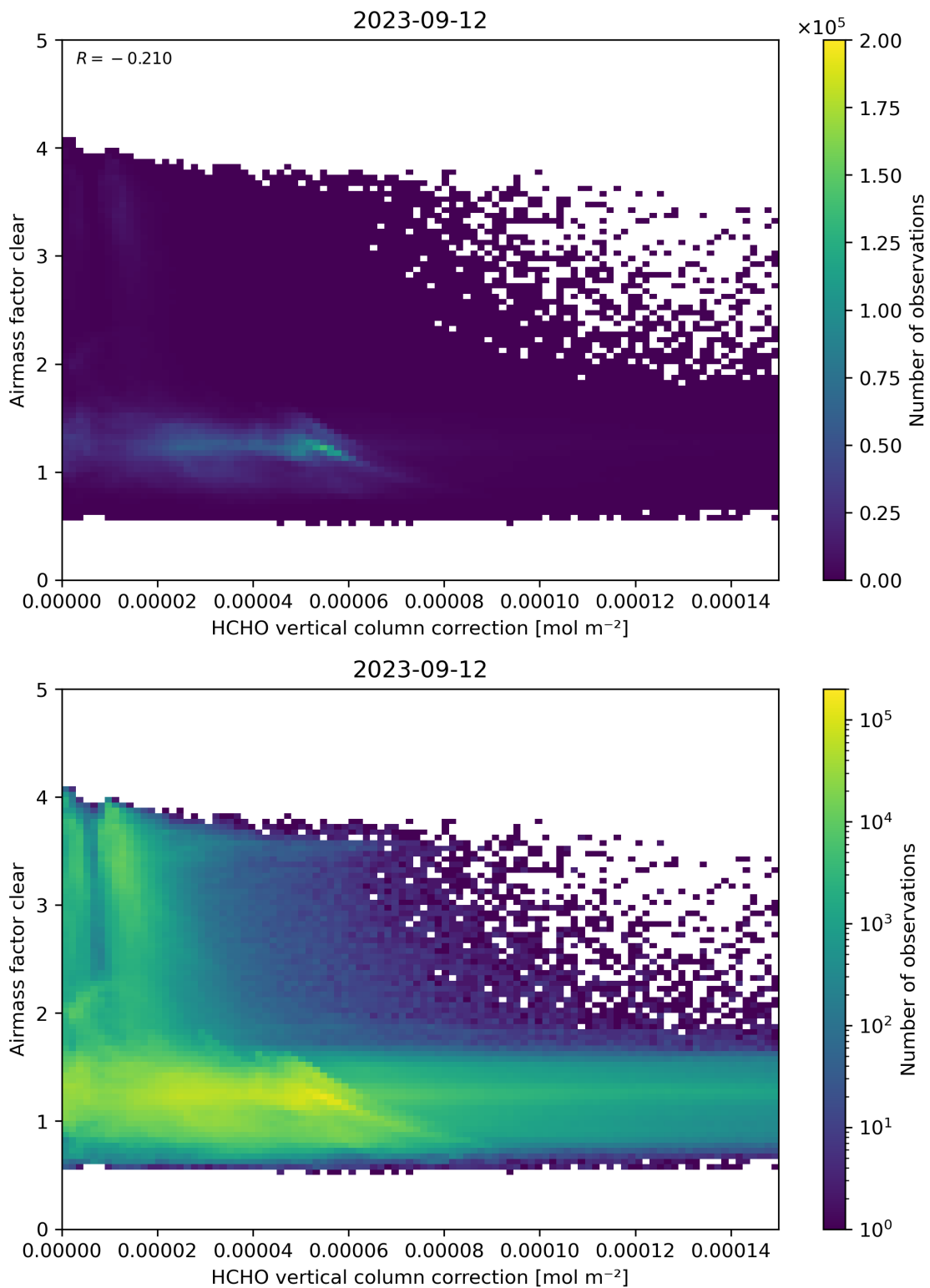


Figure 115: Scatter density plot of “HCHO vertical column correction” against “Airmass factor clear” for 2023-09-11 to 2023-09-13.

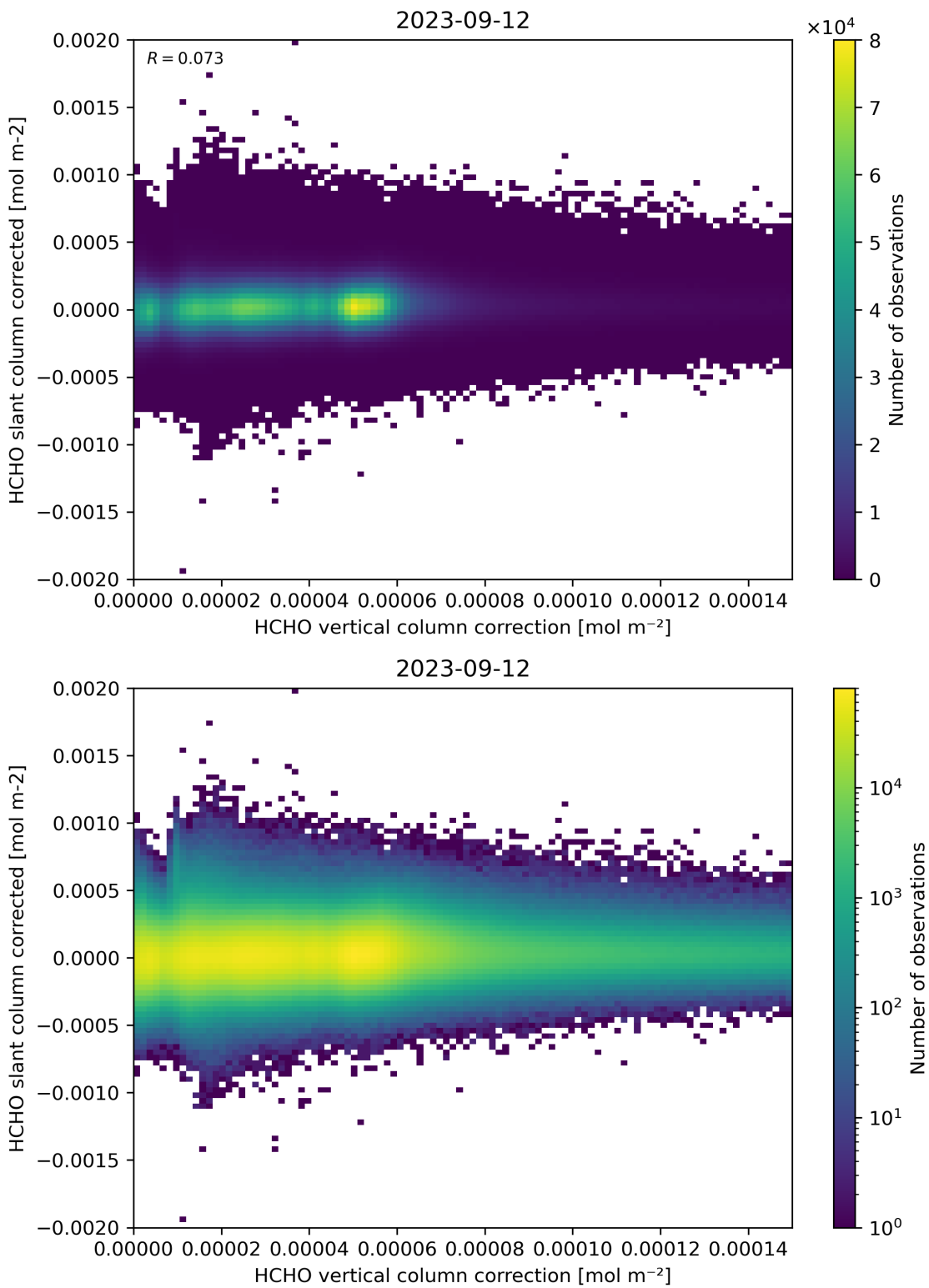


Figure 116: Scatter density plot of “HCHO vertical column correction” against “HCHO slant column corrected” for 2023-09-11 to 2023-09-13.

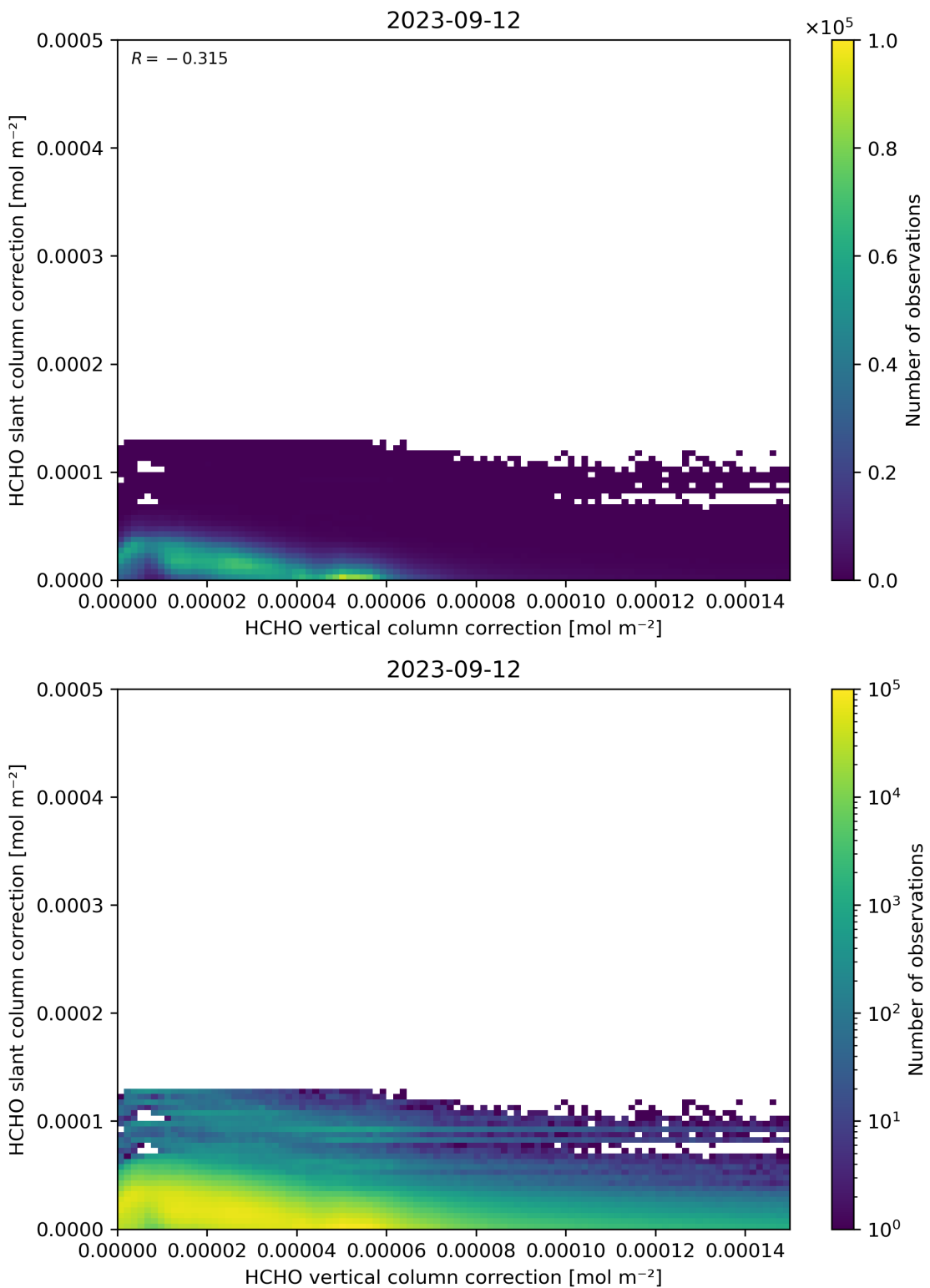


Figure 117: Scatter density plot of “HCHO vertical column correction” against “HCHO slant column correction” for 2023-09-11 to 2023-09-13.

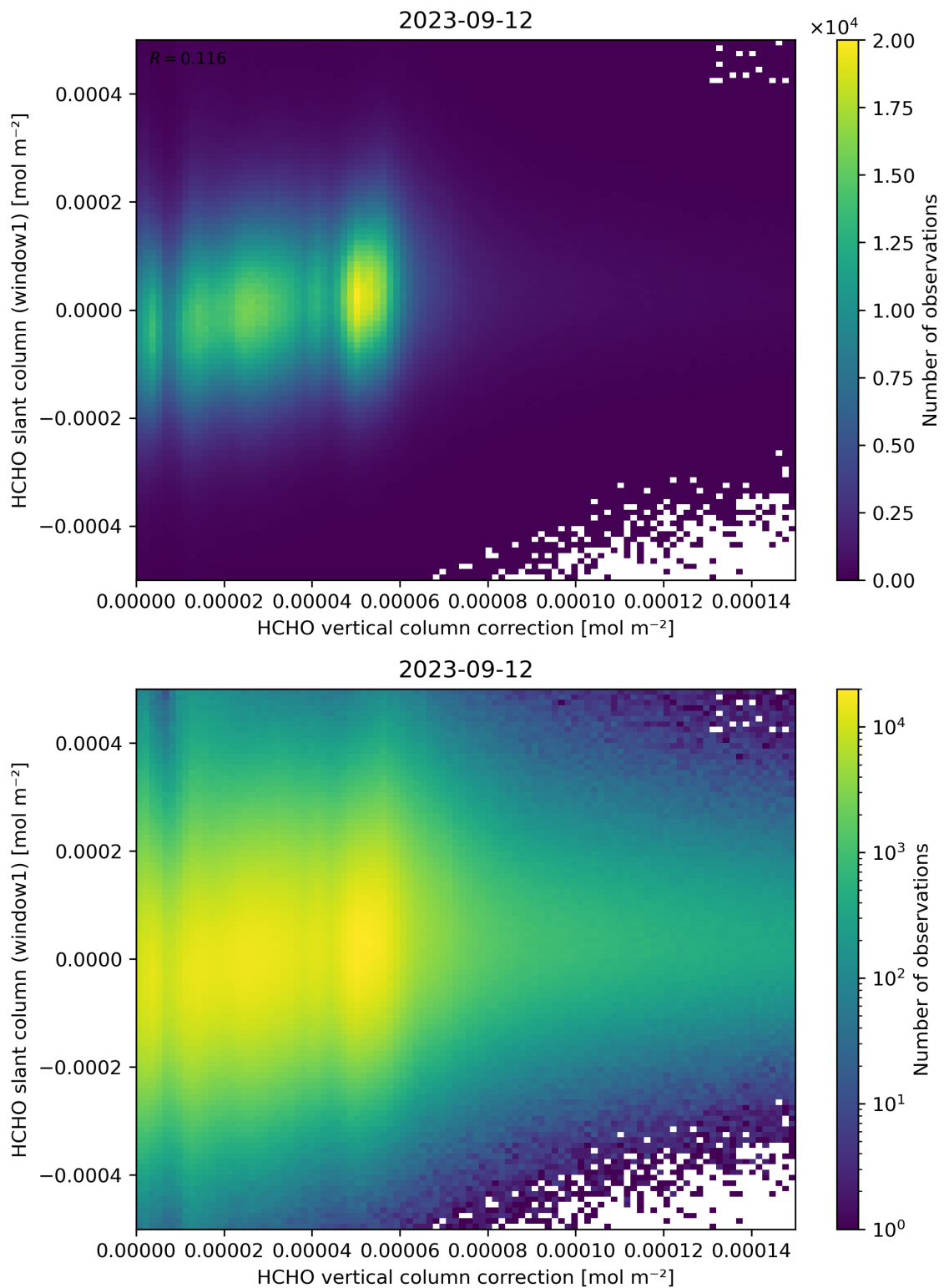


Figure 118: Scatter density plot of “HCHO vertical column correction” against “HCHO slant column (window1)” for 2023-09-11 to 2023-09-13.

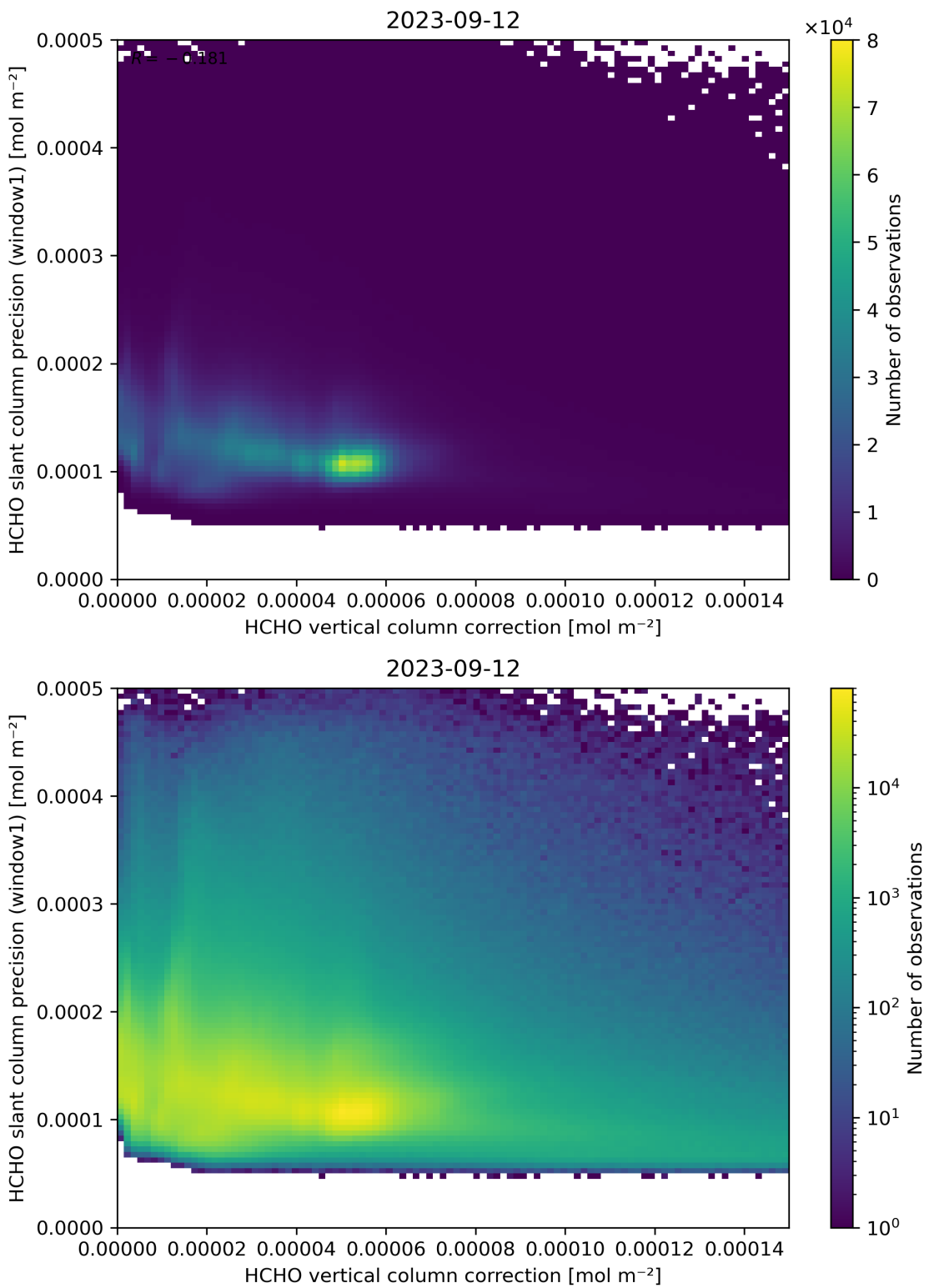


Figure 119: Scatter density plot of “HCHO vertical column correction” against “HCHO slant column precision (window1)” for 2023-09-11 to 2023-09-13.

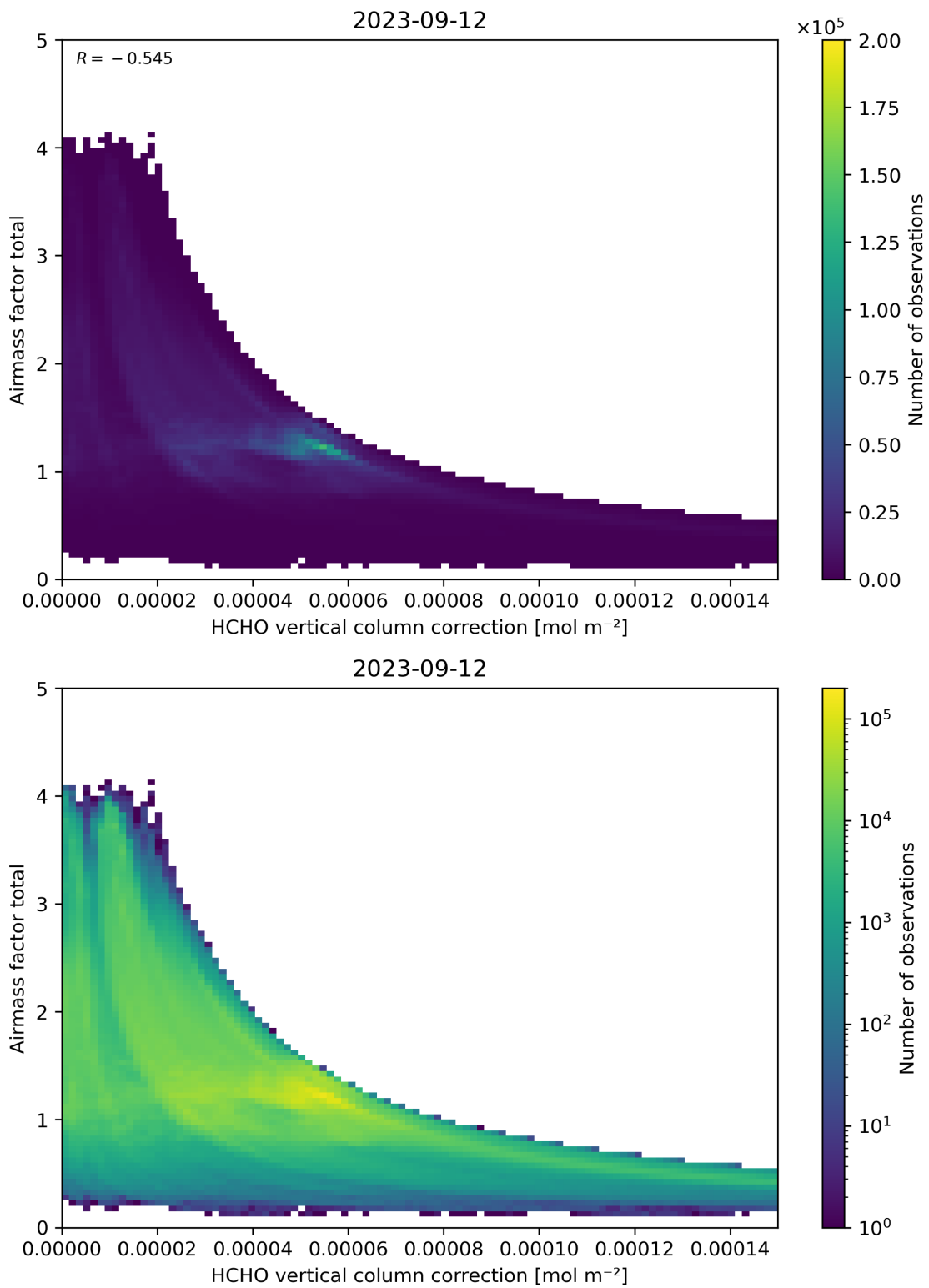


Figure 120: Scatter density plot of “HCHO vertical column correction” against “Airmass factor total” for 2023-09-11 to 2023-09-13.

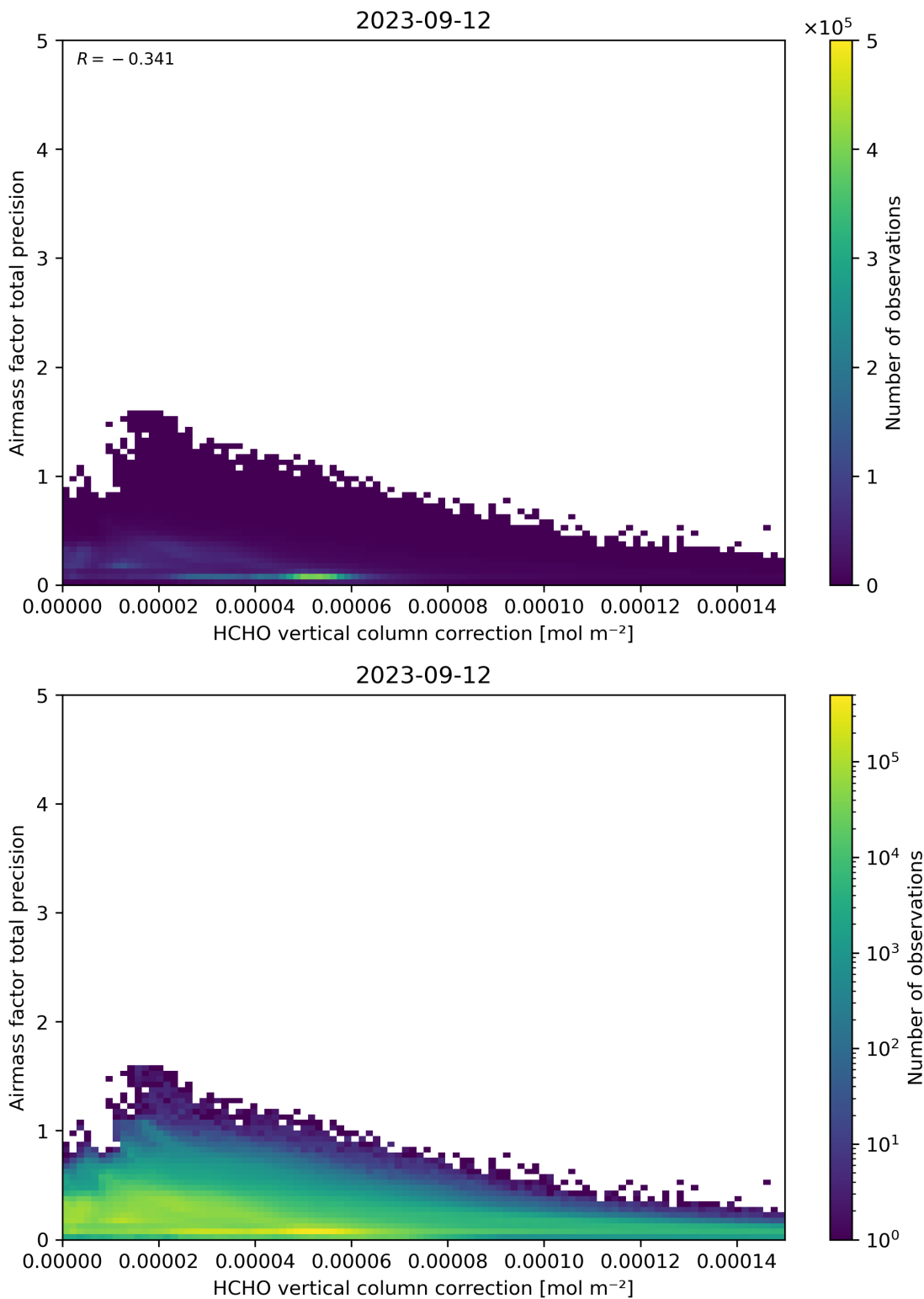


Figure 121: Scatter density plot of “HCHO vertical column correction” against “Airmass factor total precision” for 2023-09-11 to 2023-09-13.

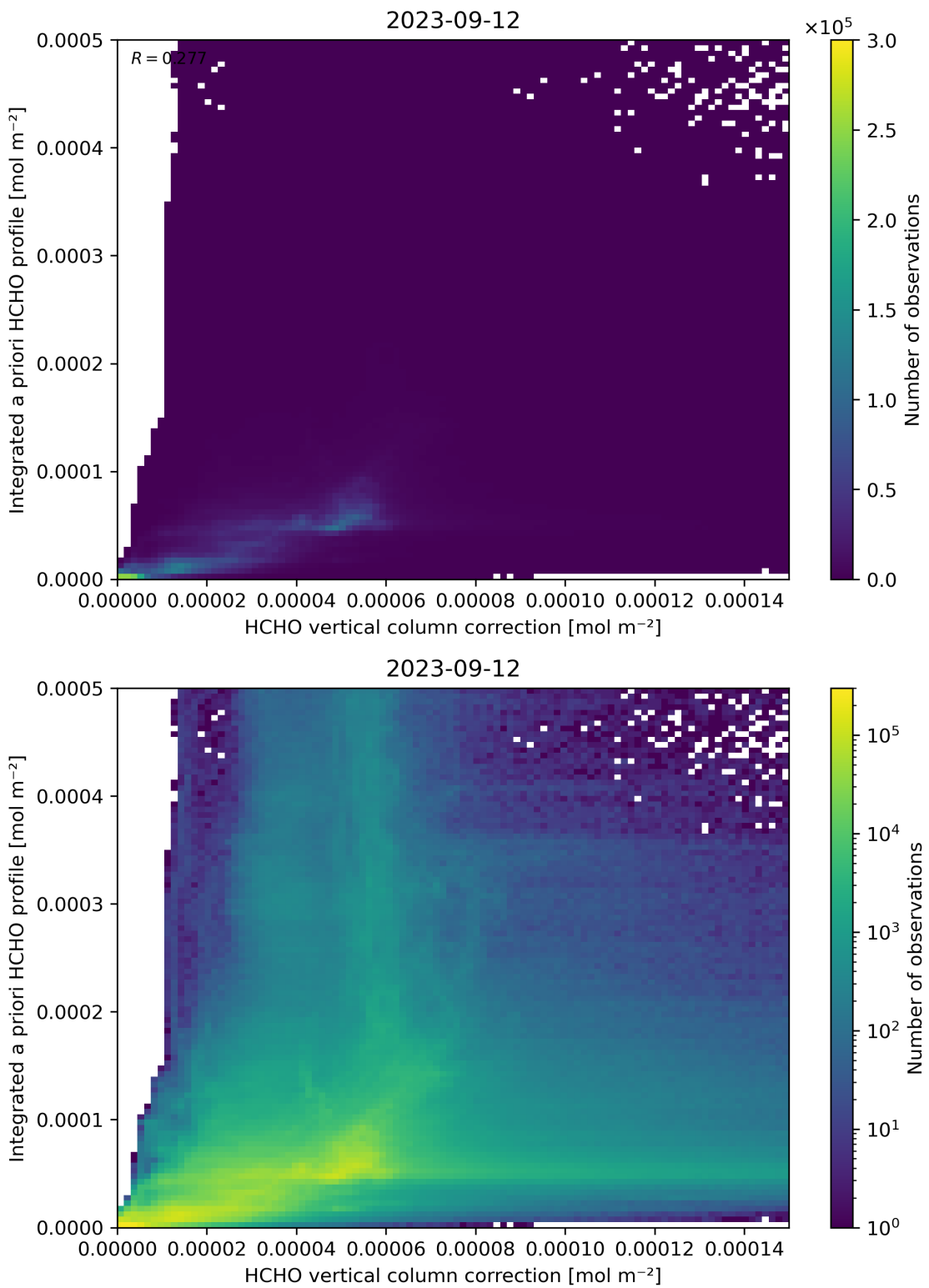


Figure 122: Scatter density plot of “HCHO vertical column correction” against “Integrated a priori HCHO profile” for 2023-09-11 to 2023-09-13.

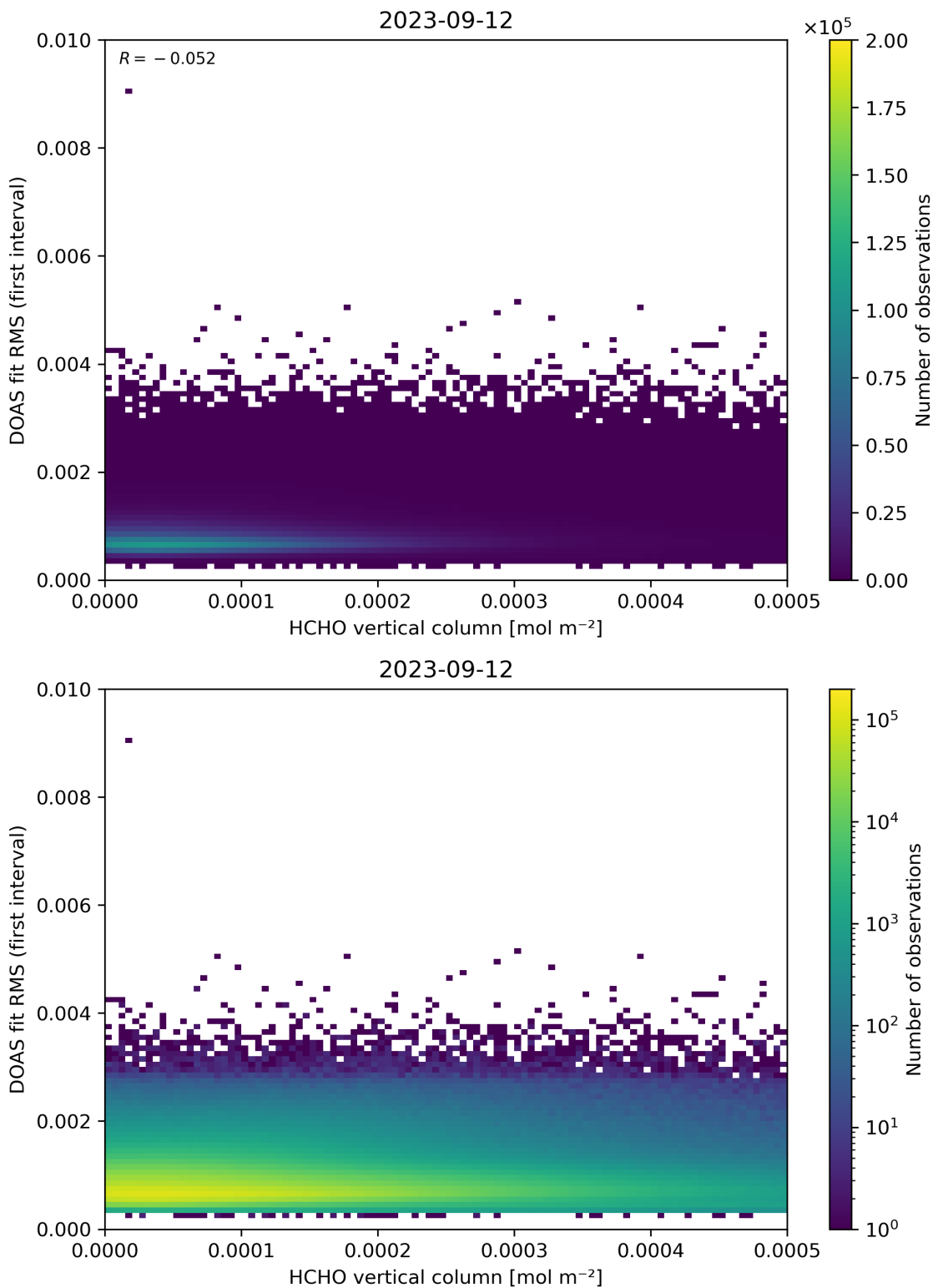


Figure 123: Scatter density plot of “HCHO vertical column” against “DOAS fit RMS (first interval)” for 2023-09-11 to 2023-09-13.

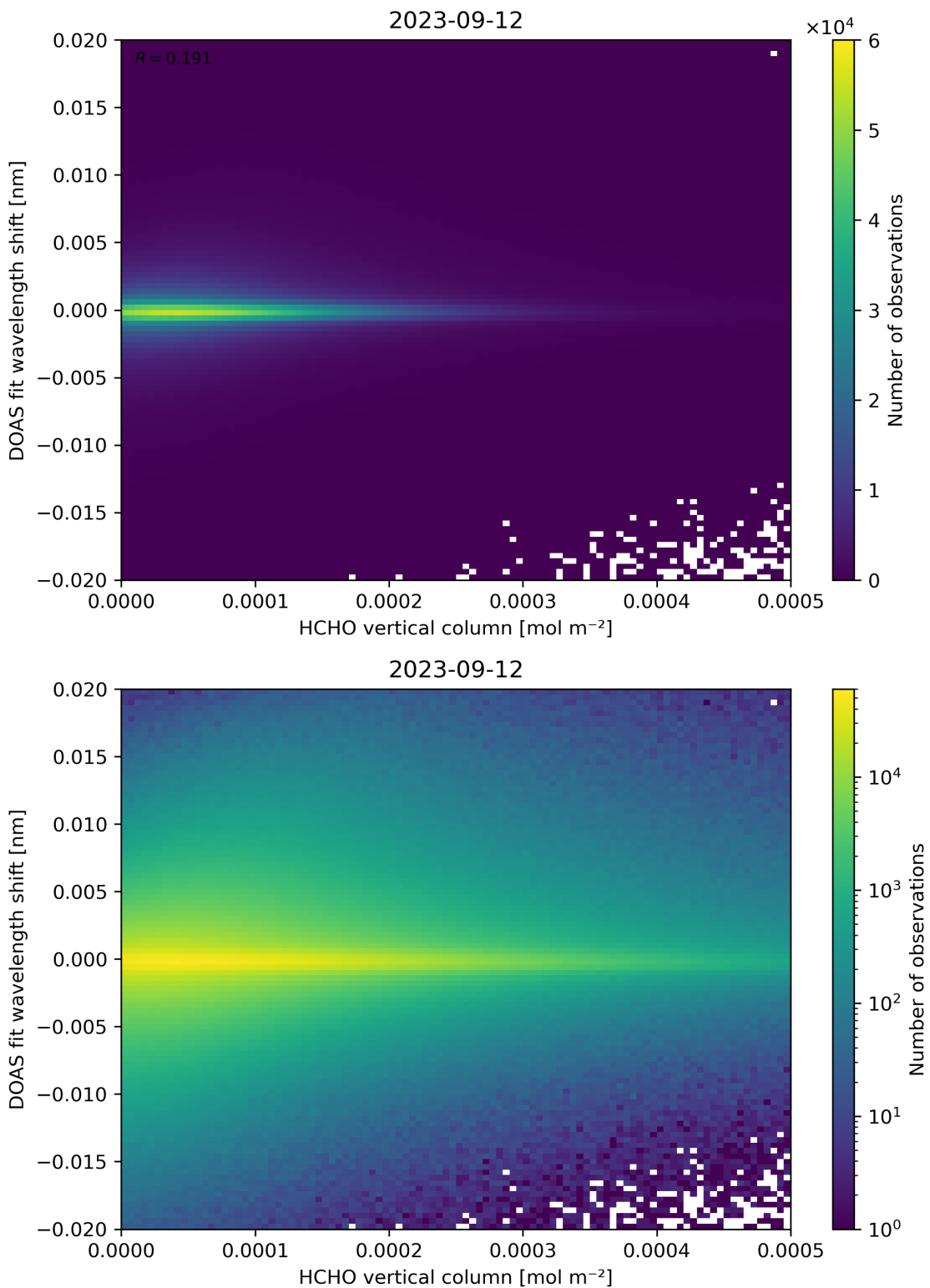


Figure 124: Scatter density plot of “HCHO vertical column” against “DOAS fit wavelength shift” for 2023-09-11 to 2023-09-13.

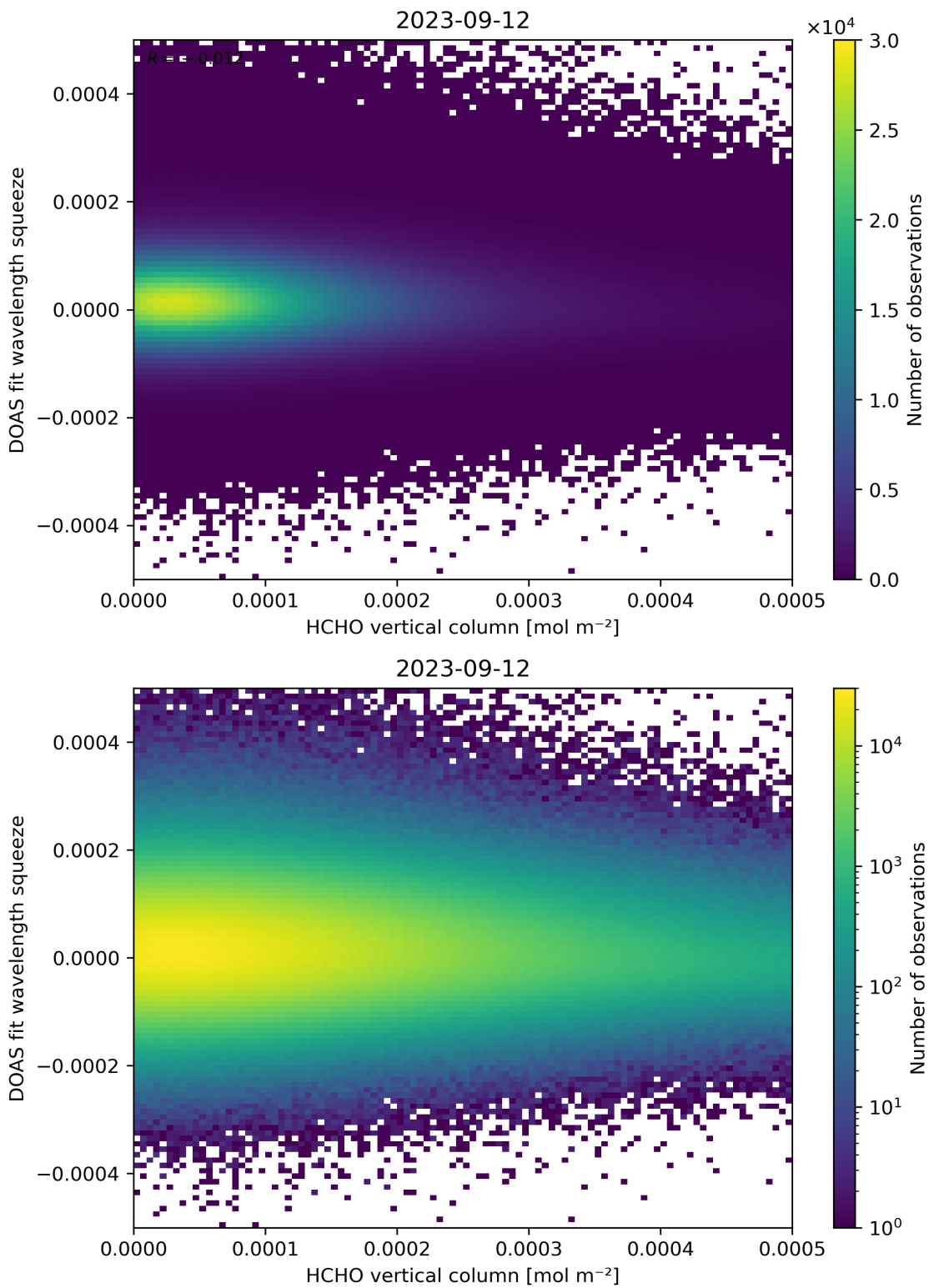


Figure 125: Scatter density plot of “HCHO vertical column” against “DOAS fit wavelength squeeze” for 2023-09-11 to 2023-09-13.

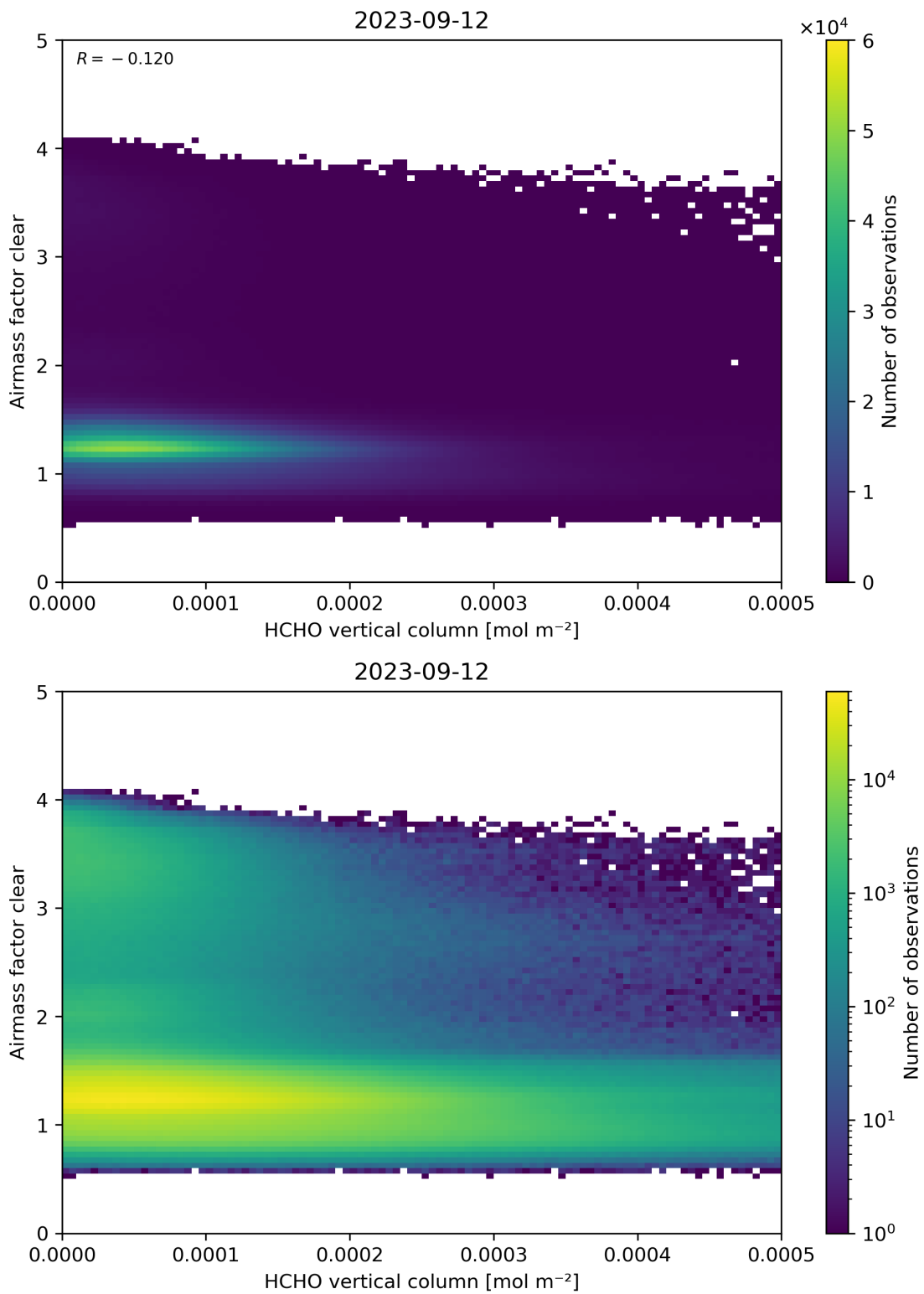


Figure 126: Scatter density plot of “HCHO vertical column” against “Airmass factor clear” for 2023-09-11 to 2023-09-13.

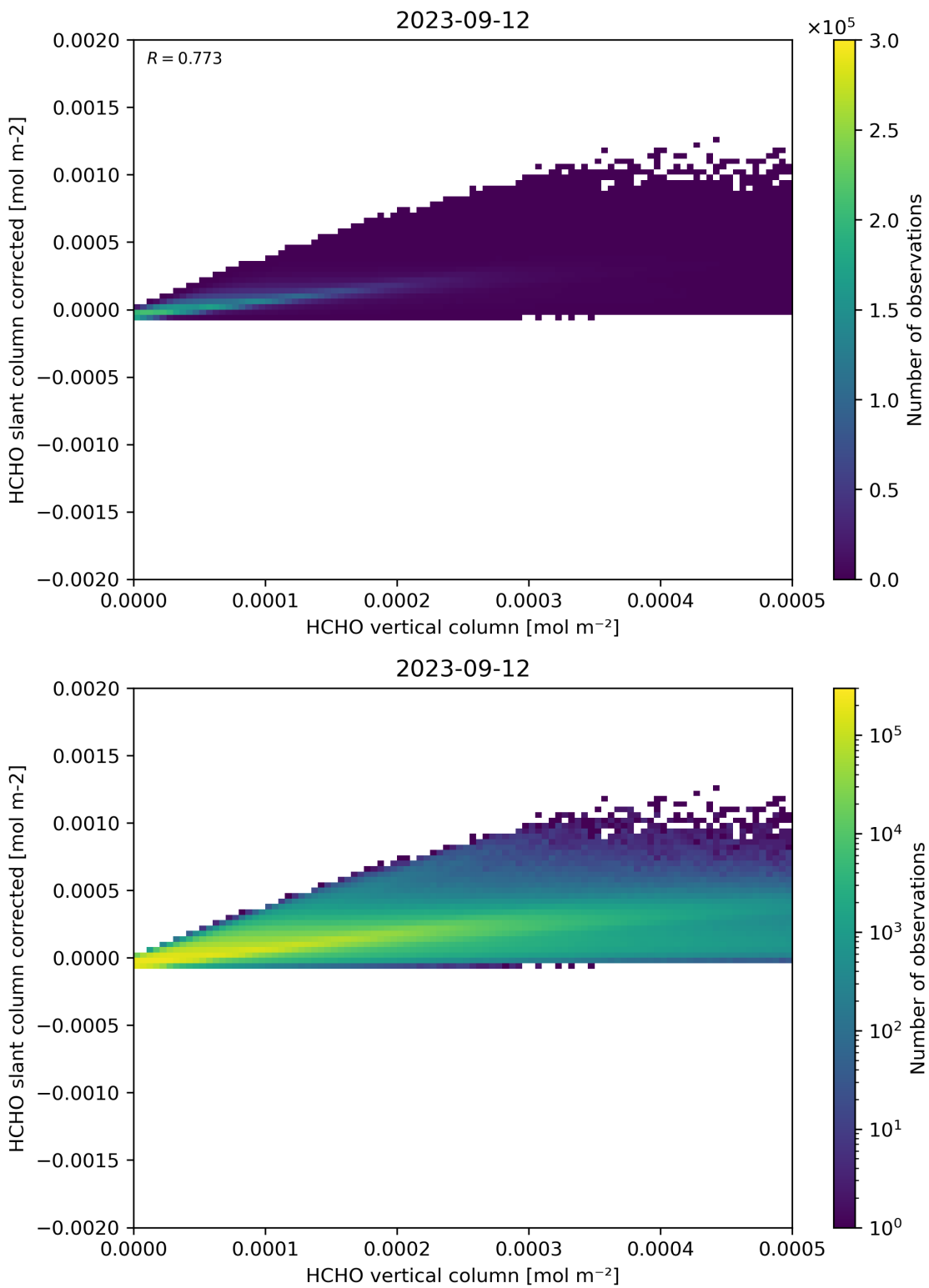


Figure 127: Scatter density plot of “HCHO vertical column” against “HCHO slant column corrected” for 2023-09-11 to 2023-09-13.

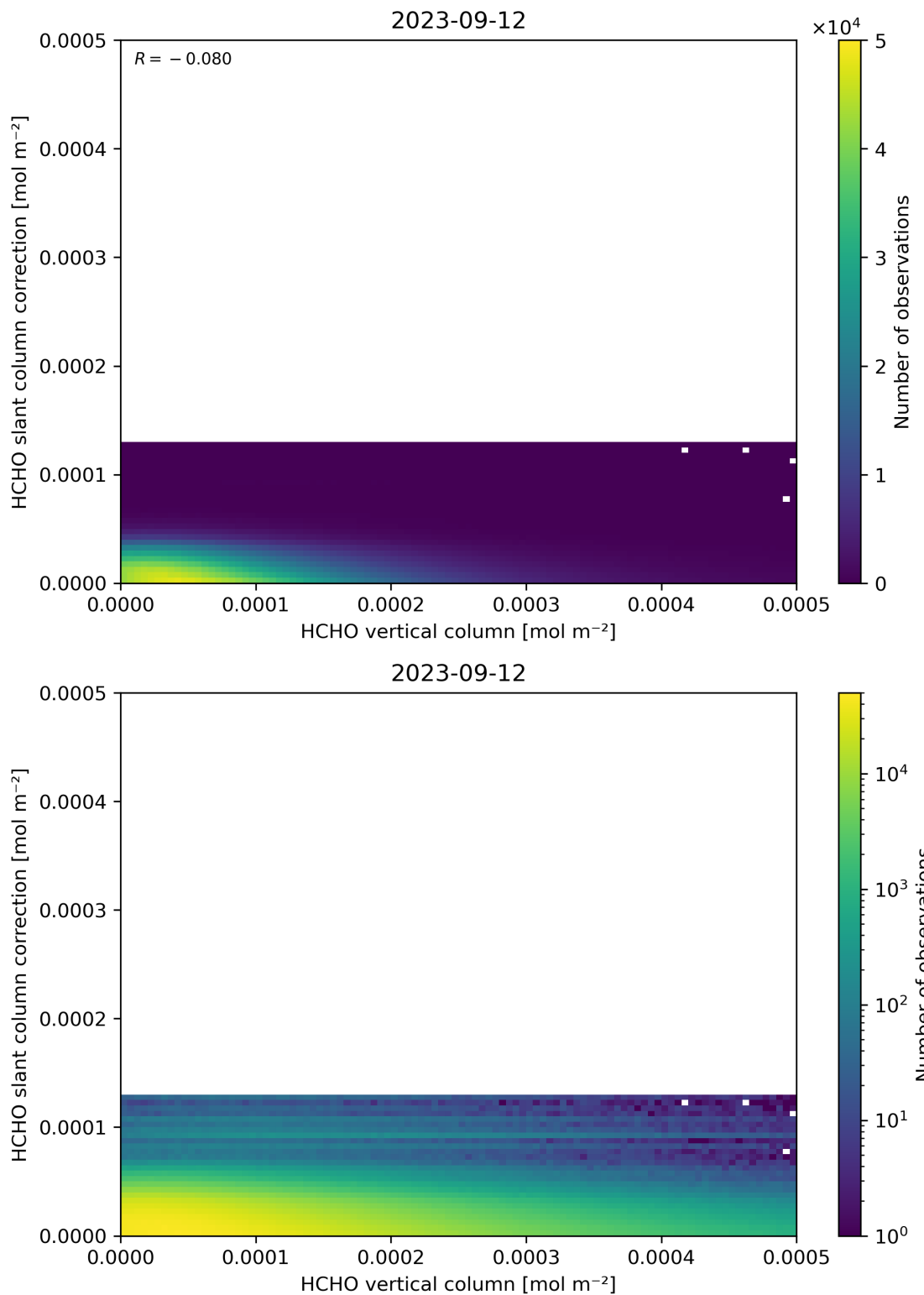


Figure 128: Scatter density plot of “HCHO vertical column” against “HCHO slant column correction” for 2023-09-11 to 2023-09-13.

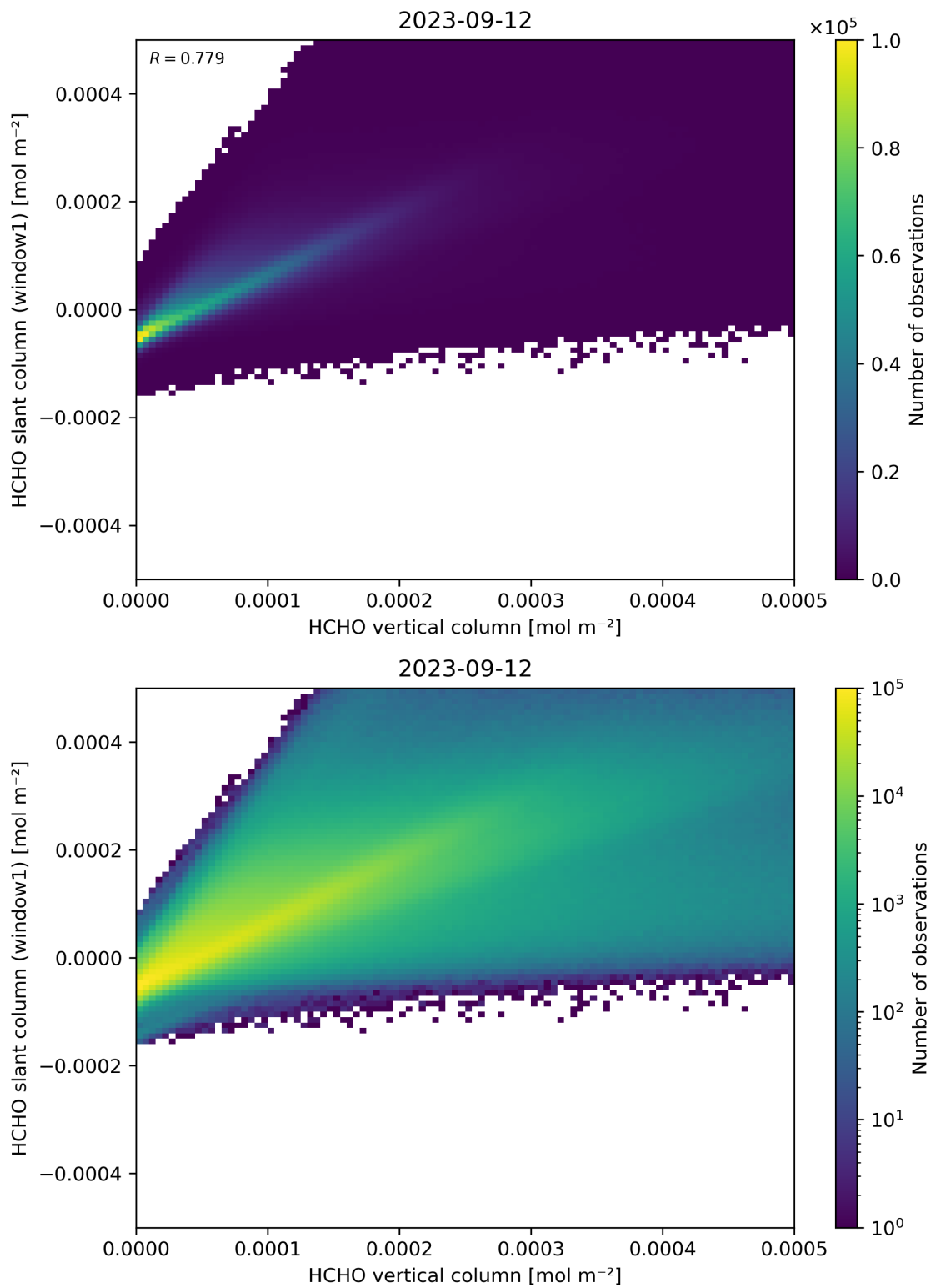


Figure 129: Scatter density plot of “HCHO vertical column” against “HCHO slant column (window1)” for 2023-09-11 to 2023-09-13.

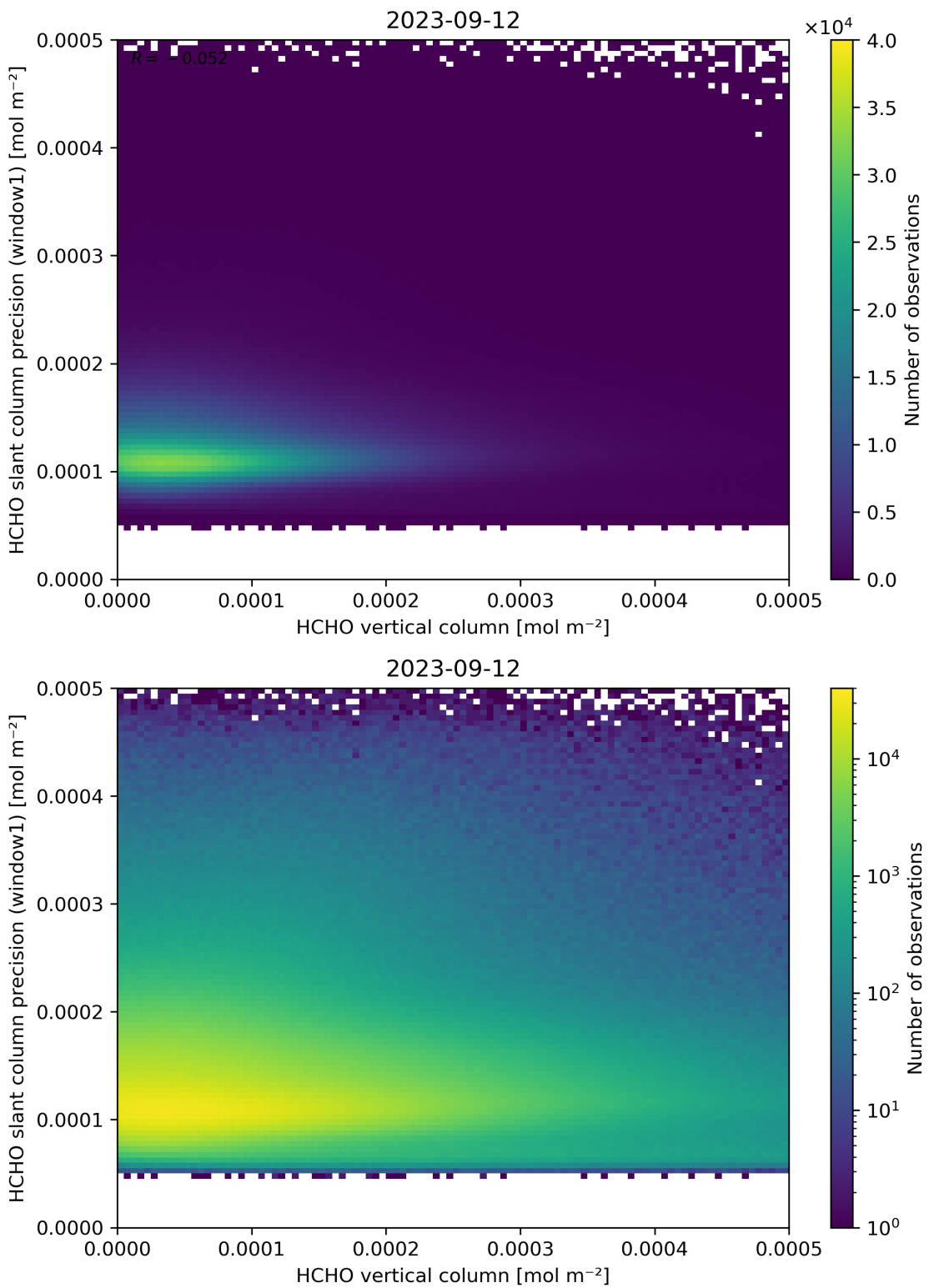


Figure 130: Scatter density plot of “HCHO vertical column” against “HCHO slant column precision (window1)” for 2023-09-11 to 2023-09-13.

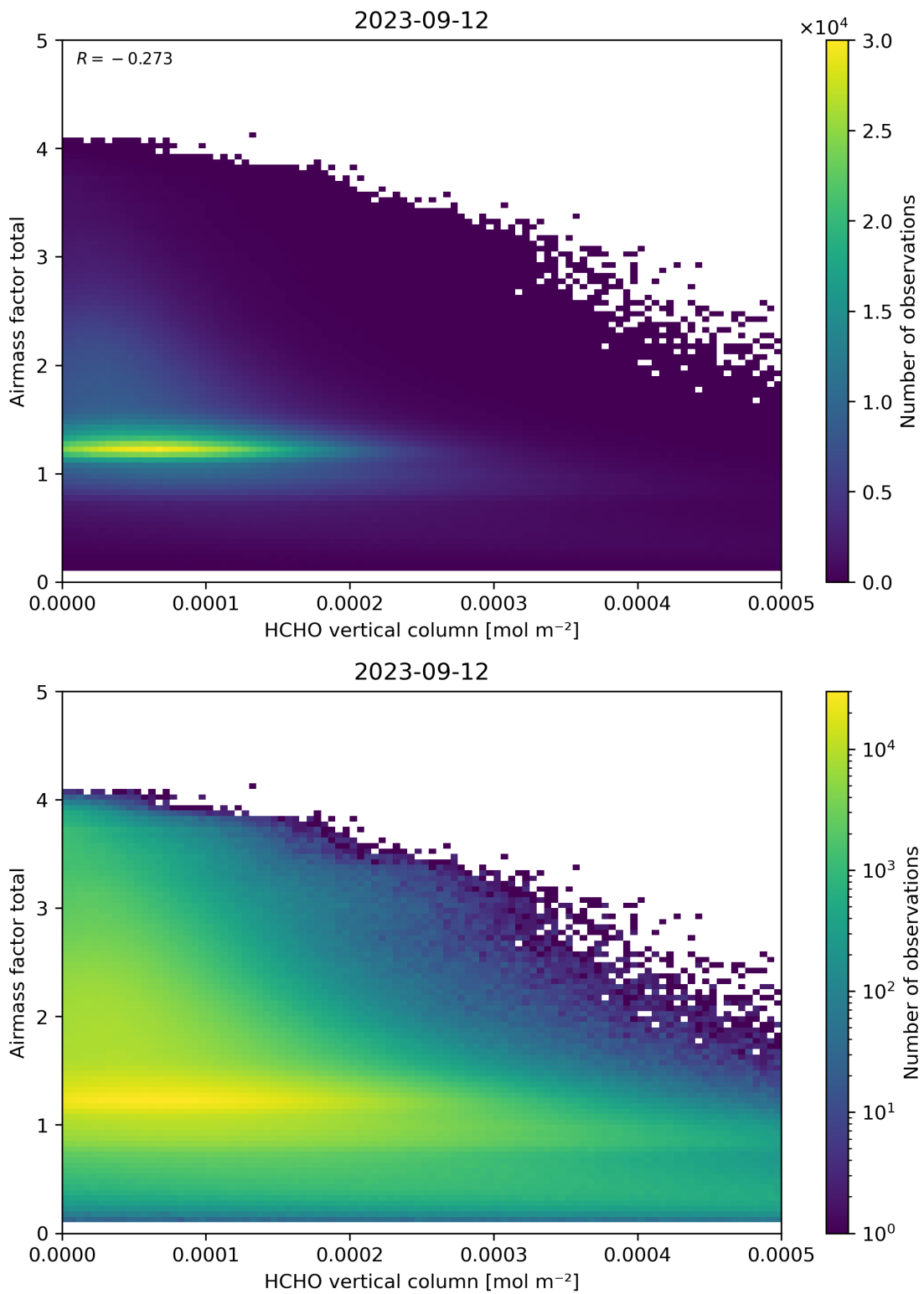


Figure 131: Scatter density plot of “HCHO vertical column” against “Airmass factor total” for 2023-09-11 to 2023-09-13.

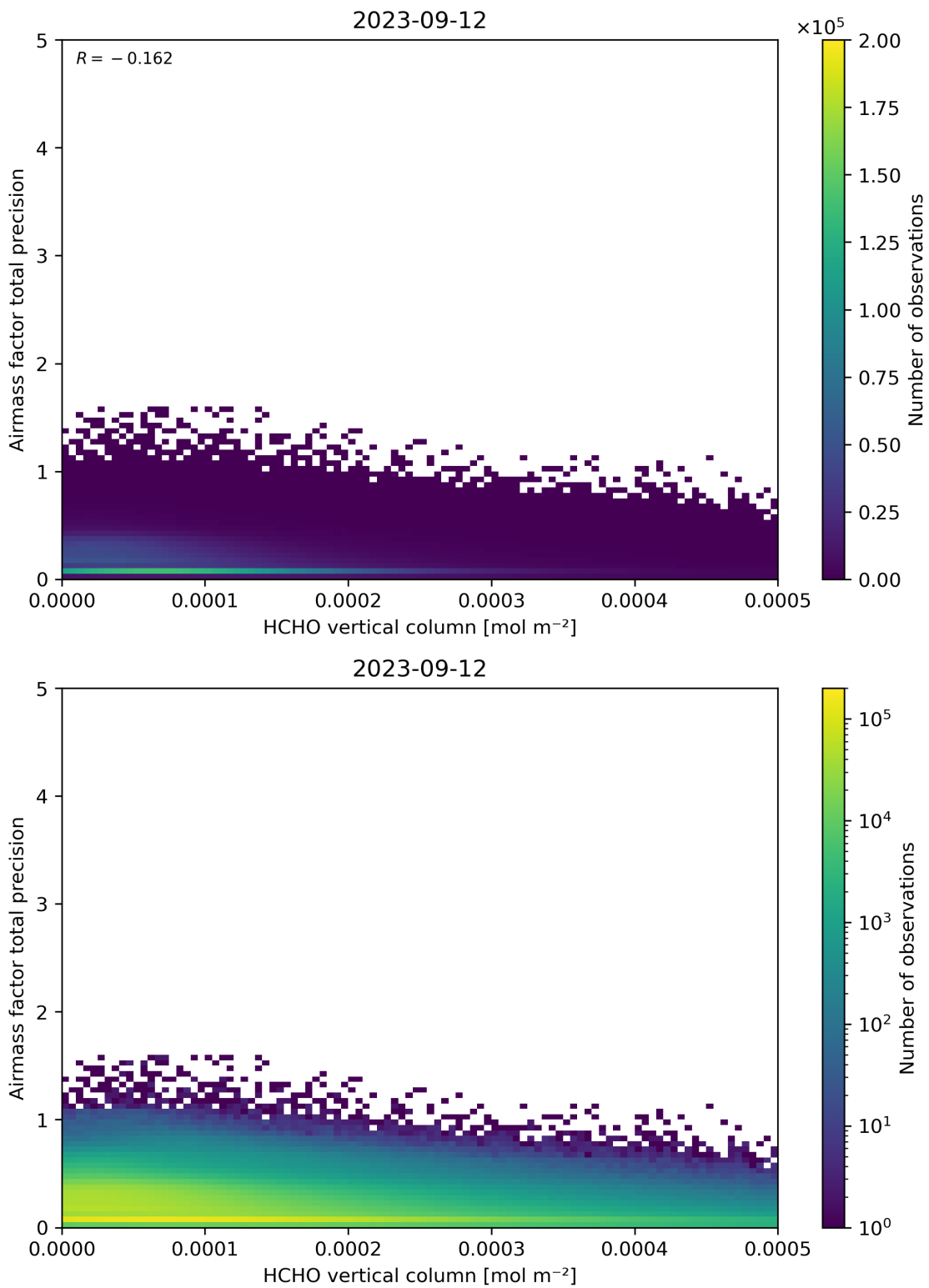


Figure 132: Scatter density plot of “HCHO vertical column” against “Airmass factor total precision” for 2023-09-11 to 2023-09-13.

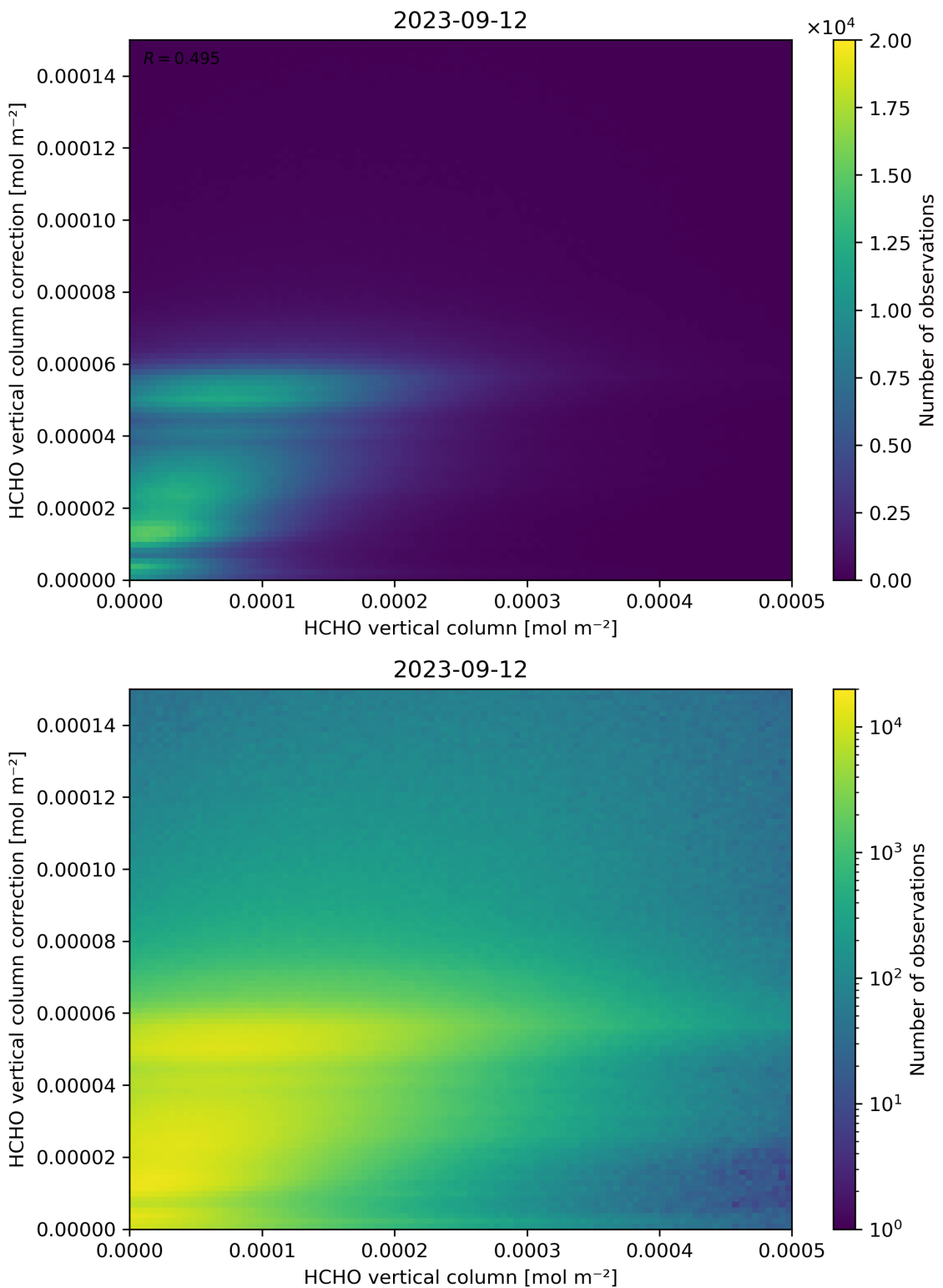


Figure 133: Scatter density plot of “HCHO vertical column” against “HCHO vertical column correction” for 2023-09-11 to 2023-09-13.

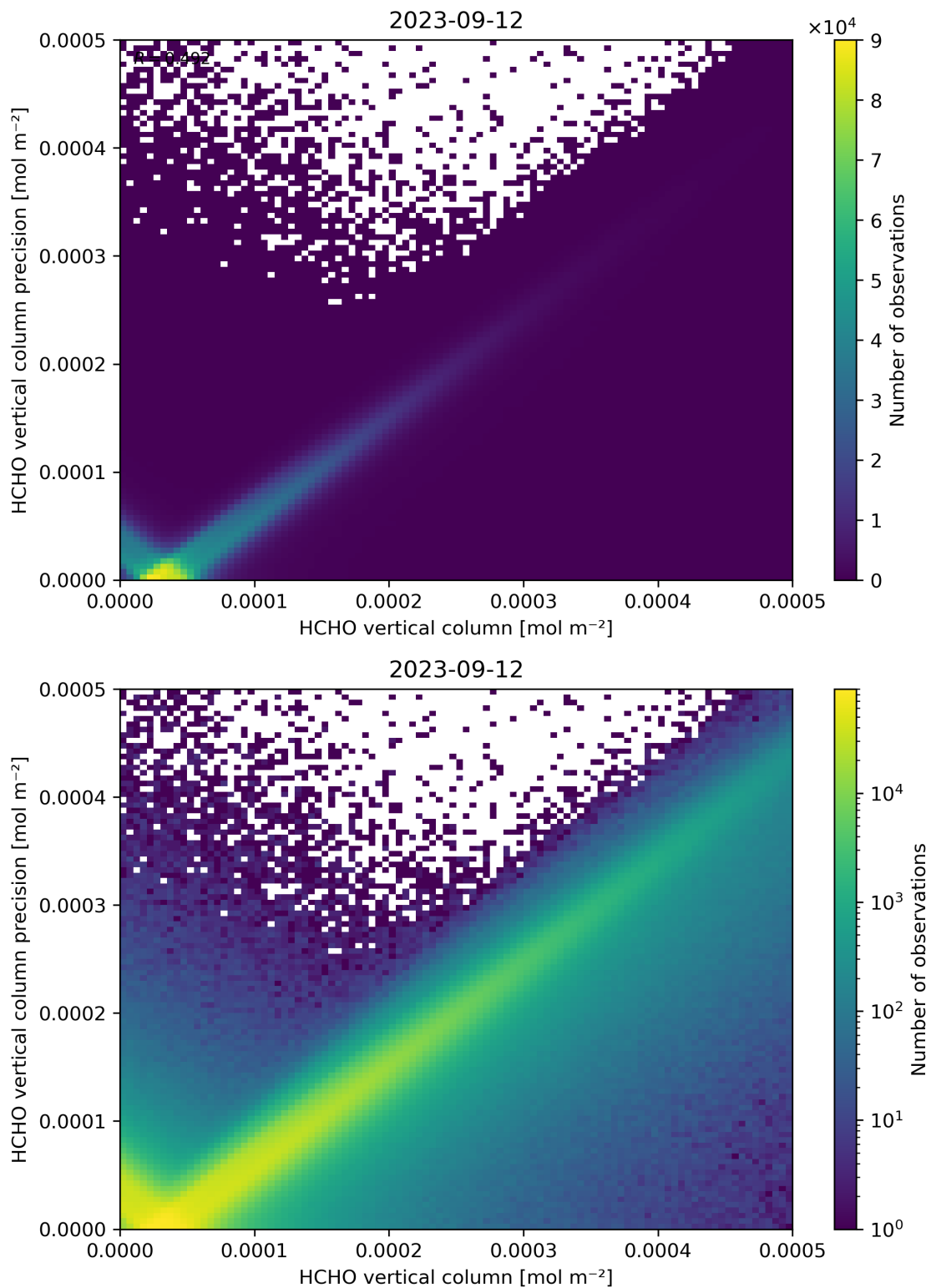


Figure 134: Scatter density plot of “HCHO vertical column” against “HCHO vertical column precision” for 2023-09-11 to 2023-09-13.

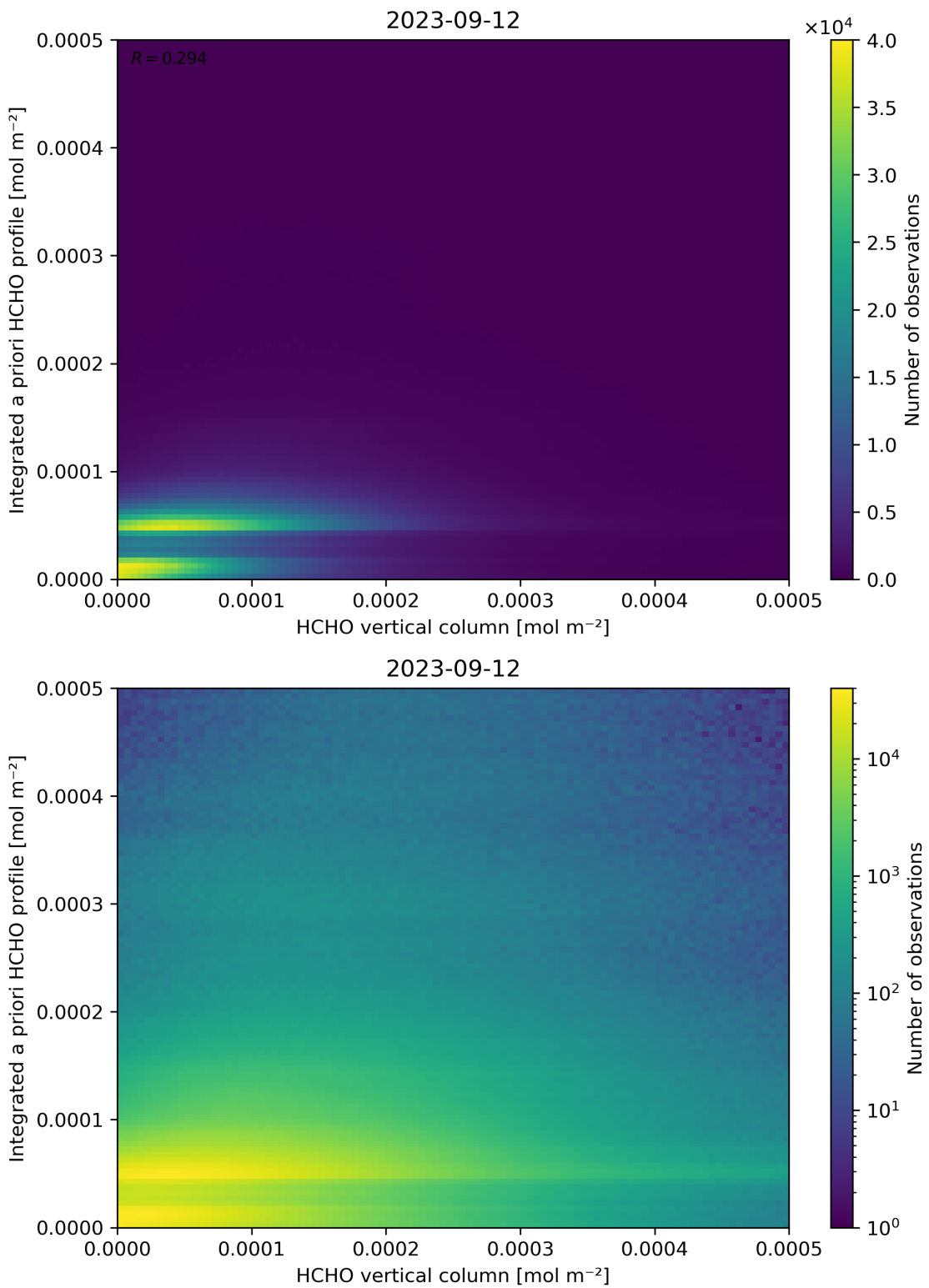


Figure 135: Scatter density plot of “HCHO vertical column” against “Integrated a priori HCHO profile” for 2023-09-11 to 2023-09-13.

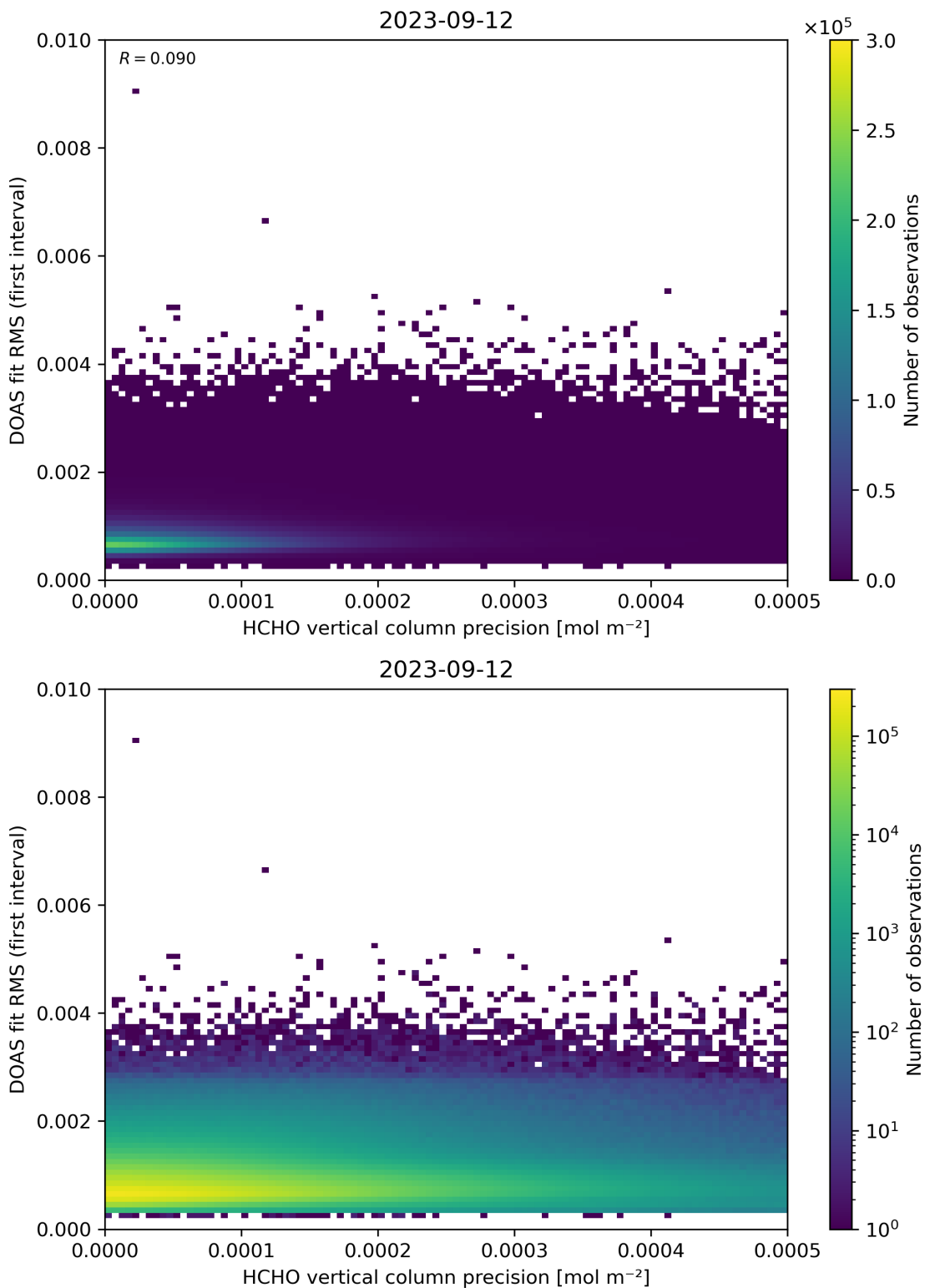


Figure 136: Scatter density plot of “HCHO vertical column precision” against “DOAS fit RMS (first interval)” for 2023-09-11 to 2023-09-13.

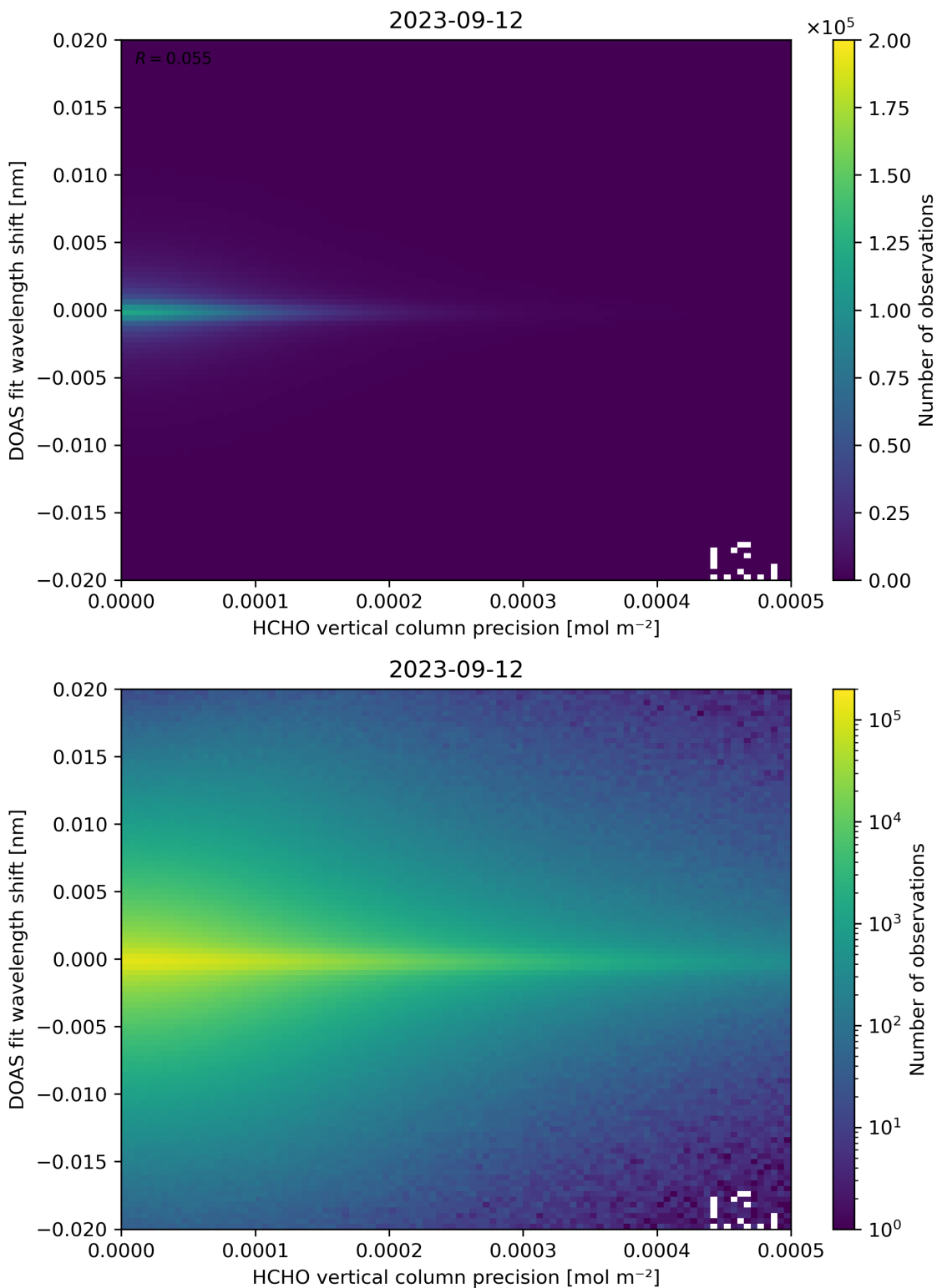


Figure 137: Scatter density plot of “HCHO vertical column precision” against “DOAS fit wavelength shift” for 2023-09-11 to 2023-09-13.

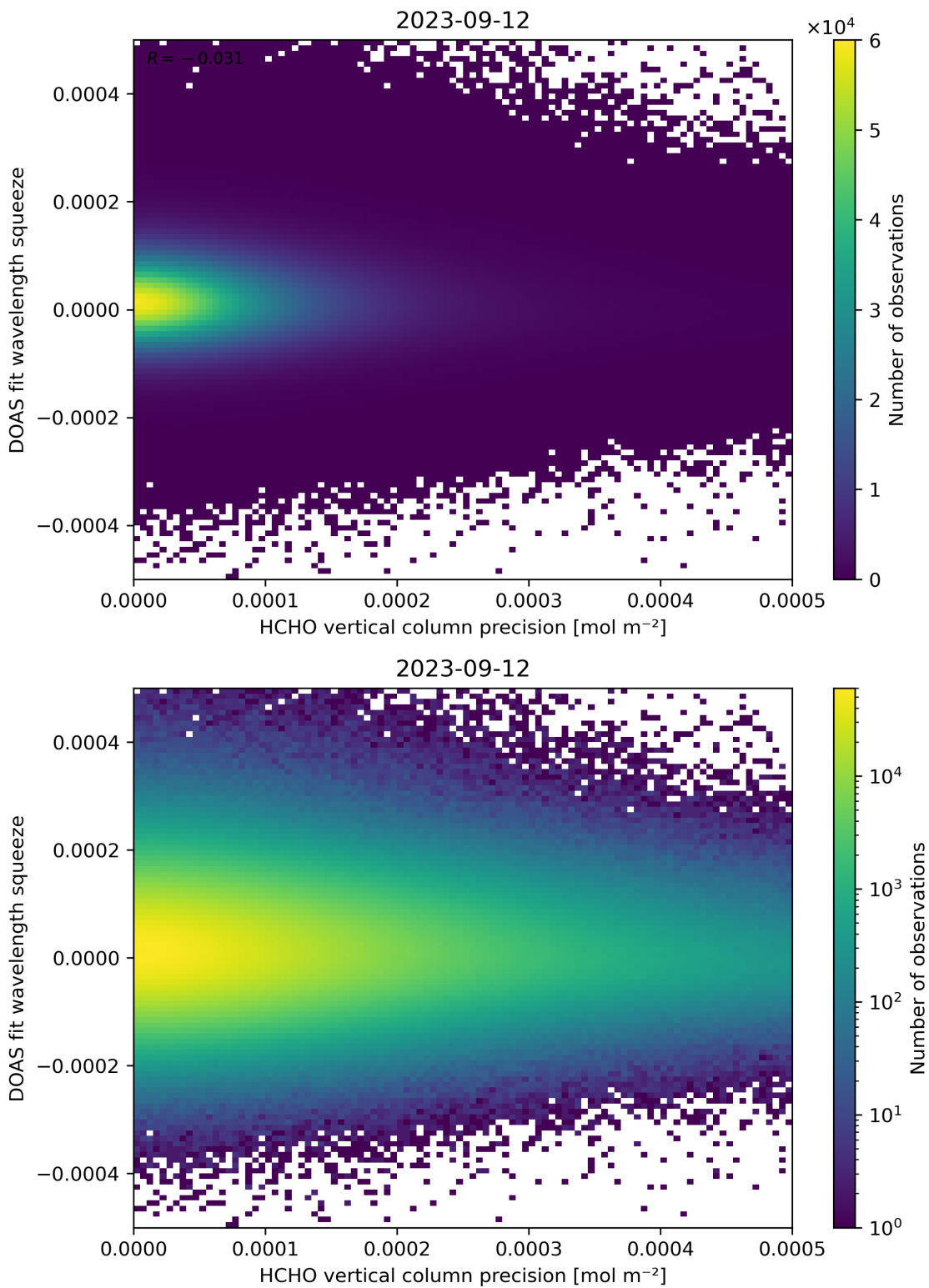


Figure 138: Scatter density plot of “HCHO vertical column precision” against “DOAS fit wavelength squeeze” for 2023-09-11 to 2023-09-13.

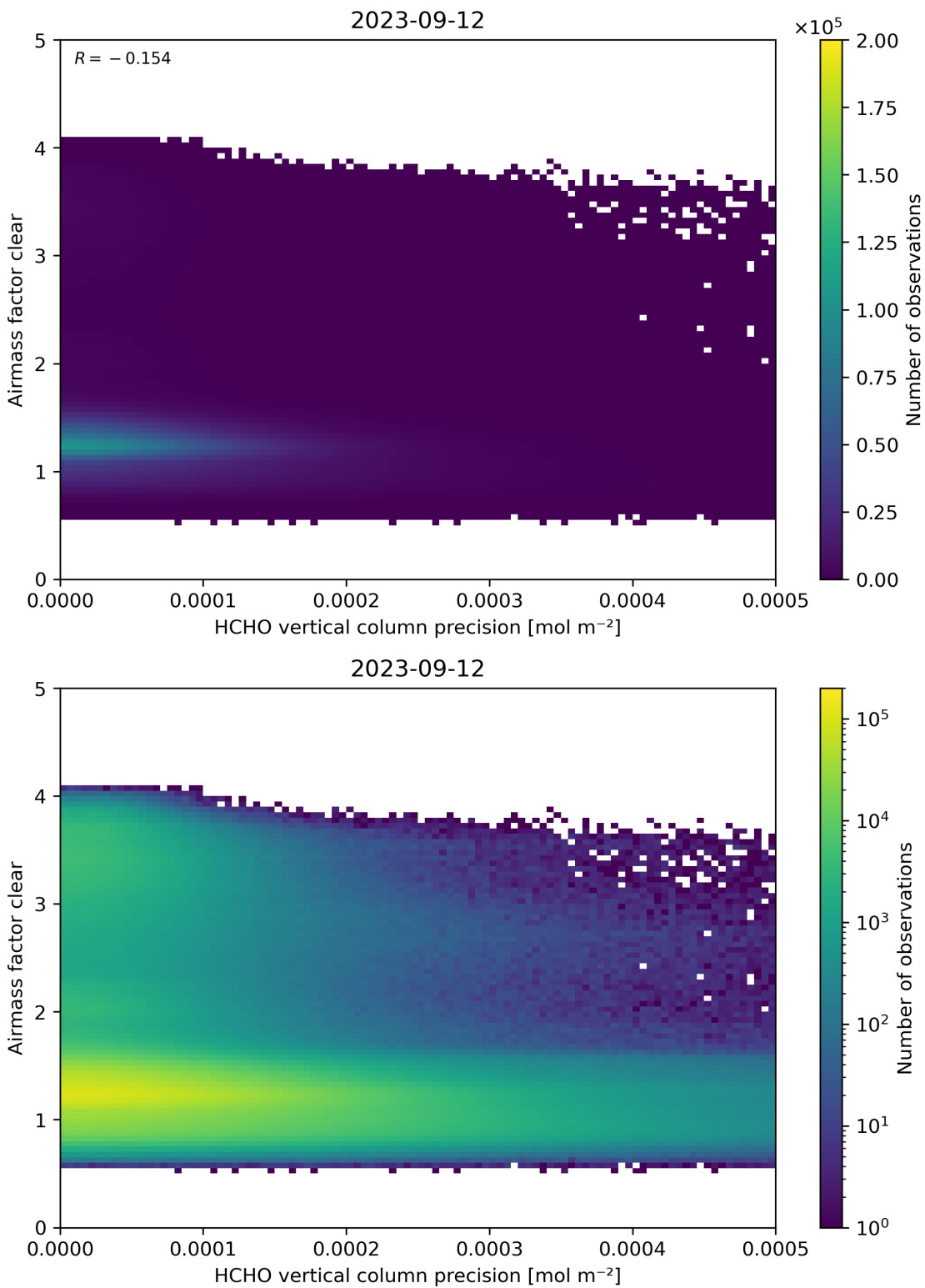


Figure 139: Scatter density plot of “HCHO vertical column precision” against “Airmass factor clear” for 2023-09-11 to 2023-09-13.

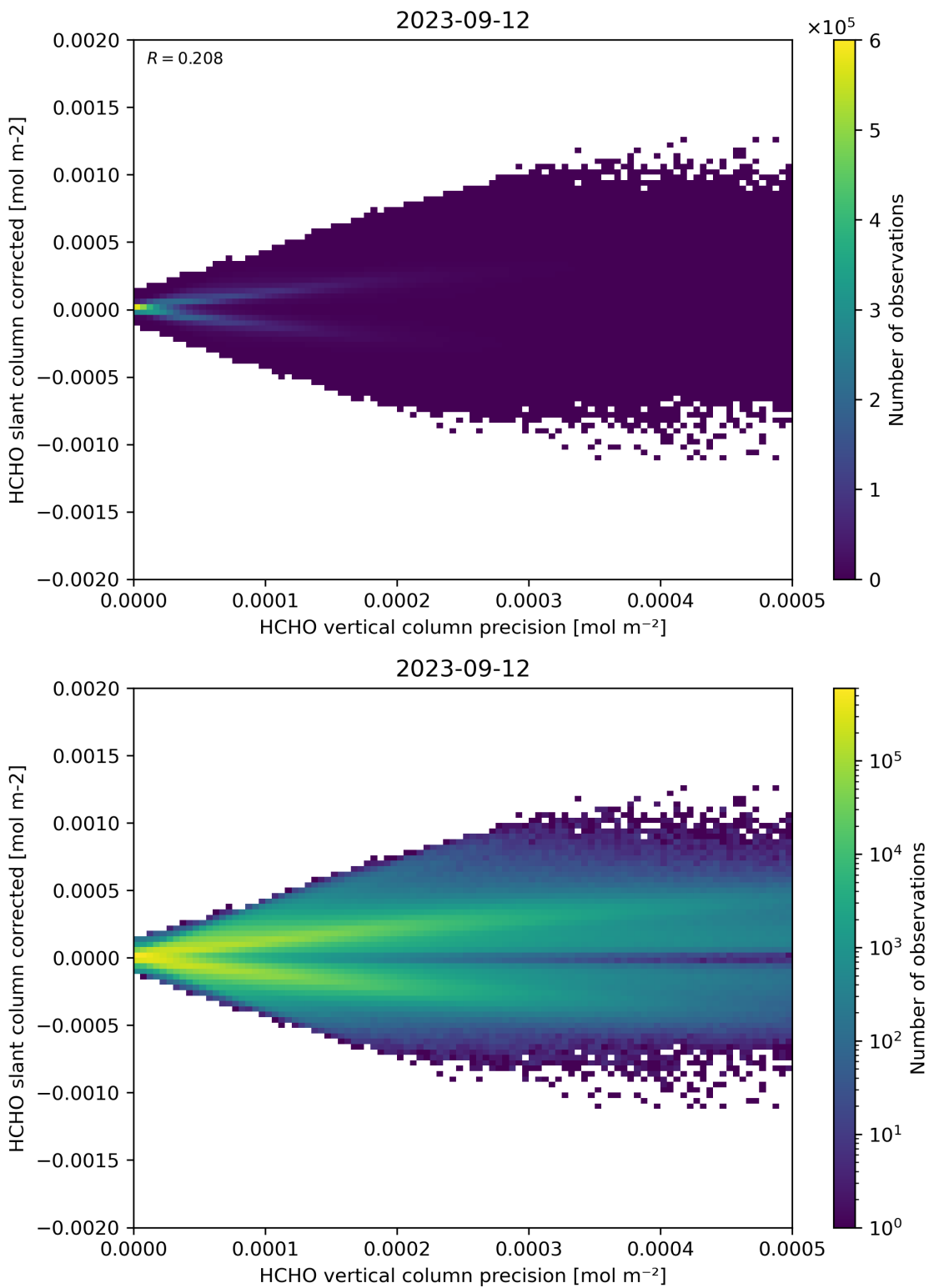


Figure 140: Scatter density plot of “HCHO vertical column precision” against “HCHO slant column corrected” for 2023-09-11 to 2023-09-13.

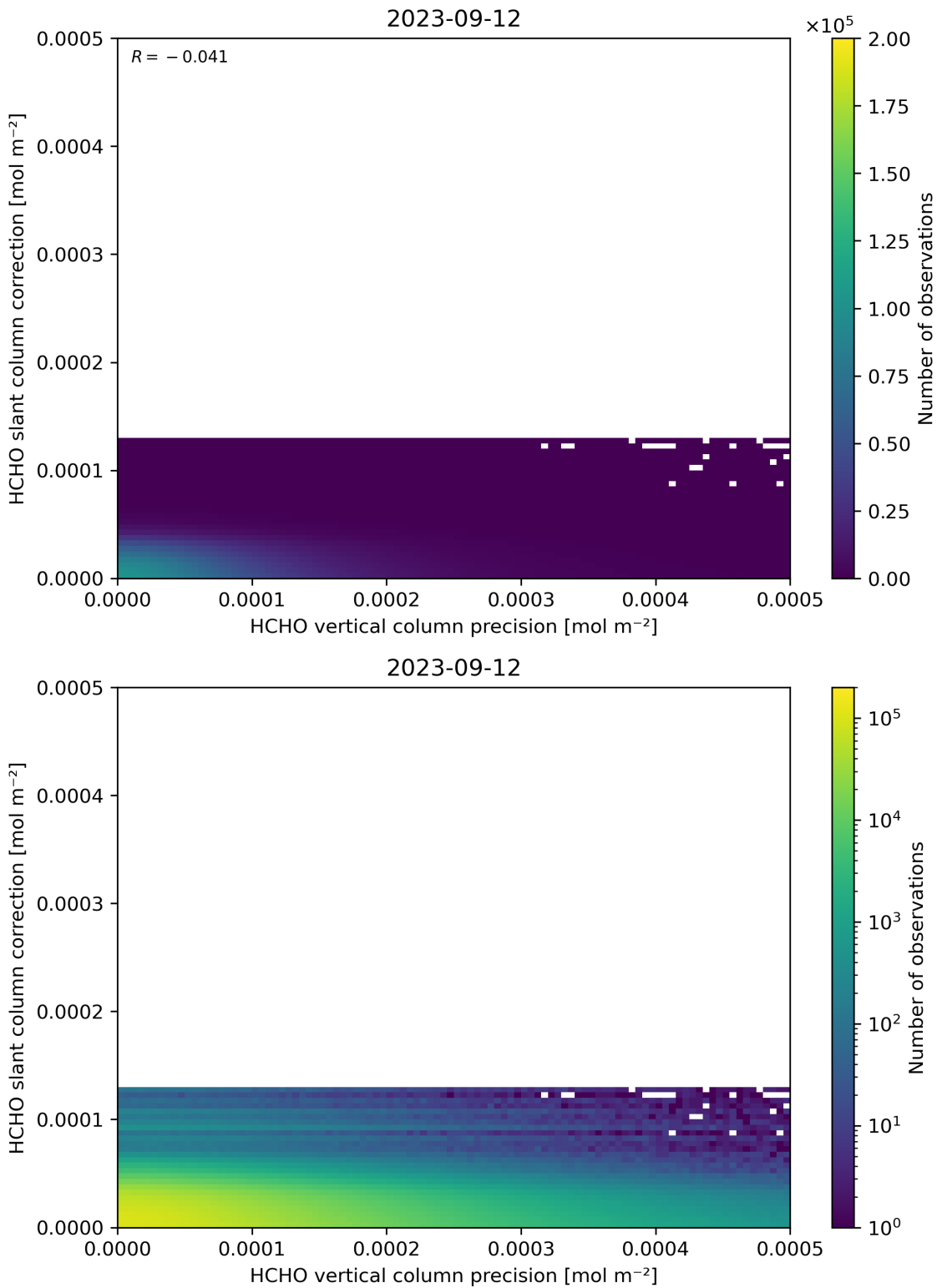


Figure 141: Scatter density plot of “HCHO vertical column precision” against “HCHO slant column correction” for 2023-09-11 to 2023-09-13.

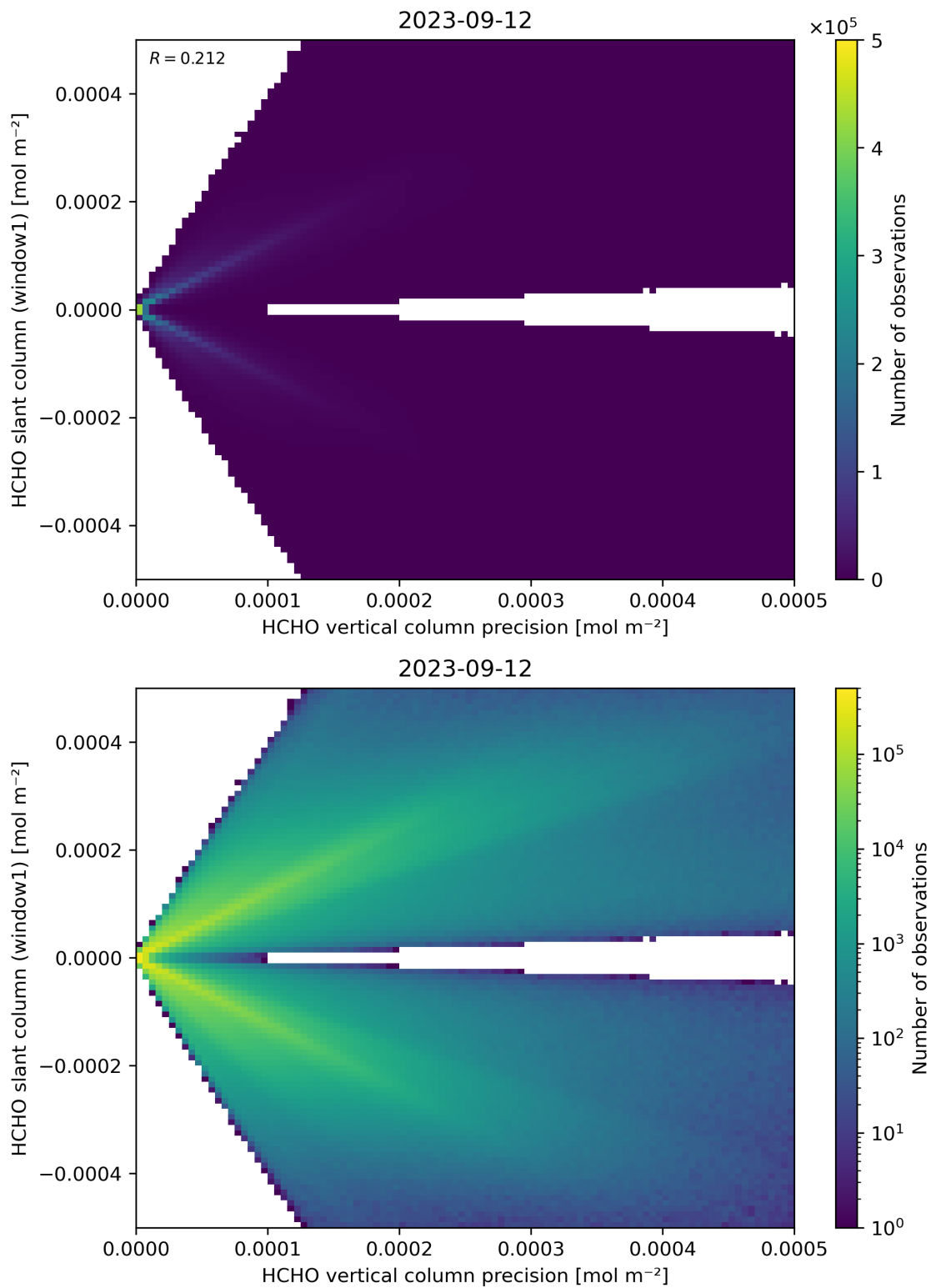


Figure 142: Scatter density plot of “HCHO vertical column precision” against “HCHO slant column (window1)” for 2023-09-11 to 2023-09-13.

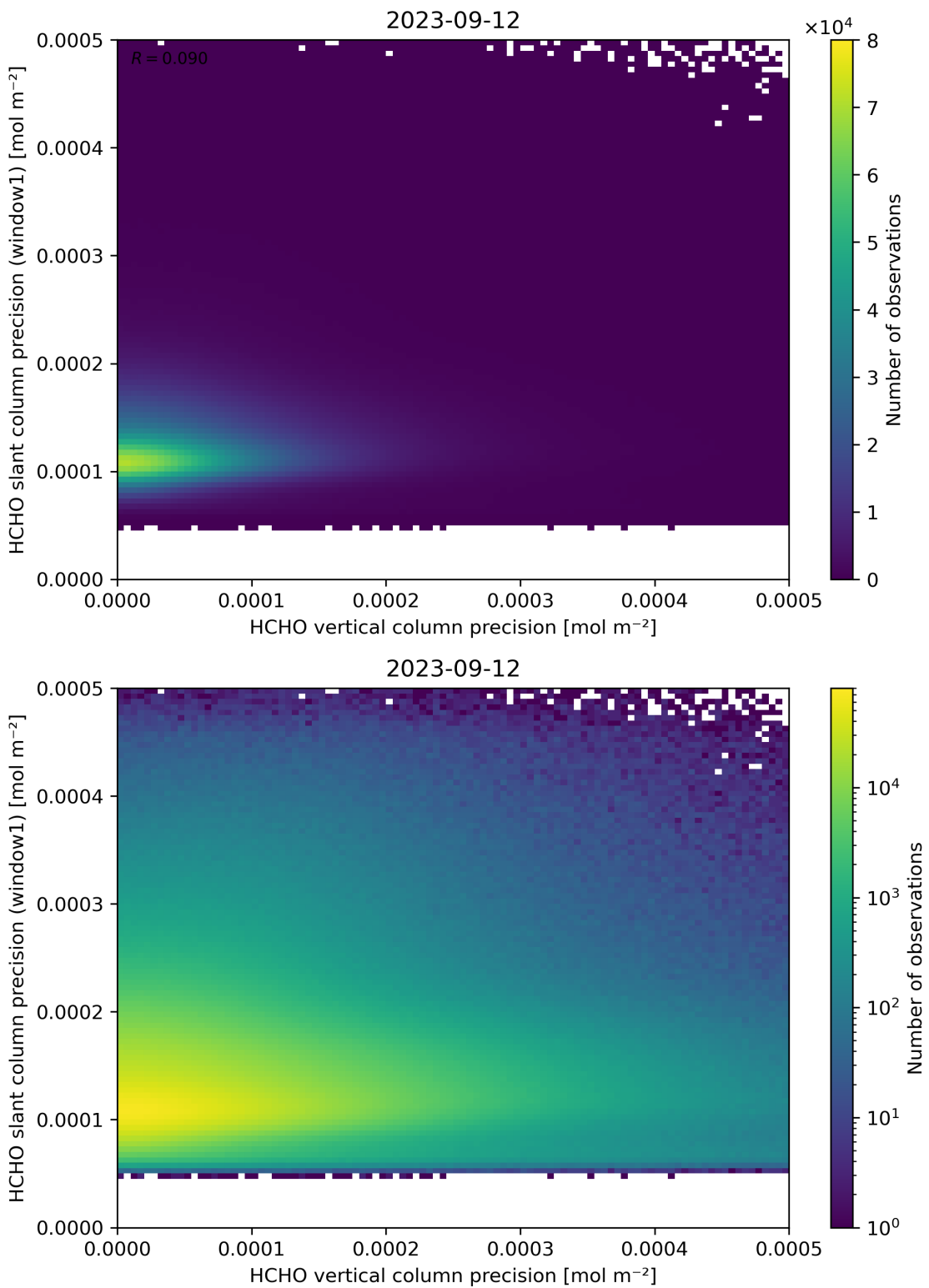


Figure 143: Scatter density plot of “HCHO vertical column precision” against “HCHO slant column precision (window1)” for 2023-09-11 to 2023-09-13.

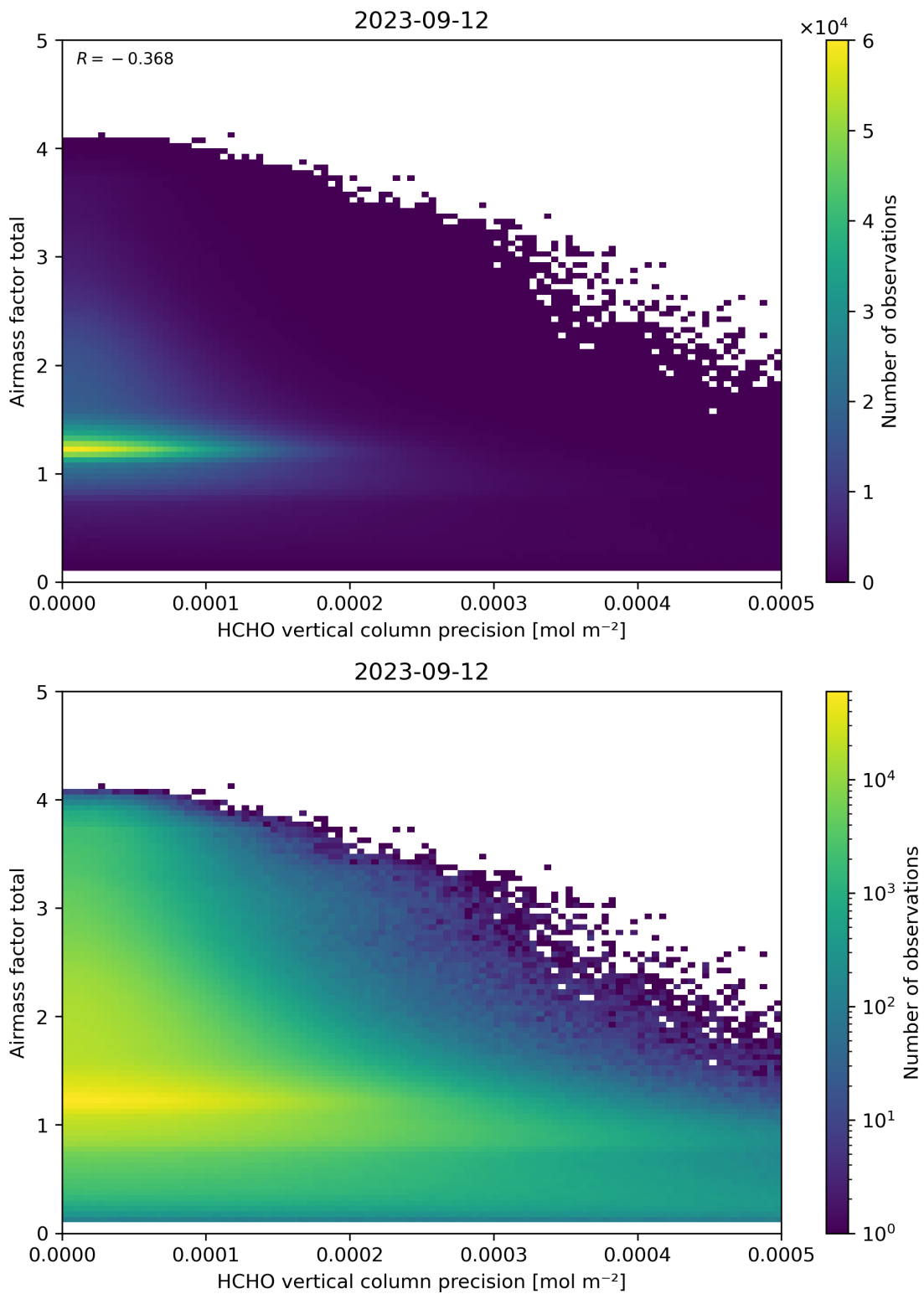


Figure 144: Scatter density plot of “HCHO vertical column precision” against “Airmass factor total” for 2023-09-11 to 2023-09-13.

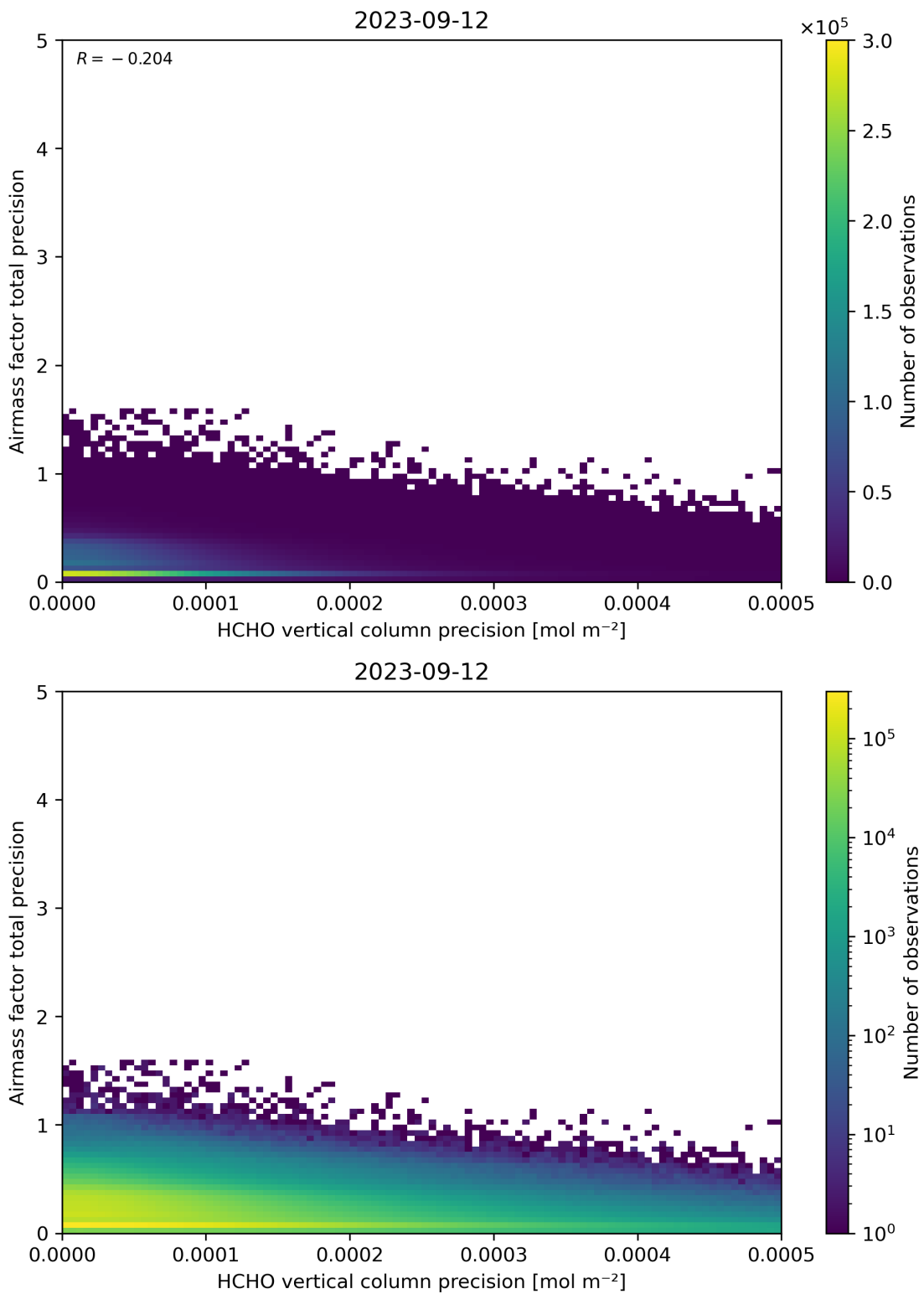


Figure 145: Scatter density plot of “HCHO vertical column precision” against “Airmass factor total precision” for 2023-09-11 to 2023-09-13.

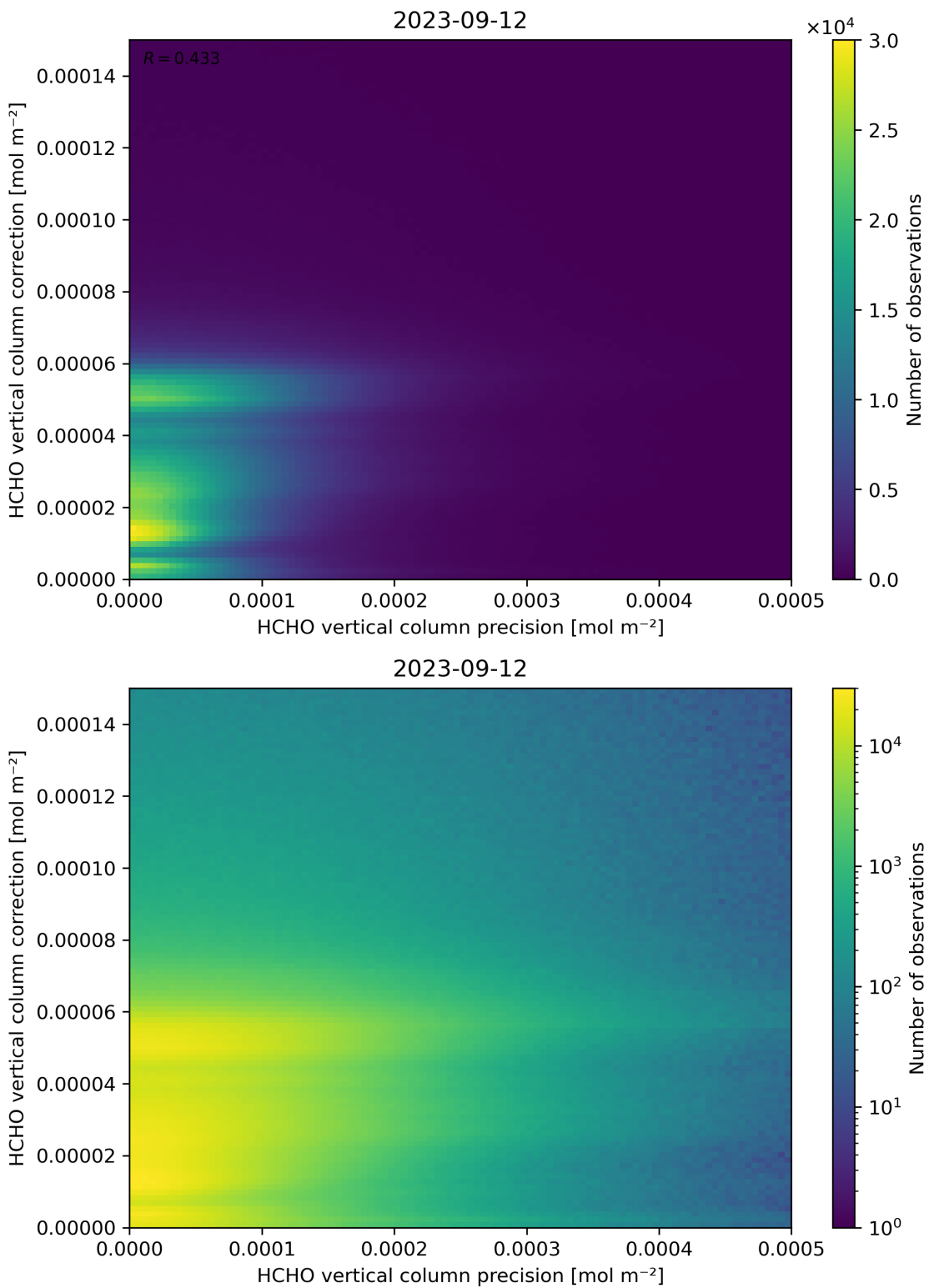


Figure 146: Scatter density plot of “HCHO vertical column precision” against “HCHO vertical column correction” for 2023-09-11 to 2023-09-13.

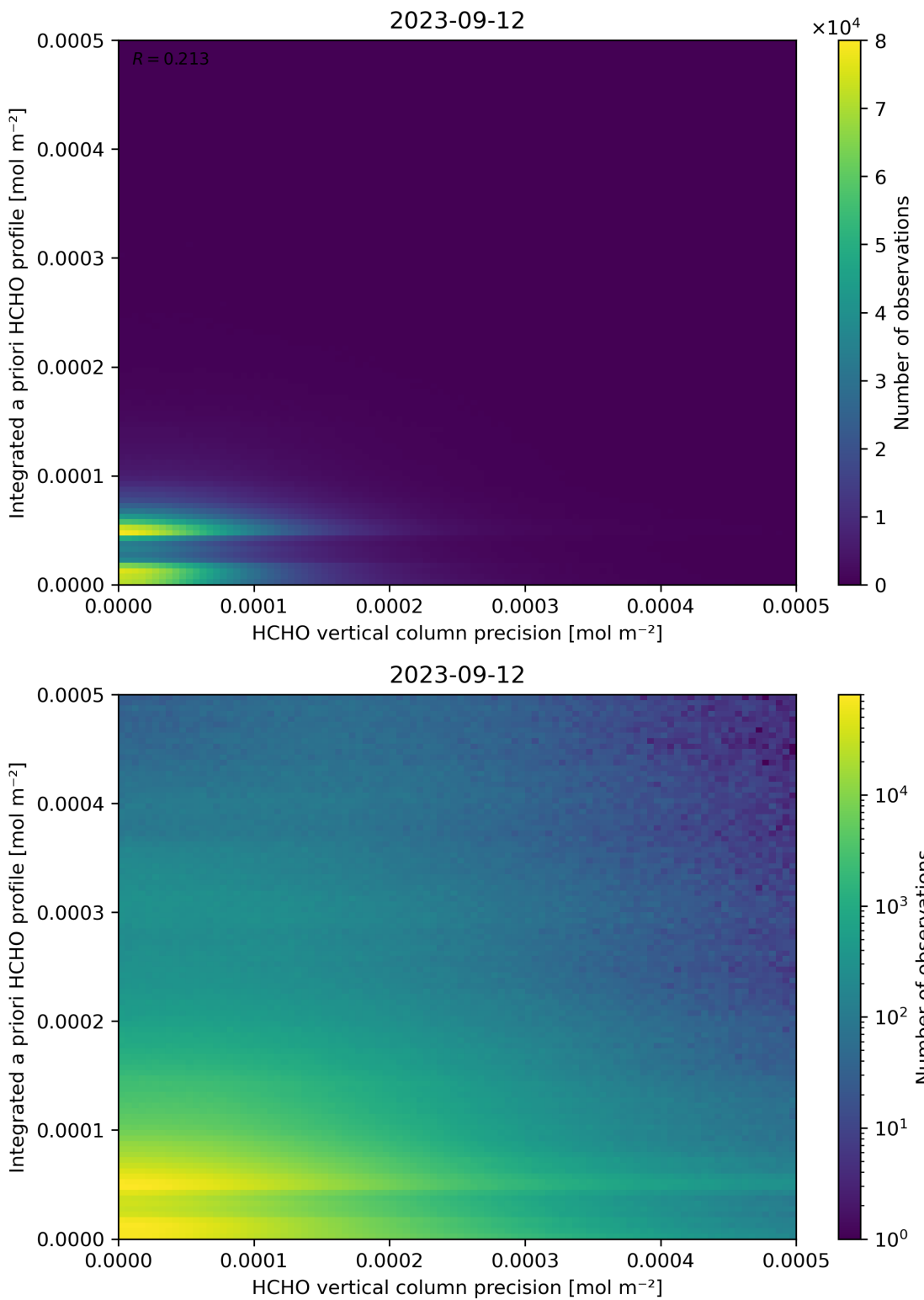


Figure 147: Scatter density plot of “HCHO vertical column precision” against “Integrated a priori HCHO profile” for 2023-09-11 to 2023-09-13.

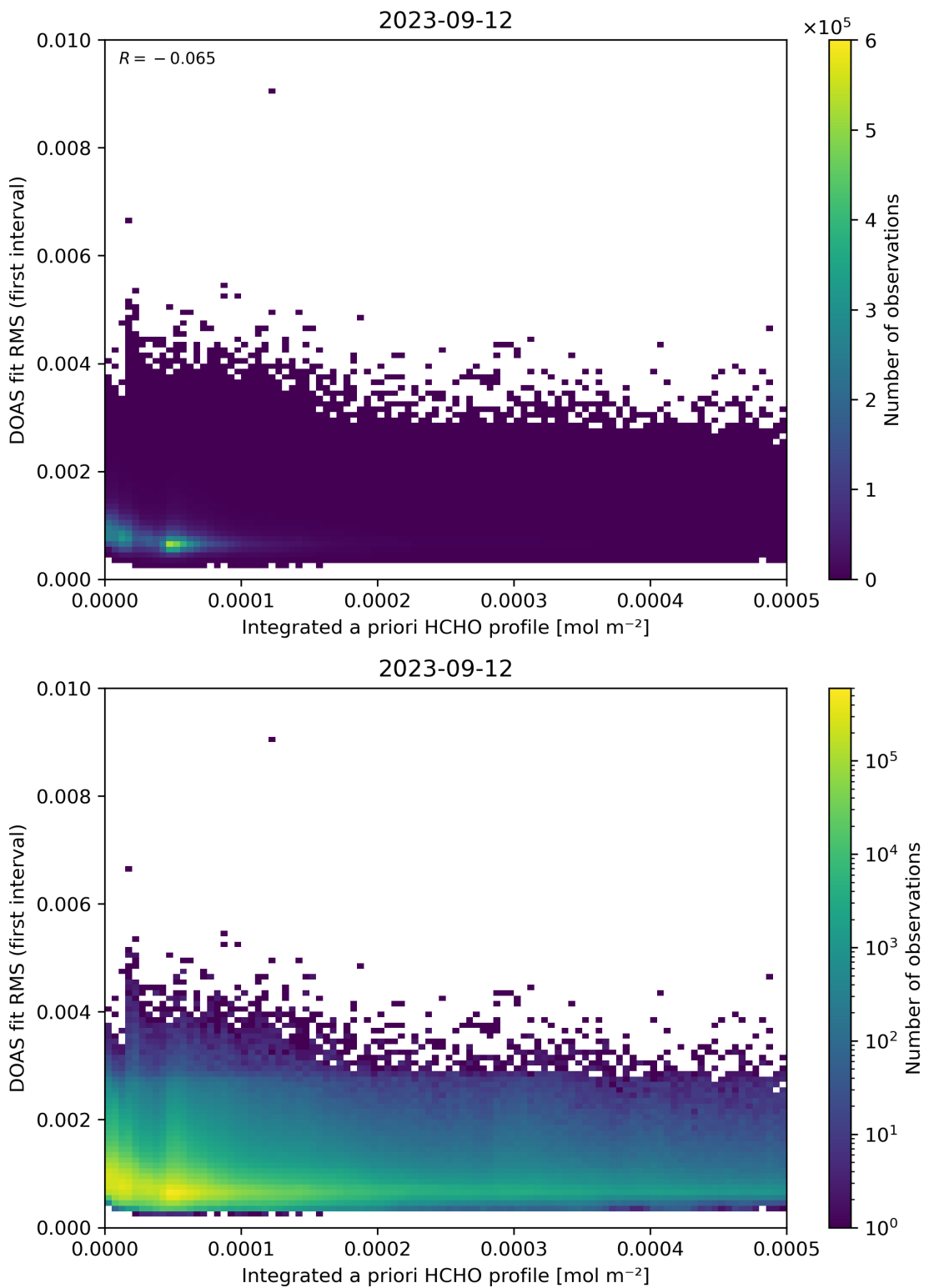


Figure 148: Scatter density plot of “Integrated a priori HCHO profile” against “DOAS fit RMS (first interval)” for 2023-09-11 to 2023-09-13.

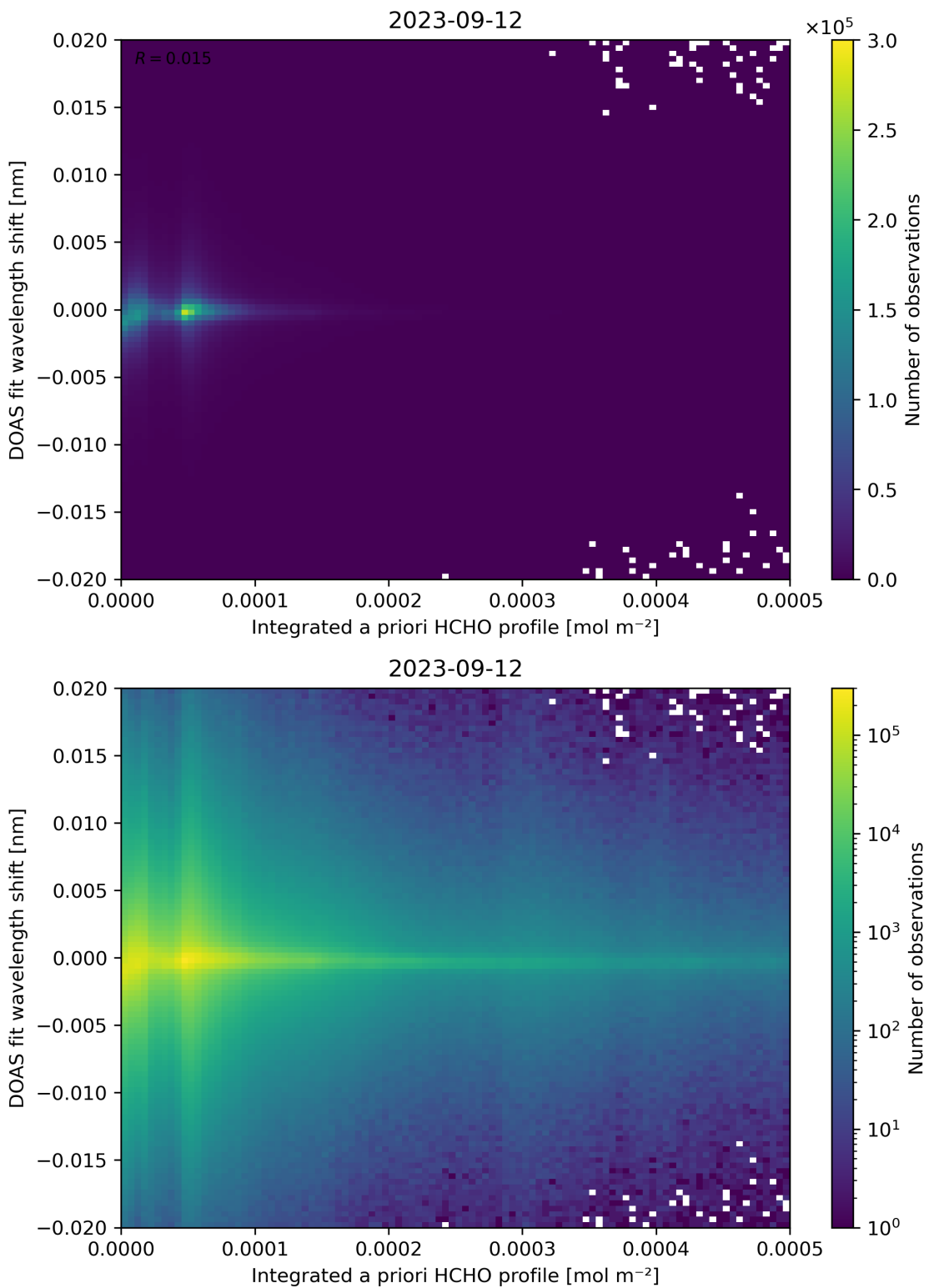


Figure 149: Scatter density plot of “Integrated a priori HCHO profile” against “DOAS fit wavelength shift” for 2023-09-11 to 2023-09-13.

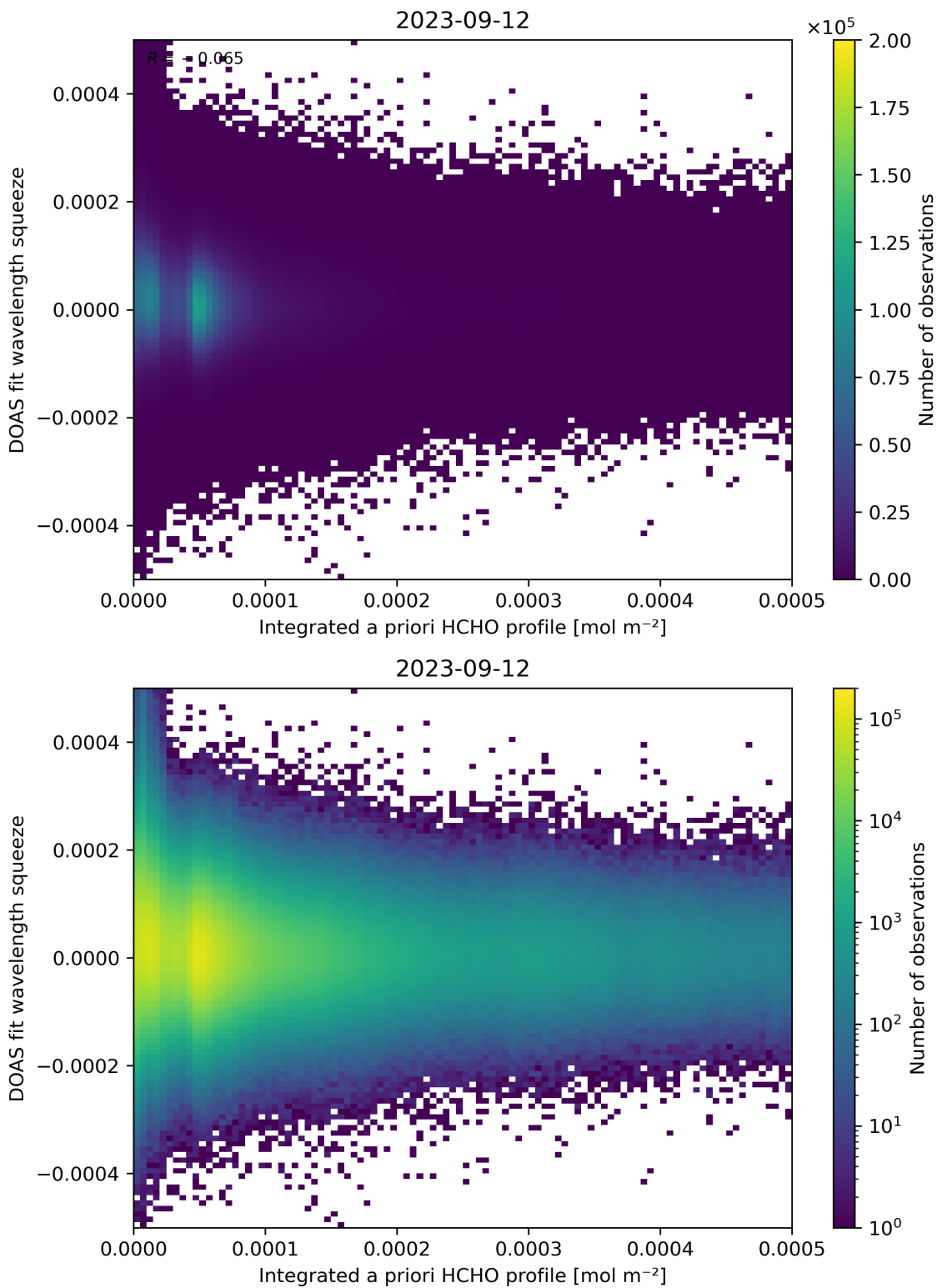


Figure 150: Scatter density plot of “Integrated a priori HCHO profile” against “DOAS fit wavelength squeeze” for 2023-09-11 to 2023-09-13.

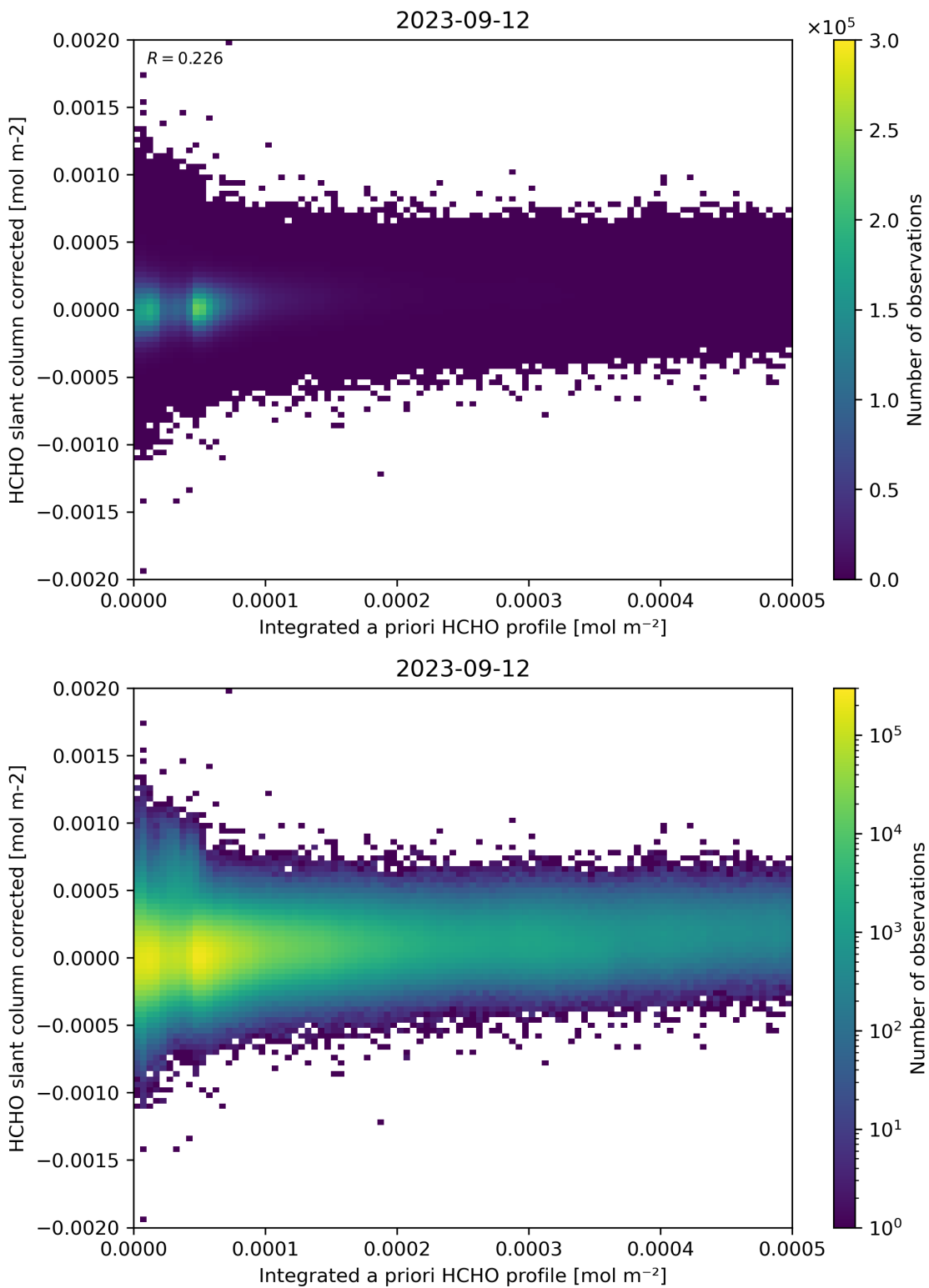


Figure 151: Scatter density plot of “Integrated a priori HCHO profile” against “HCHO slant column corrected” for 2023-09-11 to 2023-09-13.

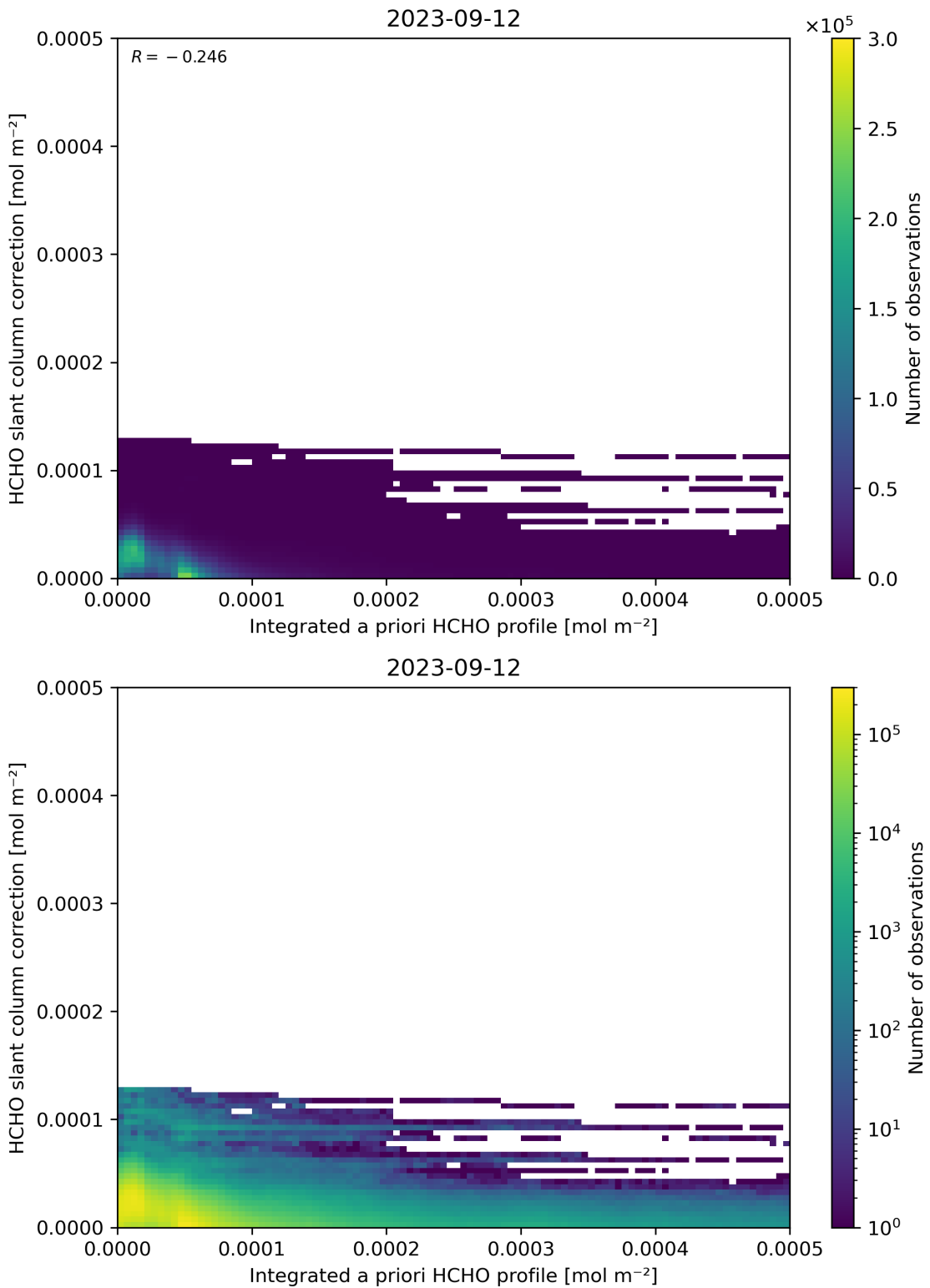


Figure 152: Scatter density plot of “Integrated a priori HCHO profile” against “HCHO slant column correction” for 2023-09-11 to 2023-09-13.

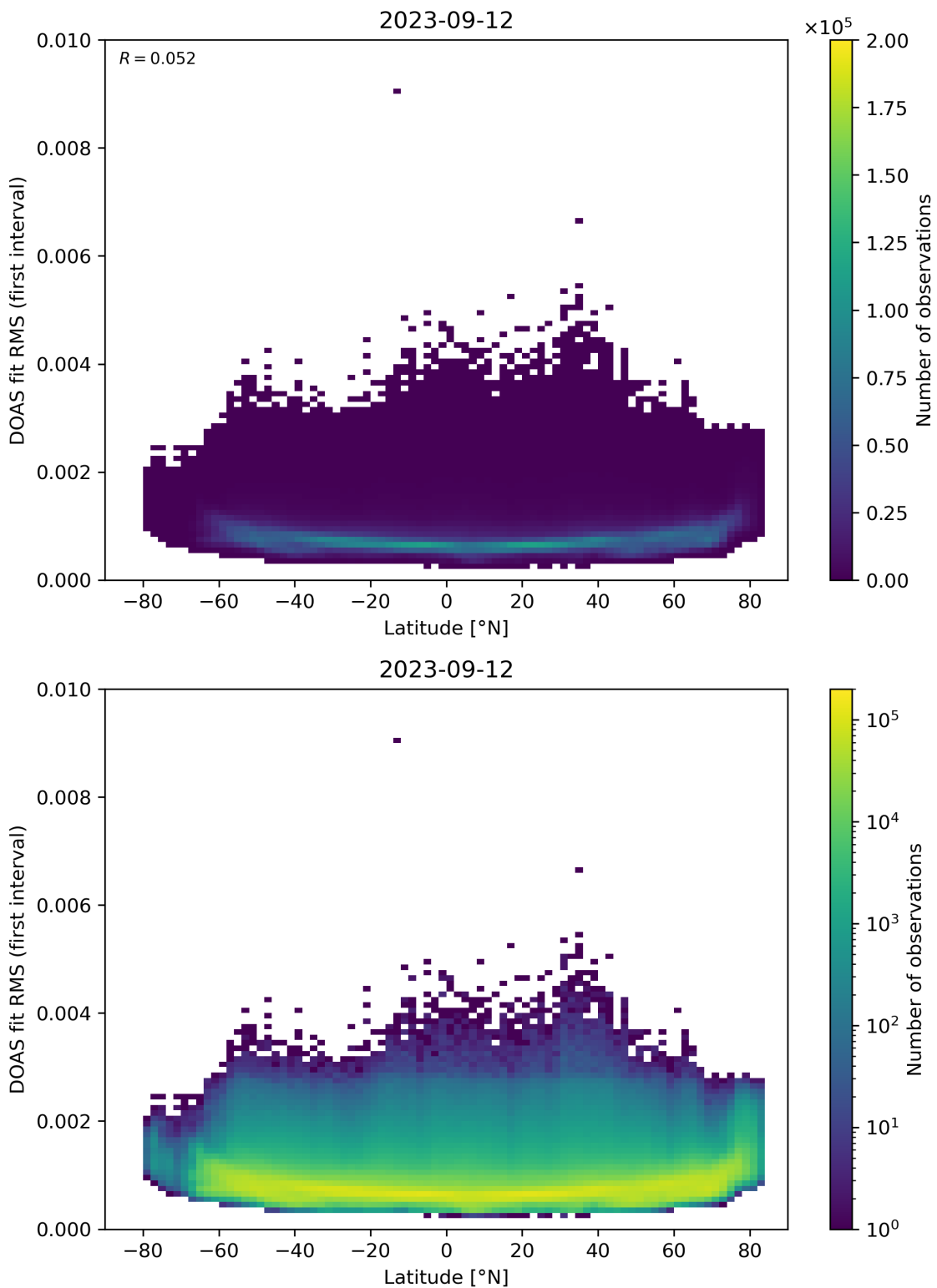


Figure 153: Scatter density plot of “Latitude” against “DOAS fit RMS (first interval)” for 2023-09-11 to 2023-09-13.

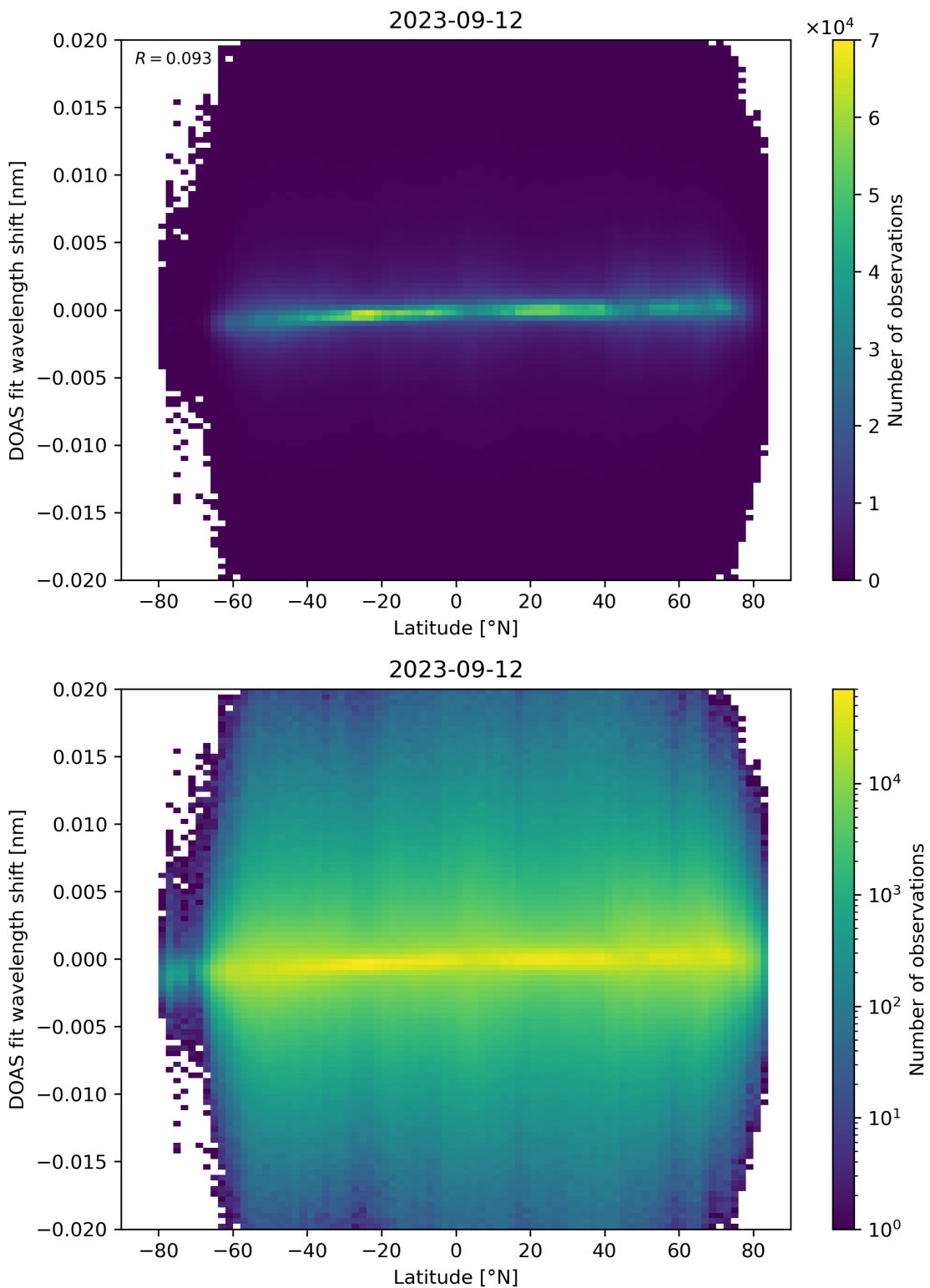


Figure 154: Scatter density plot of “Latitude” against “DOAS fit wavelength shift” for 2023-09-11 to 2023-09-13.

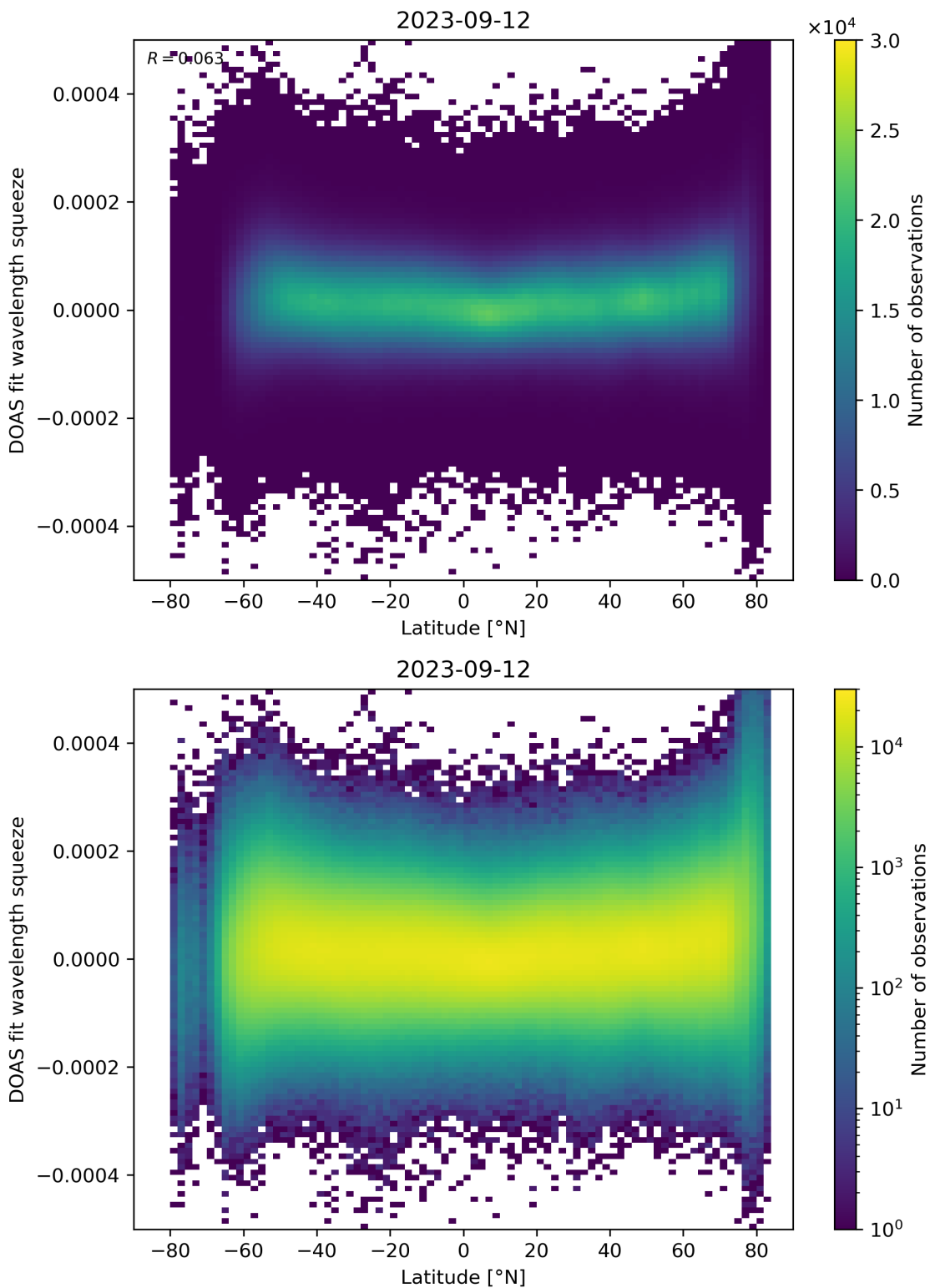


Figure 155: Scatter density plot of “Latitude” against “DOAS fit wavelength squeeze” for 2023-09-11 to 2023-09-13.

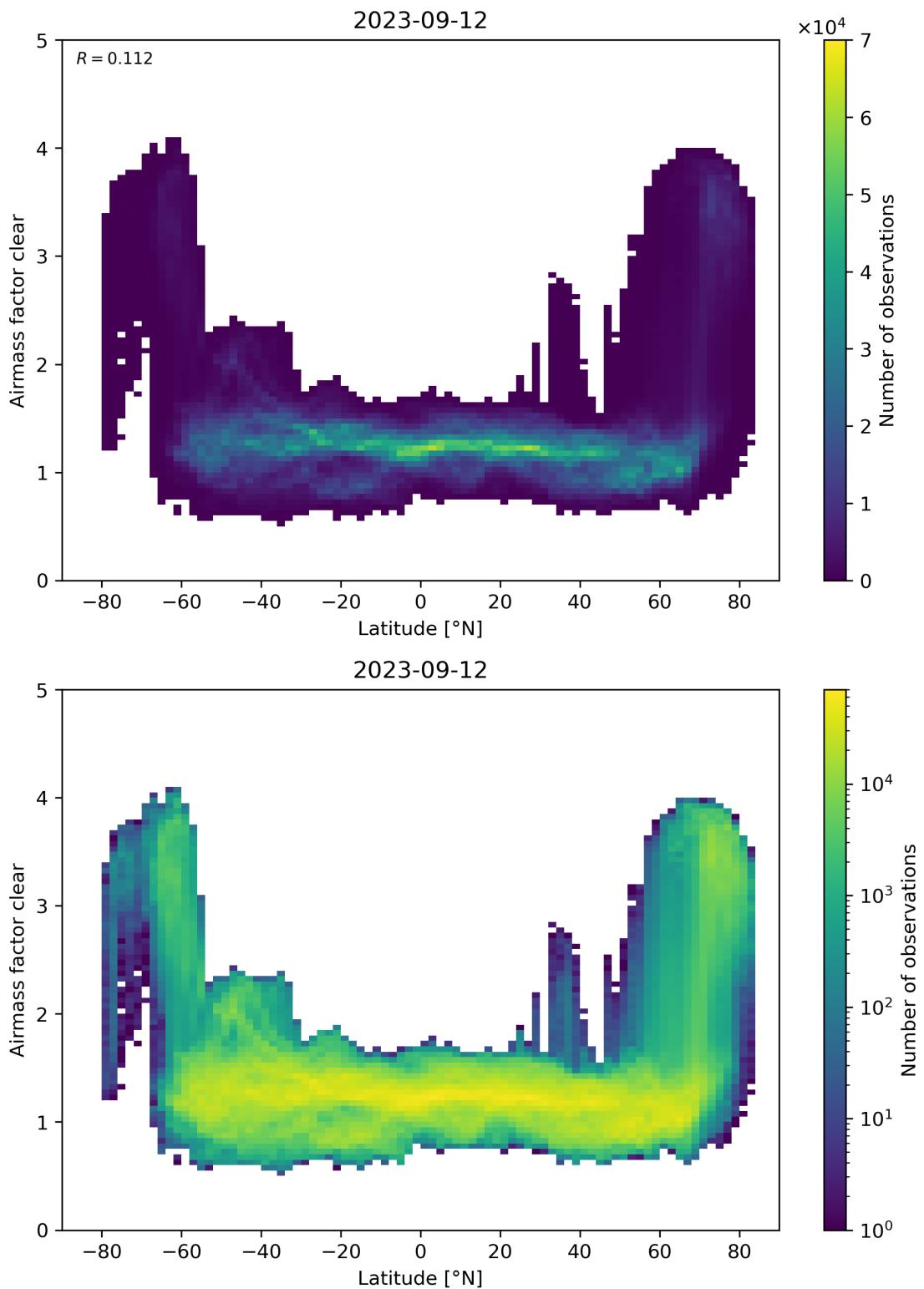


Figure 156: Scatter density plot of “Latitude” against “Airmass factor clear” for 2023-09-11 to 2023-09-13.

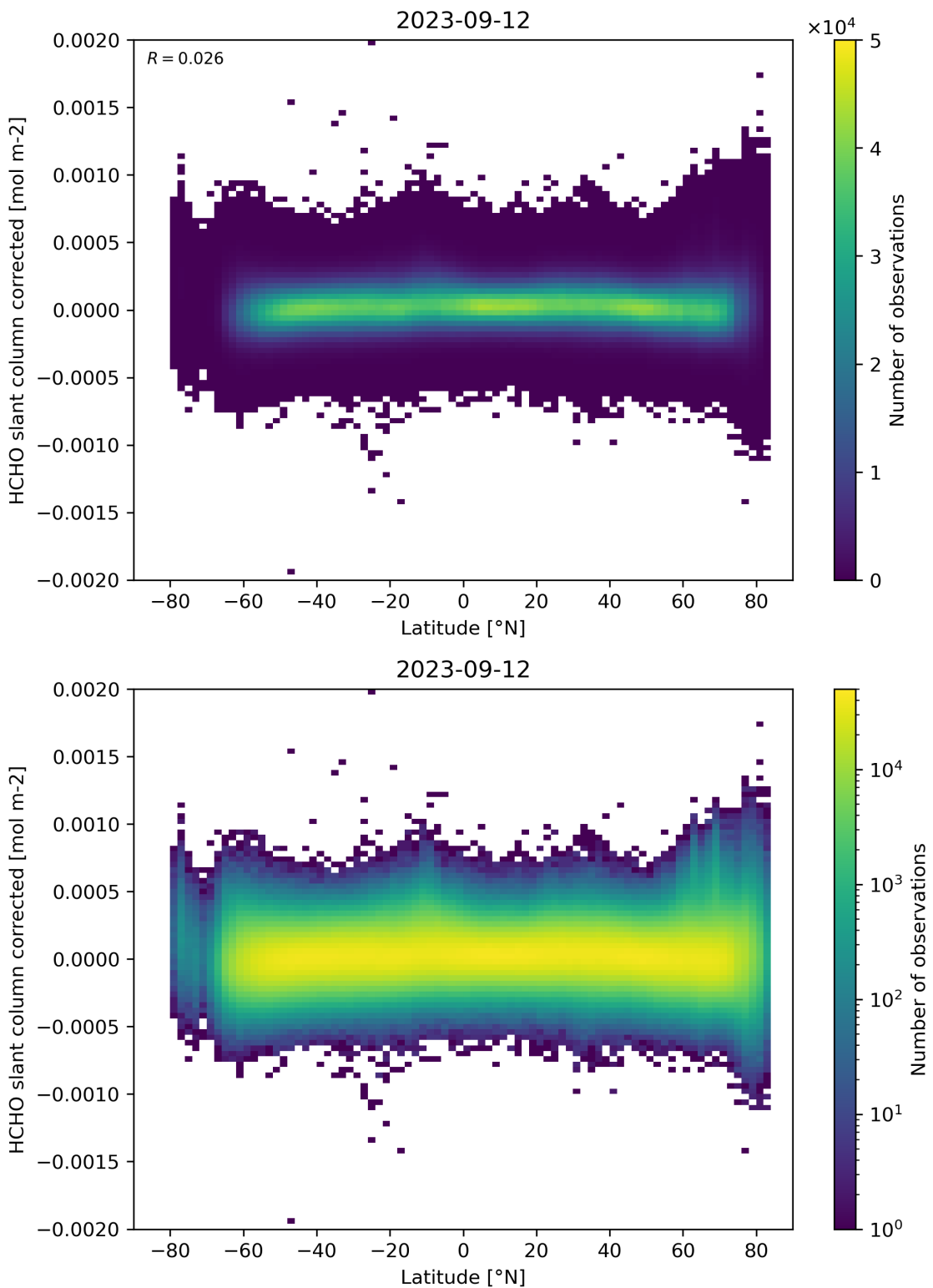


Figure 157: Scatter density plot of “Latitude” against “HCHO slant column corrected” for 2023-09-11 to 2023-09-13.

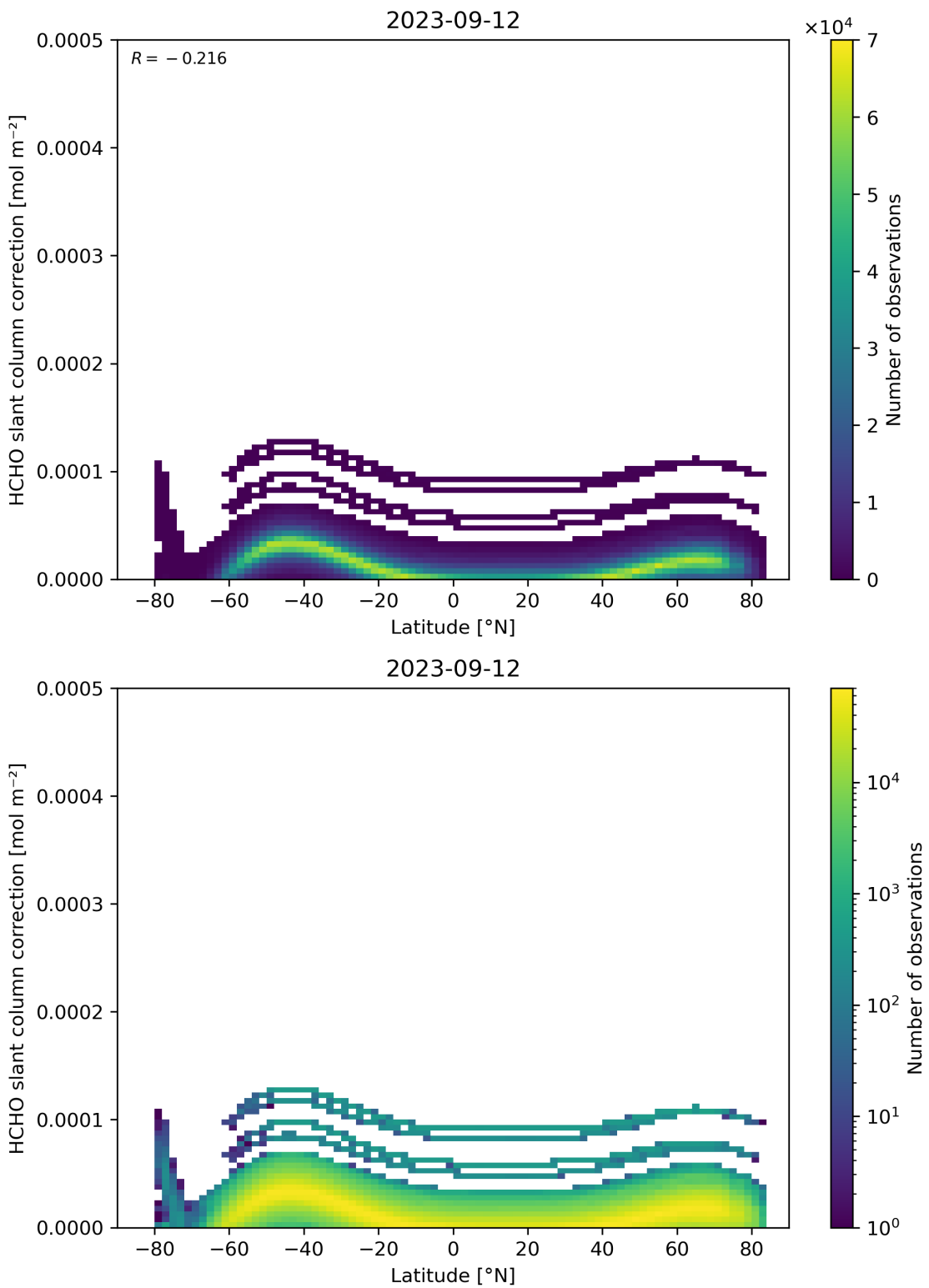


Figure 158: Scatter density plot of “Latitude” against “HCHO slant column correction” for 2023-09-11 to 2023-09-13.

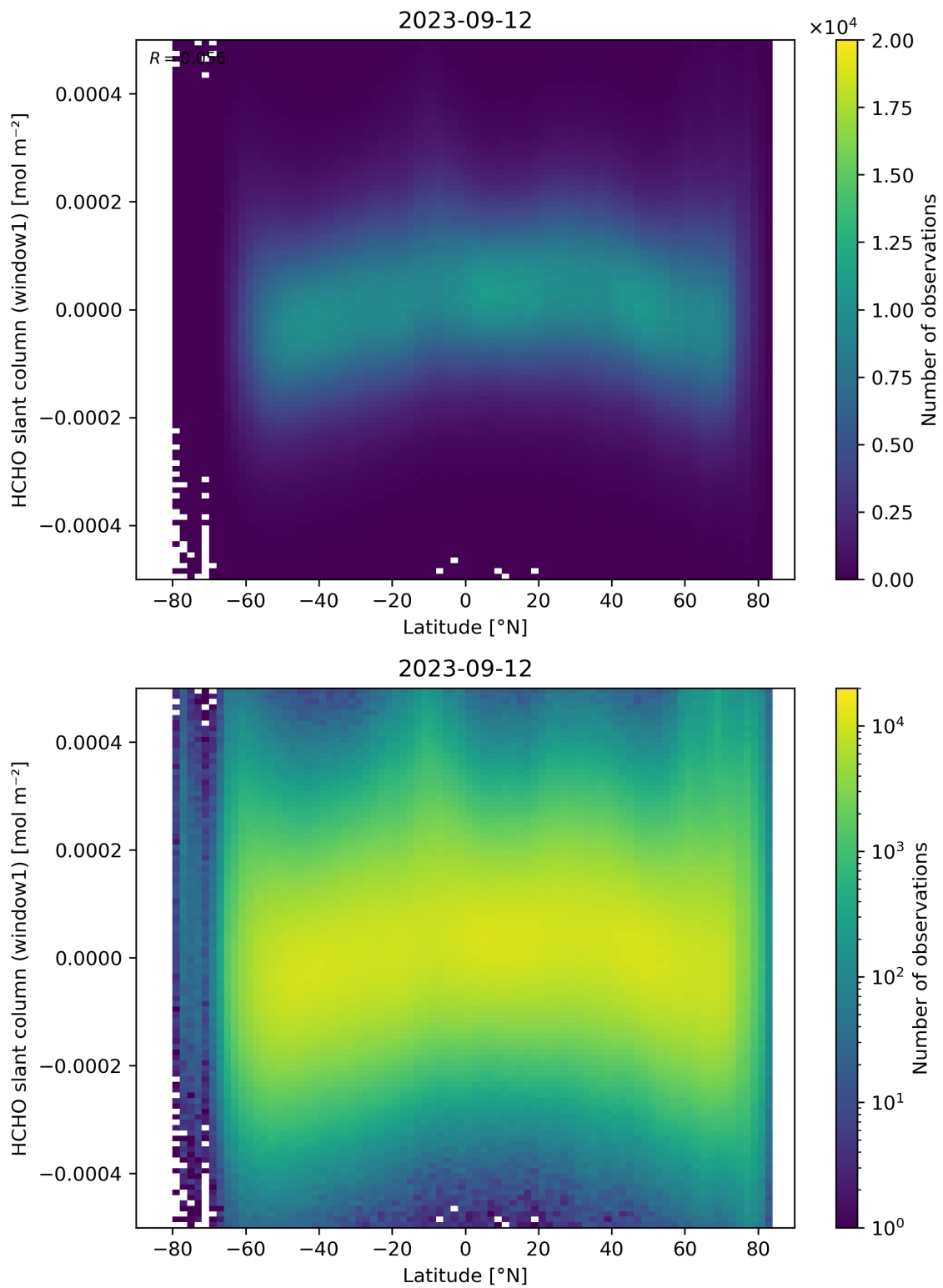


Figure 159: Scatter density plot of “Latitude” against “HCHO slant column (window1)” for 2023-09-11 to 2023-09-13.

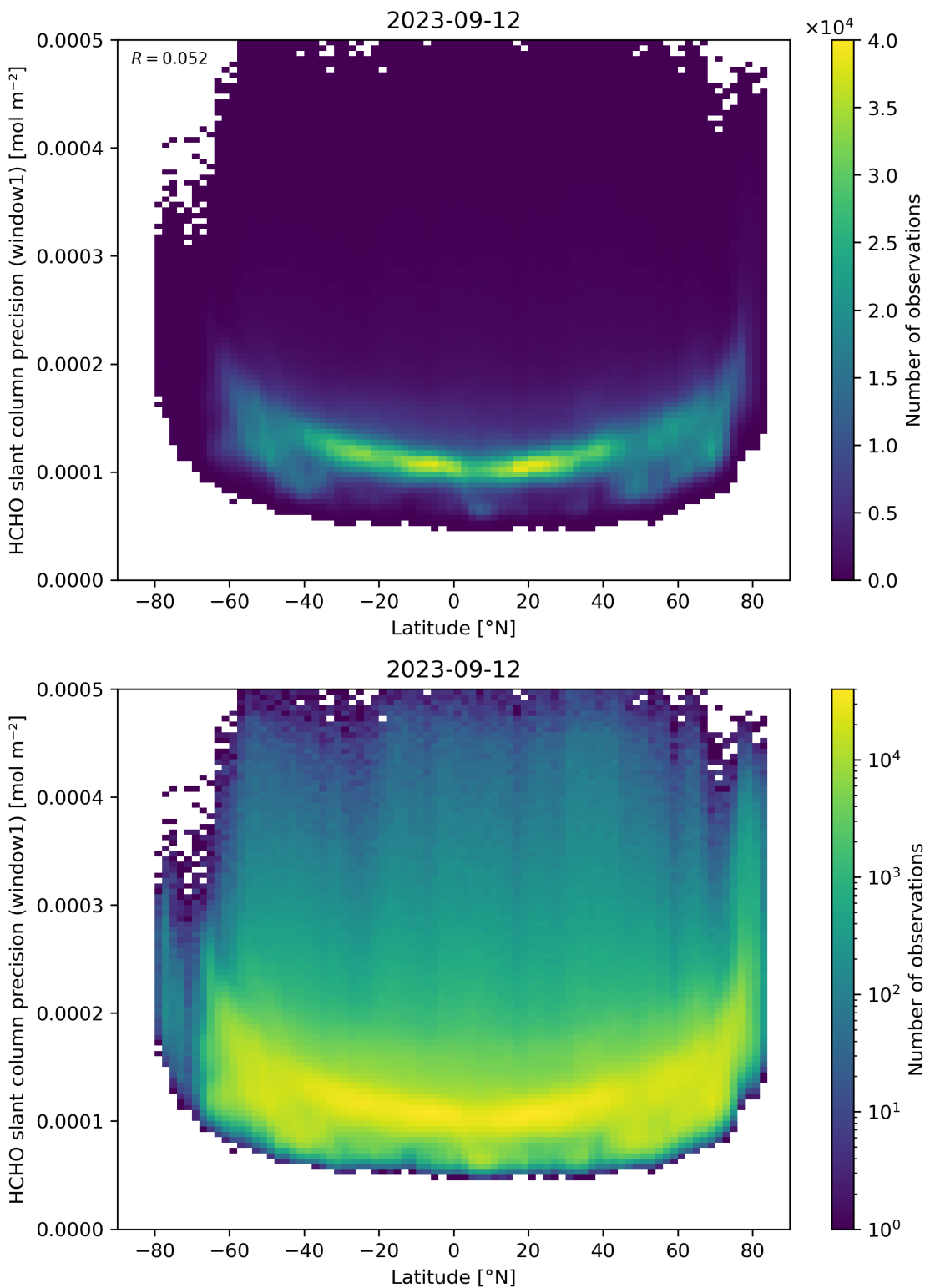


Figure 160: Scatter density plot of “Latitude” against “HCHO slant column precision (window1)” for 2023-09-11 to 2023-09-13.

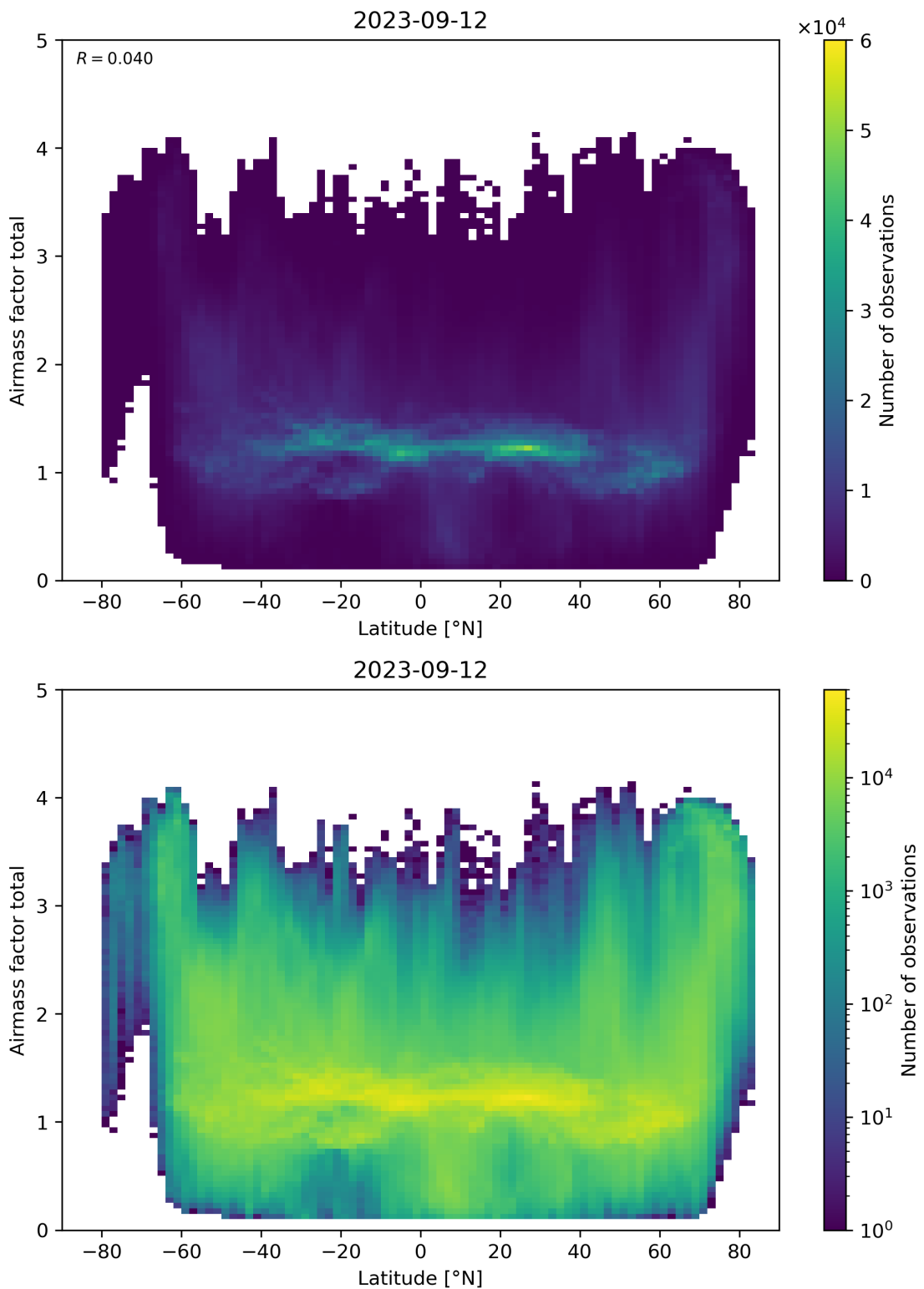


Figure 161: Scatter density plot of “Latitude” against “Airmass factor total” for 2023-09-11 to 2023-09-13.

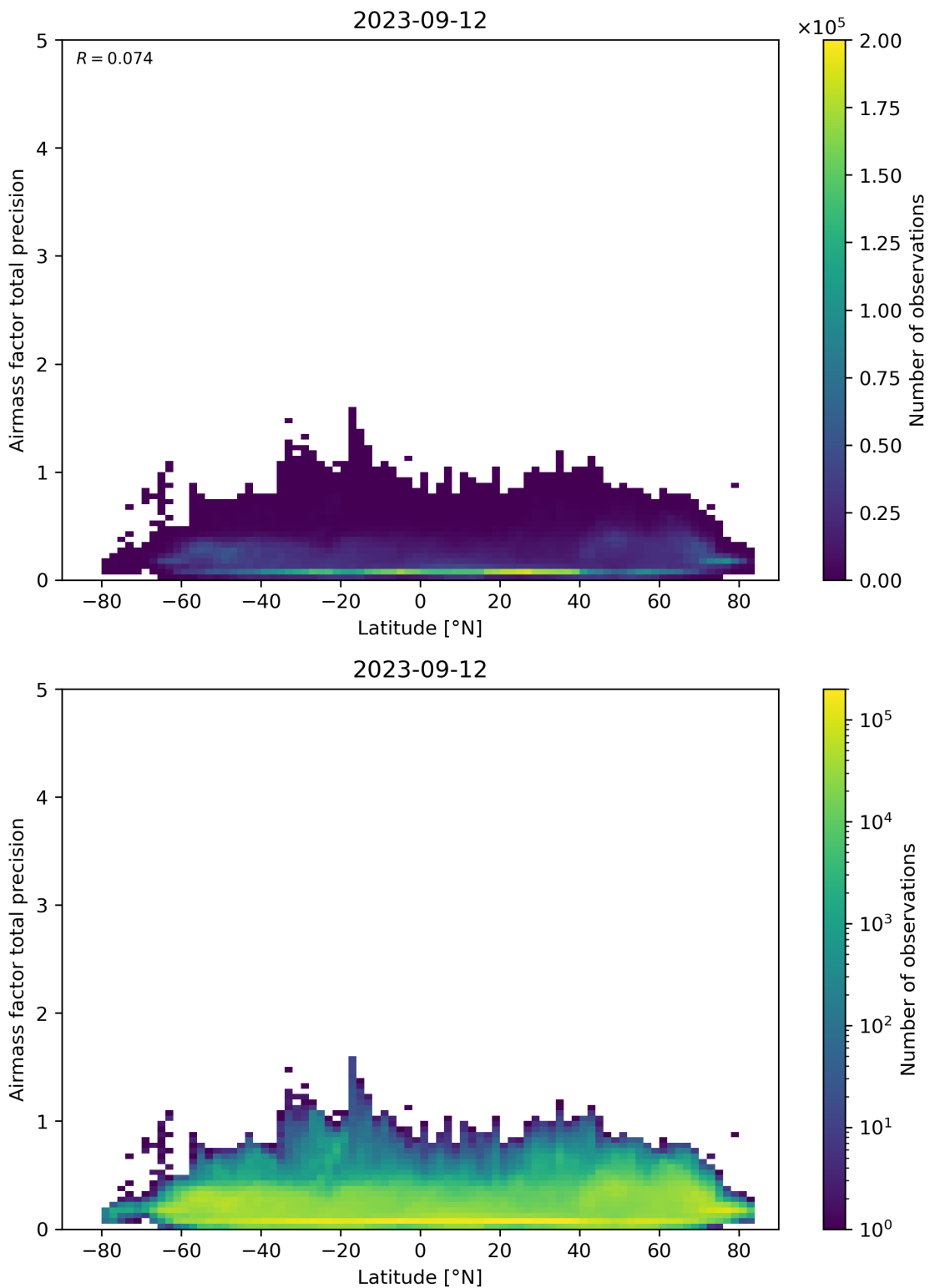


Figure 162: Scatter density plot of “Latitude” against “Airmass factor total precision” for 2023-09-11 to 2023-09-13.

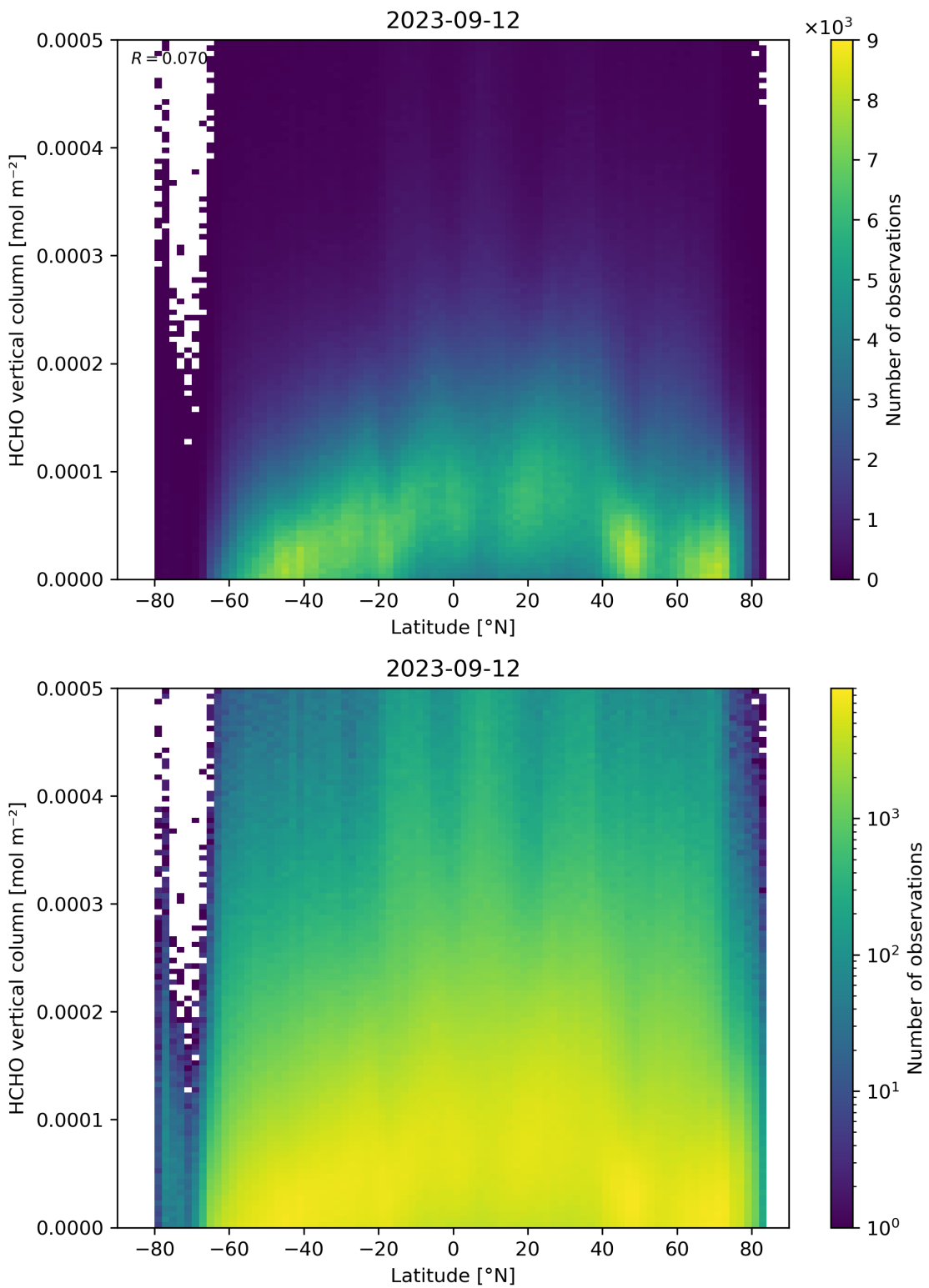


Figure 163: Scatter density plot of “Latitude” against “HCHO vertical column” for 2023-09-11 to 2023-09-13.

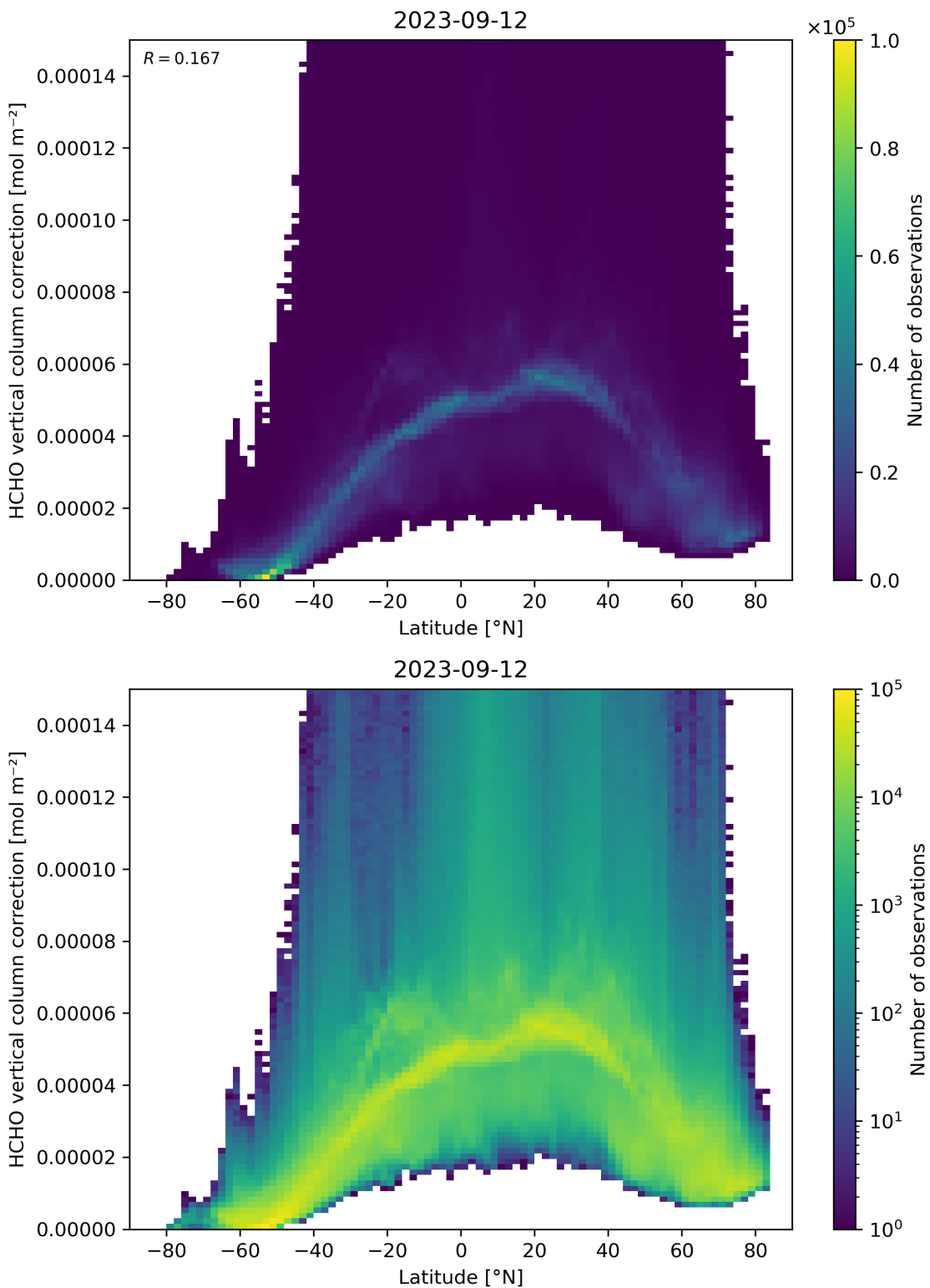


Figure 164: Scatter density plot of “Latitude” against “HCHO vertical column correction” for 2023-09-11 to 2023-09-13.

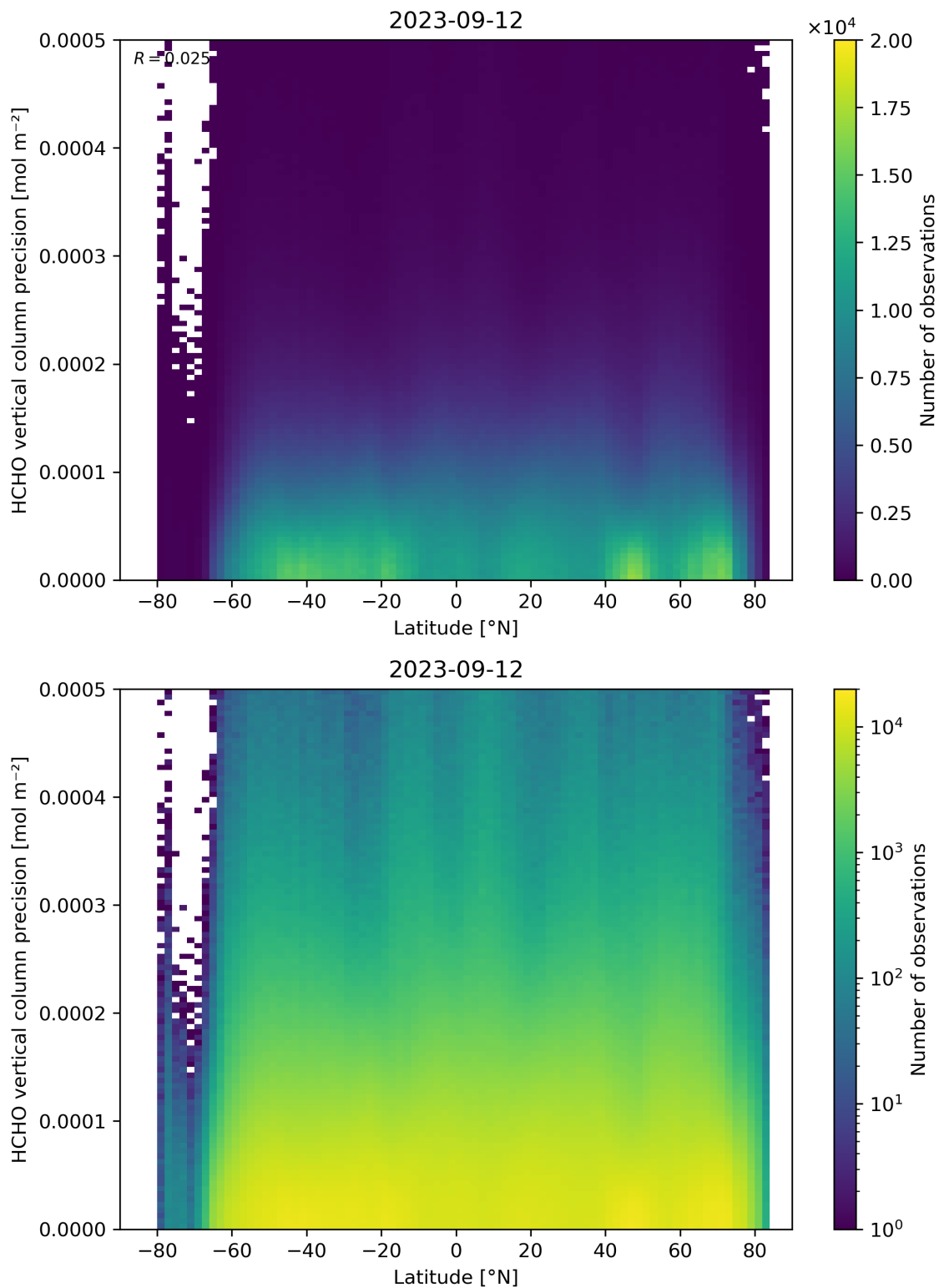


Figure 165: Scatter density plot of “Latitude” against “HCHO vertical column precision” for 2023-09-11 to 2023-09-13.

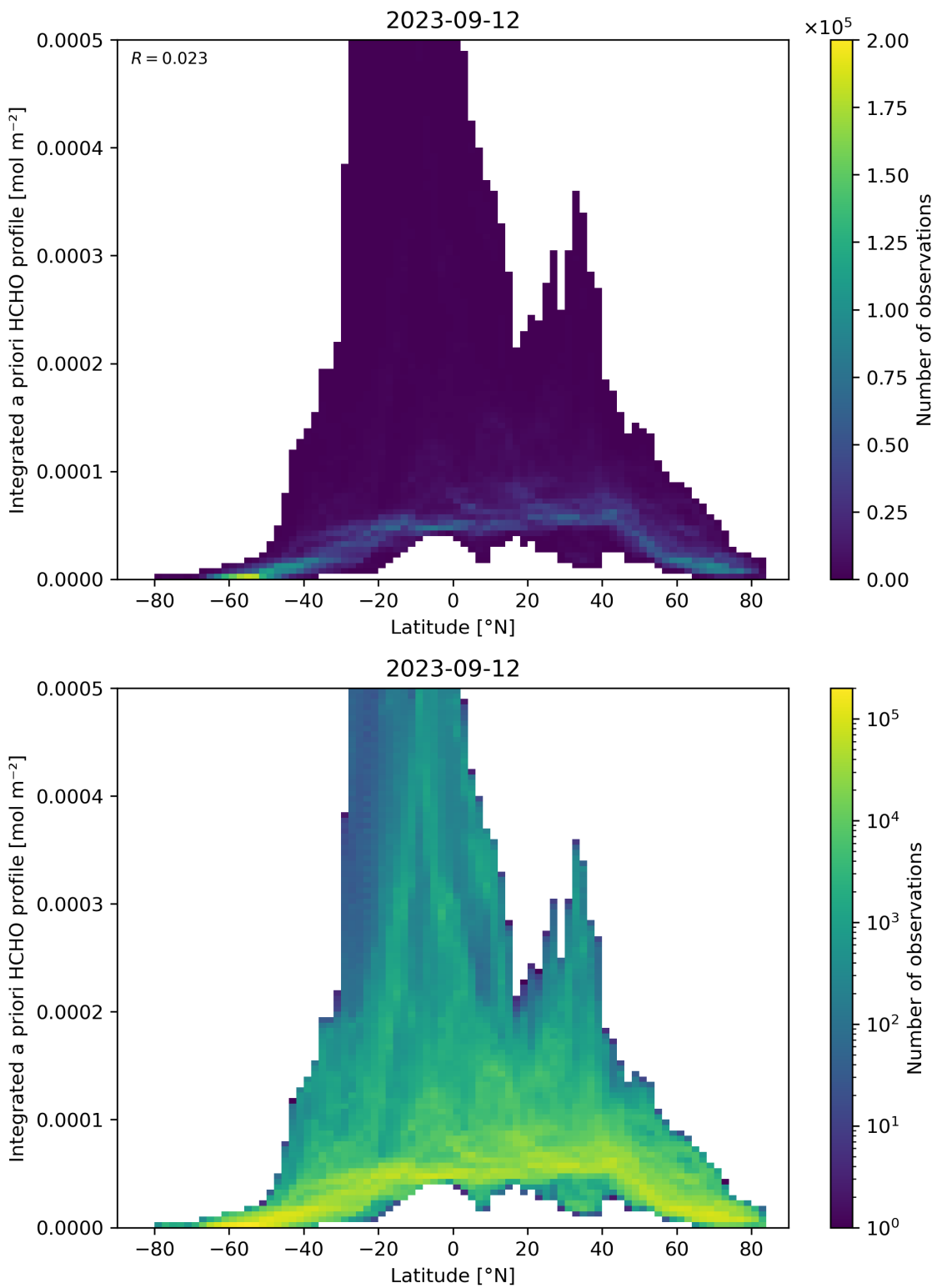


Figure 166: Scatter density plot of “Latitude” against “Integrated a priori HCHO profile” for 2023-09-11 to 2023-09-13.

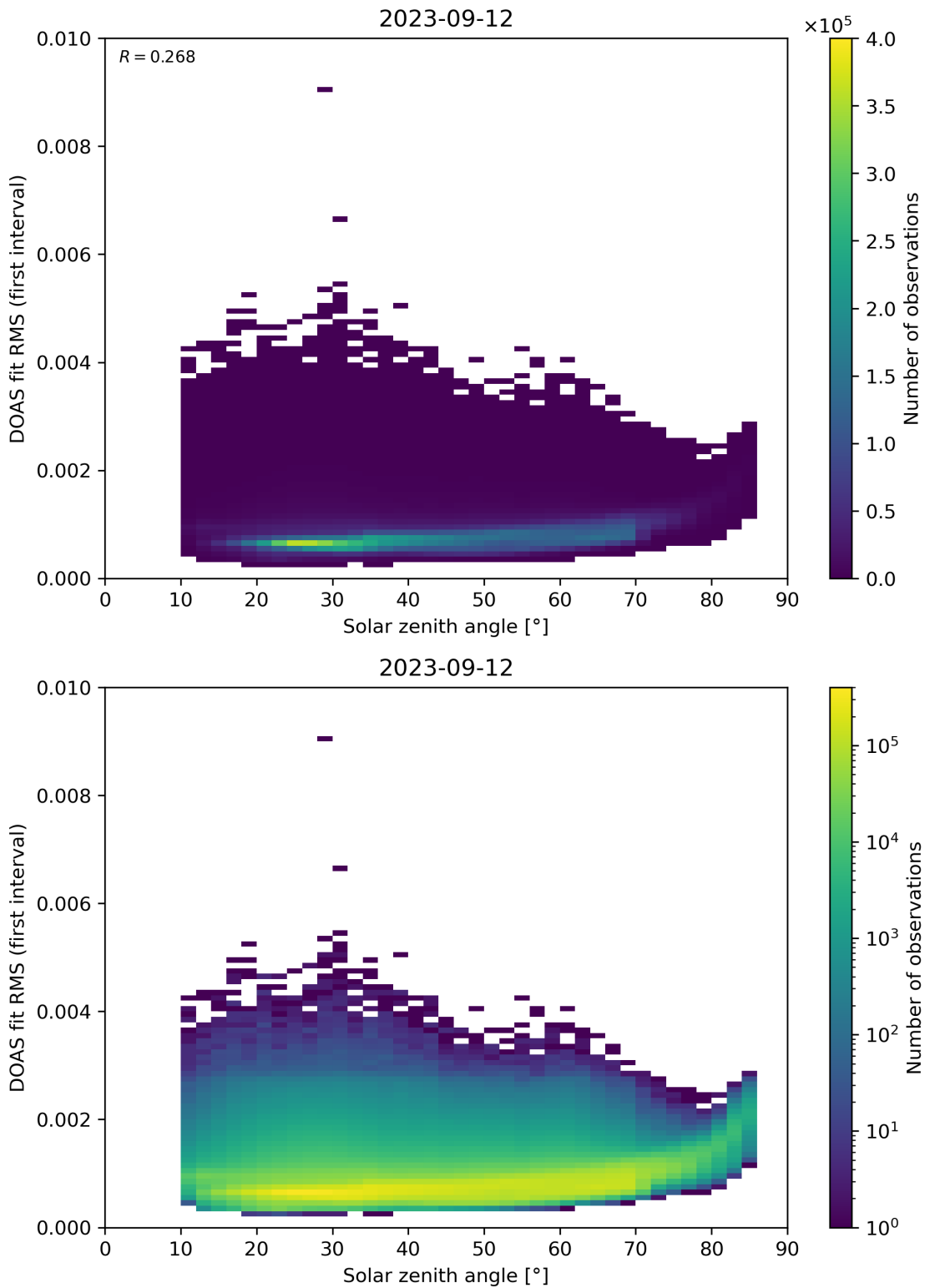


Figure 167: Scatter density plot of “Solar zenith angle” against “DOAS fit RMS (first interval)” for 2023-09-11 to 2023-09-13.

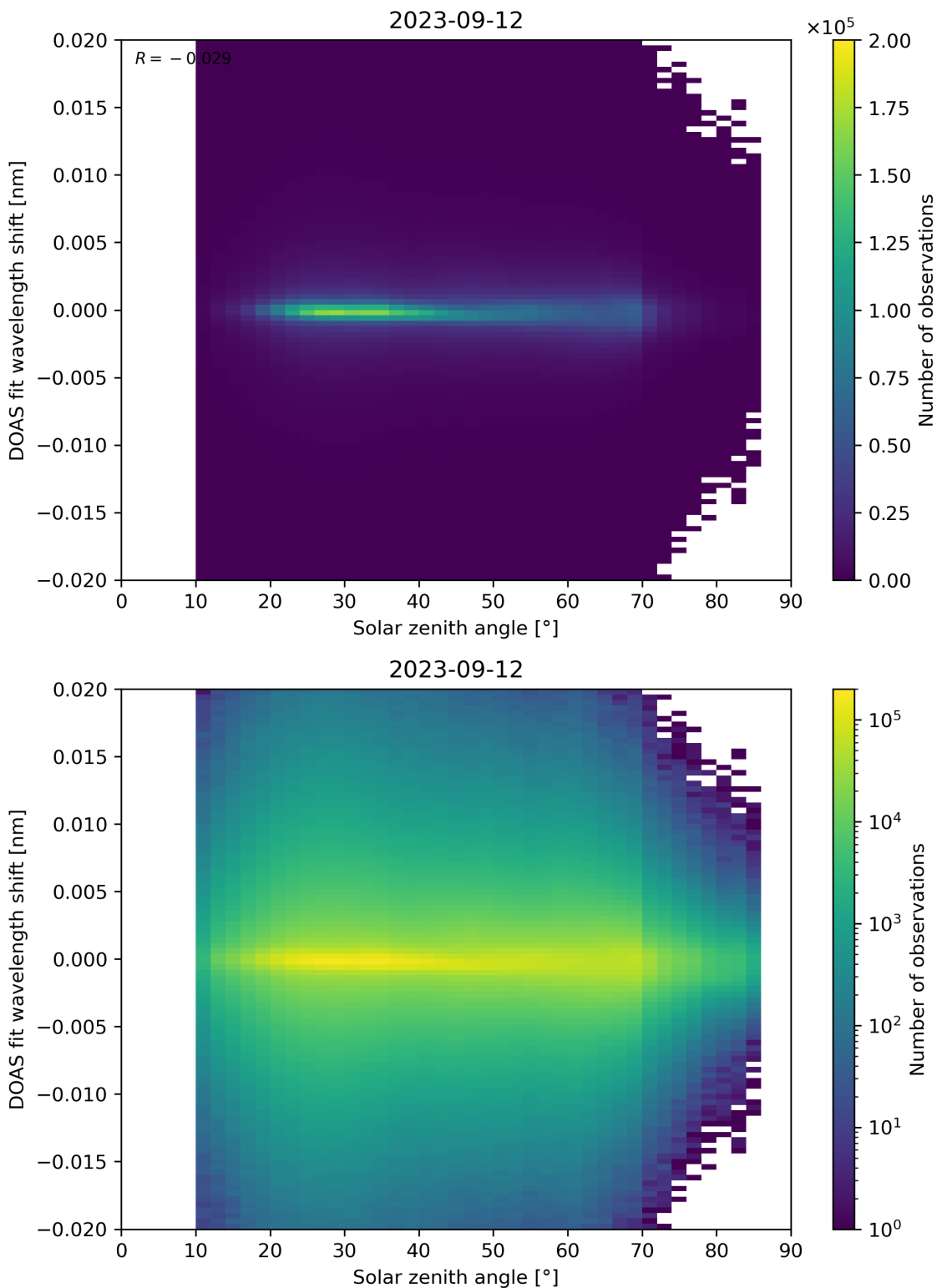


Figure 168: Scatter density plot of “Solar zenith angle” against “DOAS fit wavelength shift” for 2023-09-11 to 2023-09-13.

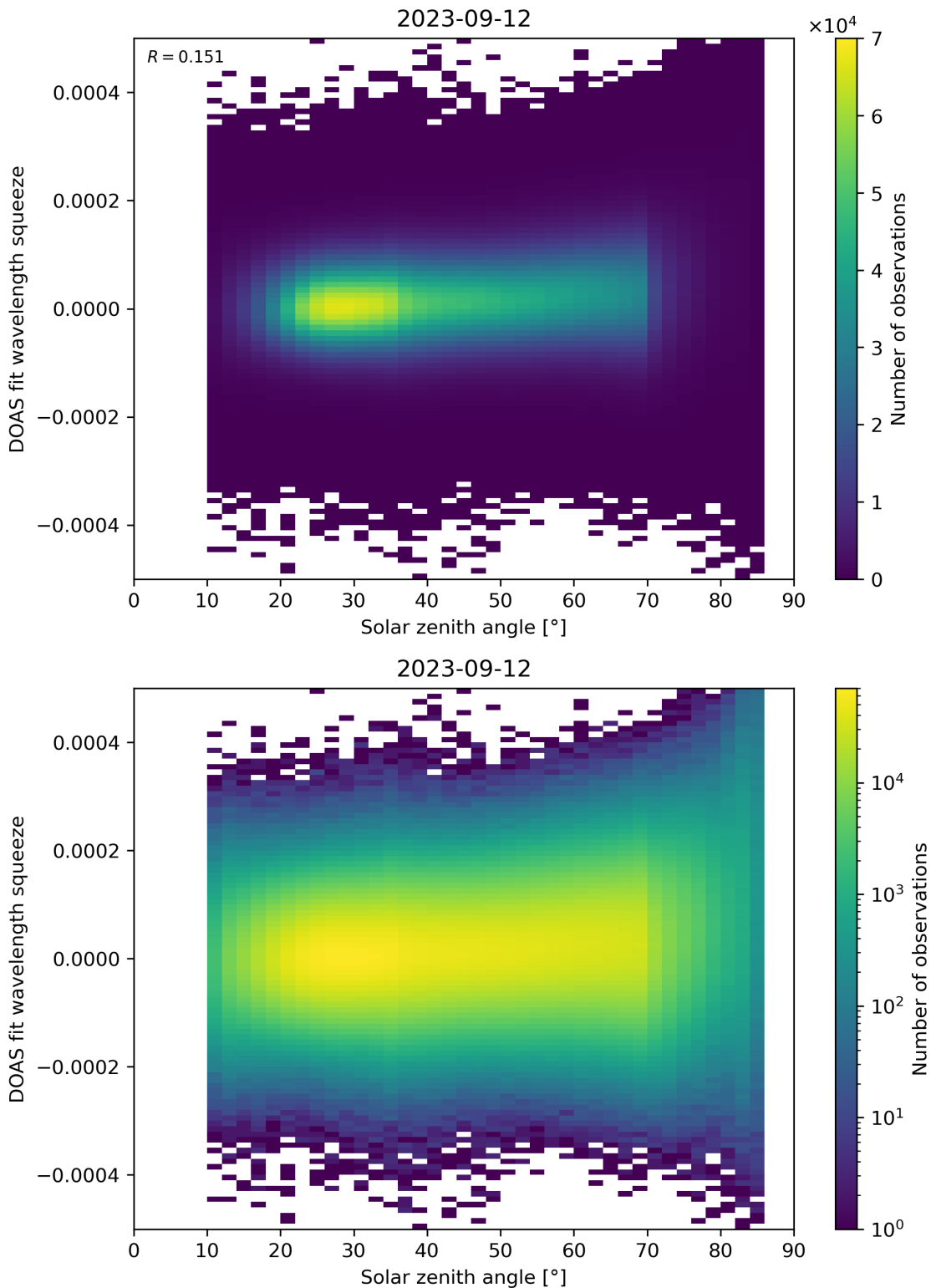


Figure 169: Scatter density plot of “Solar zenith angle” against “DOAS fit wavelength squeeze” for 2023-09-11 to 2023-09-13.

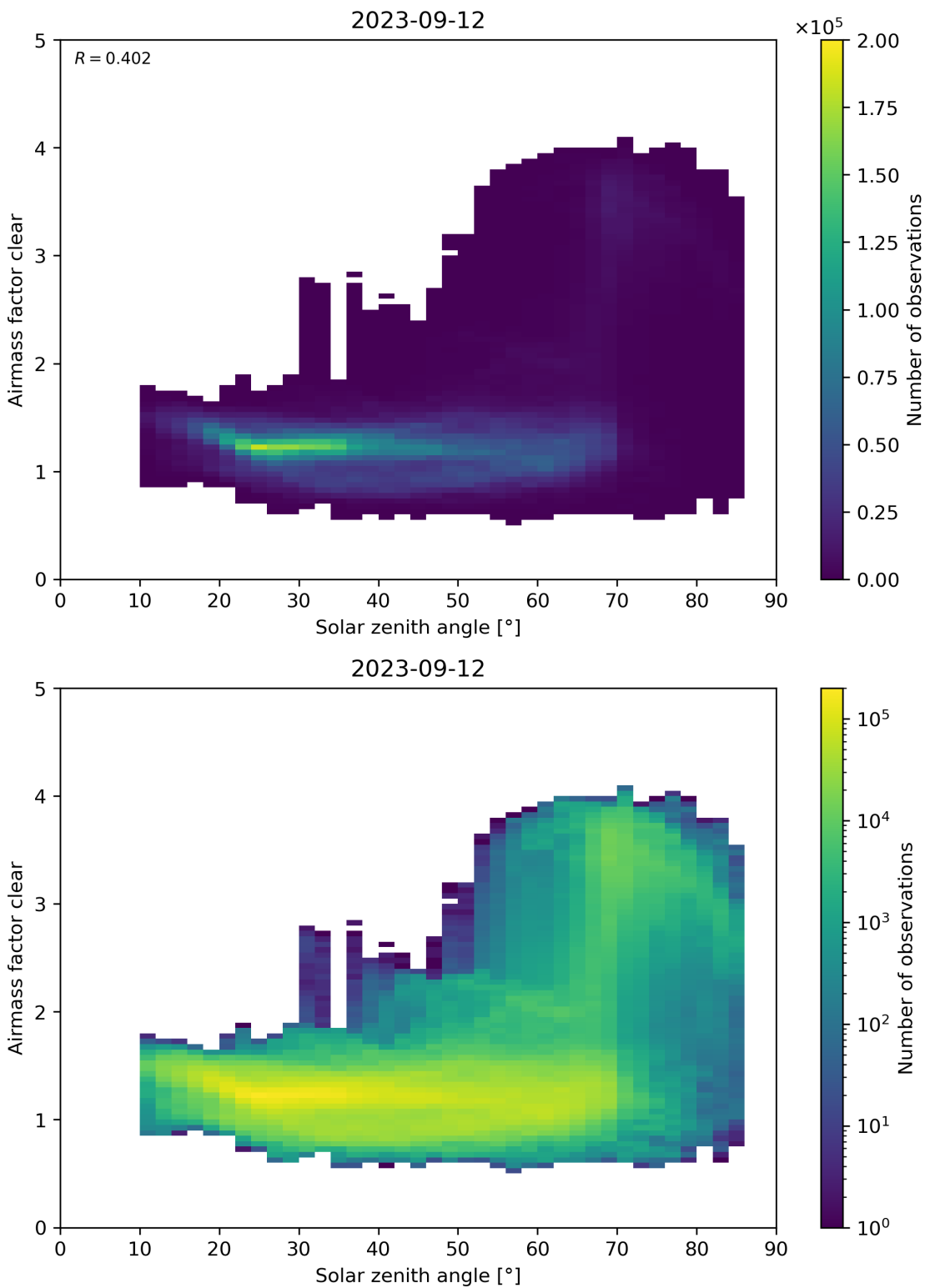


Figure 170: Scatter density plot of “Solar zenith angle” against “Airmass factor clear” for 2023-09-11 to 2023-09-13.

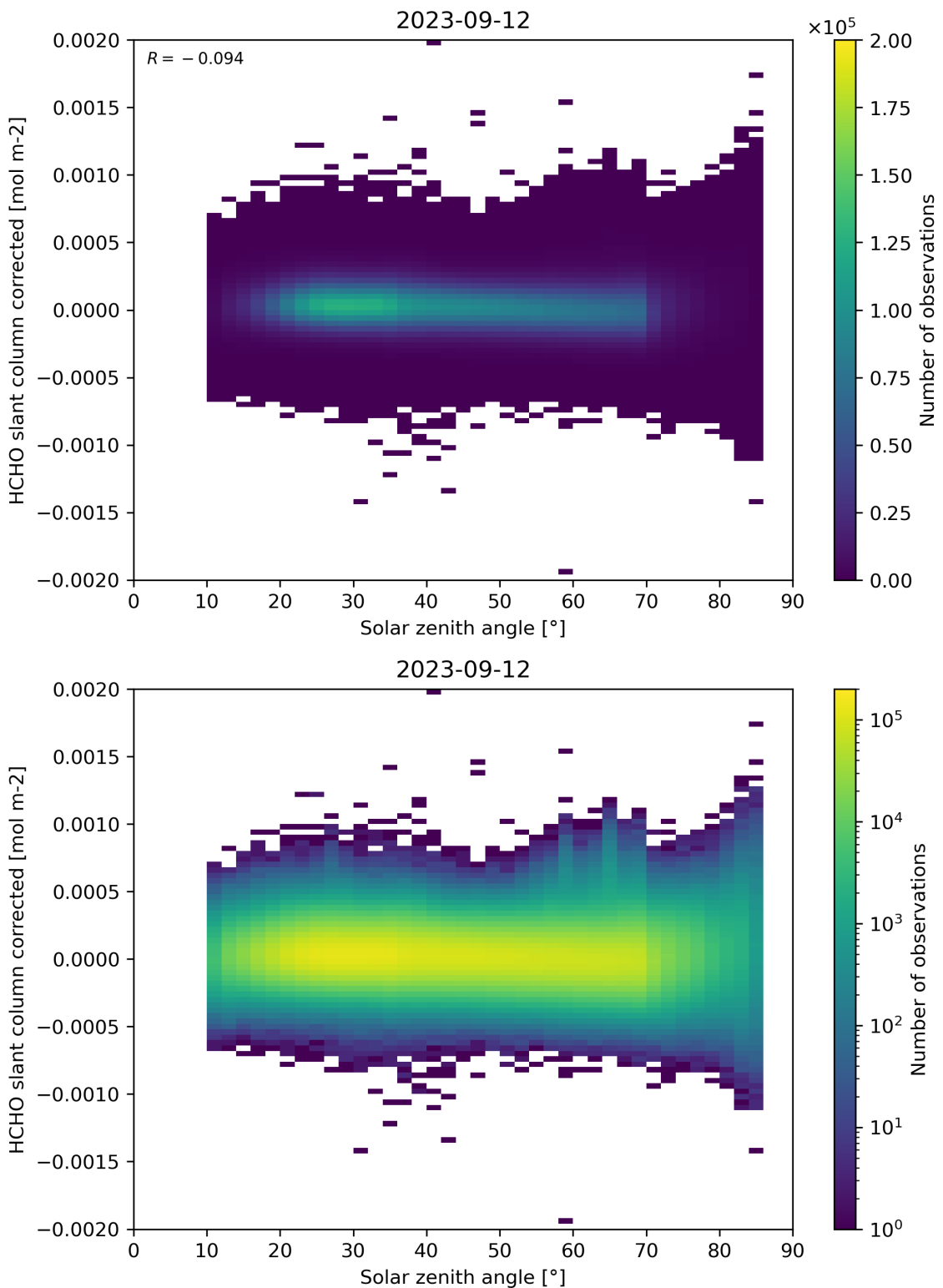


Figure 171: Scatter density plot of “Solar zenith angle” against “HCHO slant column corrected” for 2023-09-11 to 2023-09-13.

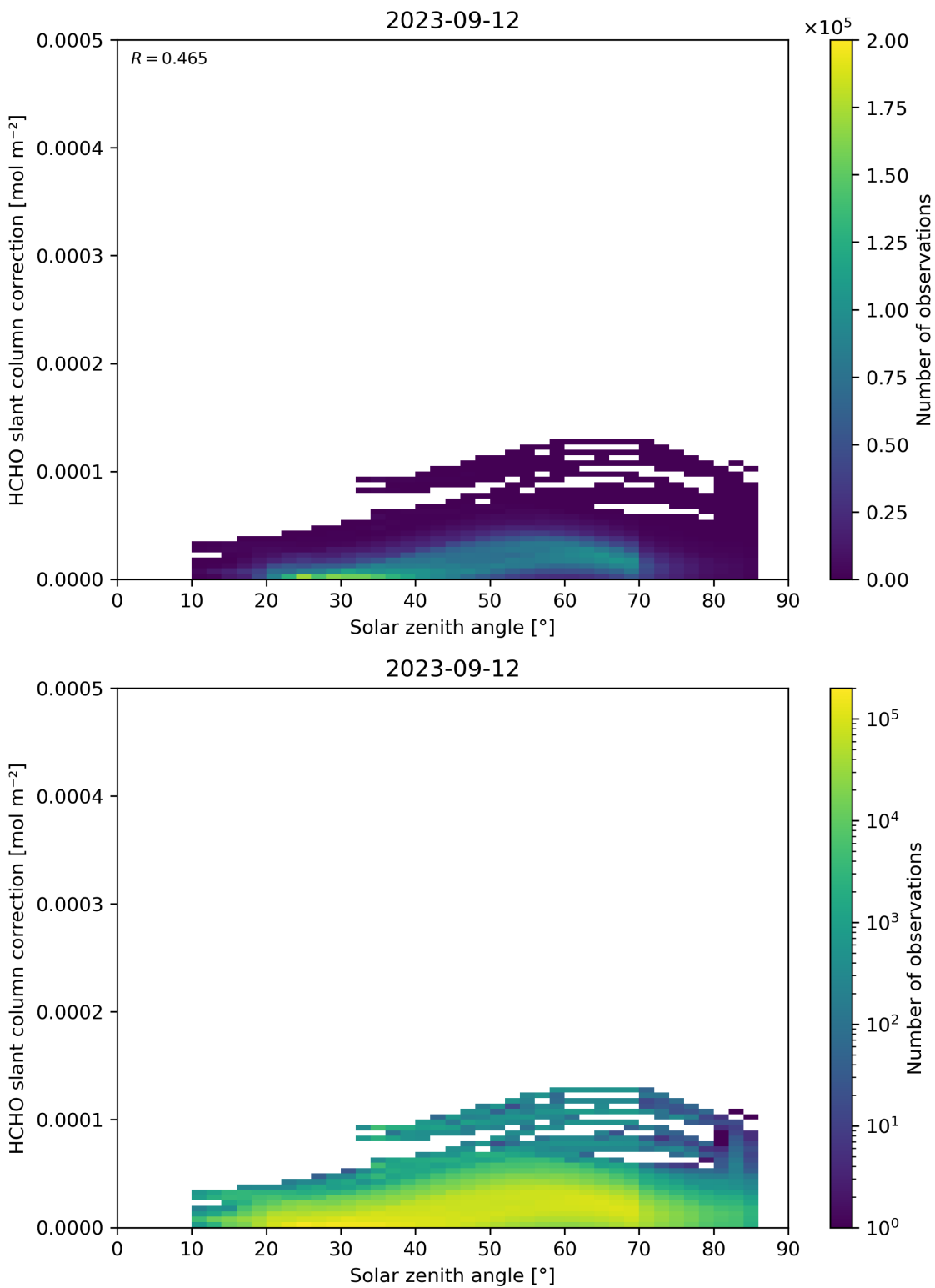


Figure 172: Scatter density plot of “Solar zenith angle” against “HCHO slant column correction” for 2023-09-11 to 2023-09-13.

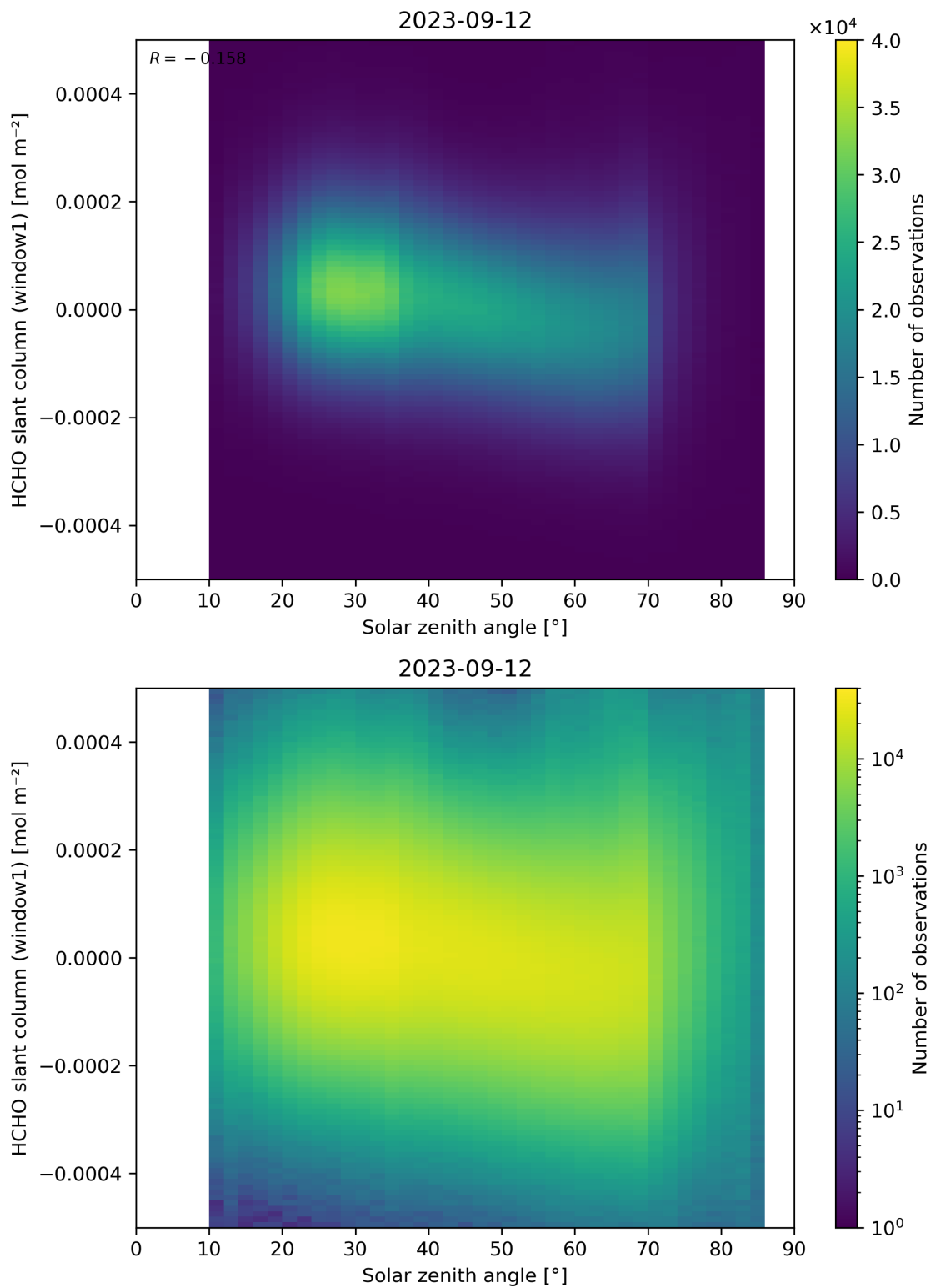


Figure 173: Scatter density plot of “Solar zenith angle” against “HCHO slant column (window1)” for 2023-09-11 to 2023-09-13.

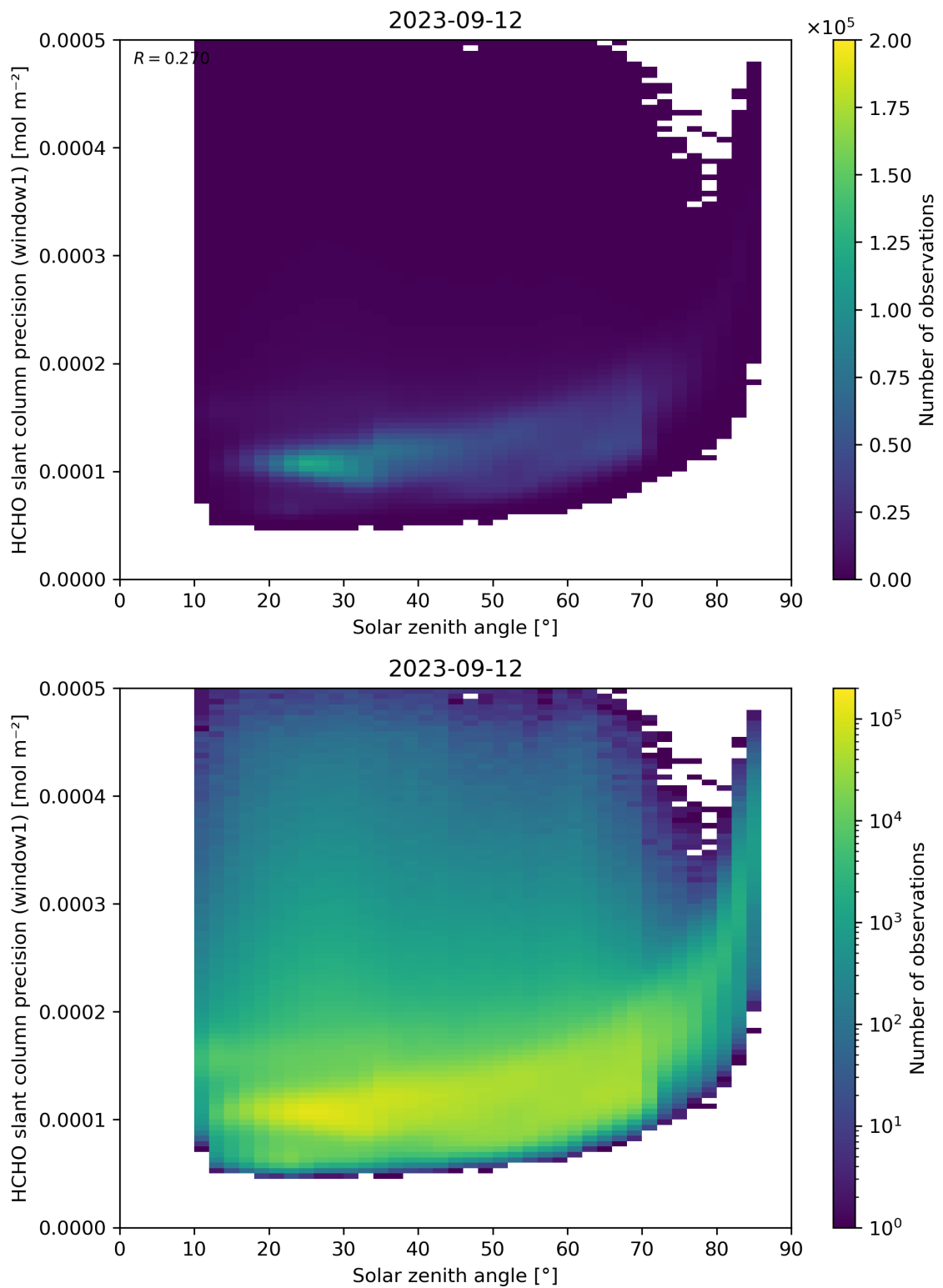


Figure 174: Scatter density plot of “Solar zenith angle” against “HCHO slant column precision (window1)” for 2023-09-11 to 2023-09-13.

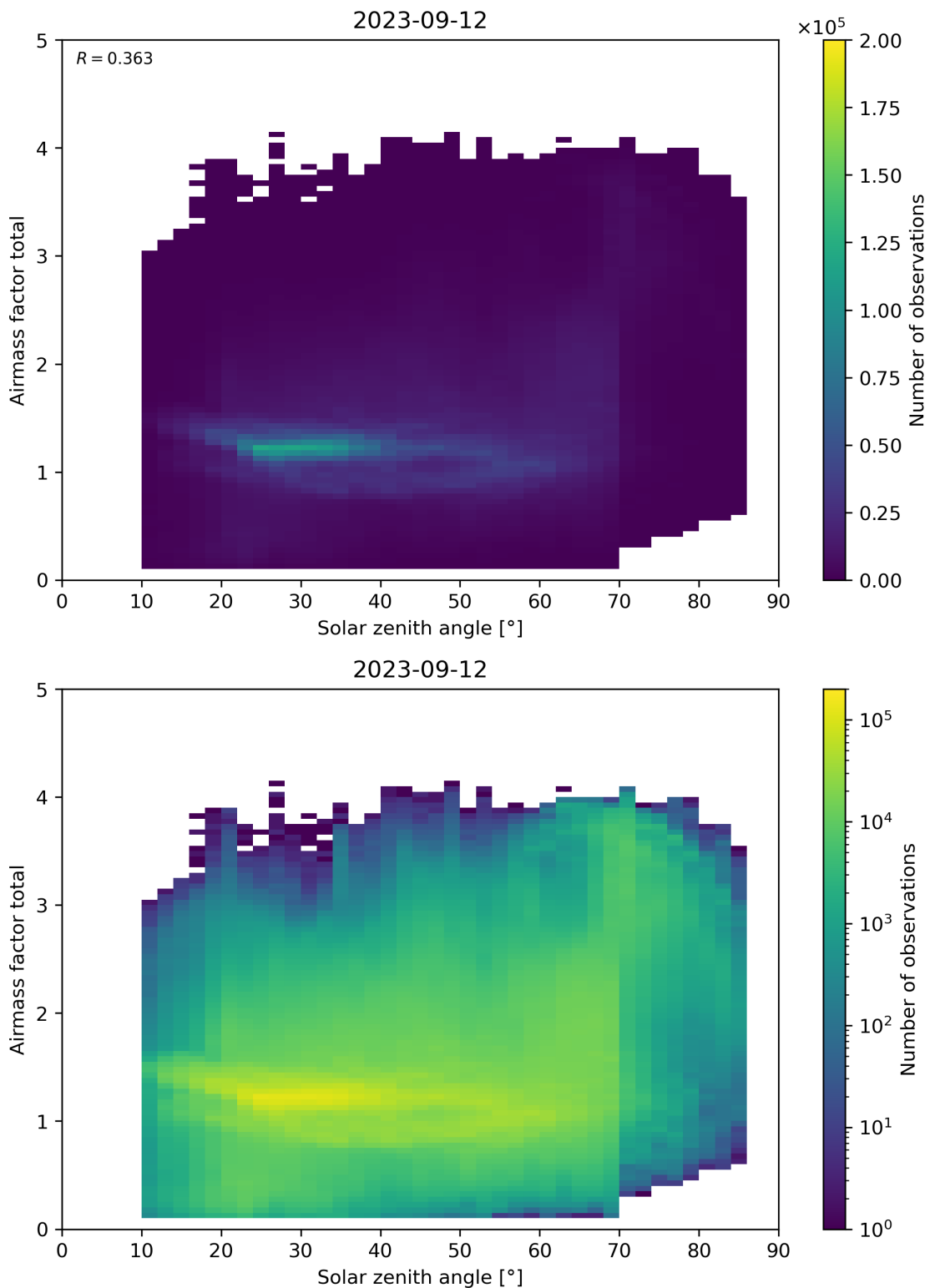


Figure 175: Scatter density plot of “Solar zenith angle” against “Airmass factor total” for 2023-09-11 to 2023-09-13.

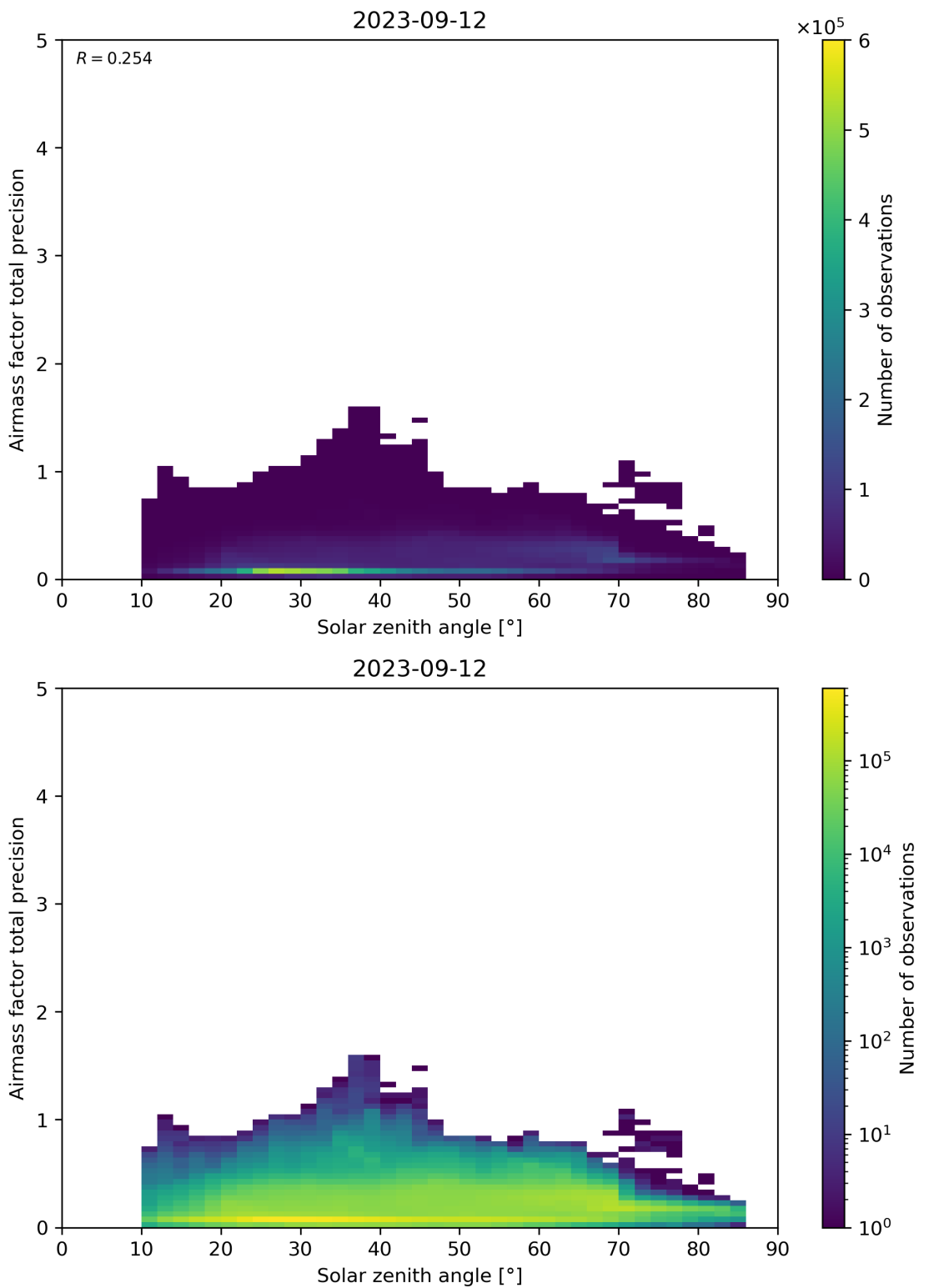


Figure 176: Scatter density plot of “Solar zenith angle” against “Airmass factor total precision” for 2023-09-11 to 2023-09-13.

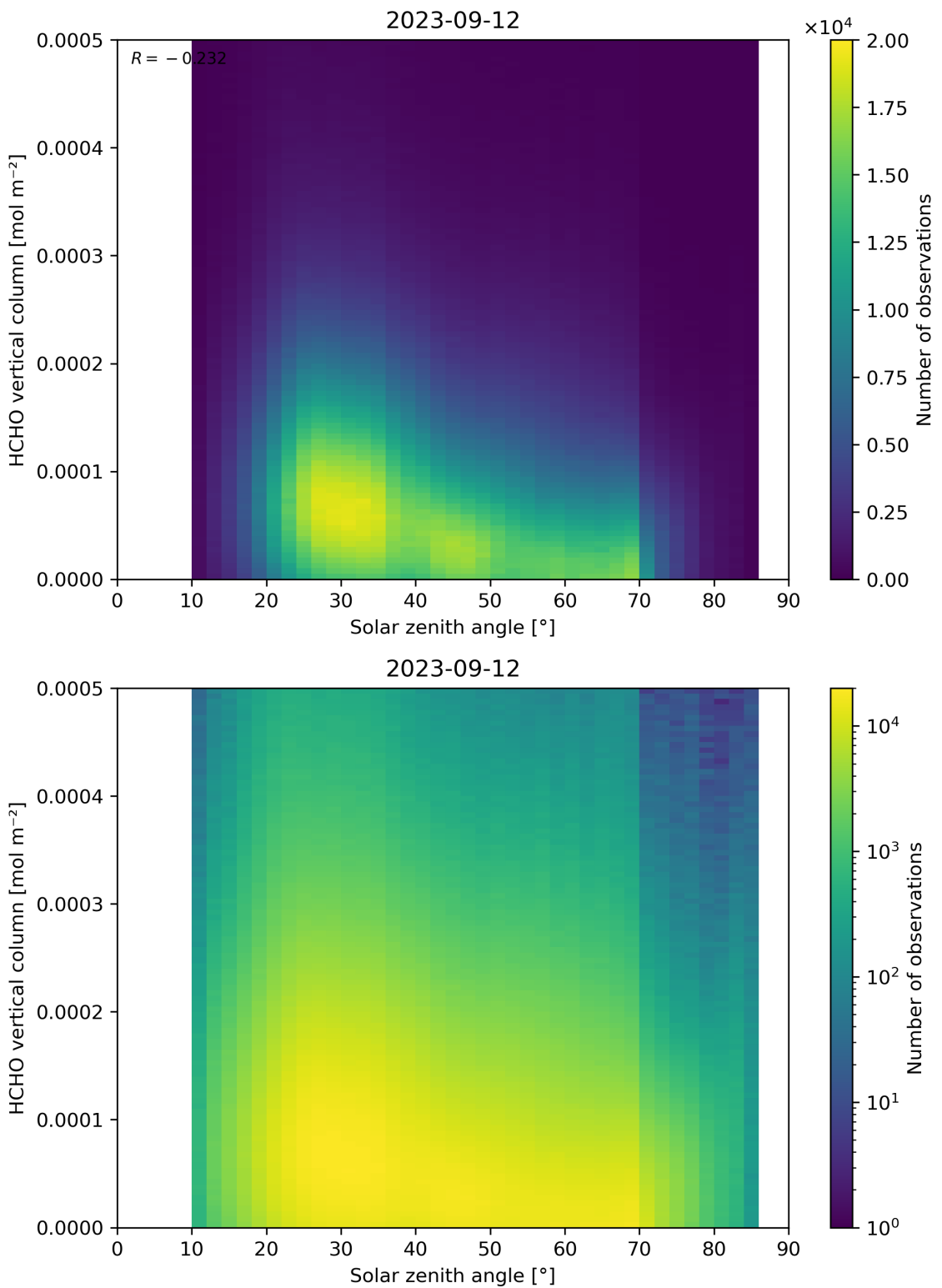


Figure 177: Scatter density plot of “Solar zenith angle” against “HCHO vertical column” for 2023-09-11 to 2023-09-13.

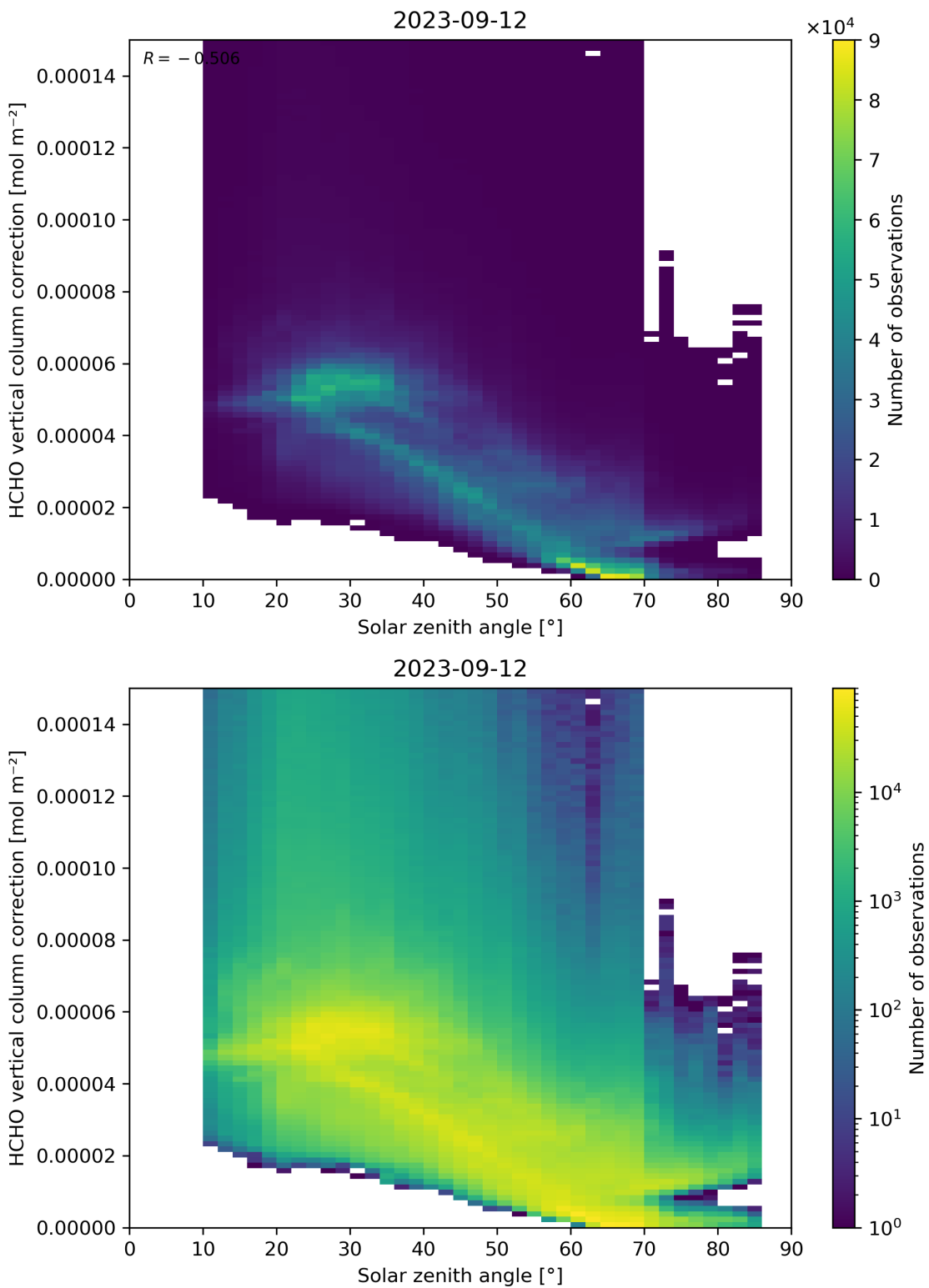


Figure 178: Scatter density plot of “Solar zenith angle” against “HCHO vertical column correction” for 2023-09-11 to 2023-09-13.

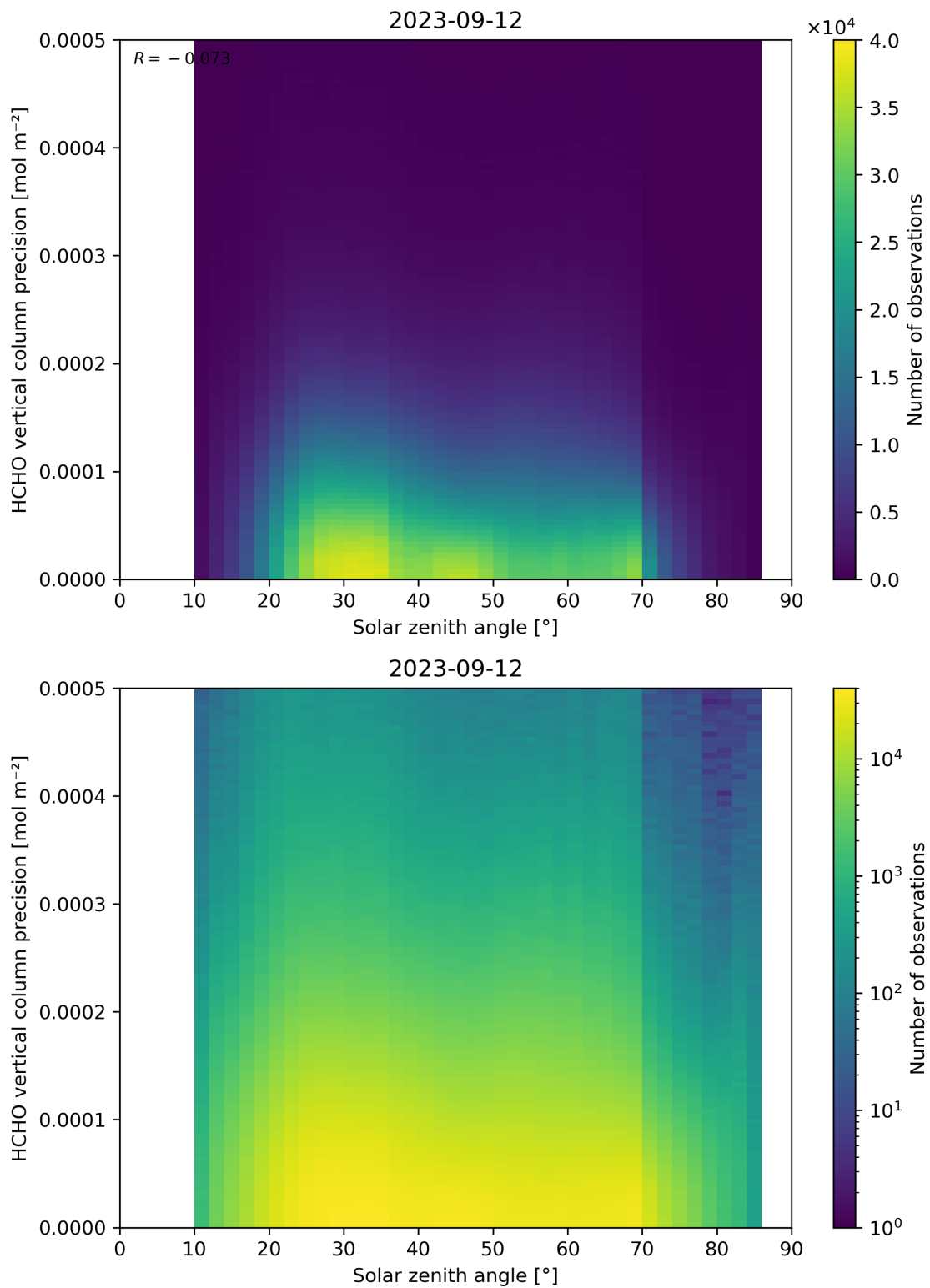


Figure 179: Scatter density plot of “Solar zenith angle” against “HCHO vertical column precision” for 2023-09-11 to 2023-09-13.

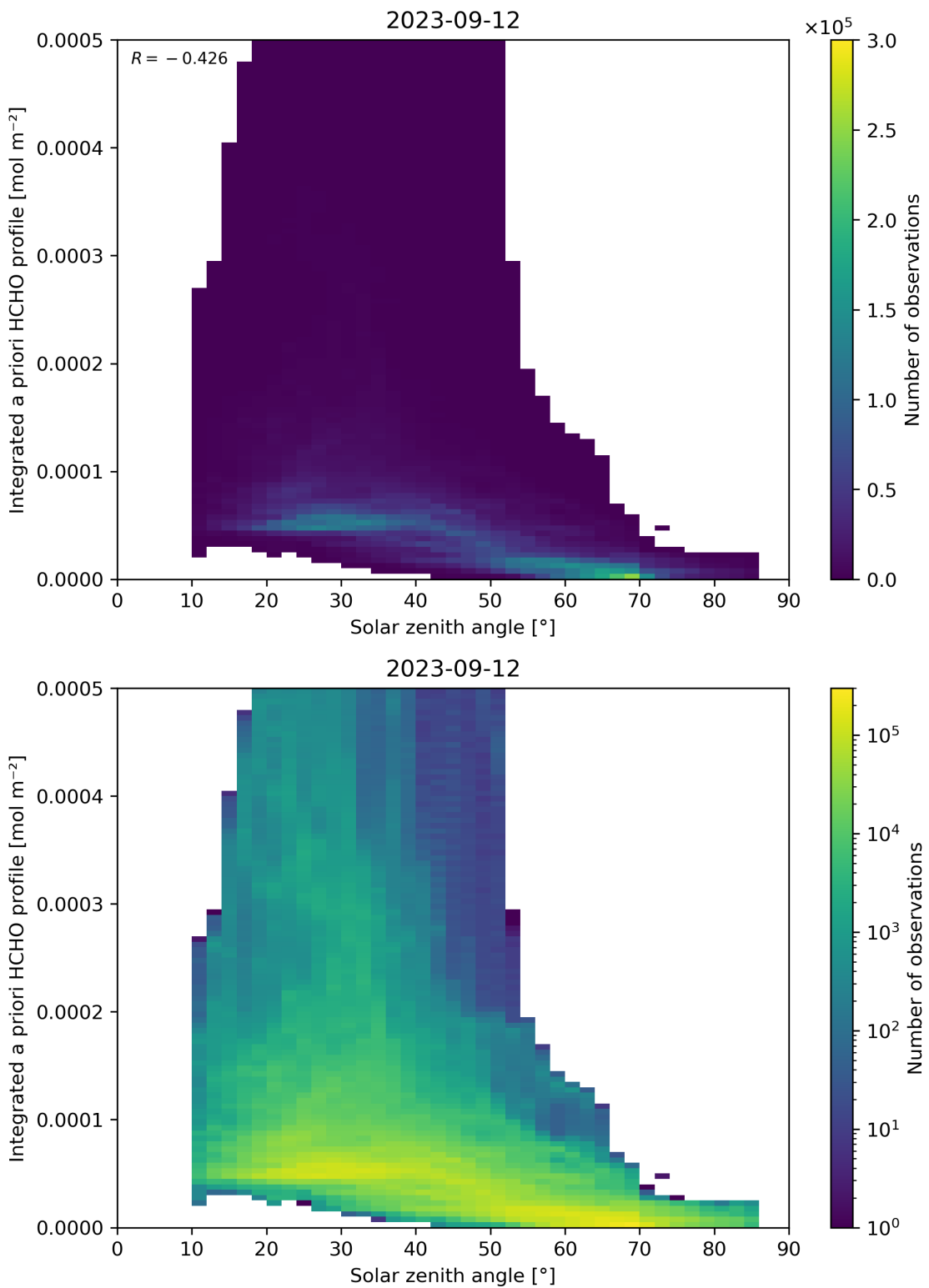


Figure 180: Scatter density plot of “Solar zenith angle” against “Integrated a priori HCHO profile” for 2023-09-11 to 2023-09-13.

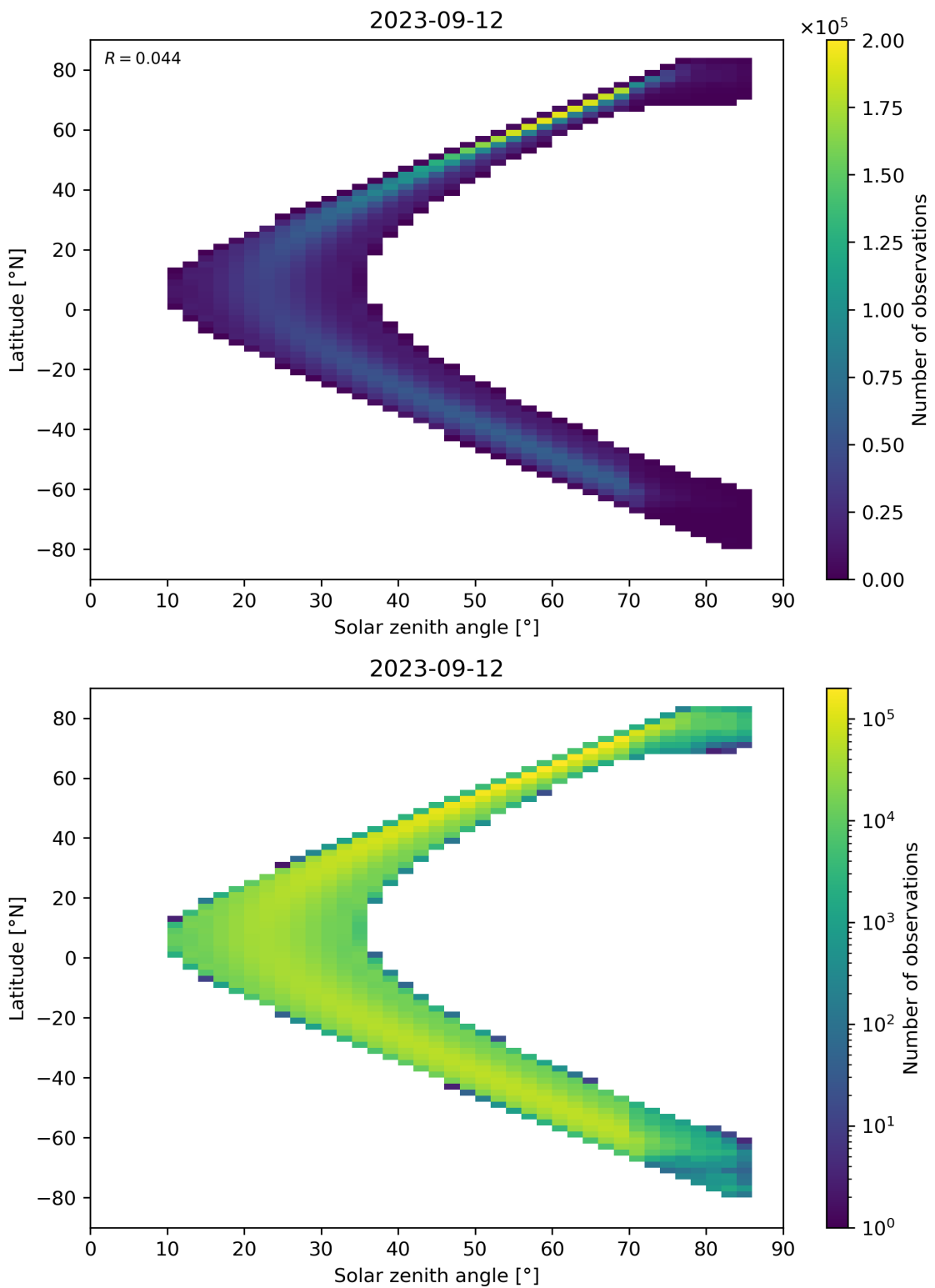


Figure 181: Scatter density plot of “Solar zenith angle” against “Latitude” for 2023-09-11 to 2023-09-13.

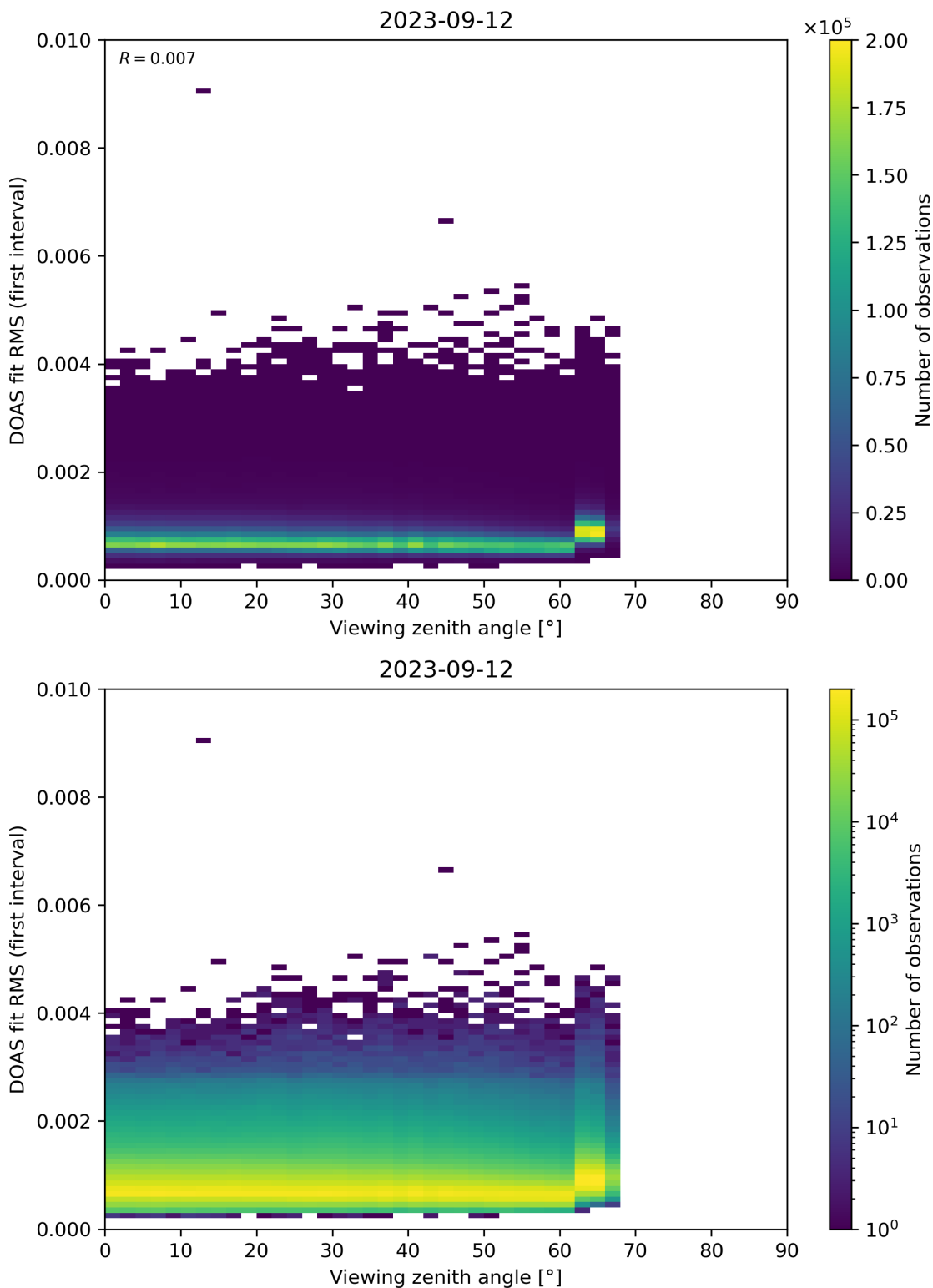


Figure 182: Scatter density plot of “Viewing zenith angle” against “DOAS fit RMS (first interval)” for 2023-09-11 to 2023-09-13.

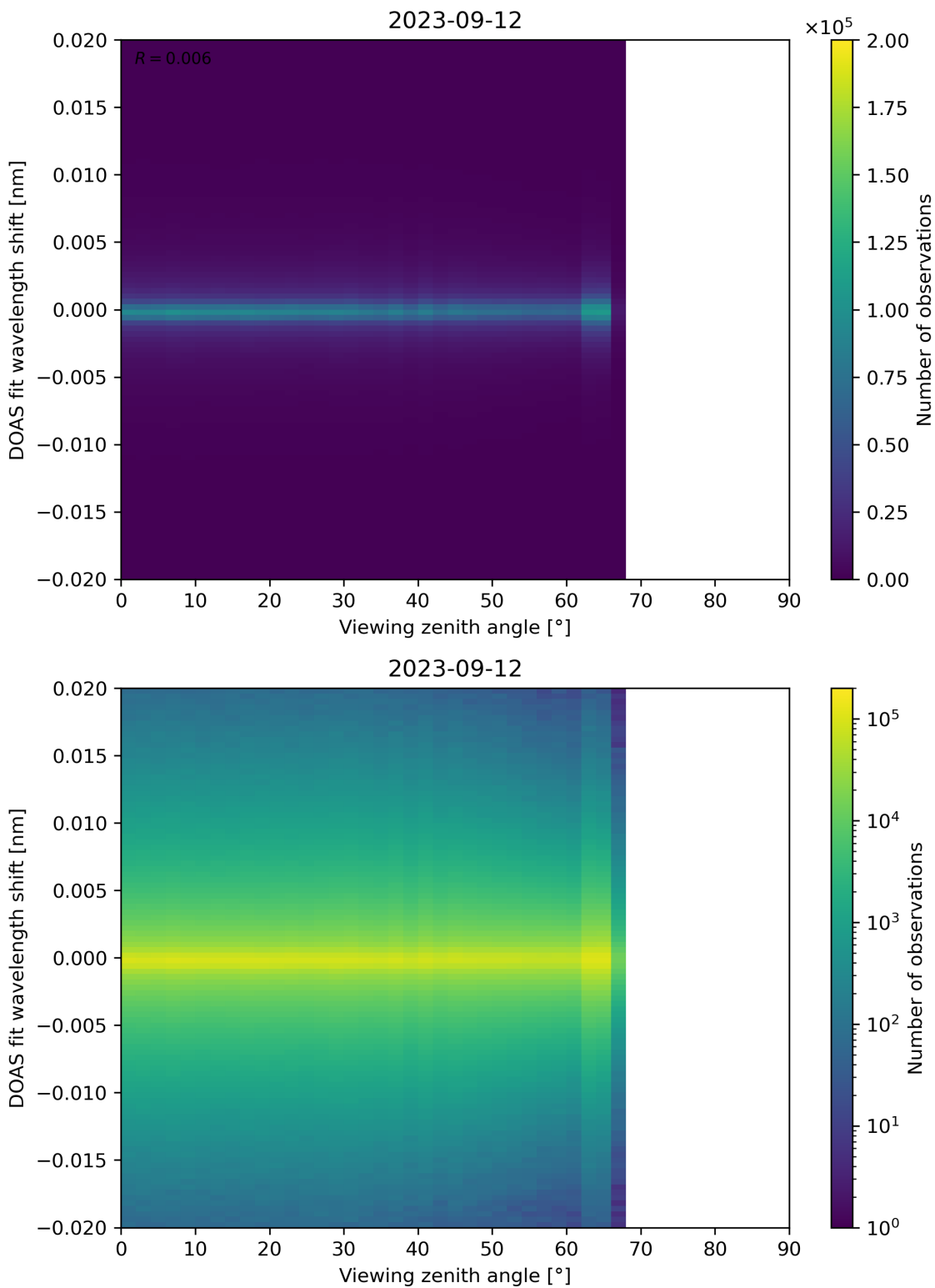


Figure 183: Scatter density plot of “Viewing zenith angle” against “DOAS fit wavelength shift” for 2023-09-11 to 2023-09-13.

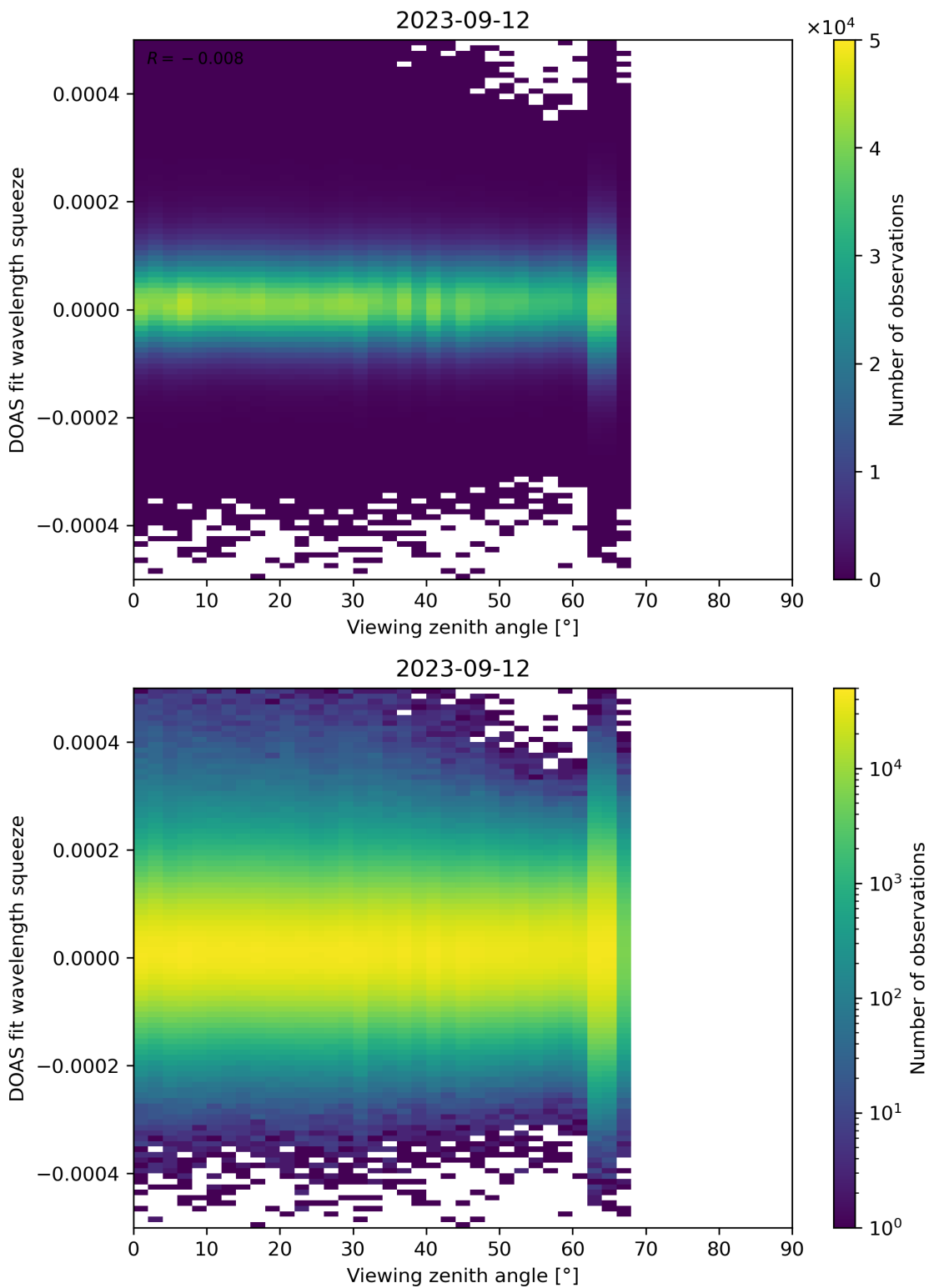


Figure 184: Scatter density plot of “Viewing zenith angle” against “DOAS fit wavelength squeeze” for 2023-09-11 to 2023-09-13.

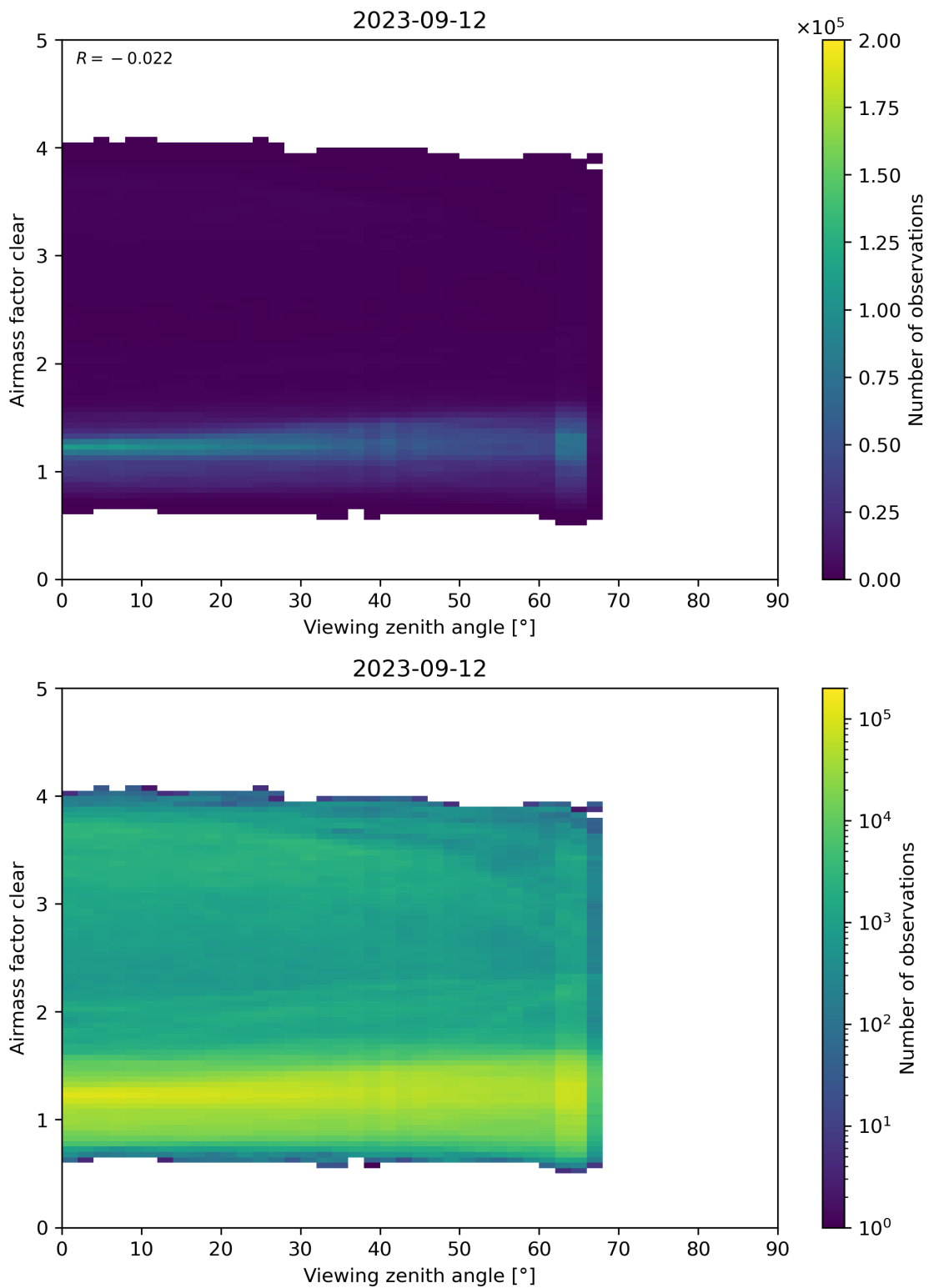


Figure 185: Scatter density plot of “Viewing zenith angle” against “Airmass factor clear” for 2023-09-11 to 2023-09-13.

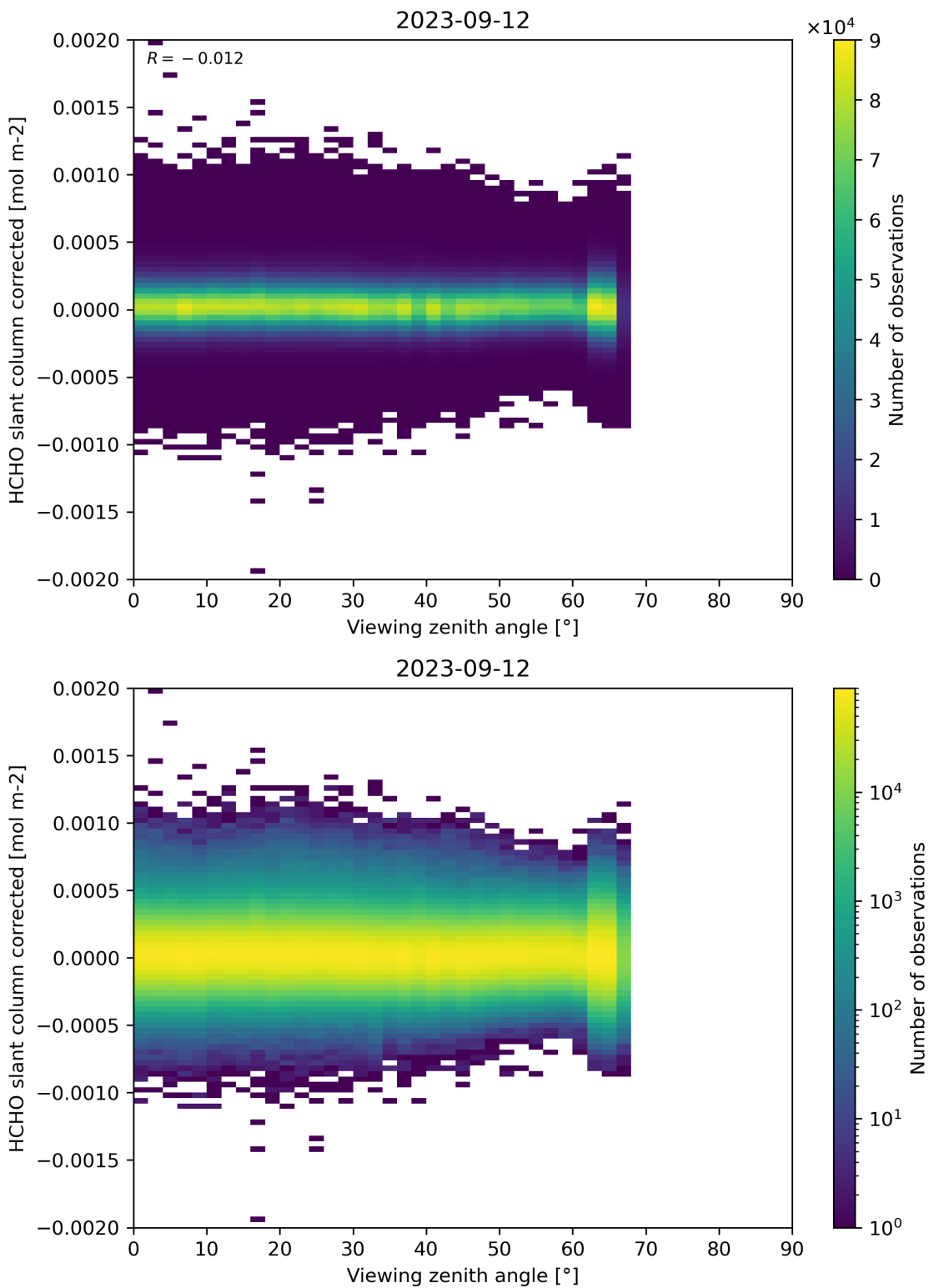


Figure 186: Scatter density plot of “Viewing zenith angle” against “HCHO slant column corrected” for 2023-09-11 to 2023-09-13.

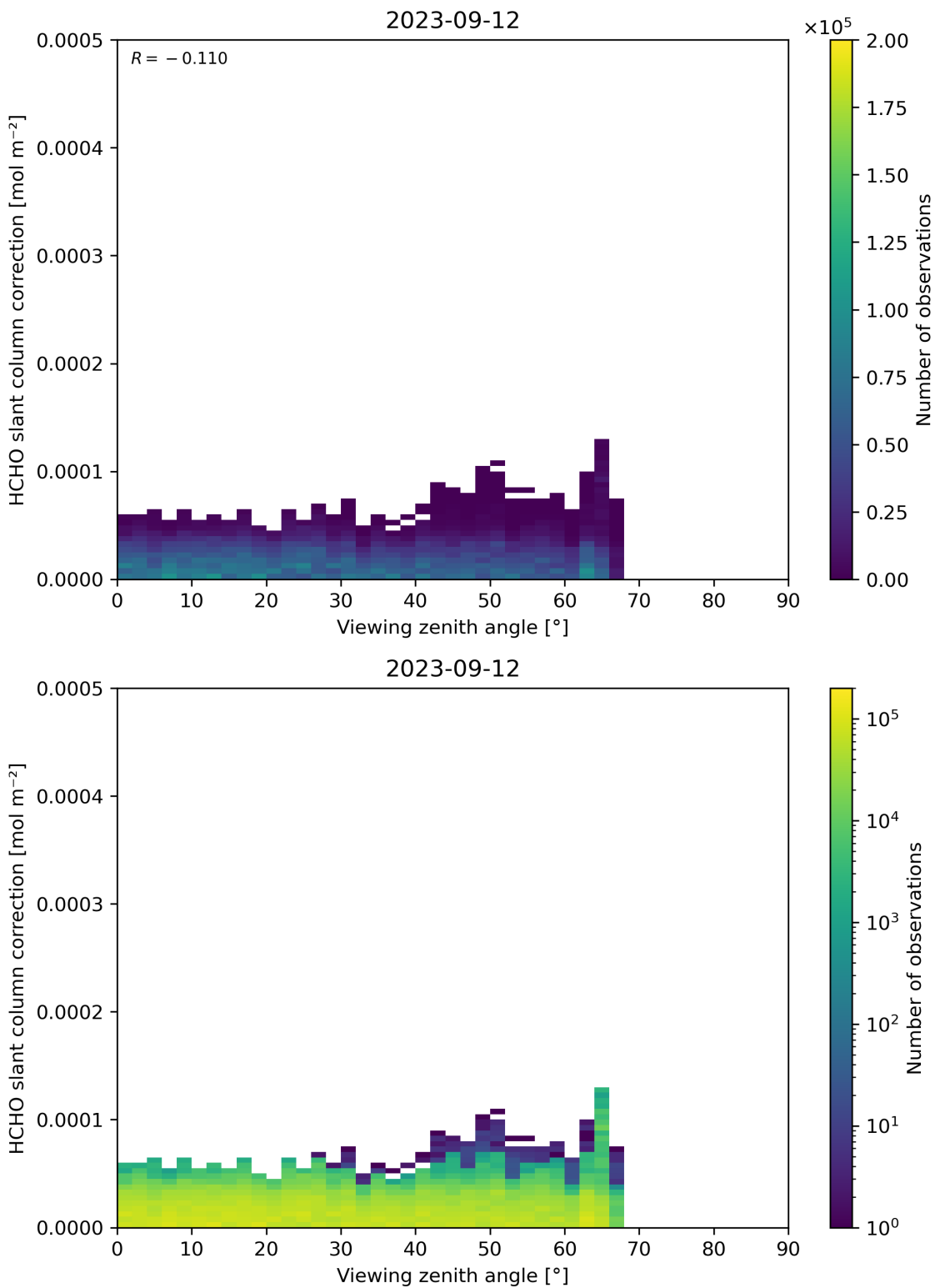


Figure 187: Scatter density plot of “Viewing zenith angle” against “HCHO slant column correction” for 2023-09-11 to 2023-09-13.

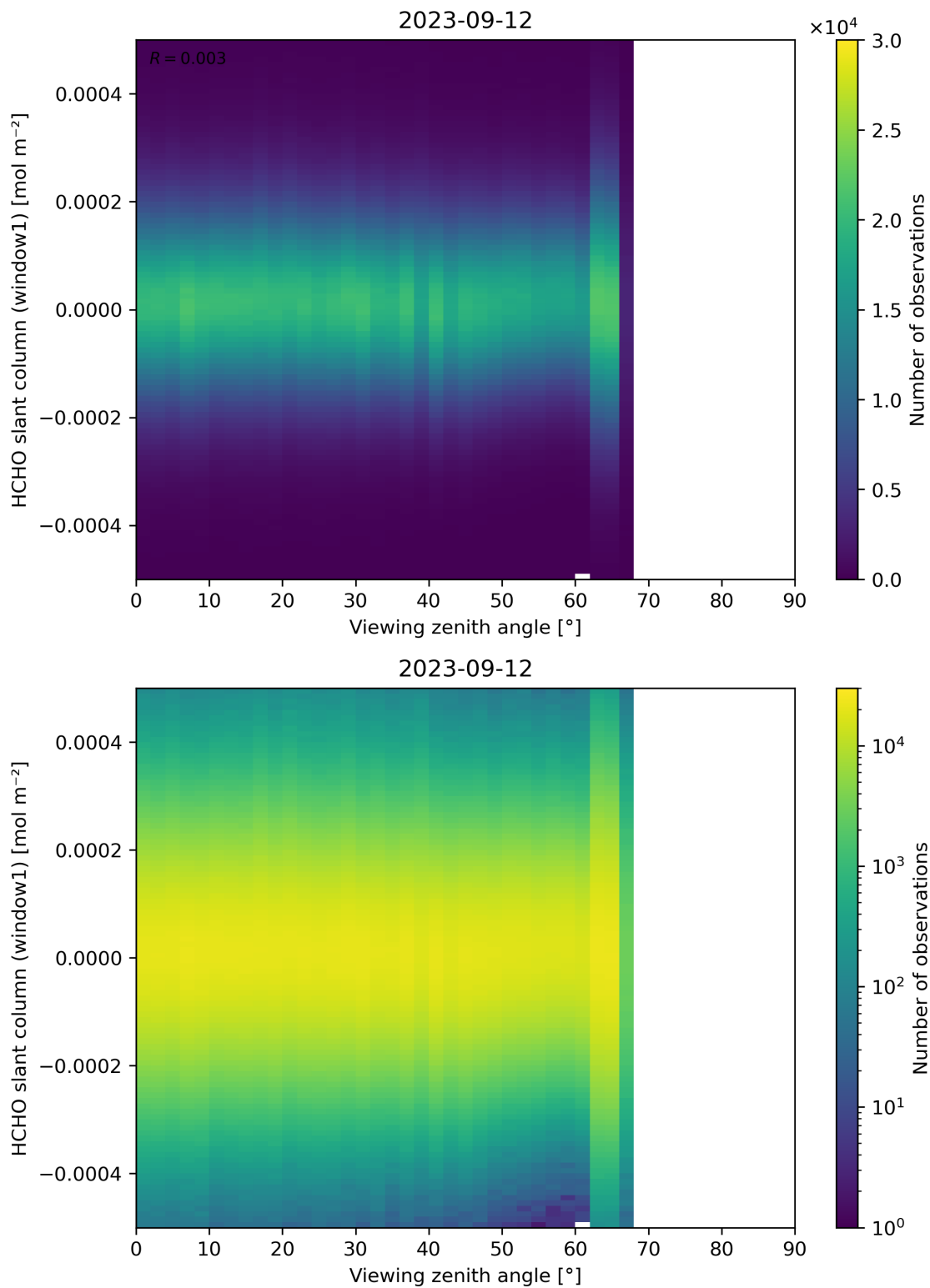


Figure 188: Scatter density plot of “Viewing zenith angle” against “HCHO slant column (window1)” for 2023-09-11 to 2023-09-13.

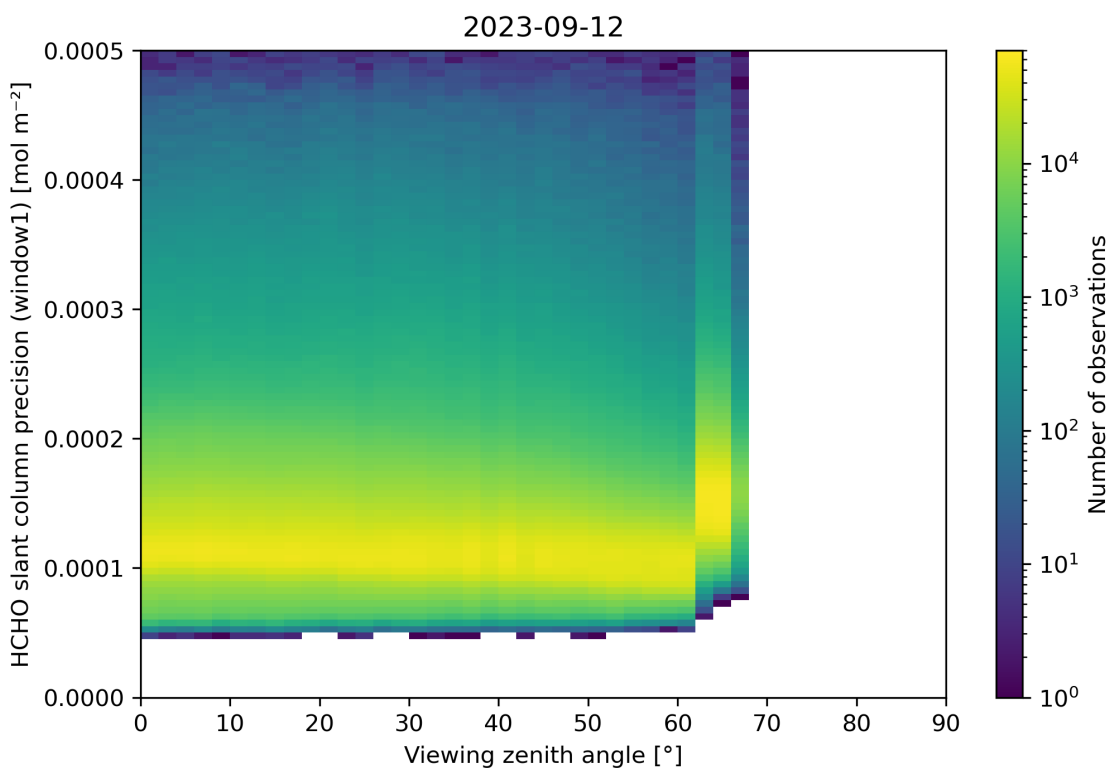
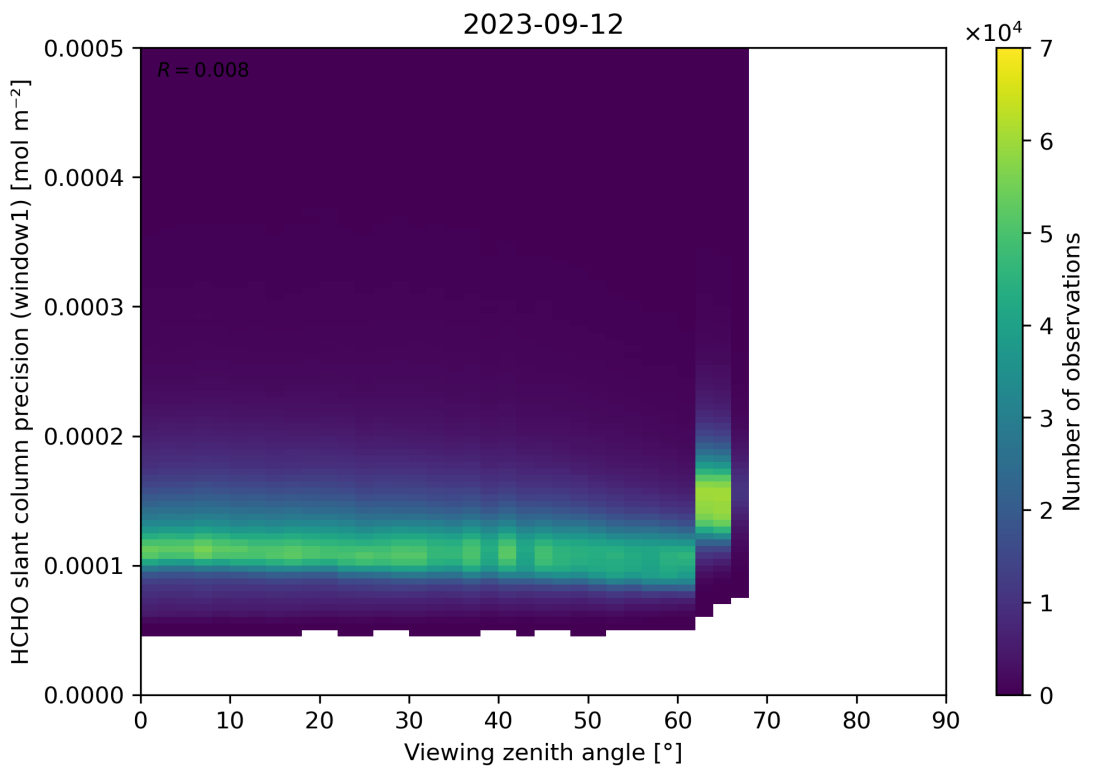


Figure 189: Scatter density plot of “Viewing zenith angle” against “HCHO slant column precision (window1)” for 2023-09-11 to 2023-09-13.

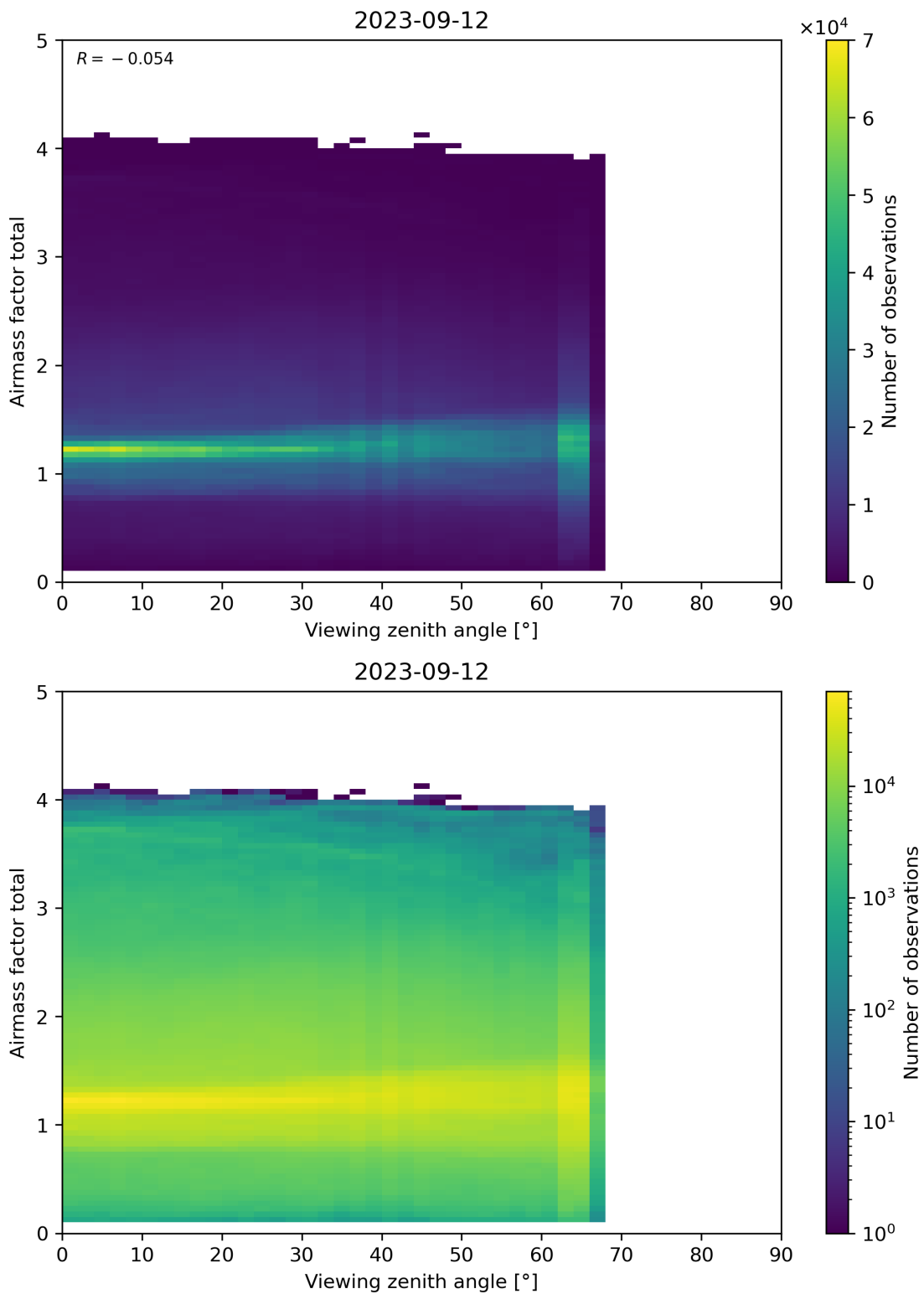


Figure 190: Scatter density plot of “Viewing zenith angle” against “Airmass factor total” for 2023-09-11 to 2023-09-13.

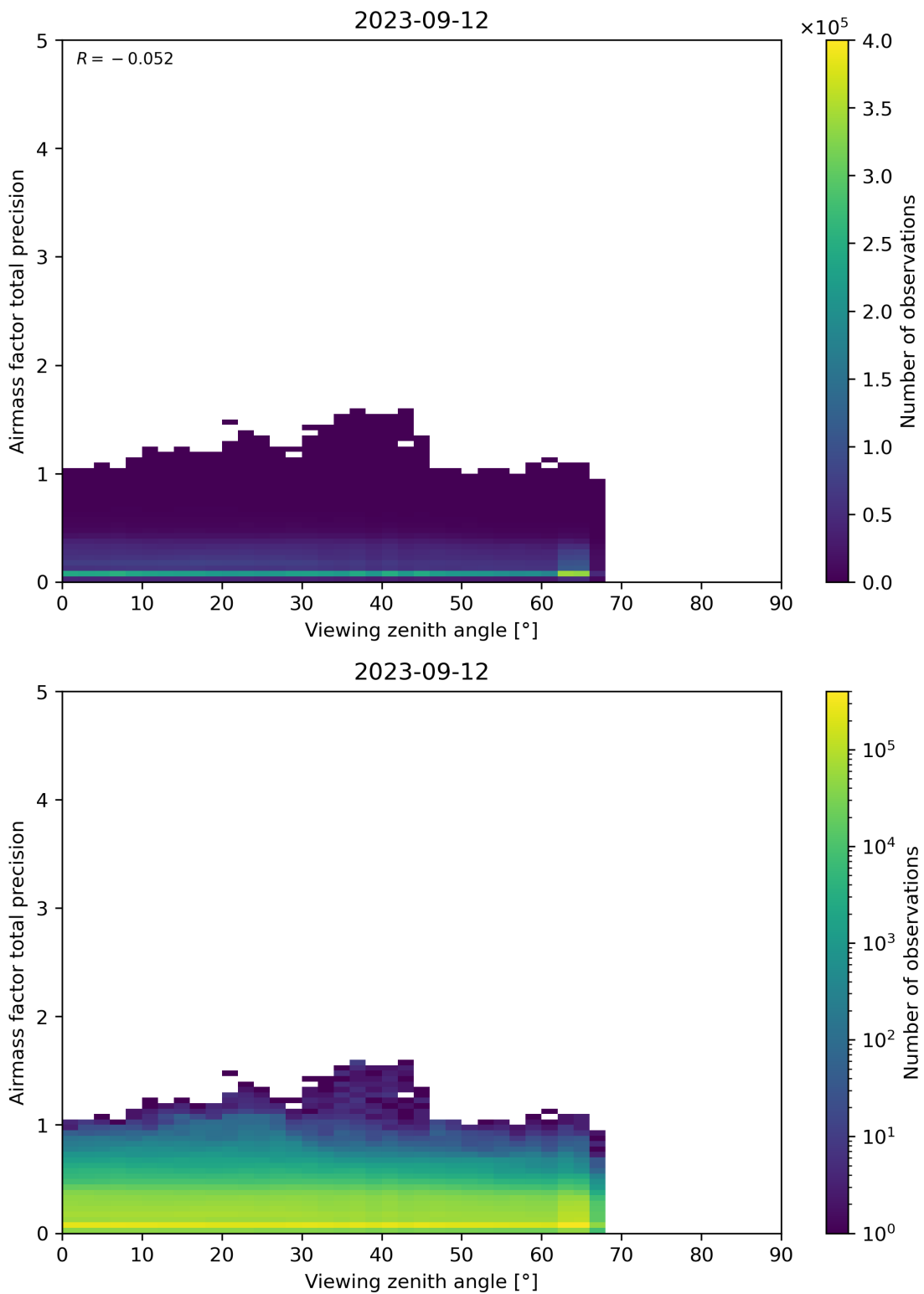


Figure 191: Scatter density plot of “Viewing zenith angle” against “Airmass factor total precision” for 2023-09-11 to 2023-09-13.

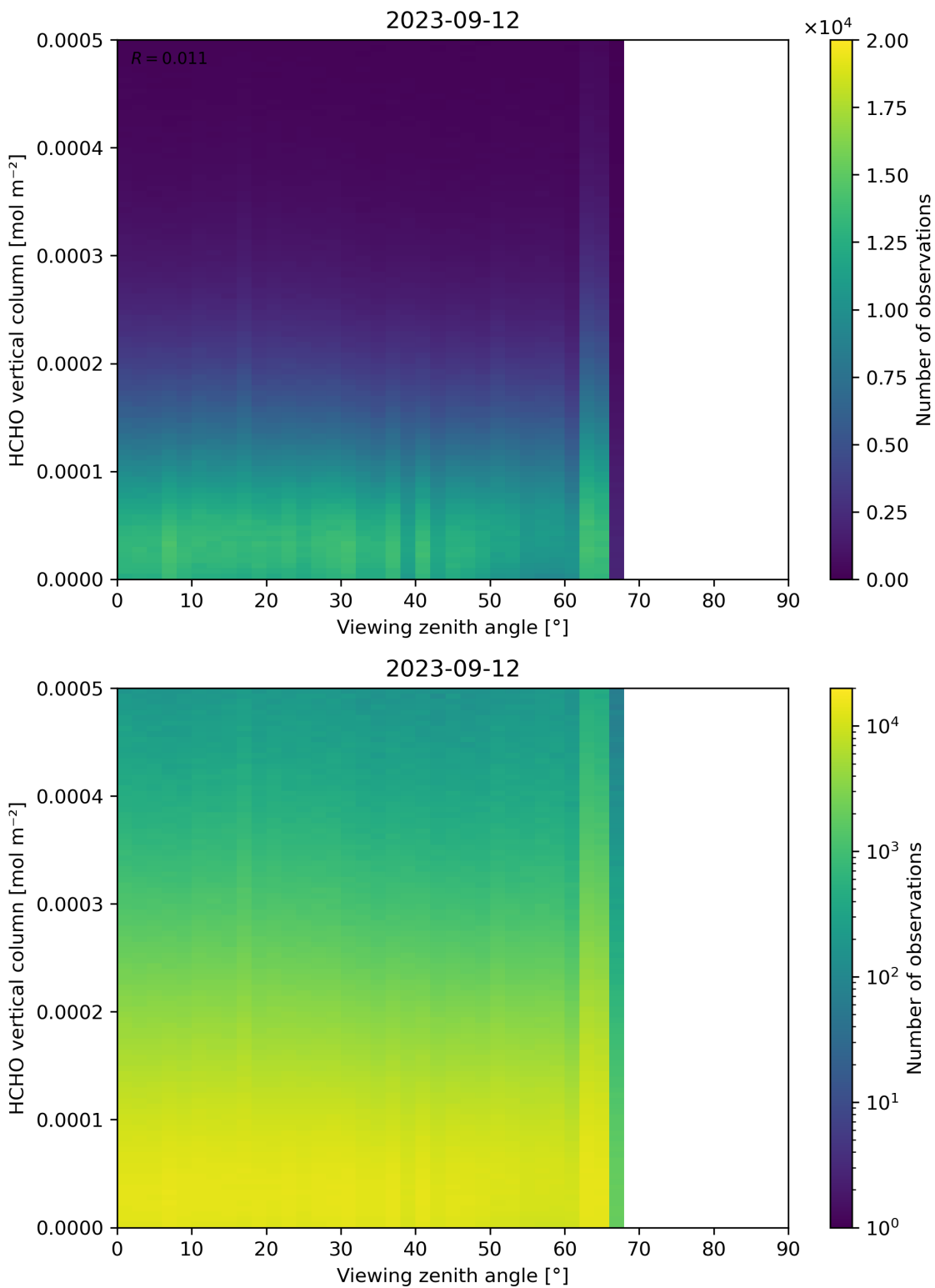


Figure 192: Scatter density plot of “Viewing zenith angle” against “HCHO vertical column” for 2023-09-11 to 2023-09-13.

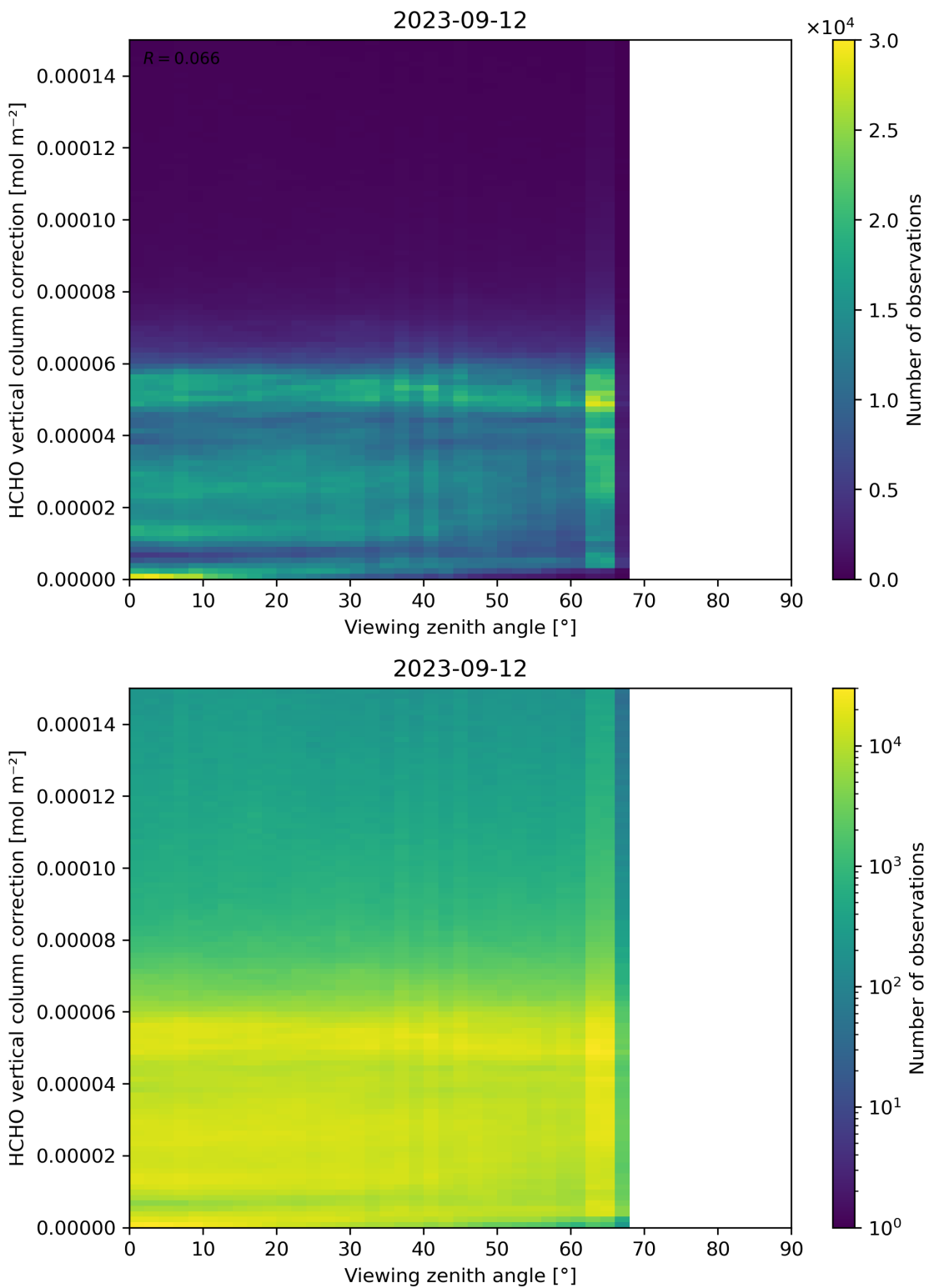


Figure 193: Scatter density plot of “Viewing zenith angle” against “HCHO vertical column correction” for 2023-09-11 to 2023-09-13.

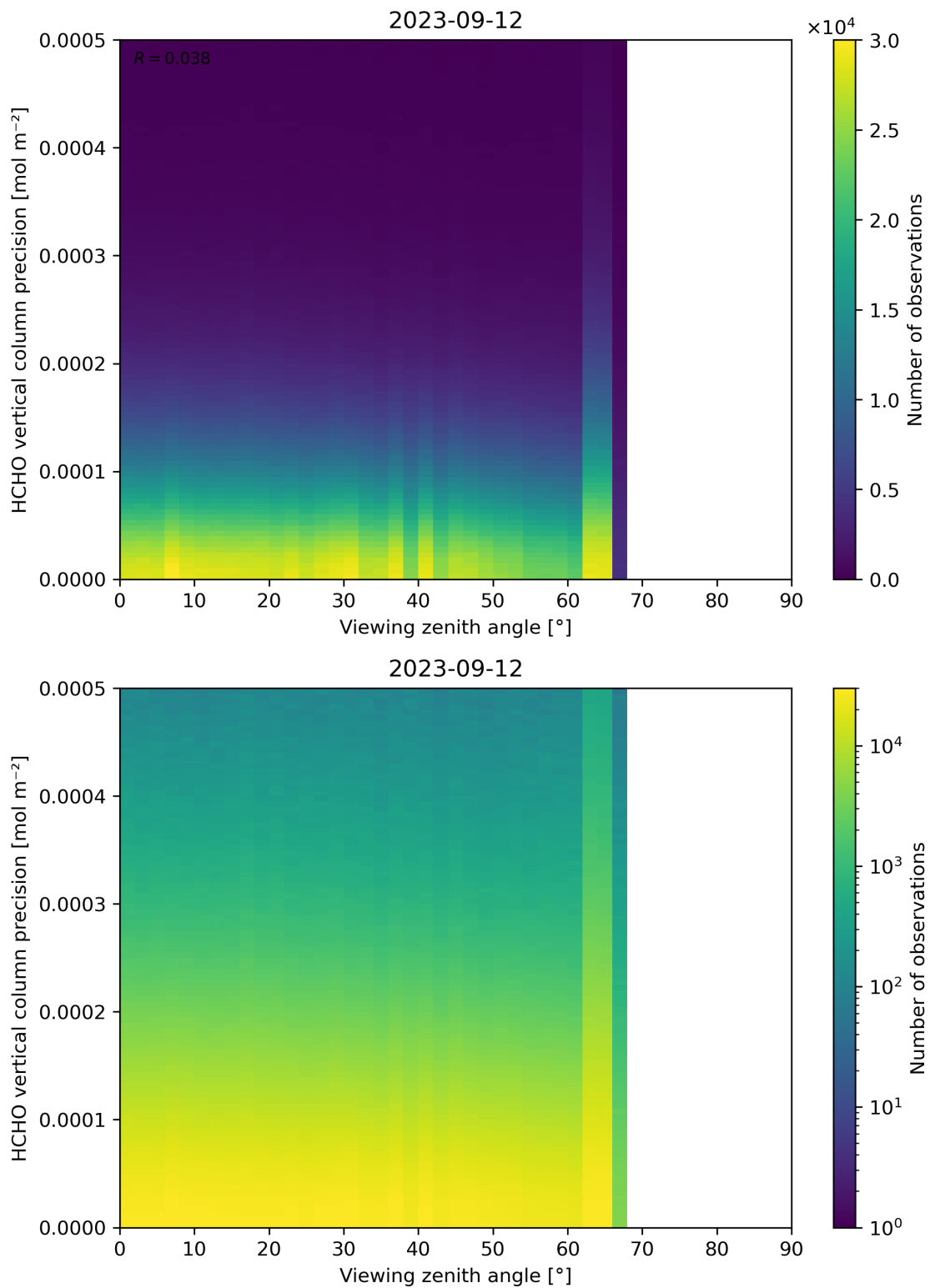


Figure 194: Scatter density plot of “Viewing zenith angle” against “HCHO vertical column precision” for 2023-09-11 to 2023-09-13.

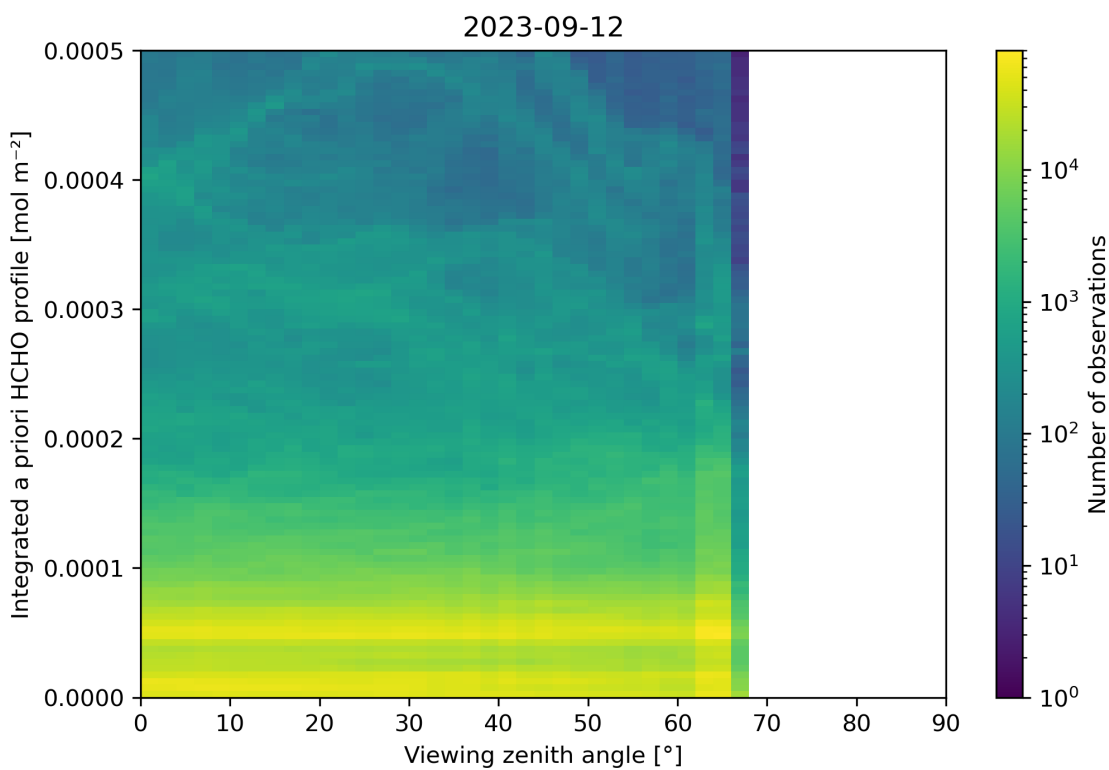
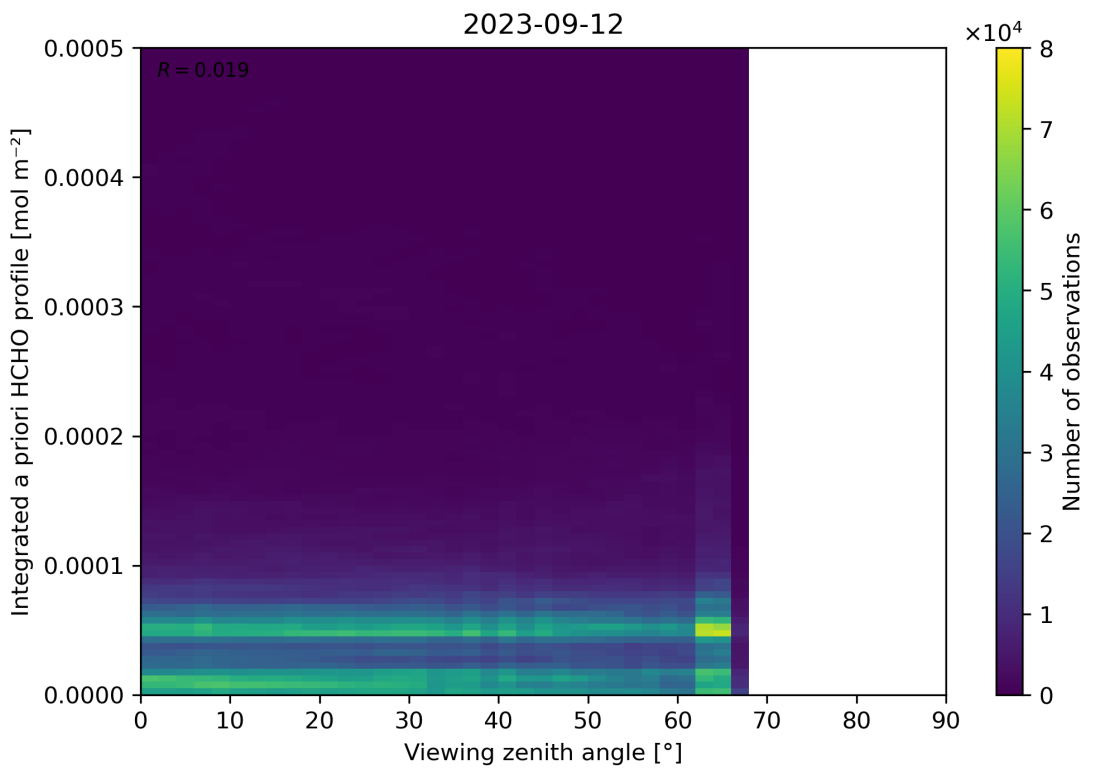


Figure 195: Scatter density plot of “Viewing zenith angle” against “Integrated a priori HCHO profile” for 2023-09-11 to 2023-09-13.

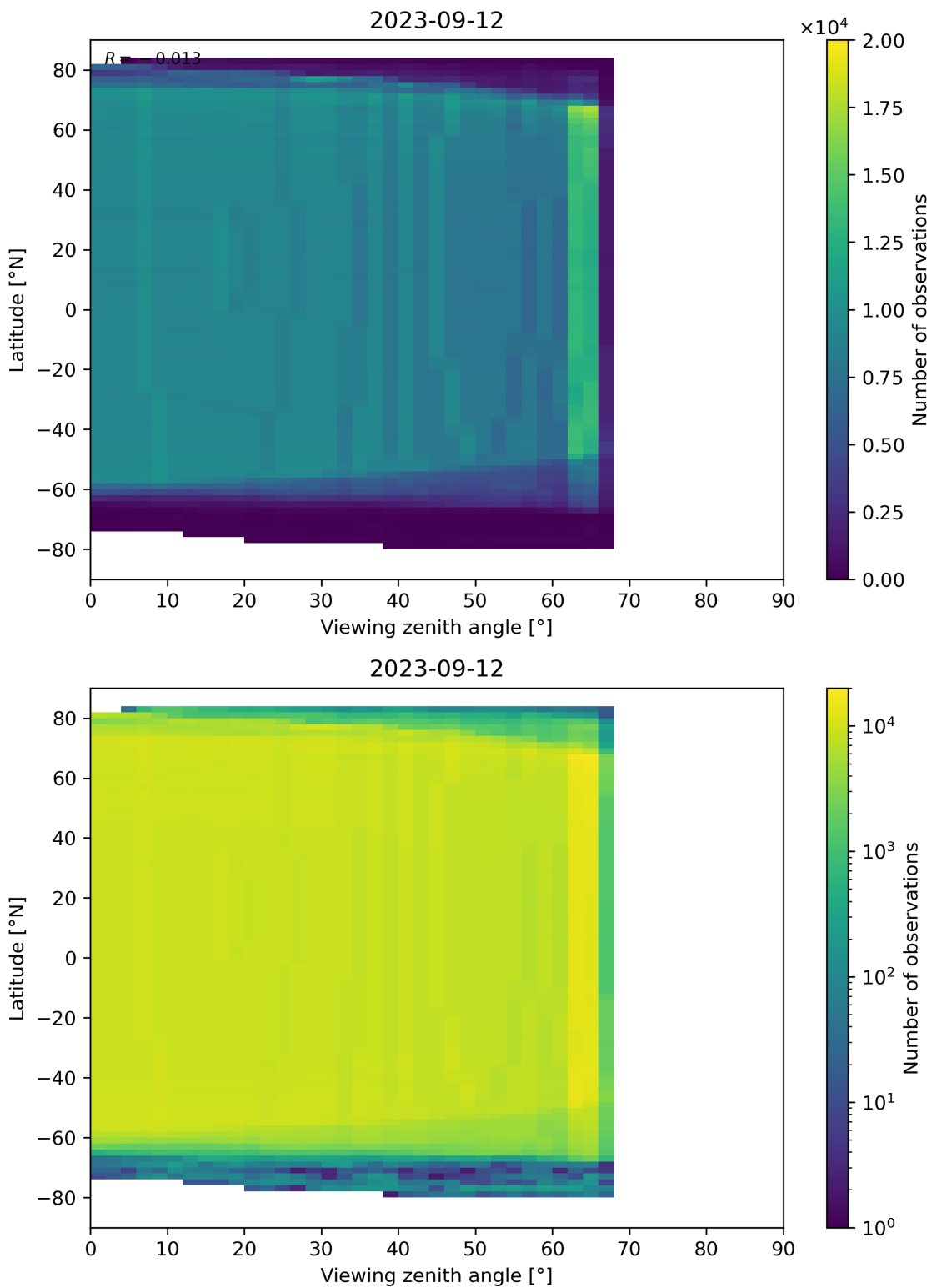


Figure 196: Scatter density plot of “Viewing zenith angle” against “Latitude” for 2023-09-11 to 2023-09-13.

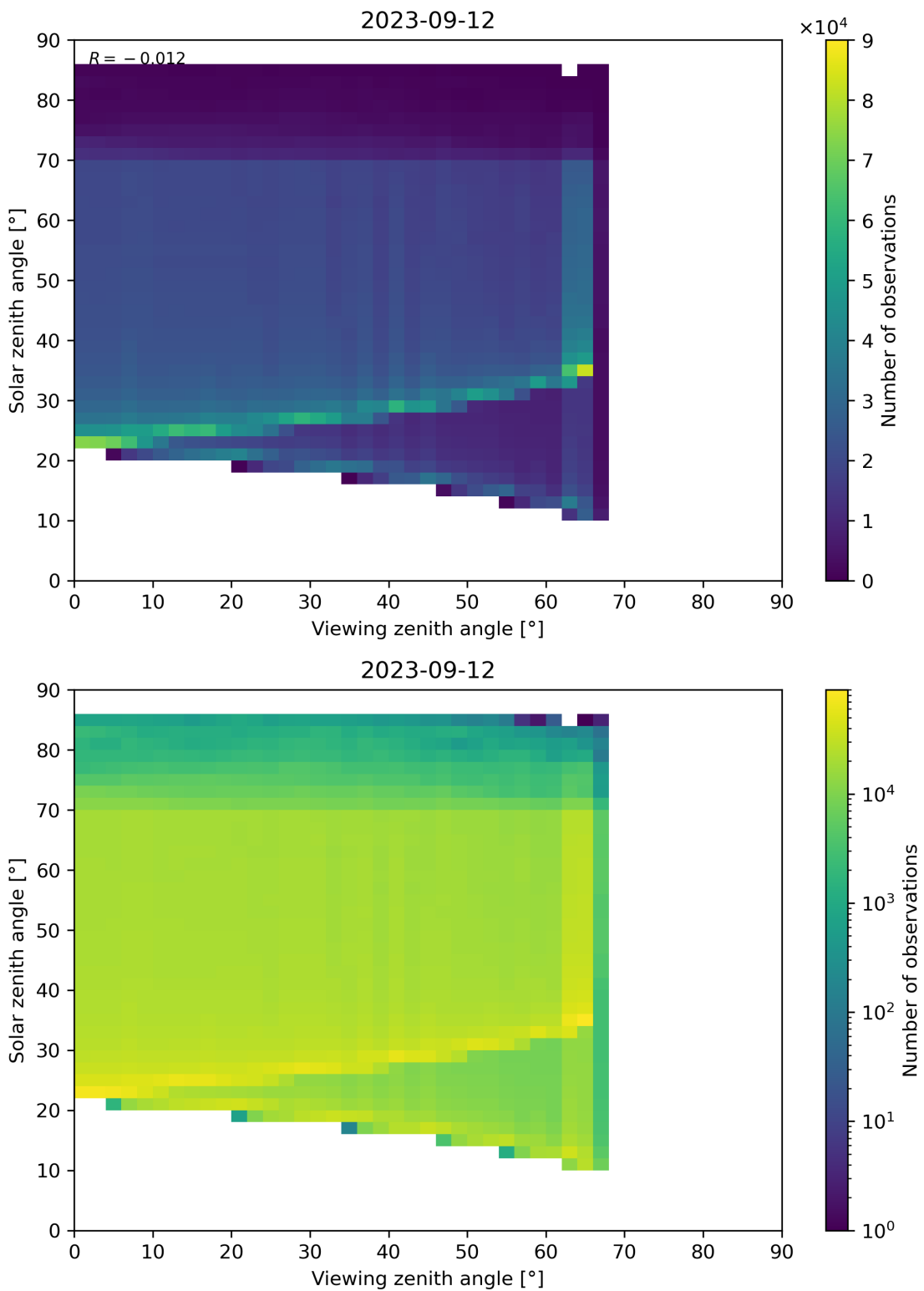


Figure 197: Scatter density plot of “Viewing zenith angle” against “Solar zenith angle” for 2023-09-11 to 2023-09-13.

Contents

| | | |
|-----------|--|------------|
| 1 | Short Introduction | 1 |
| 1.1 | The list of parameters | 1 |
| 2 | Definitions | 1 |
| 3 | Granule outlines | 12 |
| 4 | Input data monitoring | 13 |
| 5 | Warnings and errors | 14 |
| 6 | World maps | 15 |
| 7 | Zonal average | 29 |
| 8 | Histograms | 43 |
| 9 | Along track statistics | 57 |
| 10 | Coincidence density | 71 |
| 11 | Copyright information of ‘PyCAMA’ | 207 |

List of Figures

| | | |
|----|--|----|
| 1 | Map of correlation graph for 2023-09-11 to 2023-09-13. | 10 |
| 2 | Map of correlation matrix for 2023-09-11 to 2023-09-13. | 11 |
| 3 | Outline of the granules. | 12 |
| 4 | Input data per granule | 13 |
| 5 | Fraction of pixels with specific warnings and errors during processing | 14 |
| 6 | Map of “HCHO vertical column” for 2023-09-11 to 2023-09-13 | 15 |
| 7 | Map of “HCHO vertical column precision” for 2023-09-11 to 2023-09-13 | 16 |
| 8 | Map of “HCHO vertical column correction” for 2023-09-11 to 2023-09-13 | 17 |
| 9 | Map of “HCHO slant column (window1)” for 2023-09-11 to 2023-09-13 | 18 |
| 10 | Map of “HCHO slant column precision (window1)” for 2023-09-11 to 2023-09-13 | 19 |
| 11 | Map of “Airmass factor total” for 2023-09-11 to 2023-09-13 | 20 |
| 12 | Map of “Airmass factor total precision” for 2023-09-11 to 2023-09-13 | 21 |
| 13 | Map of “Airmass factor clear” for 2023-09-11 to 2023-09-13 | 22 |
| 14 | Map of “Integrated a priori HCHO profile” for 2023-09-11 to 2023-09-13 | 23 |
| 15 | Map of “DOAS fit wavelength shift” for 2023-09-11 to 2023-09-13 | 24 |
| 16 | Map of “DOAS fit wavelength squeeze” for 2023-09-11 to 2023-09-13 | 25 |
| 17 | Map of “DOAS fit RMS (first interval)” for 2023-09-11 to 2023-09-13 | 26 |
| 18 | Map of “HCHO slant column correction” for 2023-09-11 to 2023-09-13 | 27 |
| 19 | Map of the number of observations for 2023-09-11 to 2023-09-13 | 28 |
| 20 | Zonal average of “QA value” for 2023-09-11 to 2023-09-13. | 29 |
| 21 | Zonal average of “HCHO vertical column” for 2023-09-11 to 2023-09-13. | 30 |
| 22 | Zonal average of “HCHO vertical column precision” for 2023-09-11 to 2023-09-13. | 31 |
| 23 | Zonal average of “HCHO vertical column correction” for 2023-09-11 to 2023-09-13. | 32 |
| 24 | Zonal average of “HCHO slant column (window1)” for 2023-09-11 to 2023-09-13. | 33 |
| 25 | Zonal average of “HCHO slant column precision (window1)” for 2023-09-11 to 2023-09-13. | 34 |
| 26 | Zonal average of “Airmass factor total” for 2023-09-11 to 2023-09-13. | 35 |
| 27 | Zonal average of “Airmass factor total precision” for 2023-09-11 to 2023-09-13. | 36 |
| 28 | Zonal average of “Airmass factor clear” for 2023-09-11 to 2023-09-13. | 37 |
| 29 | Zonal average of “Integrated a priori HCHO profile” for 2023-09-11 to 2023-09-13. | 38 |
| 30 | Zonal average of “DOAS fit wavelength shift” for 2023-09-11 to 2023-09-13. | 39 |
| 31 | Zonal average of “DOAS fit wavelength squeeze” for 2023-09-11 to 2023-09-13. | 40 |
| 32 | Zonal average of “DOAS fit RMS (first interval)” for 2023-09-11 to 2023-09-13. | 41 |
| 33 | Zonal average of “HCHO slant column correction” for 2023-09-11 to 2023-09-13. | 42 |
| 34 | Histogram of “QA value” for 2023-09-11 to 2023-09-13 | 43 |
| 35 | Histogram of “HCHO vertical column” for 2023-09-11 to 2023-09-13 | 44 |
| 36 | Histogram of “HCHO vertical column precision” for 2023-09-11 to 2023-09-13 | 45 |

| | | |
|----|--|----|
| 37 | Histogram of “HCHO vertical column correction” for 2023-09-11 to 2023-09-13 | 46 |
| 38 | Histogram of “HCHO slant column (window1)” for 2023-09-11 to 2023-09-13 | 47 |
| 39 | Histogram of “HCHO slant column precision (window1)” for 2023-09-11 to 2023-09-13 | 48 |
| 40 | Histogram of “Airmass factor total” for 2023-09-11 to 2023-09-13 | 49 |
| 41 | Histogram of “Airmass factor total precision” for 2023-09-11 to 2023-09-13 | 50 |
| 42 | Histogram of “Airmass factor clear” for 2023-09-11 to 2023-09-13 | 51 |
| 43 | Histogram of “Integrated a priori HCHO profile” for 2023-09-11 to 2023-09-13 | 52 |
| 44 | Histogram of “DOAS fit wavelength shift” for 2023-09-11 to 2023-09-13 | 53 |
| 45 | Histogram of “DOAS fit wavelength squeeze” for 2023-09-11 to 2023-09-13 | 54 |
| 46 | Histogram of “DOAS fit RMS (first interval)” for 2023-09-11 to 2023-09-13 | 55 |
| 47 | Histogram of “HCHO slant column correction” for 2023-09-11 to 2023-09-13 | 56 |
| 48 | Along track statistics of “QA value” for 2023-09-11 to 2023-09-13 | 57 |
| 49 | Along track statistics of “HCHO vertical column” for 2023-09-11 to 2023-09-13 | 58 |
| 50 | Along track statistics of “HCHO vertical column precision” for 2023-09-11 to 2023-09-13 | 59 |
| 51 | Along track statistics of “HCHO vertical column correction” for 2023-09-11 to 2023-09-13 | 60 |
| 52 | Along track statistics of “HCHO slant column (window1)” for 2023-09-11 to 2023-09-13 | 61 |
| 53 | Along track statistics of “HCHO slant column precision (window1)” for 2023-09-11 to 2023-09-13 | 62 |
| 54 | Along track statistics of “Airmass factor total” for 2023-09-11 to 2023-09-13 | 63 |
| 55 | Along track statistics of “Airmass factor total precision” for 2023-09-11 to 2023-09-13 | 64 |
| 56 | Along track statistics of “Airmass factor clear” for 2023-09-11 to 2023-09-13 | 65 |
| 57 | Along track statistics of “Integrated a priori HCHO profile” for 2023-09-11 to 2023-09-13 | 66 |
| 58 | Along track statistics of “DOAS fit wavelength shift” for 2023-09-11 to 2023-09-13 | 67 |
| 59 | Along track statistics of “DOAS fit wavelength squeeze” for 2023-09-11 to 2023-09-13 | 68 |
| 60 | Along track statistics of “DOAS fit RMS (first interval)” for 2023-09-11 to 2023-09-13 | 69 |
| 61 | Along track statistics of “HCHO slant column correction” for 2023-09-11 to 2023-09-13 | 70 |
| 62 | Scatter density plot of “DOAS fit RMS (first interval)” against “HCHO slant column corrected” for 2023-09-11 to 2023-09-13. | 71 |
| 63 | Scatter density plot of “DOAS fit RMS (first interval)” against “HCHO slant column correction” for 2023-09-11 to 2023-09-13. | 72 |
| 64 | Scatter density plot of “DOAS fit wavelength shift” against “DOAS fit RMS (first interval)” for 2023-09-11 to 2023-09-13. | 73 |
| 65 | Scatter density plot of “DOAS fit wavelength shift” against “DOAS fit wavelength squeeze” for 2023-09-11 to 2023-09-13. | 74 |
| 66 | Scatter density plot of “DOAS fit wavelength shift” against “HCHO slant column corrected” for 2023-09-11 to 2023-09-13. | 75 |
| 67 | Scatter density plot of “DOAS fit wavelength shift” against “HCHO slant column correction” for 2023-09-11 to 2023-09-13. | 76 |
| 68 | Scatter density plot of “DOAS fit wavelength squeeze” against “DOAS fit RMS (first interval)” for 2023-09-11 to 2023-09-13. | 77 |
| 69 | Scatter density plot of “DOAS fit wavelength squeeze” against “HCHO slant column corrected” for 2023-09-11 to 2023-09-13. | 78 |
| 70 | Scatter density plot of “DOAS fit wavelength squeeze” against “HCHO slant column correction” for 2023-09-11 to 2023-09-13. | 79 |
| 71 | Scatter density plot of “Airmass factor clear” against “DOAS fit RMS (first interval)” for 2023-09-11 to 2023-09-13. | 80 |
| 72 | Scatter density plot of “Airmass factor clear” against “DOAS fit wavelength shift” for 2023-09-11 to 2023-09-13. | 81 |
| 73 | Scatter density plot of “Airmass factor clear” against “DOAS fit wavelength squeeze” for 2023-09-11 to 2023-09-13. | 82 |
| 74 | Scatter density plot of “Airmass factor clear” against “HCHO slant column corrected” for 2023-09-11 to 2023-09-13. | 83 |
| 75 | Scatter density plot of “Airmass factor clear” against “HCHO slant column correction” for 2023-09-11 to 2023-09-13. | 84 |
| 76 | Scatter density plot of “Airmass factor clear” against “Integrated a priori HCHO profile” for 2023-09-11 to 2023-09-13. | 85 |
| 77 | Scatter density plot of “HCHO slant column corrected” against “HCHO slant column correction” for 2023-09-11 to 2023-09-13. | 86 |
| 78 | Scatter density plot of “HCHO slant column (window1)” against “DOAS fit RMS (first interval)” for 2023-09-11 to 2023-09-13. | 87 |
| 79 | Scatter density plot of “HCHO slant column (window1)” against “DOAS fit wavelength shift” for 2023-09-11 to 2023-09-13. | 88 |

| | | |
|-----|--|-----|
| 80 | Scatter density plot of “HCHO slant column (window1)” against “DOAS fit wavelength squeeze” for 2023-09-11 to 2023-09-13. | 89 |
| 81 | Scatter density plot of “HCHO slant column (window1)” against “Airmass factor clear” for 2023-09-11 to 2023-09-13. | 90 |
| 82 | Scatter density plot of “HCHO slant column (window1)” against “HCHO slant column corrected” for 2023-09-11 to 2023-09-13. | 91 |
| 83 | Scatter density plot of “HCHO slant column (window1)” against “HCHO slant column correction” for 2023-09-11 to 2023-09-13. | 92 |
| 84 | Scatter density plot of “HCHO slant column (window1)” against “HCHO slant column precision (window1)” for 2023-09-11 to 2023-09-13. | 93 |
| 85 | Scatter density plot of “HCHO slant column (window1)” against “Airmass factor total” for 2023-09-11 to 2023-09-13. | 94 |
| 86 | Scatter density plot of “HCHO slant column (window1)” against “Airmass factor total precision” for 2023-09-11 to 2023-09-13. | 95 |
| 87 | Scatter density plot of “HCHO slant column (window1)” against “Integrated a priori HCHO profile” for 2023-09-11 to 2023-09-13. | 96 |
| 88 | Scatter density plot of “HCHO slant column precision (window1)” against “DOAS fit RMS (first interval)” for 2023-09-11 to 2023-09-13. | 97 |
| 89 | Scatter density plot of “HCHO slant column precision (window1)” against “DOAS fit wavelength shift” for 2023-09-11 to 2023-09-13. | 98 |
| 90 | Scatter density plot of “HCHO slant column precision (window1)” against “DOAS fit wavelength squeeze” for 2023-09-11 to 2023-09-13. | 99 |
| 91 | Scatter density plot of “HCHO slant column precision (window1)” against “Airmass factor clear” for 2023-09-11 to 2023-09-13. | 100 |
| 92 | Scatter density plot of “HCHO slant column precision (window1)” against “HCHO slant column corrected” for 2023-09-11 to 2023-09-13. | 101 |
| 93 | Scatter density plot of “HCHO slant column precision (window1)” against “HCHO slant column correction” for 2023-09-11 to 2023-09-13. | 102 |
| 94 | Scatter density plot of “HCHO slant column precision (window1)” against “Airmass factor total” for 2023-09-11 to 2023-09-13. | 103 |
| 95 | Scatter density plot of “HCHO slant column precision (window1)” against “Airmass factor total precision” for 2023-09-11 to 2023-09-13. | 104 |
| 96 | Scatter density plot of “HCHO slant column precision (window1)” against “Integrated a priori HCHO profile” for 2023-09-11 to 2023-09-13. | 105 |
| 97 | Scatter density plot of “Airmass factor total” against “DOAS fit RMS (first interval)” for 2023-09-11 to 2023-09-13. | 106 |
| 98 | Scatter density plot of “Airmass factor total” against “DOAS fit wavelength shift” for 2023-09-11 to 2023-09-13. | 107 |
| 99 | Scatter density plot of “Airmass factor total” against “DOAS fit wavelength squeeze” for 2023-09-11 to 2023-09-13. | 108 |
| 100 | Scatter density plot of “Airmass factor total” against “Airmass factor clear” for 2023-09-11 to 2023-09-13. | 109 |
| 101 | Scatter density plot of “Airmass factor total” against “HCHO slant column corrected” for 2023-09-11 to 2023-09-13. | 110 |
| 102 | Scatter density plot of “Airmass factor total” against “HCHO slant column correction” for 2023-09-11 to 2023-09-13. | 111 |
| 103 | Scatter density plot of “Airmass factor total” against “Airmass factor total precision” for 2023-09-11 to 2023-09-13. | 112 |
| 104 | Scatter density plot of “Airmass factor total” against “Integrated a priori HCHO profile” for 2023-09-11 to 2023-09-13. | 113 |
| 105 | Scatter density plot of “Airmass factor total precision” against “DOAS fit RMS (first interval)” for 2023-09-11 to 2023-09-13. | 114 |
| 106 | Scatter density plot of “Airmass factor total precision” against “DOAS fit wavelength shift” for 2023-09-11 to 2023-09-13. | 115 |
| 107 | Scatter density plot of “Airmass factor total precision” against “DOAS fit wavelength squeeze” for 2023-09-11 to 2023-09-13. | 116 |
| 108 | Scatter density plot of “Airmass factor total precision” against “Airmass factor clear” for 2023-09-11 to 2023-09-13. | 117 |
| 109 | Scatter density plot of “Airmass factor total precision” against “HCHO slant column corrected” for 2023-09-11 to 2023-09-13. | 118 |
| 110 | Scatter density plot of “Airmass factor total precision” against “HCHO slant column correction” for 2023-09-11 to 2023-09-13. | 119 |

| | | |
|-----|---|-----|
| 111 | Scatter density plot of “Airmass factor total precision” against “Integrated a priori HCHO profile” for 2023-09-11 to 2023-09-13. | 120 |
| 112 | Scatter density plot of “HCHO vertical column correction” against “DOAS fit RMS (first interval)” for 2023-09-11 to 2023-09-13. | 121 |
| 113 | Scatter density plot of “HCHO vertical column correction” against “DOAS fit wavelength shift” for 2023-09-11 to 2023-09-13. | 122 |
| 114 | Scatter density plot of “HCHO vertical column correction” against “DOAS fit wavelength squeeze” for 2023-09-11 to 2023-09-13. | 123 |
| 115 | Scatter density plot of “HCHO vertical column correction” against “Airmass factor clear” for 2023-09-11 to 2023-09-13. | 124 |
| 116 | Scatter density plot of “HCHO vertical column correction” against “HCHO slant column corrected” for 2023-09-11 to 2023-09-13. | 125 |
| 117 | Scatter density plot of “HCHO vertical column correction” against “HCHO slant column correction” for 2023-09-11 to 2023-09-13. | 126 |
| 118 | Scatter density plot of “HCHO vertical column correction” against “HCHO slant column (window1)” for 2023-09-11 to 2023-09-13. | 127 |
| 119 | Scatter density plot of “HCHO vertical column correction” against “HCHO slant column precision (window1)” for 2023-09-11 to 2023-09-13. | 128 |
| 120 | Scatter density plot of “HCHO vertical column correction” against “Airmass factor total” for 2023-09-11 to 2023-09-13. | 129 |
| 121 | Scatter density plot of “HCHO vertical column correction” against “Airmass factor total precision” for 2023-09-11 to 2023-09-13. | 130 |
| 122 | Scatter density plot of “HCHO vertical column correction” against “Integrated a priori HCHO profile” for 2023-09-11 to 2023-09-13. | 131 |
| 123 | Scatter density plot of “HCHO vertical column” against “DOAS fit RMS (first interval)” for 2023-09-11 to 2023-09-13. | 132 |
| 124 | Scatter density plot of “HCHO vertical column” against “DOAS fit wavelength shift” for 2023-09-11 to 2023-09-13. | 133 |
| 125 | Scatter density plot of “HCHO vertical column” against “DOAS fit wavelength squeeze” for 2023-09-11 to 2023-09-13. | 134 |
| 126 | Scatter density plot of “HCHO vertical column” against “Airmass factor clear” for 2023-09-11 to 2023-09-13. | 135 |
| 127 | Scatter density plot of “HCHO vertical column” against “HCHO slant column corrected” for 2023-09-11 to 2023-09-13. | 136 |
| 128 | Scatter density plot of “HCHO vertical column” against “HCHO slant column correction” for 2023-09-11 to 2023-09-13. | 137 |
| 129 | Scatter density plot of “HCHO vertical column” against “HCHO slant column (window1)” for 2023-09-11 to 2023-09-13. | 138 |
| 130 | Scatter density plot of “HCHO vertical column” against “HCHO slant column precision (window1)” for 2023-09-11 to 2023-09-13. | 139 |
| 131 | Scatter density plot of “HCHO vertical column” against “Airmass factor total” for 2023-09-11 to 2023-09-13. | 140 |
| 132 | Scatter density plot of “HCHO vertical column” against “Airmass factor total precision” for 2023-09-11 to 2023-09-13. | 141 |
| 133 | Scatter density plot of “HCHO vertical column” against “HCHO vertical column correction” for 2023-09-11 to 2023-09-13. | 142 |
| 134 | Scatter density plot of “HCHO vertical column” against “HCHO vertical column precision” for 2023-09-11 to 2023-09-13. | 143 |
| 135 | Scatter density plot of “HCHO vertical column” against “Integrated a priori HCHO profile” for 2023-09-11 to 2023-09-13. | 144 |
| 136 | Scatter density plot of “HCHO vertical column precision” against “DOAS fit RMS (first interval)” for 2023-09-11 to 2023-09-13. | 145 |
| 137 | Scatter density plot of “HCHO vertical column precision” against “DOAS fit wavelength shift” for 2023-09-11 to 2023-09-13. | 146 |
| 138 | Scatter density plot of “HCHO vertical column precision” against “DOAS fit wavelength squeeze” for 2023-09-11 to 2023-09-13. | 147 |
| 139 | Scatter density plot of “HCHO vertical column precision” against “Airmass factor clear” for 2023-09-11 to 2023-09-13. | 148 |
| 140 | Scatter density plot of “HCHO vertical column precision” against “HCHO slant column corrected” for 2023-09-11 to 2023-09-13. | 149 |
| 141 | Scatter density plot of “HCHO vertical column precision” against “HCHO slant column correction” for 2023-09-11 to 2023-09-13. | 150 |
| 142 | Scatter density plot of “HCHO vertical column precision” against “HCHO slant column (window1)” for 2023-09-11 to 2023-09-13. | 151 |

| | | |
|-----|--|-----|
| 143 | Scatter density plot of “HCHO vertical column precision” against “HCHO slant column precision (window1)” for 2023-09-11 to 2023-09-13. | 152 |
| 144 | Scatter density plot of “HCHO vertical column precision” against “Airmass factor total” for 2023-09-11 to 2023-09-13. | 153 |
| 145 | Scatter density plot of “HCHO vertical column precision” against “Airmass factor total precision” for 2023-09-11 to 2023-09-13. | 154 |
| 146 | Scatter density plot of “HCHO vertical column precision” against “HCHO vertical column correction” for 2023-09-11 to 2023-09-13. | 155 |
| 147 | Scatter density plot of “HCHO vertical column precision” against “Integrated a priori HCHO profile” for 2023-09-11 to 2023-09-13. | 156 |
| 148 | Scatter density plot of “Integrated a priori HCHO profile” against “DOAS fit RMS (first interval)” for 2023-09-11 to 2023-09-13. | 157 |
| 149 | Scatter density plot of “Integrated a priori HCHO profile” against “DOAS fit wavelength shift” for 2023-09-11 to 2023-09-13. | 158 |
| 150 | Scatter density plot of “Integrated a priori HCHO profile” against “DOAS fit wavelength squeeze” for 2023-09-11 to 2023-09-13. | 159 |
| 151 | Scatter density plot of “Integrated a priori HCHO profile” against “HCHO slant column corrected” for 2023-09-11 to 2023-09-13. | 160 |
| 152 | Scatter density plot of “Integrated a priori HCHO profile” against “HCHO slant column correction” for 2023-09-11 to 2023-09-13. | 161 |
| 153 | Scatter density plot of “Latitude” against “DOAS fit RMS (first interval)” for 2023-09-11 to 2023-09-13. | 162 |
| 154 | Scatter density plot of “Latitude” against “DOAS fit wavelength shift” for 2023-09-11 to 2023-09-13. | 163 |
| 155 | Scatter density plot of “Latitude” against “DOAS fit wavelength squeeze” for 2023-09-11 to 2023-09-13. | 164 |
| 156 | Scatter density plot of “Latitude” against “Airmass factor clear” for 2023-09-11 to 2023-09-13. | 165 |
| 157 | Scatter density plot of “Latitude” against “HCHO slant column corrected” for 2023-09-11 to 2023-09-13. | 166 |
| 158 | Scatter density plot of “Latitude” against “HCHO slant column correction” for 2023-09-11 to 2023-09-13. | 167 |
| 159 | Scatter density plot of “Latitude” against “HCHO slant column (window1)” for 2023-09-11 to 2023-09-13. | 168 |
| 160 | Scatter density plot of “Latitude” against “HCHO slant column precision (window1)” for 2023-09-11 to 2023-09-13. | 169 |
| 161 | Scatter density plot of “Latitude” against “Airmass factor total” for 2023-09-11 to 2023-09-13. | 170 |
| 162 | Scatter density plot of “Latitude” against “Airmass factor total precision” for 2023-09-11 to 2023-09-13. | 171 |
| 163 | Scatter density plot of “Latitude” against “HCHO vertical column” for 2023-09-11 to 2023-09-13. | 172 |
| 164 | Scatter density plot of “Latitude” against “HCHO vertical column correction” for 2023-09-11 to 2023-09-13. | 173 |
| 165 | Scatter density plot of “Latitude” against “HCHO vertical column precision” for 2023-09-11 to 2023-09-13. | 174 |
| 166 | Scatter density plot of “Latitude” against “Integrated a priori HCHO profile” for 2023-09-11 to 2023-09-13. | 175 |
| 167 | Scatter density plot of “Solar zenith angle” against “DOAS fit RMS (first interval)” for 2023-09-11 to 2023-09-13. | 176 |
| 168 | Scatter density plot of “Solar zenith angle” against “DOAS fit wavelength shift” for 2023-09-11 to 2023-09-13. | 177 |
| 169 | Scatter density plot of “Solar zenith angle” against “DOAS fit wavelength squeeze” for 2023-09-11 to 2023-09-13. | 178 |
| 170 | Scatter density plot of “Solar zenith angle” against “Airmass factor clear” for 2023-09-11 to 2023-09-13. | 179 |
| 171 | Scatter density plot of “Solar zenith angle” against “HCHO slant column corrected” for 2023-09-11 to 2023-09-13. | 180 |
| 172 | Scatter density plot of “Solar zenith angle” against “HCHO slant column correction” for 2023-09-11 to 2023-09-13. | 181 |
| 173 | Scatter density plot of “Solar zenith angle” against “HCHO slant column (window1)” for 2023-09-11 to 2023-09-13. | 182 |
| 174 | Scatter density plot of “Solar zenith angle” against “HCHO slant column precision (window1)” for 2023-09-11 to 2023-09-13. | 183 |
| 175 | Scatter density plot of “Solar zenith angle” against “Airmass factor total” for 2023-09-11 to 2023-09-13. | 184 |
| 176 | Scatter density plot of “Solar zenith angle” against “Airmass factor total precision” for 2023-09-11 to 2023-09-13. | 185 |
| 177 | Scatter density plot of “Solar zenith angle” against “HCHO vertical column” for 2023-09-11 to 2023-09-13. | 186 |
| 178 | Scatter density plot of “Solar zenith angle” against “HCHO vertical column correction” for 2023-09-11 to 2023-09-13. | 187 |
| 179 | Scatter density plot of “Solar zenith angle” against “HCHO vertical column precision” for 2023-09-11 to 2023-09-13. | 188 |
| 180 | Scatter density plot of “Solar zenith angle” against “Integrated a priori HCHO profile” for 2023-09-11 to 2023-09-13. | 189 |
| 181 | Scatter density plot of “Solar zenith angle” against “Latitude” for 2023-09-11 to 2023-09-13. | 190 |
| 182 | Scatter density plot of “Viewing zenith angle” against “DOAS fit RMS (first interval)” for 2023-09-11 to 2023-09-13. | 191 |

| | | |
|-----|--|-----|
| 183 | Scatter density plot of “Viewing zenith angle” against “DOAS fit wavelength shift” for 2023-09-11 to 2023-09-13. | 192 |
| 184 | Scatter density plot of “Viewing zenith angle” against “DOAS fit wavelength squeeze” for 2023-09-11 to 2023-09-13. | 193 |
| 185 | Scatter density plot of “Viewing zenith angle” against “Airmass factor clear” for 2023-09-11 to 2023-09-13. | 194 |
| 186 | Scatter density plot of “Viewing zenith angle” against “HCHO slant column corrected” for 2023-09-11 to 2023-09-13. | 195 |
| 187 | Scatter density plot of “Viewing zenith angle” against “HCHO slant column correction” for 2023-09-11 to 2023-09-13. | 196 |
| 188 | Scatter density plot of “Viewing zenith angle” against “HCHO slant column (window1)” for 2023-09-11 to 2023-09-13. | 197 |
| 189 | Scatter density plot of “Viewing zenith angle” against “HCHO slant column precision (window1)” for 2023-09-11 to 2023-09-13. | 198 |
| 190 | Scatter density plot of “Viewing zenith angle” against “Airmass factor total” for 2023-09-11 to 2023-09-13. | 199 |
| 191 | Scatter density plot of “Viewing zenith angle” against “Airmass factor total precision” for 2023-09-11 to 2023-09-13. | 200 |
| 192 | Scatter density plot of “Viewing zenith angle” against “HCHO vertical column” for 2023-09-11 to 2023-09-13. | 201 |
| 193 | Scatter density plot of “Viewing zenith angle” against “HCHO vertical column correction” for 2023-09-11 to 2023-09-13. | 202 |
| 194 | Scatter density plot of “Viewing zenith angle” against “HCHO vertical column precision” for 2023-09-11 to 2023-09-13. | 203 |
| 195 | Scatter density plot of “Viewing zenith angle” against “Integrated a priori HCHO profile” for 2023-09-11 to 2023-09-13. | 204 |
| 196 | Scatter density plot of “Viewing zenith angle” against “Latitude” for 2023-09-11 to 2023-09-13. | 205 |
| 197 | Scatter density plot of “Viewing zenith angle” against “Solar zenith angle” for 2023-09-11 to 2023-09-13. | 206 |

List of Tables

| | | |
|---|---|---|
| 1 | Parameterlist and basic statistics for the analysis | 2 |
| 2 | Percentile ranges | 3 |
| 3 | Parameterlist and basic statistics for the analysis for observations in the northern hemisphere | 4 |
| 4 | Parameterlist and basic statistics for the analysis for observations in the southern hemisphere | 5 |
| 5 | Parameterlist and basic statistics for the analysis for observations over water | 6 |
| 6 | Parameterlist and basic statistics for the analysis for observations over land | 7 |
| 7 | Correlation matrix | 8 |
| 8 | Covariance matrix | 9 |

11 Copyright information of ‘PyCAMA’

Copyright © 2005 – 2023, Maarten Sneep (KNMI).

All rights reserved.

Redistribution and use in source and binary forms, with or without modification, are permitted provided that the following conditions are met:

1. Redistributions of source code must retain the above copyright notice, this list of conditions and the following disclaimer.
2. Redistributions in binary form must reproduce the above copyright notice, this list of conditions and the following disclaimer in the documentation and/or other materials provided with the distribution.
3. Neither the name of the copyright holder nor the names of its contributors may be used to endorse or promote products derived from this software without specific prior written permission.

This software is provided by the copyright holders and contributors “as is” and any express or implied warranties, including, but not limited to, the implied warranties of merchantability and fitness for a particular purpose are disclaimed. In no event shall the copyright holder or contributors be liable for any direct, indirect, incidental, special, exemplary, or consequential damages (including, but not limited to, procurement of substitute goods or services; loss of use, data, or profits; or business interruption) however caused and on any theory of liability, whether in contract, strict liability, or tort (including negligence or otherwise) arising in any way out of the use of this software, even if advised of the possibility of such damage.

Maarten Sneep (maarten.sneep@knmi.nl).